

**TRANSESTERIFICATION OF NON-EDIBLE SEEDS OIL TO
BIODIESEL USING SOLID BASE GREEN NANO-CATALYSTS**



BY

Saman Ilyas Cheema

**Department of Plant Sciences
Quaid-i-Azam University Islamabad Pakistan
2021**

TRANSESTERIFICATION OF NON-EDIBLE SEEDS OIL TO BIODIESEL USING SOLID BASE GREEN NANO-CATALYSTS



A Thesis submitted to Quaid-i-Azam University in
Partial Fulfillment of the Requirements of the Degree of

DOCTOR OF PHILOSOPHY

In

**Plant Sciences (Botany) By
Saman Ilyas Cheema**

**Department of Plant Sciences
Quaid-i-Azam University Islamabad Pakistan
2021**

بِسْمِ اللَّهِ الرَّحْمَنِ الرَّحِيمِ

**“Allah will exalt in degree those of you who believe and those
Who have been granted knowledge.”**

[Surah Mujadilah; 58:11]

Dedicated

To

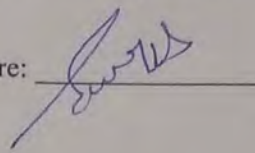
My beloved family

For being my strength

CERTIFICATE OF APPROVAL

This is to certify that research work presented in this thesis, entitled "Transesterification of Non-Edible Seeds Oil to Biodiesel using Solid Base Green Nano-Catalysts" was conducted by **Miss Saman Ilyas Cheema** under the supervision of **Prof. Dr. Mushtaq Ahmad**. No part of this thesis has been submitted anywhere else for any other degree. This thesis is submitted to the Department of Plant Sciences, Quaid-i-Azam University, Islamabad, Pakistan in partial fulfillment of the requirements for the degree of Doctor of Philosophy in the field of **Plant Sciences (Plant Systematics and Biodiversity)**, Department of Plant Sciences, Quaid-i-Azam University, Islamabad, Pakistan.

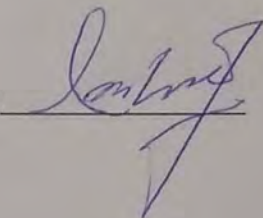
Student name: **Miss Saman Ilyas Cheema**

Signature: 

Examination committee

External Examiner 1

Prof. Dr. Muhammad Arshad
Chairperson
Department of Botany
Pir Mehr Ali Shah Arid Agriculture University,
Rawalpindi


Signature: 

External Examiner 2

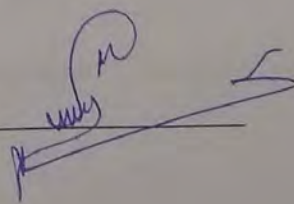
Dr. Shaikh Saeed
Associate Professor
Environmental Sciences Program
Fatima Jinnah Women University
The Mall
Rawalpindi

Signature 

Supervisor
Prof. Dr. Mushtaq Ahmad
Department of Plant Sciences
Quaid-i-Azam University, Islamabad

Signature 

Chairman
Prof. Dr. Mushtaq Ahmad
Department of Plant Sciences
Quaid-i-Azam University,
Islamabad

Signature 

Dated: 26-05-2021

FOREIGN EXAMINERS

1. Dr. Jerry Roberts

Professor
Deputy Vice Chancellor Research and Enterprise
University of Plymouth
Office of the Vice Chancellor
18 Portland Villas
Plymouth
PL4 8AA UK

2. Dr. Geoffrey Michael Gadd

Professor
Geomicrobiology Group
School of Life Sciences
University of Dundee
Dundee
DD1SEH
Scotland, United Kingdom

QAUID-I-AZAM UNIVERSITY
DEPARTMENT OF PLANT SCIENCES

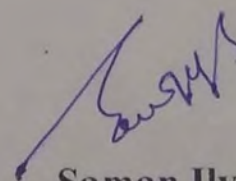
No. _____

26th May 2021

Subject: Author Declaration

I Ms. Saman Ilyas hereby state that my Ph.D. thesis titled **“Transesterification of Non-Edible Seeds Oil to Biodiesel Using Solid Base Green Nano Catalysts”** is my own work and has not been submitted previously by me for taking any degree from Department of Plant Sciences, Quaid-i-Azam University or anywhere else in the country/world.

At any time if my statement is found to be incorrect even after my Graduation the university has the right to withdraw my Ph.D. degree.



Saman Ilyas Cheema

QAUID-I-AZAM UNIVERSITY
DEPARTMENT OF PLANT SCIENCES

No. _____

26th May 2021

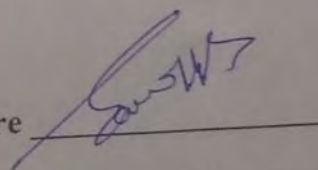
Subject: Plagiarism Undertaking

I solemnly declare that research work presented in the thesis titled "Transesterification of Non-Edible Seeds Oil to Biodiesel Using Solid Base Green Nano Catalysts" is solely my research work with no significant contribution from any other person. Small contribution/help wherever taken has been duly acknowledged and that complete thesis has been written by me.

I understand the zero-tolerance policy of the HEC and Quaid-i-Azam University towards plagiarism. Therefore, I as an author of the above titled thesis declare that no portion of my thesis has been plagiarized and any material used as reference is properly referred/cited.

I undertake that if I am found faulty of any formal plagiarism in the above titled thesis even after award of Ph.D. degree, the University reserves the rights to withdraw/revoke my Ph.D. degree and that HEC and the University has the right to publish my name on the HEC/University website on which name of students are placed who submitted plagiarized thesis.

Student / Author Signature

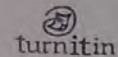


Name:

Saman Ilyas Cheema

Turnitin Originality Report

TRANSESTERIFICATION OF NON-EDIBLE SEEDS OIL TO BIODIESEL USING SOLID
BASE GREEN NANO-CATALYSTS by Saman Ilyas Cheema .



From DRSM (DRSM L)

- Processed on 19-Sep-2020 18:07 PKT
- ID: 1391202605
- Word Count: 28716

Similarity Index

7%

Similarity by Source

Internet Sources:

N/A

Publications:

N/A

Student Papers:

N/A

sources:

- 1 1% match (student papers from 28-Jun-2016)
Submitted to Higher Education Commission Pakistan on 2016-06-28
- 2 1% match (Internet from 16-Apr-2019)
<http://ramadhanupanji.blogspot.com/2014/08/penggunaanarang-aktif-limbah-tulang.html>
- 3 < 1% match (publications)
Sajjadi, Baharak, Abdul Aziz Abdul Raman, and Hamidreza Arandiyan. "A comprehensive review on properties of edible and non-edible vegetable oil-based biodiesel: Composition, specifications and prediction models", Renewable and Sustainable Energy Reviews, 2016.
- 4 < 1% match (publications)
Maryam Tanveer Akhtar, Mushtaq Ahmad, Anjuman Shaheen, Muhammad Zafar et al. "Comparative Study of Liquid Biodiesel From Sterculia foetida (Bottle Tree) Using CuO-CeO2 and Fe2O3 Nano Catalysts", Frontiers in Energy Research, 2019
- 5 < 1% match (student papers from 30-Jun-2016)
Submitted to Higher Education Commission Pakistan on 2016-06-30
- 6 < 1% match (publications)
Muhammad Dani Supardan, Satriana., Mahlinda .. "BIODIESEL PRODUCTION FROM WASTE COOKING OIL USING HYDRODINAMIC CAVITATION", MAKARA Journal of Technology Series, 2013
- 7 < 1% match (publications)
Mamoona Munir, Muhammad Saeed, Mushtaq Ahmad, Amir Waseem, Shazia Sultana, Muhammad Zafar, Gokul Raghavendra Srinivasan. " Optimization of novel Linn. Biodiesel

Table of Contents

CONTENTS		
<i>Titles</i>		<i>Page No</i>
CHAPTER 1: INTRODUCTION		
1.1	Biodiesel: A Sustainable Energy Resource	1
1.2	FeedStocks for Biodiesel Production	2
1.3	Conventional Energy Resources: A Threat to Global Environment	4
1.4	Second Generation Biodiesel: As a Sustainable Energy Option	6
1.5	Biodiesel Production Techniques	7
1.5.1	Pyrolysis/Thermal cracking	7
1.5.2	Dilution	8
1.5.3	Micro-emulsion	8
1.5.4	Transesterification/Alcoholysis	8
1.6	Natural Inorganic Clays as Green Catalysts	16
1.7	Background Justification of the Project	18
1.8	Aims and Objectives	20
CHAPTER 2: MATERIALS AND METHODS		
2.1	Chemicals and Reagents	24
2.2	Identification of Non-Edible Seeds Oil as Biodiesel Feedstock	24
2.3	Seeds Collection	24
2.4	Scanning Electron Microscopy (SEM) of Oil Seeds	24
2.5	Determination of Seeds Oil Contents Via Chemical Extraction Method	25

Table of Contents

2.6	Electric Oil Extraction	26
2.7	Purification of Crude oils	26
2.8	FFA Contents Determination of Seeds Oil	26
2.9	Synthesis of Catalysts	27
2.9.1	Clay Hybrid Composite Catalyst Synthesis	27
2.10	Characterization of Catalysts	27
2.10.1	Scanning Electron Microscopy (SEM)	27
2.10.2	Energy Dispersive X-Ray (EDS)	28
2.10.3	X-Ray Diffraction (XRD)	28
2.10.4	Fourier Transform Infrared Radiation Spectroscopy (FT-IR)	29
2.11	Biodiesel Synthesis	30
2.11.1	Transesterification	30
2.12	Biodiesel Characterization	30
2.12.1	Fourier Transform Infrared Radiation (FT-IR) Spectroscopy	31
2.12.2	Gas Chromatography-Mass Spectroscopy (GC-MS)	31
2.13	Determination of Fuel Properties	32
2.14	Optimization study of Transesterification operational factors using Response Surface Methodology (RSM)	32
CHAPTER 3: RESULTS AND DISCUSSION		
Section I: Morphological identification and Scanning Electron Micrographs of seeds of non-edible feedstock		37
3.1.1	<i>Brassica oleracea</i> L	38
3.1.2	<i>Carthamus oxyacantha</i> M. Bieb	41
3.1.3	<i>Carthamus tinctorius</i> L.	43
3.1.4	<i>Beaumontia grandiflora</i> Wall	45

Table of Contents

3.1.5	<i>Celastrus paniculatus</i> Willd.	47
3.1.6	<i>Carthamus lanatus</i> L.	49
3.1.7	<i>Acacia concinna</i> (Willd.) DC.	51
3.1.8	<i>Sapindus trifoliatus</i> L.	53
3.1.9	<i>Sesamum indicum</i> L.	55
3.1.10	<i>Ricinus communis</i> L.	57
Section II: Catalysts Characterization		62
3.2	Characterization of Montmorillonite Clay Catalysts	63
3.2.1	Characterization of Al-Mmt Clay Catalyst	63
3.2.1.1	Scanning Electron Microscopy of (Al) Montmorillonite Clay Catalyst	63
2.2.1.2	EDS Analysis of (Al) Montmorillonite Clay Catalyst	63
2.2.1.3	FT-IR of Al-Mmt Clay Catalyst	64
2.2.1.4	XRD of Al-Mmt Clay Catalyst	64
3.2.2	Characterization of Na-Ag Montmorillonite Clay Catalyst	67
3.2.2.1	Scanning Electron Microscopy of Na-Ag Montmorillonite Clay Catalyst	67
3.2.2.2	EDS Analysis of Na-Ag Montmorillonite Clay Catalyst	67
3.2.2.3	FT-IR of Na-Ag Montmorillonite Clay Catalyst	67
3.2.2.4	XRD of Na-Ag Montmorillonite Clay Catalyst	68
3.2.3	Characterization of Cu-Mg-Zn Montmorillonite Clay Catalyst	71
3.2.3.1	Scanning Electron Microscopy of Cu-Mg-Zn-Mmt Clay Catalyst	71
3.2.3.2	EDS of Cu-Mg-Zn Montmorillonite Clay Catalyst	71

Table of Contents

3.2.3.3	FTIR of Cu-Mg-Zn Montmorillonite Clay Catalyst	71
Section III: Biodiesel synthesis from ten different non-edible oil yielding seeds		75
3.3.1	<i>Brassica oleracea</i> L. Biodiesel (BOB)	80
3.3.1.1	Reaction Variables Affecting Transesterification of <i>Brassica oleracea</i> L. Seeds Oil to Biodiesel	80
3.3.1.1.1	Oil to Methanol Molar Ratio	80
3.3.1.1.2	Catalyst Concentration	81
3.3.1.1.3	Reaction Temperature (°C)	81
3.3.1.2	Chemical Characterization	81
3.3.1.2.1	GC-MS Analysis of <i>Brassica oleracea</i> L. Biodiesel (BOB)	81
3.3.1.2.2	FT-IR Analysis of BOB Biodiesel	82
3.3.1.2.3	Fuel Properties of <i>Brassica oleracea</i> L. Biodiesel (BOB)	83
3.3.1.3	Optimization Study of Transesterification Operational Factors Through Response Surface Methodology (RSM)	84
3.3.1.4	Parametric characterization of transesterification process	85
3.3.1.4.1	Interactive Impact of Catalyst Amount and Time	85
3.3.1.4.2	Interactive Impact of Catalyst Amount and Temperature	85
3.3.1.4.3	Interactive Impact of Catalyst Amount and Oil: Methanol Ratio	86
3.3.1.4.4	Interactive Impact of Time and Temperature	87
3.3.1.4.5	Interactive Impact of Time and Oil: Methanol Ratio	87
3.3.1.4.6	Interactive impact of oil: methanol ratio and temperature	88
3.3.2	<i>Carthamus oxycantha</i> Biodiesel (COB)	96
3.3.2.1	Reaction Variables Affecting Transesterification of <i>Carthamus oxycantha</i> Seeds Oil to Biodiesel	96

Table of Contents

3.3.2.1.1	Oil to Methanol Molar Ratio	96
3.3.2.1.2	Catalyst Concentration	96
3.3.2.1.3	Reaction Temperature (°C)	97
3.3.2.2	Chemical Characterization	97
3.3.2.2.1	GC-MS Analysis of <i>Carthamus oxycantha</i> Biodiesel (COB)	97
3.3.2.2.2	FT-IR of <i>Carthamus oxycantha</i> Biodiesel (COB)	98
3.3.2.2.3	Fuel Properties of <i>Carthamus oxycantha</i> Biodiesel (COB)	98
3.3.2.3	Optimization Study of Transesterification Operational Factors Through Response Surface Methodology (RSM)	99
3.3.2.4	Parametric characterization of transesterification process	100
3.3.2.4.1	Interactive Impact of Catalyst Amount and Time	100
3.3.2.4.2	Interactive Impact of Catalyst Amount and Temperature	100
3.3.2.4.3	Interactive Impact of Catalyst Amount and Oil: Methanol Ratio	101
3.3.2.4.4	Interactive impact of time and temperature	101
3.3.2.4.5	Interactive Impact of Time and Oil: Methanol Ratio	102
3.3.2.4.6	Interactive impact of oil: methanol ratio and temperature	102
3.3.3	<i>Carthamus tinctorius</i> Biodiesel (CTB)	110
3.3.3.1	Reaction Variables Affecting Transesterification of <i>Carthamus tinctorius</i> Seeds Oil to Biodiesel	110
3.3.3.1.1	Oil to Methanol Molar Ratio	110
3.3.3.1.2	Catalyst Concentration	110
3.3.3.1.3	Reaction Temperature (°C)	111
3.3.3.2	Chemical Characterization	111
3.3.3.2.1	GC-MS of <i>Carthamus tinctorius</i> Biodiesel (CTB)	111

Table of Contents

3.3.3.2.2	FT-IR of <i>Carthamus tinctorius</i> Biodiesel (CTB)	111
3.3.3.2.3	Fuel Properties of <i>Carthamus tinctorius</i> Biodiesel (CTB)	112
3.3.3.3	Optimization study of Transesterification operational factors via response surface methodology (RSM)	113
3.3.3.4	Parametric characterization of transesterification process	114
3.3.3.4.1	Interactive Impact of Catalyst Amount and Time	114
3.3.3.4.2	Interactive Impact of Catalyst Amount and Temperature	114
3.3.3.4.3	Interactive Impact of Catalyst Amount and Oil: Methanol Ratio	115
3.3.3.4.4	Interactive impact of time and temperature	115
3.3.3.4.5	Interactive Impact of Time and Oil: Methanol Ratio	116
3.3.3.4.6	Interactive impact of oil: methanol ratio and temperature	116
3.3.4	<i>Carthamus lanatus</i> Biodiesel (CLB)	125
3.3.4.1	Reaction Variables Affecting Transesterification of <i>Carthamus lanatus</i> Seeds Oil to Biodiesel	125
3.3.4.1.1	Oil to Methanol Molar Ratio	125
3.3.4.1.2	Catalyst Concentration	125
3.3.4.1.3	Reaction Temperature (°C)	126
3.3.4.2	Chemical Characterization	126
3.3.4.2.1	GC-MS of <i>Carthamus lanatus</i> Biodiesel (CLB)	126
3.3.4.2.2	FT-IR of <i>Carthamus lanatus</i> Biodiesel (CLB)	126
3.3.4.2.3	Fuel Properties of <i>Carthamus lanatus</i> Biodiesel (CLB)	127
3.3.4.3	Optimization Study of Transesterification Operational Factors Through Response Surface Methodology (RSM)	128
3.3.4.4	Parametric characterization of transesterification process	129
3.3.4.4.1	Interactive Impact of Catalyst Amount and Time	129

Table of Contents

3.3.4.4.2	Interactive Impact of Catalyst Amount and Temperature	129
3.3.4.4.3	Interactive Impact of Catalyst Amount and Oil: Methanol Ratio	130
3.3.4.4.4	Interactive impact of time and temperature	130
3.3.4.4.5	Interactive Impact of Time and Oil: Methanol Ratio	131
3.3.4.4.6	Interactive Impact of Oil: Methanol and Temperature	131
3.3.5	<i>Beaumontia grandiflora</i> Wall Biodiesel (BGB)	139
3.3.5.1	Reaction Variables Affecting Transesterification of <i>Beaumontia grandiflora</i> Wall Seeds Oil to BGB	139
3.3.5.1.1	Oil to Methanol Molar Ratio	139
3.3.5.1.2	Catalyst Concentration	139
3.3.5.1.3	Reaction Temperature °C	140
3.3.5.2	Chemical Characterization	140
3.3.5.2.1	GC-MS of <i>Beaumontia grandiflora</i> Wall Biodiesel (BGB)	140
3.3.5.2.2	FT-IR of <i>Beaumontia grandiflora</i> Wall Biodiesel	140
3.3.5.2.3	Fuel Properties of <i>Beaumontia grandiflora</i> Wall Biodiesel (BGB)	141
3.3.5.3	Optimization Study of Transesterification Operational Factors Through Response Surface Methodology (RSM)	142
3.3.5.4	Parametric characterization of transesterification process	143
3.3.5.4.1	Interactive Impact of Catalyst Amount and Time	143
3.3.5.4.2	Interactive Impact of Catalyst Amount and Temperature	143
3.3.5.4.3	Interactive Impact of Catalyst Amount and Oil: Methanol Ratio	144
3.3.5.4.4	Interactive impact of time and temperature	144
3.3.5.4.5	Interactive Impact of Time and Oil: Methanol Ratio	144

Table of Contents

3.3.5.4.6	Interactive impact of oil: methanol ratio and temperature	145
3.3.6	<i>Acasia concinna</i> Biodiesel (ACB)	153
3.3.6.1	Reaction Variables Affecting Transesterification of <i>Acasia concinna</i> Seeds Oil to ACB	153
3.3.6.1.1	Oil to Methanol Molar Ratio	153
3.3.6.1.2	Catalyst Concentration	153
3.3.6.1.3	Reaction Temperature (°C)	154
3.3.6.2	Chemical Characterization	154
3.3.6.2.1	GC-MS of <i>Acasia concinna</i> Biodiesel (ACB)	154
3.3.6.2.2	FT-IR of <i>Acasia concinna</i> Biodiesel (ACB)	154
3.3.6.2.3	Fuel Properties of <i>Acasia concinna</i> Biodiesel (ACB)	155
3.3.6.3	Optimization Study of Transesterification Operational Factors Through Response Surface Methodology (RSM)	156
3.3.6.4	Parametric characterization of transesterification process	156
3.3.6.4.1	Interactive Impact of Catalyst Amount and Time	156
3.3.6.4.2	Interactive Impact of Catalyst Amount and Temperature	157
3.3.6.4.3	Interactive Impact of Catalyst Amount and Oil: Methanol Ratio	157
3.3.6.4.4	Interactive impact of time and temperature	158
3.3.6.4.5	Interactive Impact of Time and Oil: Methanol Ratio	158
3.3.6.4.6	Interactive impact of oil: methanol ratio and temperature	158
3.3.7	<i>Sapindus trifoliatus</i> Biodiesel (STB)	167
3.3.7.1	Reaction Variables Affecting Transesterification of <i>Sapindus trifoliatus</i> Seeds Oil to ACB	167
3.3.7.1.1	Oil to Methanol Molar Ratio	167
3.3.7.1.2	Catalyst Concentration	167

Table of Contents

3.3.7.1.3	Reaction Temperature	168
3.3.7.2	Chemical Characterization	168
3.3.7.2.1	GC-MS of <i>Sapindus trifoliatus</i> Biodiesel (STB)	168
3.3.7.2.2	FT-IR of <i>Sapindus trifoliatus</i> Biodiesel (ACB)	168
3.3.7.2.3	Fuel Properties of <i>Sapindus trifoliatus</i> Biodiesel (ACB)	169
3.3.7.3	Optimization Study of Transesterification Operational Factors Through Response Surface Methodology (RSM)	170
3.3.7.4	Parametric characterization of transesterification process	170
3.3.7.4.1	Interactive Impact of Catalyst Amount and Time	171
3.3.7.4.2	Interactive Impact of Catalyst Amount and Temperature	171
3.3.7.4.3	Interactive Impact of Catalyst Amount and Oil: Methanol Ratio	171
3.3.7.4.4	Interactive impact of time and temperature	172
3.3.7.4.5	Interactive Impact of Time and Oil: Methanol Ratio	172
3.3.7.4.6	Interactive impact of oil: methanol ratio and temperature	173
3.3.8	<i>Sesamum indicum</i> Biodiesel (SIB)	181
3.3.8.1	Reaction Variables Affecting Transesterification of <i>Sesamum indicum</i> Seeds Oil to SIB	181
3.3.8.1.1	Oil to Methanol Molar Ratio	181
3.3.8.1.2	Catalyst Concentration	181
3.3.8.1.3	Reaction Temperature	182
3.3.8.2	Chemical Characterization	182
3.3.8.2.1	GC-MS of <i>Sesamum indicum</i> Biodiesel (SIB)	182
3.3.8.2.2	FT-IR of <i>Sesamum indicum</i> Biodiesel (SIB)	182
3.3.8.2.3	Fuel Properties of <i>Sesamum indicum</i> Biodiesel (SIB)	183

Table of Contents

3.3.8.3	Optimization Study of Transesterification Operational Factors Through Response Surface Methodology (RSM)	184
3.3.8.4	Parametric characterization of transesterification process	184
3.3.8.4.1	Interactive Impact of Catalyst Amount and Time	185
3.3.8.4.2	Interactive Impact of Catalyst Amount and Temperature	185
3.3.8.4.3	Interactive Impact of Catalyst Amount and Oil: Methanol Ratio	185
3.3.8.4.4	Interactive impact of time and temperature	186
3.3.8.4.5	Interactive Impact of Time and Oil: Methanol Ratio	186
3.3.8.4.6.	Interactive impact of oil: methanol ratio and temperature	187
3.3.9	<i>Ricinus communis</i> Biodiesel (RCB)	196
3.3.9.1	Reaction Variables Affecting Transesterification of <i>Ricinus communis</i> Seeds Oil to RCB	196
3.3.9.1.1	Oil to Methanol Molar Ratio	196
3.3.9.1.2	Catalyst Concentration	196
3.3.9.1.3	Reaction Temperature	197
3.3.9.2	Chemical Characterization	197
3.3.9.2.1	GC-MS of <i>Ricinus communis</i> Biodiesel (RCB)	197
3.3.9.2.2	FT-IR of <i>Ricinus communis</i> Biodiesel (RCB)	197
3.3.9.2.3	Fuel Properties of <i>Ricinus communis</i> Biodiesel (RCB)	198
3.3.9.3	Optimization Study of Transesterification Operational Factors Through Response Surface Methodology (RSM)	199
3.3.9.4	Parametric characterization of transesterification process	199
3.3.9.4.1	Interactive Impact of Catalyst Amount and Time	199
3.3.9.4.2	Interactive Impact of Catalyst Amount and Temperature	200

Table of Contents

3.3.9.4.3	Interactive Impact of Catalyst Amount and Oil: Methanol Ratio	200
3.3.9.4.4	Interactive impact of time and temperature	201
3.3.9.4.5	Interactive Impact of Time and Oil: Methanol Ratio	201
3.3.9.4.6	Interactive impact of oil: methanol ratio and temperature	202
3.3.10	<i>Celastrus paniculatus</i> Biodiesel (CPB)	210
3.3.10.1	Reaction Variables Affecting Transesterification of <i>Celastrus paniculatus</i> Seeds Oil to RCB	210
3.3.10.1.1	Oil to Methanol Molar Ratio	210
3.3.10.1.2	Catalyst Concentration	210
3.3.10.1.3	Reaction Temperature	211
3.3.10.2	Chemical Characterization	211
3.3.10.2.1	GC-MS of <i>Celastrus paniculatus</i> Biodiesel RCB	211
3.3.10.2.2	FT-IR of <i>Celastrus paniculatus</i> Biodiesel RCB	211
3.3.10.2.3	Fuel properties of <i>Celastrus paniculatus</i> Biodiesel (CPB)	212
3.3.10.3	Optimization Study of Transesterification Operational Factors Through Response Surface Methodology (RSM)	213
3.3.10.4	Parametric characterization of transesterification process	213
3.3.10.4.1	Interactive Impact of Catalyst Amount and Time	214
3.3.10.4.2	Interactive Impact of Catalyst Amount and Temperature	214
3.3.10.4.3	Interactive Impact of Catalyst Amount and Oil: Methanol Ratio	214
3.3.10.4.4	Interactive impact of time and temperature	215
3.3.10.4.5	Interactive Impact of Time and Oil: Methanol Ratio	215
3.3.10.4.6	Interactive impact of oil: methanol ratio and temperature	216

Table of Contents

Section IV: Comparison of Catalytic Efficiency of Catalysts		223
3.4.1	Catalytic Efficiency of Al-Mmt Clay Catalyst	224
3.4.1.1	Reusability of Al-Mmt Clay Catalyst	224
3.4.2	Catalytic Efficiency of Na-Ag-Mmt Clay Catalyst	225
3.4.2.1	Reusability of Na-Ag-Mmt Clay Catalyst	225
3.4.3	Catalytic Efficiency of Cu-Mg-Zn-Mmt Clay Catalyst	225
3.4.3.1	Reusability of Cu-Mg-Zn-Mmt Clay Catalyst	225
4	Concluding Remarks and Recommendations	230
REFERENCES		236
PUBLICATION		

List of Tables

<i>Table No</i>	<i>Title</i>	<i>Page No</i>
3.1	Micro morphological characteristics of oil yielding seeds determined via LM and SEM.	59-61
3.3.1	Characteristics of oil yielding seeds	77-78
3.3.1.1	Optimized Conditions for BOB Synthesis Using Na-Mmt, Na-Ag-Mmt, Cu-Mg-Zn-Mmt Clay Catalysts	91
3.3.1.2.1	Identified Esters in <i>Brassica oleracea</i> L. Derived Biodiesel (BOB) Using GC-MS	91
3.3.1.2.2	FT-IR Spectrum of <i>Brassica oleracea</i> L. Obtained biodiesel	92
3.3.1.2.3	Fuel Properties of <i>Brassica oleracea</i> L. Derived Biodiesel	92
3.3.1.4	Experimental and Pridicted yield of <i>Brassica oleracea</i> L. Biodiesel (BOB) using Box-Behnken Design	93
3.3.1.4.1	Analysis of Variance (ANOVA) from Achieved Results	94
3.3.2	Optimized Conditions for COB Synthesis Using Na-Mmt, Na-Ag-Mmt, Cu-Mg-Zn-Mmt Clay Catalysts	105
3.3.2.2.1	Identified Esters in <i>Carthamus oxycantha</i> Biodiesel (COB) Using GC-MS	105
3.3.2.2.2	FT-IR Spectrum of <i>Carthamus oxycantha</i> Obtained biodiesel (COB)	106
3.3.2.2.3	Fuel Properties of <i>Carthamus oxycantha</i> Biodiesel (COB)	106
3.3.2.4	Experimental and Pridicted yield of <i>Carthamus oxycantha</i> Biodiesel (COB) using Box-Behnken Design	107
3.3.2.4.1	Analysis of Variance (ANOVA) from Achieved Results	108
3.3.3	Optimized Conditions for CTB Synthesis Using Na-Mmt, Na-Ag-Mmt, Cu-Mg-Zn-Mmt Clay Catalysts	119
3.3.3.2.1	Identified Esters in <i>Carthamus tinctorius</i> Biodiesel (CTB) Using GC-MS	119
3.3.3.2.2	FT-IR Spectrum of <i>Carthamus tinctorius</i> Obtained biodiesel (CTB)	120

3.3.3.2.3	Fuel Properties of <i>Carthamus tinctorius</i> Biodiesel (CTB)	121
3.3.3.4	Experimental and Pridicted yield of <i>Carthamus tinctorius</i> Biodiesel (CTB) using Box-Behnken Design	122
3.3.3.4.1	Analysis of Variance (ANOVA) from Achieved Results	123
3.3.4	Optimized Conditions for CLB Synthesis Using Na-Mmt, Na-Ag-Mmt, Cu-Mg-Zn-Mmt Clay Catalysts	134
3.3.4.2.1	Identified Esters in <i>Carthamus lanatus</i> Biodiesel (CLB) Using GC-MS	134
3.3.4.2.2	FT-IR Spectrum of <i>Carthamus lanatus</i> Biodiesel (CLB)	135
3.3.4.2.3	Fuel Properties of <i>Carthamus lanatus</i> Biodiesel (CLB)	135
3.3.4.4	Experimental and Pridicted yield of <i>Carthamus lanatus</i> Biodiesel (CLB) using Box-Behnken Design	136
3.3.4.4.1	Analysis of Variance (ANOVA) from Achieved Results	137
3.3.5	Optimized Conditions for BGB Synthesis Using Na-Mmt, Na-Ag-Mmt, Cu-Mg-Zn-Mmt Clay Catalysts	148
3.3.5.2.1	Identified Chemical Compounds in. <i>Beaumontia grandiflora</i> Wall Biodiesel (BGB) Using GC-MS	148
3.3.5.2.2	FT-IR of <i>Beaumontia grandiflora</i> Wall (BGB) biodiesel	149
3.3.5.2.3	Fuel Properties of <i>Beaumontia grandiflora</i> Wall Biodiesel (BGB)	149
3.3.5.4	Experimental and Pridicted yield of <i>Beaumontia grandiflora</i> Wall Biodiesel (BGB) using Box-Behnken Design	150
3.3.5.4.1	Analysis of Variance (ANOVA) from Achieved Results	151
3.3.6	Optimized Conditions for ACB Synthesis Using Na-Mmt, Na-Ag-Mmt, Cu-Mg-Zn-Mmt Clay Catalysts	162
3.3.6.2.1	Identified Esters in. <i>Acasia concinna</i> Biodiesel (ACB) Using GC-MS	162
3.3.6.2.2	FT-IR of <i>Acasia concinna</i> Biodiesel (ACB)	163
3.3.6.2.3	Fuel Properties of <i>Acasia concinna</i> Biodiesel (ACB)	163
3.3.6.4	Experimental and Pridicted yield of <i>Acasia concinna</i> Biodiesel (ACB) using Box-Behnken Design	164
3.3.6.4.1	Analysis of Variance (ANOVA) from Achieved Results	165

3.3.7	Optimized Conditions for STB Synthesis Using Na-Mmt, Na-Ag-Mmt, Cu-Mg-Zn-Mmt Clay Catalysts	176
3.3.7.2.1	Identified Esters in. <i>Sapindus trifoliatius</i> Biodiesel (STB) Using GC-MS	176
3.3.7.2.2	FT-IR of <i>Sapindus trifoliatius</i> Biodiesel (STB)	176
3.3.7.2.3	Fuel Properties of <i>Sapindus trifoliatius</i> Biodiesel (STB)	177
3.3.7.4	Experimental and Pridicted yield of <i>Brassica oleracea</i> L. Biodiesel (BOB) using Box-Behnken Design	178
3.3.7.4.1	Analysis of Variance (ANOVA) from Achieved Results	179
3.3.8	Optimized Conditions for SIB Synthesis Using Na-Mmt, Na-Ag-Mmt, Cu-Mg-Zn-Mmt Clay Catalysts	190
3.3.8.2.1	Identified Esters in. <i>Sesamum indicum</i> Biodiesel (SIB) Using GC-MS	190
3.3.8.2.2	FT-IR of <i>Sesamum indicum</i> Biodiesel (SIB)	191
3.3.8.2.3	Fuel Properties of <i>Sesamum indicum</i> Biodiesel (SIB)	192
3.3.8.4	Experimental and Pridicted yield of <i>Sesamum indicum</i> Biodiesel (SIB) using Box-Behnken Design	193
3.3.8.4.1	Analysis of Variance (ANOVA) from Achieved Results	194
3.3.9	Optimized Conditions for RCB Synthesis Using Na-Mmt, Na-Ag-Mmt, Cu-Mg-Zn-Mmt Clay Catalysts	205
3.3.9.2.1	Identified Esters in. <i>Ricinus communis</i> Biodiesel (RCB) Using GC-MS	205
3.3.9.2.2	FT-IR of <i>Ricinus communis</i> Biodiesel (RCB)	206
3.3.9.2.3	Fuel Properties of <i>Ricinus communis</i> Biodiesel (RCB)	206
3.3.9.4	Experimental and Pridicted yield of <i>Ricinus communis</i> Biodiesel (RCB) using Box-Behnken Design	207
3.3.9.4.1	Analysis of Variance (ANOVA) from Achieved Results	208
3.3.10	Optimized Conditions for CPS Synthesis Using Na-Mmt, Na-Ag-Mmt, Cu-Mg-Zn-Mmt Clay Catalysts	219
3.3.10.2.1	Identified Esters in. <i>Celastrus paniculatus</i> Biodiesel (CPB) Using GC-MS	219
3.3.10.2.2	FT-IR of <i>Celastrus paniculatus</i> Biodiesel (CPB)	220
3.3.10.2.3	Fuel Properties of <i>Celastrus paniculatus</i> Biodiesel (CPB)	220

3.3.10.4	Experimental and Predicted yield of <i>Celastrus paniculatus</i> Biodiesel (BOB) using Box-Behnken Design	221
3.3.10.4.1	Analysis of Variance (ANOVA) from Achieved Results	222
3.4	Best Catalytic Yield against Selected Feed Stock	229
4	Comparative Key Findings of the Study	232-233

Flow Chart

<i>Flow Chart No</i>	<i>Title</i>	<i>Page No</i>
1	Steps Involved in Synthesis and Charaterization of Biodiesel	36

List of Plates

<i>Plate No</i>	<i>Title</i>	<i>Page No</i>
1	(a) <i>Brassica oleraceae</i> L. Plant, (b) Seeds, (c, d) SEM of Seeds and Sculpturing	40
2	(a) <i>Carthamus oxyacantha</i> M.Bieb. (b) Plant, Seeds, (c, d) SEM of Seeds and Sculpturing	42
3	(a) <i>Carthamus tinctorius</i> L. Plant, (b) Seeds, (c, d) SEM of Seeds and Sculpturing	44
4	(a) <i>Beaumontia grandiflora</i> Wall Plant, (b) Seeds, (c, d) SEM of Seed surface and wing	46
5	(a) <i>Celastrus paniculatus</i> Willd. Plant, (b) Seeds, (c, d) SEM of Seed surface and sculpturing	48
6	(a) <i>Carthamus lanatus</i> L. Plant, (b) Seeds, (c, d) SEM of Seed surface and sculpturing	50
7	(a) <i>Acacia concinna</i> (Willd.) DC. Plant, (b) Seeds, (c, d) SEM of Seed surface and sculpturing	52
8	(a) <i>Sapindus trifoliatus</i> L. (b) Plant, Seeds, (c, d) SEM of Seed surface and sculpturing	54
9	(a) <i>Sesamum indicum</i> L. Plant, (b) Seeds, (c, d) SEM of Seed surface and sculpturing	56
10	(a) <i>Ricinus communis</i> L. Plant, (b) Seeds, (c, d) SEM of Seed surface and sculpturing	57

List of Figures

<i>Figure No</i>	<i>Title</i>	<i>Page No</i>
2.1	Experimental Strategy of the Work Done	23
3.2.1.1	Scanning Electron Micrograph of Raw Mmt Clay (A), Scanning Electron Micrograph of Calcined Mmt Clay (B), Electron Micrograph of Al-Mmt Clay Catalyst (C, D)	65
3.2.1.2	Energy Dispersive X-ray Spectroscopy of Al-Mmt Clay Catalyst	65
3.2.1.3	FT-IR Spectra of Al-Mmt Clay Catalyst (500°C)	66
3.2.1.4	XRD Pattern of Al-Mmt Clay Catalyst	66
3.2.2.1	Scanning Electron Micrograph of Raw Mmt Clay (A), Scanning Electron Micrograph of Calcined Mmt Clay (B), Scanning Electron Micrograph of Na-Ag-Mmt Clay Catalyst (C, D)	69
3.2.2.2	Energy Dispersive X-ray Spectroscopy of Na-Ag-Mmt Clay Catalyst	69
3.2.2.3	FT-IR Spectra of Na-Ag-Mmt Clay Catalyst (500°C)	70
3.2.2.4	XRD Pattern of Na-Ag-Mmt Clay Catalyst	70
3.2.3.1	Scanning Electron Micrograph of Raw Mmt Clay (A), Scanning Electron Micrograph of Calcined Mmt Clay (B), Scanning Electron Micrograph of Electron Micrograph of Cu-Mg-Zn-Mmt Clay Catalyst (C, D)	73
3.2.3.2	Energy Dispersive X-ray Spectroscopy of Cu-Mg-Zn-Mmt Clay Catalyst.	73
3.2.3.3	FT-IR Spectra of Cu-Mg-Zn-Mmt Clay Catalyst (500°C)	74
3.3.1.2.1	GCMS of <i>Brassica oleracea</i> L Biodiesel (BOB)	89
3.3.1.2.2	FTIR Spectrum of <i>Brassica oleracea</i> L. biodiesel	89
3.3.1.4	3D surface Plots showing the impact of different parameters on <i>Brassica oleracea</i> L. biodiesel (BOB) yield	90
3.3.2.2.1	GCMS <i>Carthamus oxycantha</i> Biodiesel (COB)	103
3.3.2.2.2	FTIR Spectrum of <i>Carthamus oxycantha</i> Biodiesel (COB)	103
3.3.2.4	3D surface Plots showing the impact of different parameters on <i>Carthamus oxycantha</i> biodiesel (COB) yield	104

3.3.3.2.1	GCMS of <i>Carthamus tinctorius</i> Biodiesel (CTB)	117
3.3.3.2.2	FTIR Spectrum of <i>Carthamus tinctorius</i> Biodiesel (COB)	117
3.3.2.4	surface Plots showing the impact of different parameters on <i>Carthamus tinctorius</i> biodiesel (CTB) yield.	118
3.3.4.2.1	GC-MS of <i>Carthamus lanatus</i> Biodiesel (CLB)	132
3.3.4.2.2	FT-IR of <i>Carthamus lanatus</i> Biodiesel (CLB)	132
3.3.4.4	3D surface Plots showing the impact of different parameters on <i>Carthamus lanatus</i> biodiesel (CLB) yield	133
3.3.5.2.1	GC-MS of <i>Beaumontia grandiflora</i> Wall Biodiesel (BGB)	146
3.3.5.2.2	FT-IR of <i>Beaumontia grandiflora</i> Wall Biodiesel (BGB)	146
3.3.5.4	3D surface Plots showing the impact of different parameters on <i>Beaumontia grandiflora</i> Wall biodiesel (BGB) yield	147
3.3.6.2.1	GC-MS of <i>Acasia concinna</i> Biodiesel (ACB)	160
3.3.6.2.2	FT-IR of <i>Acasia concinna</i> Biodiesel (ACB)	160
3.3.6.4	3D surface Plots showing the impact of different parameters on <i>Acasia concinna</i> biodiesel (ACB) yield	161
3.3.7.2.1	GC-MS of <i>Sapindus trifoliatus</i> Biodiesel (STB)	174
3.3.7.2.2	FT-IR of <i>Sapindus trifoliatus</i> Biodiesel (STB)	174
3.3.7.4	3D surface Plots showing the impact of different parameters on <i>Sapindus trifoliatus</i> biodiesel (STB) yield	175
3.3.8.2.1	GC-MS of <i>Sesamum indicum</i> Biodiesel (SIB)	188
3.3.8.2.2	FT-IR of <i>Sesamum indicum</i> Biodiesel (SIB)	188
3.38.4	3D surface Plots showing the impact of different parameters on <i>Sesamum indicum</i> biodiesel (SIB) yield	189
3.3.9.2.1	GC-MS Spectrum of <i>Ricinus communis</i> Biodiesel (RCB)	203
3.3.9.1.2	FT-IR of <i>Ricinus communis</i> Biodiesel (RCB)	203
3.3.9.4	3D surface Plots showing the impact of different parameters on <i>Ricinus communis</i> biodiesel (RCB) yield	204
3.3.10.2.1	GC-MS of <i>Celastrus paniculatus</i> Biodiesel (CPB)	217
3.3.10.2.2	FT-IR of <i>Celastrus paniculatus</i> Biodiesel (CPB)	217

3.3.10.4	3D surface Plots showing the impact of different parameters on <i>Celastrus paniculatus</i> biodiesel (CPB) yield	218
3.4	Comparison of Catalytic Efficiencies of Catalysts, Al-Mmt, Na-Ag-Mmt & Cu-Mg-Zn-Mmt (from Left to Right Respectively), Time and Their Reusability	227
3.4.1.1	Reusability of Al-Mmt Catalyst in Transesterification Reaction	227
3.4.2.1	Reusability of Na-Ag-Mmt Catalyst in Transesterification Reaction	228
3.4.3.1	Reusability of Cu-Mg-Zn-Mmt Catalyst in Transesterification Reaction	228

ACKNOWLEDGMENTS

All praises belong to ALLAH, the Almighty, the most merciful, the most kind, the creator, the light of the heavens and the earth and the source of all knowledge and wisdom, who enabled me to complete this great task successfully. I also offer my countless salutations to the Messenger of Allah, Muhammad (SAW), who Enlightened the humanity with knowledge and gave a direction to astrayed mankind.

Though only my name appears on the cover of this dissertation, a great many people have contributed to its production. I owe my gratitude to all those people who have made this dissertation possible and because of whom my research experience has been one that I will cherish forever.

*I felt highly privileged in taking opportunity to express my deep gratitude to my respectable supervisor **Professor Dr. Mushtaq Ahmad, Head of the department, Department of Plant Sciences** for his guidance, kind behavior and suggestions during the entire research work that have made it possible for me to complete this manuscript. I must say that he is an asset of our department and I have been fortunate enough to have a mentor like him.*

*I am extremely grateful to **Dr. Muhammad Zafar**, Associate Professor, Department of Plant Sciences, Quaid-i-Azam University, Islamabad, for his keen interest, encouragement, immense help, valuable guidance, constructive criticism, and guidance to enhance my research work, and future capabilities.*

*I take this opportunity to record my sincere thanks to **Dr. Mir Ajab Khan**, Ex Dean, FBS, for his unceasing encouragement and moral support. I place on record my sincere gratitude to **Dr. Shazia Sultana** for her moral encouragement.*

*I am very grateful to my lab fellows, respected seniors, and juniors, especially **Ayesha**, who helped me in various ways during my research. I also felt my gratitude and thanks to **Muhammad Sufyan**, and **Farooq Ahmad** who cooperated with me within this time.*

*Words always seem to shallow whenever it comes to my dearest parents nothing would have been possible without their love, support, encouragement, and prayers. This journey would not have been possible if not for them. I am truly blessed to have loving siblings (**Yasir, Sehar** and **Hafsa**), and beautiful sister-in-law **Saqiba**. I feel lucky to*

have a brother like you *Bhia!* Thank you for being my rock when I needed it the most and for supporting me for every decision that I made. We know that we can always count on each other. *Sehar!* you know I love you and you mean the world to me. Thank you for lending an ear when nobody else would, and for the bond we share. *Hafsa,* you know that you are my mirror image-same yet opposite! Thank you for the friendship that we share, for the hang outs, sweet, crazy conversations full of half sentences, daydreams, and misunderstandings more thrilling than understanding could ever be. *Saqiba,* even though we live miles apart, you will always be dear to my heart. Thank you for not just been the best sister-in-law, but also a sincere friend.

At last, I would like to acknowledge my best friends *Rimsha Baig, Rubab Nasir and Rutaba Gull* for their unconditional love and support. I will always cherish this friendship. There is no one like you girls and I am fortunate to have you as friends.

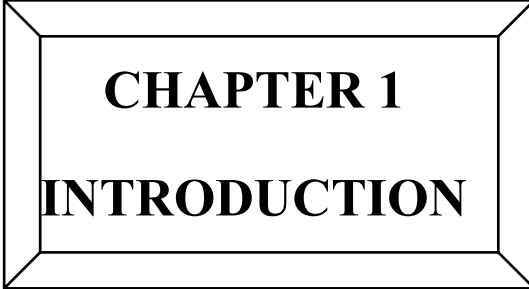
Finally, I would like to thank everybody who was important in the successful completion of this thesis, and I truly apologize that I was not able to mention everyone personally.

Saman Ilyas Cheema

ABSTRACT

This study is confined to identification of ten novel non-edible oil seeds as feedstock for biodiesel- a sustainable alternate of petro diesel. Ten non-edible seeds oils have been studied systematically comprising; collection, morphological identification and SEM studies, estimation analysis of total oil content of seeds, mechanical oil extraction, transesterification of seeds oil to biodiesel, optimization and physico-chemical characterization of synthesized biodiesel and its comparison with international standards. Plants selected as a feed stock in the study include; *Brassica oleracea* L., *Carthamus lanatus* L., *Carthamus tinctorius* L., *Carthamus oxycantha* M.Bieb., *Beaumontia grandiflora* (Roxb.) Wall., *Acacia concinna* (Willd.) DC., *Sapindus trifoliatus* L., *Sesamum indicum* L., *Ricinus communis* L. and *Celastrus paniculatus* Willd. Three different (single, double and triple metal) Montmorillonite clay-metal composites were synthesized through in-situ wet impregnation method. Sustainability of catalysts was also determined. Synthesized biodiesel was synthesized using analytical techniques like GC-MS and FT-IR.

Free fatty acid value estimation revealed that all the selected seeds oils have less than 3 % of FFA content. Thus, require one step transesterification for conversion into biodiesel. Optimization of biodiesel yield was achieved through reaction variables (alcohol:oil, catalyst conc., temperature) for transesterification. Highest biodiesel yield (95%) was reported for *Carthamus tinctorius* L. using Al-Mmt clay catalyst (1:7 of oil to methanol, 0.2 g of catalyst at 100°C for 5 hours) followed by *Sesamum indicum* L. (93%) using Cu-Mg-Zn-Mmt (1:3 of oil to methanol, 0.2 g of catalyst at 90°C for 3 hours). However, the lowest yield was obtained for *Ricinus communis* L. (85%) with Na-Ag-Mmt (1:3 of oil to methanol, 3 g of catalyst at 110°C for 6 hours). It is stated that the synthesized clay-metal hybrid catalysts have promising catalytic efficiency and sustainability. Three of the seeds oils i.e. *Brassica oleracea* L., *Carthamus lanatus* and *Beaumontia grandiflora* (Roxb.) Wall. were reported as Novel feedstocks used in this study for biodiesel synthesis. Catalytic efficiency and cost effectiveness of the clay hybrid nanocatalysts makes them a better substitute of other available counterparts. Economical feasibility of the feedstocks is positive and can be used for commercial level biodiesel production. The study further recommends the mass cultivation of non-edible feedstock as a feedstock crops for biodiesel production.



CHAPTER 1
INTRODUCTION

1.1 Biodiesel: A Sustainable Energy Resource

Biodiesel is not only renewable but also an environment friendly alternative to the existing fuel resource i.e. fossil fuel based petro-diesel which not only is squeezing fast but is also the leading cause of environmental pollution (Ullah et al., 2018). Thus, a dire need to find the alternate to the traditional energy resource brings Biodiesel to the spotlight in the scientific community which is greener and pollution free substitute of the fossil fuel derived diesel.

The seed oil or animal fat derived long chain fatty acids are converted into mono-alkyl esters with or without the help of catalyst to obtain what is called biodiesel. It is eco-friendly, biodegradable, carbon neutral, readily available, non-flammable, non-explosive and of non-toxic nature (Atabani et al., 2013). The conversion of fatty acids to mono-alkyl esters is carried out through different processes including micro emulsion, thermal cracking/pyrolysis and transesterification (Yusuf et al., 2011). But transesterification is the most popular, simple, cost effective favorable method of biodiesel production among the other methods. It is the process in which one molecule of triglyceride reacts with alcohol in a reversible manner yielding three molecules of ester and one molecule of glycerol in the presence or absence of catalyst. In stoichiometric terms three molecules of alcohol are required to convert one molecule of fatty acid to ester but actually more alcohol is used to derive the reaction in forward direction. And glycerol which is the byproduct of this reaction, also has numerous applications in the chemical and pharmaceutical industry (Ramadhas et al., 2005).

The popularity of the biodiesel mostly comes from the fact that it is environment friendly which can be explained by the fact that it has very low or no aromatic compounds and sulfur contents, leading cause of environmental pollution, and 10-11% oxygen by weight. Another important aspect of biodiesel is that it has higher cetane number which is associated with the ignition quality; higher the cetane number, higher the fuel quality. Biodiesel can be used as pure fuel or as a blend with the petroleum in different proportions i.e. B2 having 2% biodiesel and 98% petroleum diesel, B5 with 5% biodiesel and 95% petroleum diesel and B20 which contains 20% biodiesel fraction and 80% petroleum diesel. These low fraction biodiesel blends do

not require any engine modification but higher blends i.e. B100 (pure biodiesel) may require little modifications of engine (Balat & Balat, 2010).

According to an estimate, the world energy demand will rise at the pace of 1.7%/year and this will reach 16.5 billion tons of oil by the end of year 2030 and the amount of available fossil fuel reserves are limited (Khan & Pervaiz, 2013). Global climate change, hike in fossil fuels based petro-diesel and growing gap in demand and supply of non-renewable energy resources has made sustainable or renewable resources an attractive alternate candidate to compensate the world's energy demands (Nematollahi et al., 2016). And biodiesel industry is growing at a fast pace, with an annual increase of 7.3% and will be a total worth of 54.8 billion USD industry by the year 2025 (Sekoai et al., 2019). Many countries like Indonesia, China, Brazil, USA, France, Malaysia, Germany, Italy and other European countries are considering biodiesel to satisfy their demands of energy. Therefore, biodiesel could be one of the sustainable energy resources to cope with the global concerns of environmental pollution and to fill the growing demand and supply gap of fossil fuel derived petro-diesel and its consumption.

1.2 FeedStocks for Biodiesel Production

Fossil fuels i.e. petroleum, coal and natural gas contribute the major fraction of the world energy reservoirs but are facing stress due to imbalance of demand and supply. This has paved way to alternate energy resources; renewable energy resources, which offer a clean, nature friendly, cheap and yet reliable source of energy (Gui et al., 2008). One of the most attractive attributes of biodiesel is the wide range of feed stocks for its production unlike fossil fuels. Feed stock should fulfill two chief requirements: cheap and abundant. As seventy five percent of the overall production cost of biodiesel is due to feed stock. Thus, selection of feed stock to start the process of biodiesel production is first and crucial step. Overall, there are four types of feed stocks for biodiesel synthesis as mentioned below (Atabani et al., 2012).

1. Edible vegetable oils: rapeseed oil, sunflower oil, peanut oil etc.
2. Non-edible vegetable oils: jatropha, sea mango, algae, halophytes etc.
3. Waste or used oils
4. Animal fats: tallow, chicken fats etc.

Feed stock divides biodiesel into three generations; first generation biofuels, second generation biofuels and third generation biofuels (Enamala et al., 2018). Biodiesel produced from edible plant oils is categorized under first-generation biofuels. Major fraction of feed stocks for biodiesel production comes from edible plant oils for example 84% of biodiesel is produced from rapeseed oil, 13% from sunflower oil, 1% from palm oil and 2% from soy and other sources. The fact that presently about ninety-five percent of biodiesel is obtained from edible sources is gathering a global concern that it is no more like biofuels replacing fossil fuels rather its food versus fuel contest. Exploitation of edible resources for fuel production may cause an imbalance in food supply-demand ratio. And huge proportion of agricultural land is now being utilized for growing crops for fuel production otherwise used to grow crops to meet the food demands of the world. Another argument that is adding fuel to the matter is that cultivation of crops on large scale for fuel purposes is resulting in deforestation as observed in Indonesia, Malaysia and Brazil. One percent of world's total agricultural land was documented to be used for crop production for biodiesel in 2006. Given that biofuel has only 1 % share in world's fuel transportation, increasing the proportion of biodiesel will simply result in occupying the whole portion of world's arable land (Gui et al., 2008, Ajanovic, 2011).

Edible seeds oil use for diesel production may cause the shortage in the supply of edible oil globally. So, the world is moving towards another greener alternate of fossil fuels i.e. non-edible oil resources for biodiesel production (Gui et al., 2008). Biodiesel produced from non-edible plants oil is placed under second generation biofuels. Besides not being threat to the food market, popularity of non-edible oil crops also comes from the fact that they grow on marginal land and require less maintenance and water. Edible sources of biodiesel are also criticized for not being cost effective which, alongside catalyst cost and land management, is an important factor. On contrary non-edible sources are cheaper than their counter parts and would reduce the demand of edible ones (Bhuiya et al., 2016). According to an estimate about 17% of total grain production is used for biodiesel production (Asif et al., 2017). Some of the major non-edible sources of biodiesel, which are used globally, are: *Jatropha curcas*, *Pongamia pinnata* or *Pongamia glabra*, *Aleurites moluccana*, *Pachira glabra*, *Calophyllum inophyllum*, *Hevea brasiliensis*, *Balanites aegyptiaca*, *Croton megalocarpus*, *Cerbera odollam*, *Terminalia belerica*, *Azadirachta indica*, *Madhuca*

indica, *Madhuca longifolia*, *Nicotiana tabacum*, *Sapindus mukorossi*, *Sterculia feotida*, *Sapium sebiferum* Roxb, *Ceiba pentandra*, *Simmondsia chinensis*, *Euphorbia tirucalli*, Rice bran, Babassu tree and micro-algae (Bhuiya et al., 2016).

Animal fats, grease and waste oils were also regarded as second-generation feed stock. Although such feed stocks have their benefits, but problems are also associated with their extensive application (Mardhiah et al., 2017). Fatty acid profile plays a key role in conversion of oil to biodiesel and presence of saturated fatty acids in animal fats is an undesirable character which limits their feasibility for the process of transesterification. Whereas, use of waste cooking oils, WCO, as a feed stock for biodiesel synthesis has its own limitations like collection, transportation and pretreatment (Ullah et al., 2015).

In recent years, a third generation of biofuels has also been emerged in which biodiesel is produced from fungi and micro algae and macro algae (Enamala et al., 2018; Raheem et al., 2018; Ullah et al., 2015). These resemble plant source in a way as they can also harvest sun light into chemical energy i.e. photosynthesis. Micro algae, one of the oldest creatures on earth, can also capture atmospheric carbon dioxide and convert it to oxygen thus, are natural filters which reduce environmental pollution and enhance air quality. Chief qualities of algal biomass are possession of large quantities of lipids, do not require fertile land for growth, higher catalytic efficiency and no or negligible presence of recalcitrant lignin. But, pretreatment of algae is the huge challenge for its use on large scale that uplifts the total production cost of the procedure (Raheem et al., 2018).

1.3 Conventional Energy Resources: A Threat to Global Environment

World energy resources can be categorized into to two broader categories i.e. non-renewable energy resources, fossil fuels, and renewable energy resources, wind energy, solar energy, biofuels. A huge problem associated with the consumption of fossil fuels is the emission of carbon dioxide and other undesirable gases like oxides of nitrogen and sulfur and aromatic compounds which cause environmental pollution (Nematollahi et al., 2016). The global population is estimated to reach nine million by the mid of this millennium, with most part of population residing in the developing and

poor countries of the world. (Asif et al., 2017). Energy and population growth have a direct relation i.e. more population results in more food demand as well as that of energy resources for life sustenance. Fast growing population will result in increased consumption of fossil fuels which not only would cause their depletion but will also harm the already damaged environment by the emission of large amounts of GHGs, greenhouse gasses, thus, adding fuel to the already existing hot issue of global warming (Omer, 2008). According to International Energy Agency report, the world's energy need will increase by 50% rise by the year 2030 and 45% of this fraction will be used by China and India. This growth in demand is directly linked to the increase in vehicles in transport sector. This transportation energy demand is expected to grow at the rate of 1.8% annually from 2005 to 2035. This sector is the second largest energy consumer after industrial sector and almost all the energy demand of this sector is fulfilled by oils derived from fossil fuels (97.6%) (Atabani et al., 2012). It is important to mention that 22% of total GHGs comes from fossil fuels derived oil burning from vehicles. And according to the predictions of International Energy Agency, carbon dioxide emission will increase 92% by the year 2020 and 8.6 billion metric tons of it will be unleashed to the atmosphere from 2020 to 2035 (Conti et al., 2016, Mahmudul et al., 2017).

Globally, climate change and global warming are the most pressing issues of today. Policy makers have consensus that the world temperature rise due to fossil fuels emission should not exceed 2°C above the average global temperature of the pre-industrial times. And any increases in the temperature above the expected degree would result in loss life of approximately one million species including hundreds of millions of people losing life (McKelvey, 1972). And to achieve this target It has been estimated that if the cumulative carbon emissions are limited to 1,100 giga tons of CO₂ (Gt CO₂) between 2011 to 2050 then there would be fifty percent chances of retention of pace of temperature change (average 2°C) throughout the 21st century. But, at present there are approximately three times higher green-house gases constrained in unburnt fossil fuels than this, thus persistent and unchecked use of present reserves of fossil fuels is mismatched with warming limit of 2°C. globally, out of total fossil fuel reserves a third of oil reserves, half of gas reserves and about eighty per cent of existing coal reserves should remain unexploited from 2010 to 2050 to meet the target of 2°C (Meinshausen et al, 2009, Clarke et al, 2014, McGlade & Ekins, 2015).

1.4 Second Generation Biodiesel: as a Sustainable Energy Option

At present 350 oil bearing crops are identified as feed stock for biodiesel production, but feed stock selection is a crucial step as it alone costs 75% of the cost of the whole process of biodiesel production (Lin et al., 2011, Atabani et al., 2012). Currently 14% of global energy demand is fulfilled by renewable energy resources and approximately 10% of this fraction comes from biomass (Chisti, 2007). A significant proportion, 95%, of biodiesel is produced from edible plant oils which has raised concerns about food security. This has started the debate of food vs fuel, according to which use of edible sources for fuel production will ultimately cause price hike and starvation. One such example is found in Malaysia where extensive use of palm oil for biodiesel production has caused its shortage in market and thus, 70% increase in price (Balat, 2011). Thus, recently focus of researchers is shifted towards the exploration of non-edible resources. Main cost of biodiesel production process comes from the price and availability of the feed stocks. Edible plant oils as feed stock are expensive and make the production costly (Chhetri et al, 2008).

An alternate feed stock for biodiesel production is non-edible plant seed oils which neither compete with food chain nor with the arable land and are cost effective (Atabani et al., 2014). Also, there is no issue of availability as they are abundantly present throughout the world (Demirbas, 2009). Non-edible feedstocks are quite promising for the sustainable synthesis of biodiesel. Some examples of non-edible oil seed crops include *Jatropha curcas*, *Calophyllum inophyllum*, *Sterculia feotida*, *Madhuca indica*, *Pongamia glabra*, *Linseed*, *Pongamia pinnata*, *Hevea brasiliensis*, *Azadirachta indica*, *Camelina sativa*, *Lesquerella fendleri*, *Nicotiana tabacum*, *Deccan hemp*, *Ricinus communis* L., *Babassu*, *Simmondsia chinensis*, *Eruca sativa*. L *Cerbera odollam*, *Coriandrum sativum* L., *Croton megalocarpus*, Salmon oil, Pilu, Crambe, syringa, *Scheleichera triguga*, *Stillingia*, *Shorea robusta*, *Terminalia belerica roxb*, *Cuphea*, *Camellia*, *Champaca*, *Simarouba glauca*, *Garcinia indica*, Rice bran, Hingan, Desert date, Cardoon, *Asclepias syriaca*, *Guizotia abyssinica*, Radish Ethiopian mustard, Syagrus, Tung, *Idesia polycarpa* var. *vestita*, Alagae, *Argemone mexicana* L., *Putranjiva roxburghii*, *Sapindus mukorossi*, *M. azedarach*, *Thevetia peruviana*, Copaiba, Milk bush, Laurel, Cumaru, Andiroba, Almond, Piqui, *B. napus*, Tomato seed, *Zanthoxylum bungeanum* etc. (Demirbas, 2009, Sekhar et al., 2009, Singh &

Singh, 2010). Non-edible oil seed plants grow in arid, semi-arid environments and need low fertility and moisture content to grow. Likewise, they are generally propagated through seeds or cuttings. Meanwhile they do not compete with food crops for water, land and food requirements as they grow on marginal land and after oil extraction seed cake may be utilized as compost for soil improvement (Azam et al, 2005). Some of the advantages of non-edible plants as second generation feed stock include: they grow on nonagricultural or barren land, require no care, need no fertilizers, resistant to pest borne diseases, do not compete for food with the edible crops, liquid nature of fuel, useful byproducts i.e. seed cakes after oil extraction can be used as a fertilizer, biodegradability higher heat content and presence of sulfur and aromatic compounds in minor quantities (Atabani et al, 2013). Hence, as a biodiesel feed stock nonedible seeds oils have great potential to overcome the environmental, social and economic problems on broad spectrum.

1.5 Biodiesel Production Techniques

According to available literature plant derived oils because of their higher viscosity cannot be used directly in diesel engine and require modification prior to their application (Jayed et al., 2009, Bhuiya et al., 2016). For conversion of plant oil to biodiesel available techniques include micro-emulsion, pyrolysis/thermal cracking, dilution and transesterification/alcoholysis (Demirbas et al., 2005, Balat, 2011, Silitonga et al., 2011).

1.5.1 Pyrolysis/Thermal cracking

In the process of pyrolysis, organic matters are thermally decomposed in the presence of catalyst and absence of oxygen. Reactants can be fatty acids (FA) or fatty acid methyl esters, plant oils and animal fats. Pyrolysis is widely used by many scientists for biodiesel production. Thermally decomposition of triglycerides disintegrates them into alkanes, alkenes, alkadienes, aromatics and carboxylic acids (Srivastava & Prasad, 2000, Balat & Balat, 2010, Yusuf et al., 2011). The process of pyrolysis is admired for being simple in nature, no undesired products and nature friendly (pollution free). Positive attributes of biodiesel produced via thermal decomposition are higher cetane number, low viscosity, reasonable sulfur, sediments and water content and tolerable copper corrosion values. Whereas, undesirable

biodiesel properties include ash content, carbon deposits and pour point (Sharma et al., 2008, Singh & Singh, 2010).

1.5.2 Dilution

Dilution of does not require any chemical modification rather in this process vegetable oils are diluted by mixing with diesel to reduce their viscosity to enhance engine performance. Pure vegetable oil is not compatible with the diesel engine and requires modifications, but among different blending mixtures its twenty percent blend i.e. 20% vegetable oil and 80% petro diesel is found successful (Balat & Balat, 2010, Parawira, 2010, Yusuf et al., 2011). The option of direct use of vegetable oils is not considered suitable and practical as it (vegetable oil) is neither compatible with direct diesel engine nor indirect diesel engine. Some of the problems associated with its use are; high viscosity, acid composition, free fatty-acid (FFA) content, gum production because of oxidation, polymerization during storage and combustion, carbon residues and condensation of lubrication-oil (Yusuf et al., 2011).

1.5.3 Micro-emulsion

Micro-emulsion is a process of emulsification in which isotropic, translucent and stable (in thermodynamic dimension) dispersions of oil, water, surfactant, usually along with co-surfactant (small amphiphilic molecule) are obtained. In this colloidal equilibrium, dimensions of isotropic microstructure two immiscible liquids range from 1-150nm (Balat & Balat, 2010, Singh & Singh, 2010). The solvents used in this process include methanol, ethanol, butanol, 1-butanol and hexanol. Micro-emulsions of these solvents have the maximum velocity requirement for diesel fuels (Jain & Sharma, 2010, Parawira, 2010).

1.5.4 Transesterification/Alcoholysis

It is the most efficient and simple method of biodiesel production among all other methods. In this process, a triglyceride molecule reacts in a reversible manner with alcohol in the presence or absence of catalyst in a two-step reaction to produce fatty acid alkyl esters (biodiesel) along with glycerol which is the byproduct of this reaction (Sharma & Singh, 2009, Balat & Balat 2010). Stoichiometric ratio of oil and alcohol is 1:3 but actually more alcohol is used to carry the reaction in forward

direction. At commercial level, mostly used alcohols are methanol and ethanol due to their cost effectiveness but other alcohols such as propanol, isopropanol, butanol and other branch chain alcohols can also be used but are costly thus, are not best choice. Both methanol and ethanol also have physical and chemical advantages as they have great dissolving and reacting powers. Glycerol produced as side product also has uses in cosmetic industry (Yusuf et al., 2011).

Usually transesterification reactions are categorized into two classes' i.e. catalyzed transesterification and non-catalyzed transesterification reaction. A catalyst is used to start the reaction as it lowers the activation energy. As alcohol is non soluble or barely soluble in oil/fat this makes role of catalyst very essential. Use of the catalyst increases the solubility of alcohols, accelerating the rate of the reaction. Hence, catalyzed transesterification is the mostly used process of biodiesel production (Karmakar et al., 2010).

1.5.4.1 Catalyzed Transesterification for Biodiesel Production

This process involves the reaction of alcohol (methanol) with oil in the presence of catalyst. Catalyst plays a crucial role as it lowers the activation energy and speeds the reaction rate. It also helps in the mixing process of oil and methanol. Nevertheless, catalysts are of various types/natures and catalyst selection is purely based upon chemical properties of the oil and its FFA content (free fatty acids). Based on the FFA content of the vegetable oil, this reaction can be of single step or two steps (esterification, transesterification). Vegetable oils which have low free fatty acid content (0.5% to >3%), require single step transesterification and basic/alkaline catalysts are used. Whereas, oils with higher FFA levels are converted to biodiesel via two step esterification and transesterification using acidic catalysts. However, based on the solubility in reaction mixture, catalysts are grouped into homogeneous, acid/base, heterogeneous, acid/base, and enzymes.

1.5.4.1.1 Alkali and Acid Catalysts

The mechanism for base-catalyzed transesterification reaction was framed as three steps (Eckey, 1956). In the first step there is an attack on the carbonyl carbon atom of the triglyceride molecule by the anion of the alcohol (methoxide ion) to

procedure a tetrahedral intermediate. In the second step, the tetrahedral intermediate reacts with methanol to regenerate the methoxide ion. In the final step, realignment of the tetrahedral intermediate leads to the production of a fatty acid ester and a diglyceride. The end product is less viscous as compared to the vegetable oil (Pinto et al., 2005). Examples of base or alkaline catalysts include sodium hydroxide (NaOH), potassium hydroxide (KOH), sodium methoxide (NaOCH₃), potassium methoxide (KOCH₃), potassium carbonate (K₂CO₃) etc. however, commercially most used catalysts are NaOH and KOH. Base catalyzed transesterification is said to be the fastest and cost effective of all other catalyzed methods. For instance a base catalyzed reaction proceeds approximately 4000 times faster than the reaction with same amount of acidic catalyst. Thus, reaction time reduces significantly i.e. 30-60 minutes approximately. Furthermore, product obtained has high purity and yield is maximum. These factors make it commercially most used method of biodiesel synthesis. Nevertheless, like all other processes this also has limitations i.e. FFA content of the reactant vegetable oil should be >0.5% to >3%, otherwise desired end product will not be obtained (soap and water are formed). Other drawbacks include; energy intensive, separation of glycerol is difficult from the product, catalyst recovery is difficult, wastewater (alkaline nature) needs treatment and lastly saponification makes the product separation difficult (Sharma & Singh, 2009, Janaun & Ellis, 2010, Shahid & Jamal, 2011).

Exploration for more effective catalyst for biodiesel synthesis through transesterification which are less sensitive to impurities and efficient against low quality feedstocks such as waste cooking oil, has led to the use of acid catalysts as these seem beneficial against such issues. Some inorganic catalysts e.g HCl and H₂SO₄ are also used. Acid catalyzed alcoholysis is a two-step process i.e. acid catalyzed esterification followed by base catalyzed transesterification (Aranda et al., 2008). Transesterification in acidic medium is a relatively slower process than the reaction in basic media. However, for designing of new catalytic processes, a thorough understanding of reaction kinetics and computational modeling would be very effective. Acid catalysts are more tolerant to the feedstocks with high FFA content, free fatty acid level is reduced to desirable limit via esterification using acid catalysts and then process proceeds towards transesterification. Saponification which is a real problem in base catalyzed reaction can be avoided using acid catalyzed transesterification. However, it (acid catalyzed alcoholysis) has its own problems like

slow speed (approximately 3 to 48 hours) of reaction and requires more extreme conditions like high temperature and pressure (pinto et al., 2005, Shahid & Jamal, 2011, Bombarelli et al., 2013, Silva et al., 2015).

1.5.4.1.2 Homogeneous and Heterogeneous Catalysts

Catalysts are also classified on the basis of their physical nature i.e. homogeneous catalysts (liquid in nature) and heterogeneous catalysts (solid in nature). And chemically they are usually either acidic or basic in nature. Homogeneous catalysts are the most used acid/base industrial catalysts for transesterification reaction. Reaction mechanism of both base and acid catalyzed reaction has fundamental difference i.e. alkali catalyzed reaction follows the nucleophilic approach; the nucleophilic alkoxide ion (produced from alcohol) attacks the electrophilic carbonyl group of triglyceride molecule. Whereas in acid catalyzed reaction there is protonation of the carbonyl group making it nucleophile followed by the electrophilic attack by the proton (acid) (Schuchardt et al., 1998, Aransiola et al., 2014). Homogeneous alkali catalyzed transesterification reaction is the most common lab and industrial procedure for biodiesel production. NaOH and KOH are most used base catalysts because of their fast catalysis rate and cost effectiveness. Homogeneous Acid catalyzed alcoholysis is suitable for the vegetable oils which have high level of free fatty acids and involves two steps (Aransiola et al., 2014).

But the hitches of their use include; no reusability of the catalyst as they are in the same phase with the products formed, this makes their recovery impossible, because they cannot be recovered after the completion of reaction this makes their use costly, another problem associated with their use is saponification which makes product separation a difficult process and also decreases product yield and last but not the least water produced during the reaction requires pretreatment before releasing into the sewerage system. All these problems have limited the use of homogeneous catalysts in biodiesel industry (Chouhan & Sarma, 2011).

Heterogeneous catalyst can be defined as a spinal mixed oxide of two metals (should not be Noble metals) (Helwani et al., 2009). Like homogeneous catalysts, heterogenous catalysts are also of acidic and basic nature which makes them suitable for transesterification reaction. Likewise, they show some reaction mechanism

resemblances with that of homogenous catalyzed reaction. Heterogenous catalysts are divided into two classes on the basis of temperature i.e. high temperature and low temperature catalysts (Serio et al., 2008, Endalew et al., 2011). Reusability problems associated with homogeneous can be overcome by the use of heterogeneous catalysts, can be re-used more than a few times e.g. copper doped zinc oxide can be used more than six times, likewise, catalyst reusability can be increased over eight times using K_2CO_3 which is quite remarkable (Gurunathan & Ravi, 2015, Zhao et al., 2018). They are easy to separate from the reaction mixture after reaction completion thus product quality is increased, and production cost is reduced. The process is environment friendly and waste-water production is greatly reduced and does not require any pre-treatment which is a costly procedure thus, lowers the overall reaction cost (Yan et al 2010). Moreover, heterogeneously catalyzed transesterification enhances both the quality (99%) and quantity ($\approx 100\%$) of the product. Purity of the glycerol produced as side product is significantly increased from 80% (homogeneous catalyzed transesterification) to 98% (heterogeneously catalyzed reaction) (Helwani et al., 2009). Manipulation of heterogenous catalyst for desired properties can be done easily according to reaction requirements, thus, free fatty acids or water does not affect the reaction. Heterogeneously catalyzed reaction like homogeneously catalyzed transesterification follows either alkaline or acid catalyzed reaction mechanism (Serio et al., 2008, Endalew et al., 2011). Heterogeneous catalysts usually require high oil to methanol ratio, more catalyst concentration and long reaction time to obtain higher yields of biodiesel. For example, Mn doped ZnO gives yield as high as 97% at the reaction conditions of; oil to methanol ratio is 1:7, catalyst conc. 8% and reaction is carried out at 50°C for fifty minutes (Baskar et al., 2017).

Heterogeneous catalysts due to the presence of multiple acid sites having different strengths of Bronsted/Lewis acidity, are commercially more preferred than the homogeneous ones. Sulfur based heterogeneous catalysts affective catalysts against the transesterification of acidic oils (high FFA content), examples of these low temperature heterogeneous catalysts include sulphated zirconia, zeolites, ion exchange resins and mixed metal oxides. Among these, SO_4^{2-}/ZrO_2 (sulfated zirconia) shows high efficiency in esterification process (Yan et al., 2010). Tungststed-zirconia, WO_3/ZrO_2 (pallet type) successfully converts oil to diesel via transesterification however, it's a lengthy reaction i.e. takes 140 hours, at 75°C and gives sixty five percent biodiesel yield

(Park et al., 2008). Other examples of low temperature heterogeneous catalysts include heteropoly acids (HPAs). It gives approximately 99% biodiesel yield in short time span (45 minutes) and temperature (55°C) (Narasimharao et al., 2007). Heteropoly acids as catalyst ($\text{Cs}_{2.5}\text{H}_{0.5}\text{PW}_{12}\text{O}_{40}$) gives maximum yield of 96.22% using optimum reaction conditions and recovered catalyst can be used up to 9 times (Zhang et al., 2010). Lewis acid catalyst (zirconocene perfluorooctanesulphonate) is stable in air and also shows resistance to water. This catalyst can be used in both esterification and transesterification and recovery of the catalyst at the end of reaction is very easy as during the reaction, it changes from homogeneous to heterogeneous form (white solid precipitate) (Deng et al., 2018).

High temperature heterogeneous acid catalysts like low temperature ones also include some sulfated acids and HPAs (heteropoly acids). These are also broadly studied in literature. Tungstated zirconia-alumina, Solid super acid catalyst, is an efficient catalyst and shows high catalytic power during the transesterification of soybean oil to biodiesel (90%), following two step esterification and transesterification process (Furuta et al., 2004).

Heterogeneous base catalysts offer important advantages over acidic catalysts. Heterogeneous alkali catalyzed process allows easy product formation and purification methods. Other advantages include; less wastewater (alkaline) formation and less reaction equipment requirement thus, reduction of process cost and decrease in negative impact on environment (Zhang et al., 2010). At the same reaction conditions, both homogeneous base catalyst and solid base catalyst show same properties except that of catalyst recovery, which is easy in case of heterogeneous catalysts e.g. sodium/sodium hydroxide/aluminium oxide (heterogeneous catalysts) show resemblance to homogeneous sodium hydroxide at same operating conditions (Kim et al., 2004). However, unlike homogeneous ones, they are sensitive to the water and free fatty acid content of feedstock so, can't be used against feedstocks with higher acid values (Lee & Saka, 2010). Another problem associated with their use is leaching of base catalysts and can be overcome by using alkaline earth metal oxides as catalysts (Yan et al., 2010). Other examples of heterogeneous base catalysts include; $\text{K}_2\text{CO}_3/\text{Al}_2\text{O}_3$, MgO , CaO , SrO , $\text{KF}/\text{Al}_2\text{O}_3$, KF/ZnO , ion exchange resins, base zeolites, Mg/Al , Li/Al (Wan et al., 2009, Gama et al., 2010, Vyas et al., 2010, Gama et al., 2015). These catalysts flake

like crystal morphology containing strong basic sites and give high biodiesel yield (>92%) at optimal conditions (Navajas et al., 2018). CaO is often preferred due to its nature friendly constituents which enable its long life, high catalytic efficiency at mild reaction conditions (Borges & Díaz, 2012). Usually, $\text{Ca}(\text{NO}_3)_2$ and $\text{Ca}(\text{OH})_2$ are the precursors for calcium oxide production. However, it also has rich raw materials in nature like; Ca rich waste materials (eggshells of chicken, shells of mollusks, bones) thus, deals with waste disposal problems and is cheap as well. Use of calcium oxide nano-catalyst has higher conversion efficiency (yield), i.e. 93% of jatropha oil (Huaping et al., 2006). Calcium oxide shows effectiveness in biodiesel formation but percolation of calcium ions which lowered the produced biodiesel quality. The leaked calcium ions react with free fatty acids present in oil and causes saponification and disable the catalyst. This problem can be solved using appropriate support materials. One more drawback of its use is the requirement of thermal energy for activation of catalyst for removal of CO_2 and moisture content (Kouzu et al., 2009, Borges & Díaz, 2012).

1.5.4.1.3 Biocatalysts

Lipase catalysts show tolerance for high FFA content (free fatty acid content) of the biodiesel feedstock. They act more efficiently on long chain fatty acids than on short chain fatty acids. Thus, transesterification carried via ethanol is more effective than that of which is carried through methanol. Likewise, product separation from glycerol and separation of soap and catalyst are relatively simple procedures. But, conversion efficiency of oils to biodiesel (reaction yield) and time of reaction are disapproving than base catalyzed reactions. Furthermore, lipases are not cost effective and can't be implemented on industrial scale biodiesel production. They fail to offer the ASTM standard fuel specifications for degree of reaction completion. However, utilization of lipases which are tolerant towards solvent, immobilized lipases and other multiple enzymes can be economical alternative (Shahid & Jamal, 2011). Typically, acid/base catalyzed reactions are considered more favorite than enzyme catalyzed ones (Atabani et al., 2012).

1.5.4.1.4 Waste Materials as Catalysts

Lately, waste materials have also been effectively benefited as catalysts. And cheap waste materials have shown potential to catalyze the transesterification

reaction for biodiesel production. Mostly used mineral wastes include; Cement waste (basic nature because of mineral matrix), calcite, sodium/calcium aluminosilicates, albite and portlandite (Kumar et al., 2018). Calcium carbonate catalyst gives 93% yield of FAMES in alcoholysis. It can be formed through the calcination (900°C) of eggshell (Farooq et al., 2018). Other examples of such catalysts include; catalysts derived from organic waste (plantain peels, coconut shells, woods etc.), K₂O Na₂O catalysts (obtained from peels of banana). The sodium and potassium are converted to corresponding oxides via oven drying of peels at 80°C before calcination at 700°C (48 hours) (Ezebor et al., 2014, Uprety et al., 2016, Endut et al., 2017, Gohain et al., 2017, Etim et al., 2018). Moreover, use of waste materials in catalyst synthesis may somehow resolve the waste disposal problems and the value-added constituents are beneficial for various industrial processes (Farooq et al., 2018).

However, heterogeneous catalysts have some constrains i.e. active moieties in these catalysts cannot be accessed in a liquid medium thus, catalytic activity is reduced. Moreover, active sites of solid support (porous) also play role in reducing catalytic activity. This arises need for development of new catalysts that not only have great catalytic efficiency and selective nature but also can be easily separated and reused. This can be accomplished by grafting via covalent binding and adsorption. Nano-catalysts are a way forward and act as a bridge, linking homogeneous and heterogeneous catalysts and have attributes of both types of catalysts (Thangaraj et al., 2016).

1.5.4.1.5 Heterogeneous Nano-Catalysts

These catalysts offer a great variety of possibilities to researchers to mould their surface functionality, elemental constitution/ no of atoms present in the nano particle. They are of highly selective nature and have surface to volume ratio, making them extremely efficient reaction media thus, obtain high yields of product (Thangaraj et al., 2015, Thangaraj et al., 2016). Metal oxide nano-catalysts offer high catalyst loading and enhance the efficiency of methanolysis. Moreover, excess presence of active sites on nano-catalysts makes them desirable (Wagner et al., 2000). Calcium oxide nano-catalyst is good choice for transesterification of oils to biodiesel, it gives about 98.54% conversion and can be reused for nine times (~95.8% yield for six cycles) (Reddy et al., 2016). Nano-catalyst formed doping of calcium oxide with lithium show

good conversion efficiency of oils to FAMES at mild temperature conditions (Kaur & Ali, 2011). Nano-catalysts of calcium and magnesium oxide are also found effective (98.95% yield) in biodiesel synthesis. It was also found that mixed oxides of various metals are more efficient than calcium oxide alone (Tahvildari et al., 2015). Other examples of calcium-based nano-catalysts used in biodiesel synthesis include; Ca/(Fe₃O₄@SiO₂), KF/CaO both of these show great catalytic power in transesterification and can be reused (Wen et al., 2010, Feyzi & Norouzi, 2016). Other nano-catalysts, effective in esterification reaction are; CdO and SnO₂ (Alves et al., 2014), other examples of nano-sized catalysts useful in biodiesel production are; magnetic nanoparticles, MNP, (magnetite, magnetite supported on silica), Fe₃O₄-TBD (Santos et al., 2015), K₂O/ γ -Al₂O₃ (heterogeneous base catalyst) (Han & Guan., 2009), KOH supported on Al₂CaO₄ or Al₂O₃ (Nayebzadeh et al., 2016), ZnO:Fe (Baskar & Soumiya, 2016), HPA-ZnO (Thangaraj & Piraman, 2016), ZnO:Ni (Baskar et al., 2018), ZnO:Mn (Baskar et al., 2017), nanotubes of zinc and aluminum (Zn_{1.2}H_{0.6}PW₁₂O₄₀ and Al_{0.9}H_{0.3}PW₁₂O₄₀ respectively) (Li et al., 2009, Wang et al., 2009), acid-base bifunctional HPA nano-catalyst (C₆H₁₅O₂N₂)₂HPW₁₂O₄₀ (Zhao et al., 2013), Cs-MgO (Woodford et al., 2014) etc. All the aforementioned nano-catalysts give more than 90% biodiesel yield, are easy to separate from reaction medium and have the capacity to be reused. All these qualities make them a strong candidate to catalyze the transesterification reaction.

1.6 Natural Inorganic Clays as Green Catalysts

Clay and clay minerals belong to the class of incrustated inorganic compounds, principal part of earth crust, are inert in nature, and are widely exploited due to their potential as catalysts in green chemistry. Other advantages of inorganic clays as catalysts include economical to use, non-toxic and decomposable. They are used successfully in many industrial processes as catalyst i.e. porcelain, paper industry and cement industry, waste management, water and air purification (Nafees & Waseem, 2014; Nafees et al., 2013; Ullah et al., 2017).

Generally, clays and clay minerals are made by the eroding or hydrothermal degradation of primary silicates groups. Chemically clay is the hydrous sheet-silicate or layered silicate of aluminum (aluminosilicate) and magnesium holding cation in its crystalline assembly besides some amount of metal oxides such as Cr, Ni/Fe

(Choudhary et al., 2012). Naturally present clays are considered as finely grounded soil because of their alignment that comprises of mixture of diverse clay minerals, metal oxides, eroded minerals and organic materials (Kim et al., 2013).

Microscopically, clay minerals are made up of ultra-thin, 1 nm, Al_2SiO_5 layers compactly stacked on interlayered hydrated ions. Based on the type of ions present, clays can either be cationic or anionic. Former occur more commonly in nature. They comprise of layers of Al_2SiO_5 (negatively charged), stabilized through interlayer cations. Their acidic nature is attributed to the presence of hydroxyl group on surface (Zhou, 2011). Anionic clays do not occur abundantly they have metal hydroxide sheets balanced by anions and water molecules. However, they are simple to manufacture in the labs (Zhang et al., 2010). Clays can hold various ions i.e. potassium, calcium, nitrate due to the large surface area and high polarity. They have also been used to eliminate heavy metals and toxins due to their absorbent properties. Structurally, clays are phyllosilicate with 2D layers of silicate hydrous. These layers are formed through the condensation of tetrahedral silicate unit, which is highly stable, having extra unshared oxygen positioned distantly from tetrahedral layer.

Condensation of silicates layer with various octahedral units through unshared atoms of oxygen results in the formation of many classes of clay minerals. This octahedral sheet is formed by the edge-sharing and polymerization of octahedral MO_6 (M being aluminum or Magnesium etc.). Two unshared oxygen atoms are present above and below the plane of polymerization in every octahedron making it negatively charged. Al because of being trivalent, occupies only 2/3 of octahedral spaces whereas, Mg being divalent, fills all the available holes. This makes clay minerals of di and tri-octahedral type. Usually, all layers of Al_2SiO_5 have one or two Si-O tetrahedral panes and one Al-O/ Mg-O octahedral sheet (Schoonheydt et al., 2011).

Clay minerals have been considered as heterogeneous catalysts as are abundantly available, stable, economic and of ecological nature. Most frequently used clay-based catalysts are made of Montmorillonite, Bentonite and Kaolin and are grouped under smectite and kaolinite groups. Like any other catalyst, they (montmorillonite, bentonite and kaolin) have also been manipulated to enhance catalytic potential. For this purpose, most commonly used methods include; ion exchange and in-situ wet impregnation method. They significantly increase the catalyst

quality i.e. making it recyclable without diminution of catalytic activity and enhance strength of acid sites (Bronsted and Lewis). In comparison with other catalysts (heterogeneous), manipulated/unmanipulated natural and commercially offered clays give good results for biodiesel synthesis via alcoholysis. Clearly, most of the moulded clays have caught much attention in transesterification than of the naturally present counterparts for their low activity. Various metal ions have been impregnated in the clay by the method of cation exchange and successfully used as catalyst for alcoholysis of succinic acid with Iso-butanol, and stearic acid with alcohol (Almadani et al., 2018).

1.7 Background Justification of the Project

Vast majority of world resources have been invested in biodiesel industry to encounter the energy crisis. However, majority (95%) of the produced biodiesel comes from edible crops making it a food security concern rather than a fossil fuel alternate. Thus, there is a huge potential of non-edible oil yielding crops to be used as an alternate. Unfortunately, not much effort is made to explore non-edible seeds oil for biodiesel synthesis. Another issue which has raised concerns regarding the use of edible plants/crops as biodiesel feedstock is deforestation for the cultivation of energy feedstock, causing drastic effects on global environment one such example of deforestation for feedstock cultivation can be found in Malaysia. Pakistan is not different from the rest of the world and is facing serious energy crisis. Currently Pakistan mainly relies on fossil fuels for its energy needs and among these oil makes the highest proportion i.e. 38% followed by hydro 32%, natural gas 27%, and coal only 3%. Due to high reliance on oil, the country imports oil which over burdens already suffering economy. Pakistan is fifth most populous country of the world after China, India, United States and Indonesia according to the U.S. Census Bureau. And the demand-supply gap of energy is becoming sharper certainly due to high population growth rate i.e. 2% approximately. And the effect of global climate change is also visible from the drastic changes in rain fall pattern. Salinity and drought turn formally agricultural land to barren land. The government of Pakistan in 2006 first came up with the policy for development of renewable energy resources for power generation to cope with the country's ever-growing demand of energy. In the year 2010 the total input of renewable energy resources to the power sector was less than one percent however the government aims to grow this proportion to five percent by the year 2030. There is a

huge potential for biomass based renewable energy resource as the country's interior part mostly consists of arable land, appropriate for feedstock development. About 28-million-hectare area in Pakistan is marginal and unfit for cultivation mainly due to water scarcity, intense radiation exposure, salinity and soil erosion. Non-edible crops/plants growing on these marginal waste land can be a potential non-edible biodiesel feedstock.

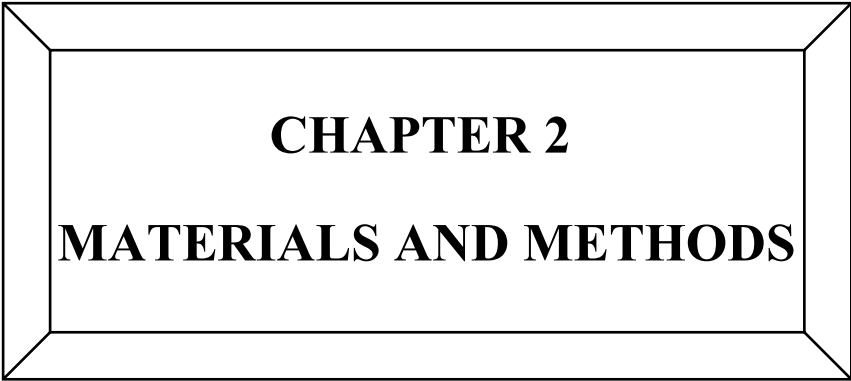
Use of non-edible oil-bearing plants as biodiesel feedstock offers several advantages over edible counterparts i.e., they do not compete with the food chain (have toxins which are poisonous to humans/animals), grow on waste land, require less water for life sustenance and are eco-friendly. They also enhance the soil quality through nitrogen fixation. Thus, current study deals with the exploration, identification and utilization of ten novel potential non-edible biodiesel feedstocks for future biodiesel industry. These feedstocks include; *Brassica oleracea* var. *alboglabra*, *Carthamus lanatus*, *Carthamus tinctorius*, *Carthamus oxycantha*, *Beaumontia grandiflora*, *Acacia concinna*, *Sapindus trifoliatus*, *Sesamum indicum*, *Ricinus communis*, *Celastrus paniculatus*. The seed of these plants are not fit for human consumption, have significant oil content with low free fatty acid content with few exceptions.

Attributes like cost effectiveness, utilization of marginal land make non-edible feedstock derived biodiesel an inexpensive and pro-environment alternative of fossil fuels. Its commercialization could lead to less pollutant green fuel burning in automobile engines. Results of current study highlight the impact of biofuel synthesis from non-edible feedstocks that affirm that biodiesel is economical source of sustainable energy.

1.8 Aims and Objectives

The aims and objectives of this project are:

- Identification of the non-edible oil yielding seeds for biodiesel synthesis.
- Chemical oil extraction of seeds oils for determination of oil content and FFA analysis.
- Synthesis and application of different solid base green nano-catalysts (single, double and triple metal modified clays) for biodiesel production.
- Catalyst characterization using different techniques like SEM, EDS, XRD and FTIR.
- Chemical characterization of synthesized biodiesel using techniques of FT-IR and GC-MS.
- Determination of fuel properties of prepared biodiesel and their comparison with International Standards of China GB/T 20828 (2007), American (ASTM-951, 6751) and European Union (EU-14214).
- Optimization of synthesized biodiesel using statistical techniques of Response Surface Methodology (RSM) and ANOVA.



CHAPTER 2
MATERIALS AND METHODS

This chapter contains the experimental strategy adopted in the current study for the synthesis and characterization of the solid base nano-catalysts as well as biodiesel production. Pictorial presentation of the experimental strategy is presented in figure 2.1.

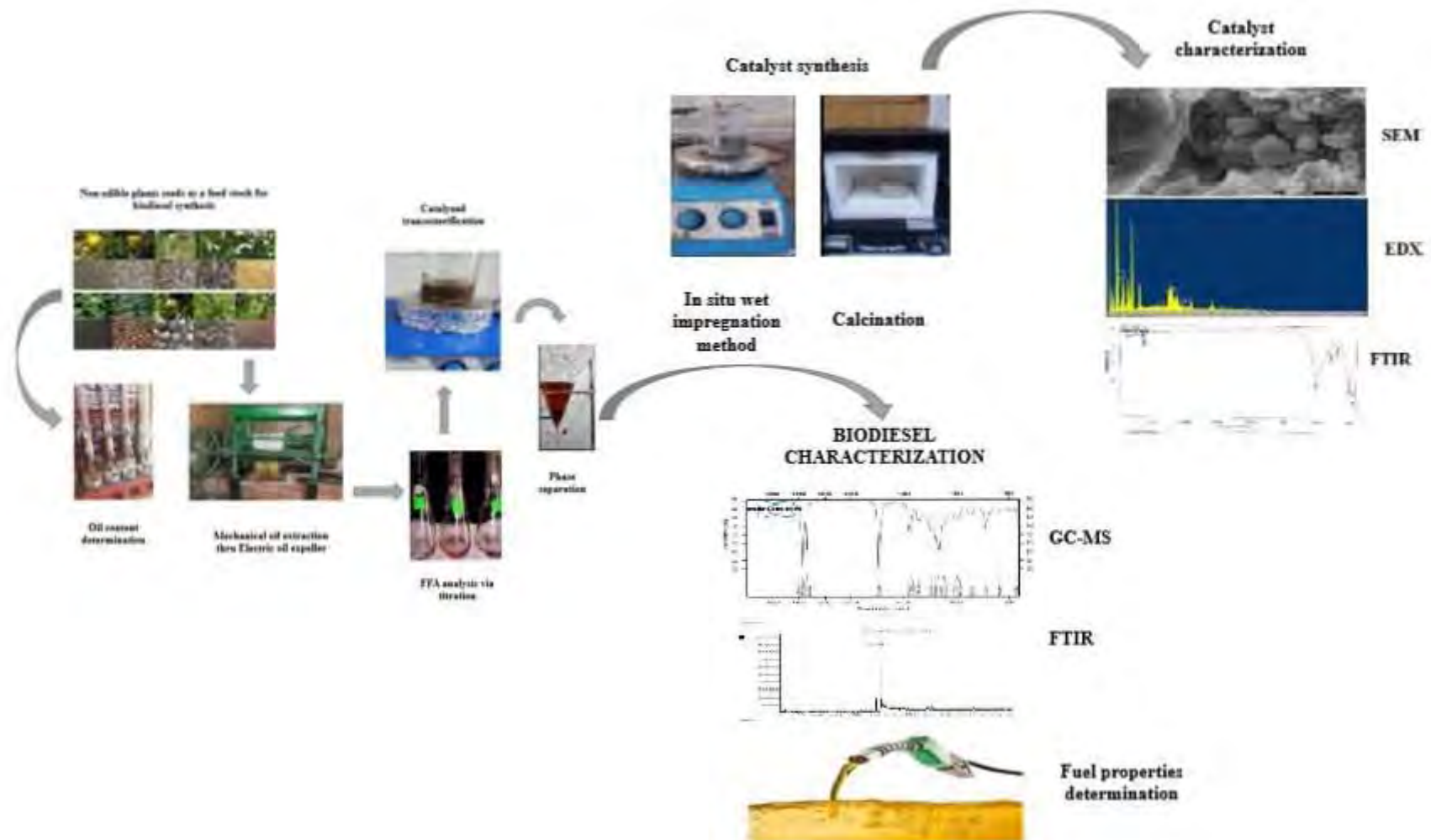


Figure 2.1: Experimental Strategy of the Work Done

2.1 Chemicals and Reagents

Different chemicals and reagents used in the experimental lab work include; Methanol, 99.9% (analytical grade), n-hexane (99%), chloroform, montmorillonite clay, bentonite clay, MgO, CuSO₄, ZnO, NaOH, AgNO₃, NaCl, Al₂O₃, NaOH pallet (99%), iso-propyl alcohol. All the chemicals were of analytical grade, purchased from Merck (Germany).

2.2 Identification of Non-Edible Plants as Biodiesel Feedstock

Morphological identification of the selected ten non-edible plants i.e. *Brassica oleracea* L., *Carthamus lanatus* L., *Carthamus tinctorius* L., *Carthamus oxycantha* M.Bieb., *Beaumontia grandiflora* (Roxb.) Wall., *Acacia concinna* (Willd.) DC., *Sapindus trifoliatus* L., *Sesamum indicum* L., *Ricinus communis* L. and *Celastrus paniculatus* Willd. was done using Binocular Light Microscope (Bausch and Lomb model W, New York) under 10X, 20X, 30X and 40X resolutions. Morphological features like leaves, stem, flower and seeds were studied using ruler via dissecting microscope and 3-5 consecutive readings were recorded for the accuracy in the data. Qualitative and quantitative morphological characters were studied and confirmed by the Flora of Pakistan, Flora of China as well as from the persevered Herbarium specimens from Herbarium of Pakistan (ISL), Quaid-i-Azam University, Islamabad. The names of species and citation was confirmed via International Plant Name Index.

2.3 Seeds Collection

Seeds of the non-edible plants were collected from different parts of the country in appropriate seasons during various field trips. These were shade dried and stored at ambient temperature before oil extraction.

2.4 Scanning Electron Microscopy of Oil Yielding Seeds

SEM is routinely used to generate high-resolution images of shapes of objects (SEI) and to show spatial variations in chemical compositions. Accelerated electrons in SEM carry significant amounts of kinetic energy, and this energy is dissipated as a variety of signals produced by electron-sample interactions when the incident electrons are decelerated in the solid sample. These signals include secondary electrons (that

produce SEM images), backscattered electrons (BSE), diffracted backscattered electrons (EBSD that are used to determine crystal structures and orientations of minerals), photons (characteristic X-rays that are used for elemental analysis and continuum X-rays), visible light (cathodoluminescence--CL), and heat. Secondary electrons and backscattered electrons are commonly used for imaging samples: secondary electrons are most valuable for showing morphology and topography on samples and backscattered electrons are most valuable for illustrating contrasts in composition in multiphase samples (i.e. for rapid phase discrimination). X-ray generation is produced by inelastic collisions of the incident electrons with electrons in discrete orbitals (shells) of atoms in the sample. As the excited electrons return to lower energy states, they yield X-rays that are of a fixed wavelength (that is related to the difference in energy levels of electrons in different shells for a given element). Thus, characteristic X-rays are produced for each element in a mineral that is "excited" by the electron beam. SEM analysis is "non-destructive"; that is, x-rays generated by electron interactions do not lead to volume loss of the sample, so it is possible to analyze the same materials repeatedly (Fatima et al., 2018). Micromorphological of seed surface features i.e. shape, surface, margins, periclinal wall arrangements, seed coat sculpturing variation was examined through SEM, scanning electron microscopy (Model JEOL JSM-5910). The seeds were washed, dried and then soaked in 100% acetone for one hour. Approximately 450Å of gold were deposited onto the mounted samples in a vacume evaporator, International Scientific Instruments (ISI) Model PS-2. The specimens were viewed at an accelerating voltage of HV 30 KV. These were visualized and photographed at different resolutions for better details (polaroid films p/n665) (Alves & Pozza, 2009).

2.5 Determination of Seeds Oil Content Via Chemical Extraction Method

Prior to oil content analysis using soxhlet apparatus (VWR VELP Scientifica, Germany), seeds were oven dried for one day at 60°C. Dried seeds were then finely grinded to make a powder. Then 5g of this powder was placed in thimble, placed at the center of the apparatus. The round bottom flask was filled with 250 ml of the n-hexane, which was used as a solvent. And was heated up to 68°C with water circulating reflux system. The reaction was carried out for 4-5 hours. After the completion of the reaction,

the wet powder was placed in oven at 60°C overnight (Shimelis & Hugo, 2011). After that, it was weighed, and oil percentage of the seeds was accessed using the following formula

$$\text{Oil content \%} = \frac{W3 - W1}{W2} \times 100 \quad \text{Equation 1}$$

Where W1 is weight of empty flask, W2 is weight of empty flask + powdered sample whereas, W3 is weight of sample used.

2.6 Electric Oil Extraction

Electric oil expeller (KEK P0015-10127) is one of the suitable methods used for extraction of seed oils in large quantity. These seeds were fed in the electric oil expeller and oil is extracted on large scale. Oil seed cake was produced as a side product and was passed several times through the expeller to maximize the oil quantity. Obtained crude oils were kept in dark at appropriate temperature to prevent the photo-oxidation of oils (Karaj & Müller, 2011).

2.7 Purification of Crude oils

Crude oils were then purified from dust and other debris via filtration using Whatman grade 2 filter paper. After that the oils were boiled to remove the moisture content (water) to enhance the oil quality. Purified oils were then stored in air-tight jars for further use (Kongjao et al., 2010).

2.8 FFA Content Determination of Oils

Free fatty acid content (FFA value) of the oils was determined using standard acid-base titration method. For this purpose, blank and sample titrations were performed. For the purpose of blank titration, basic solution (0.025 M KOH prepared in distilled water) was taken in burette and blank solution (10 ml of iso-propanol with 2-3 drops of Phenolphthalein indicator) in conical flask was titrated against it by the drop wise addition of burette solution in it. In case of sample titration, sample solution was prepared by the addition of 1 ml of oil to the 9 ml of iso-propanol along with few drops of indicator. And then was titrated by the basic solution till the appearance of

resistant pink color (Lam & Proctor, 2001). The procedure was repeated for few times to get the accurate figure. FFA was determined using following equation below

$$\text{Acid Number} = \frac{A - B}{V} \quad \text{Equation 2}$$

Where, A is volume of KOH sol. used in sample titration, B is volume of KOH sol. used in sample titration and V is the volume of oil used.

2.9 Synthesis of Catalysts

In this study three different types of novel catalysts have been synthesized and effectively used to produce biodiesel thru the process of transesterification. To overcome the problems associated with the heterogeneous catalysts (single metal based in majority) like leaching, poisoning and blockage of active sites, clay composites of single, double and triple metals have been synthesized in this study. They are also efficient in conversion of oil to biodiesel.

2.9.1 Clay Hybrid Composite Catalyst Synthesis

Different single, double and triple metal clay hybrid catalysts were synthesized by *in situ* wet impregnation method as adopted by (Manikandan et al., 2012, Munir et al, 2019). For this purpose, 3g of clay, Montmorillonite and Bentonite, was swelled in 500 mL distilled water for 5 hours at room temperature to hydrate the interlayer cation and expand the lamellae. And then, known amount of different salts (sodium, silver, copper, manganese, zinc, iron) were added to the hydrated clay suspension as metal precursors. NaOH (few drops) were added to the solution to attain the final base. This slurry was stirred with magnetic stirrer at 100°C for approximately 7 hours to evaporate the water. After that the resultant wet material was washed several times (with DH₂O) to attain 8 pH. The product was oven dried overnight at 105°C. Then was finally grinded, sieved and calcined in muffle furnace at 500°C (Zhou, 2011).

2.10 Characterization of Catalysts

Catalysts were characterized using different techniques like SEM, EDS, XRD and FT-IR.

2.10.1 Scanning Electron Microscopy (SEM)

Morphology (surface) of catalyst was examined through Scanning Electron Microscopy (SEM) (NOVA Nano). And directions were followed as per manual instructions of Nova NanoSEM These were visualized and photographed (polaroid films p/n665) (Sokolova et al., 2011).

2.10.2 Energy Dispersive X-Ray (EDS)

EDS analysis is also called energy dispersive X-ray analysis or energy dispersive X-ray microanalysis. It is an analytical technique used for the elemental analysis or chemical characterization of a sample. It relies on an interaction of some source of X-ray excitation and a sample. Its characterization capabilities are due in large part to the fundamental principle that each element has a unique atomic structure allowing a unique set of peaks on its X-ray emission spectrum. A sample excited by an energy source (such as the electron beam of an electron microscope) dissipates some of the absorbed energy by ejecting a core-shell electron. A higher energy outer-shell electron then proceeds to fill its place, releasing the difference in energy as an X-ray that has a characteristic spectrum based on its atom of origin. This allows for the compositional analysis of a given sample volume that has been excited by the energy source. The position of the peaks in the spectrum identifies the element, whereas the intensity of the signal corresponds to the concentration of the element. Compositional information, down to the atomic level, can be obtained with the addition of an EDS detector to an electron microscope. As the electron probe is scanned across the sample, characteristic X-rays are emitted and measured; each recorded EDS spectrum is mapped to a specific position on the sample. The quality of the results depends on the signal strength and the cleanliness of the spectrum. Signal strength relies heavily on a good signal-to-noise ratio, particularly for trace element detection and dose minimization (which allows for faster recording and artifact-free results). Cleanliness has impact on the number of spurious peaks seen; this is a consequence of the materials that make up the electron column (Peng et al., 2008). Elemental characterization of the catalysts was identified by Energy Dispersive X-Ray (EDS/EDX) EDX spectra were measured with a Si(Li) EDS detector (Thermo Scientific) or an XFlash® SDD detector (Bruker), both having an active area of 10 mm² (Carta et al., 2013).

2.10.3 X-Ray Diffraction (XRD)

X-Ray Powder Diffraction (XRD) is a nondestructive technique that obtains detailed information such as chemical composition of the material, the crystallographic structure or morphology of the atoms or molecules inside the material, as well as the physical properties of the material. XRD is most widely used to study the phase and crystal structure of substances. Each chemical molecule or phase has a unique diffraction pattern when the material is analyzed by XRD. The XRD analysis has the advantages of no damage to the sample, no pollution, quickness and high measurement accuracy, and it can offer a large amount of information about crystal integrity. Therefore, XRD analysis, as a modern scientific method of material structure and composition analysis, has gradually been widely used in the research of various disciplines, such as geology, environmental science, material science, engineering, and polymer science (Agarwal et al., 2017). The crystalline structure of catalyst was verified by Powder X-ray diffraction (XRD) using powder diffractometer by means of $\text{Cu-K}\alpha = 1.54 \text{ \AA}$ at the scanning rate of 2θ in $2\theta/\text{minutes}$ ($2\theta = 5-70^\circ$) (Vorontsov et al., 2018).

2.10.4 Fourier Transform Infrared Radiation Spectroscopy (FT-IR)

Fourier transform infrared (FTIR) spectroscopy is a rapid, economical, easy, and non-destructive technique. The IR spectrum of a clay mineral is sensitive to its chemical composition, isomorphous substitution, layer stacking order, or structural modifications. This makes FTIR spectroscopy the most informative single technique not only for clay mineral composition and structure but also for interactions of the clay minerals with inorganic or organic compounds. Basically, by applying infrared radiation (IR) to samples of materials, FTIR analysis measures a sample's absorbance of infrared light at various wavelengths to determine the material's molecular composition and structure. The Fourier transform spectrometer works to convert the raw data from the broad-band light source to obtain the absorbance level at each wavelength. The x-axis or horizontal axis represents the infrared spectrum, which plots the intensity of infrared spectra. The peaks, which are also called absorbance bands, correspond with the various vibrations of the sample's atoms when it's exposed to the infrared region of the electromagnetic spectrum. For mid-range IR, the wave number on the infrared spectrum is plotted between $4,000$ to 400 cm^{-1} . The y-axis or vertical

axis represents the amount of infrared light absorbed or transmitted by the material being analyzed. Typically, absorbance bands are grouped within two types: Group frequencies and fingerprint frequencies. Group frequencies are characteristic of small groups of atoms or functional groups such as CH₂, OH, and C=O. These types of bands are typically seen above 1,500cm⁻¹ in the infrared and they're usually unique to a specific functional group, making them a reliable means of identifying functional groups in a molecule. As for fingerprint frequencies, these are highly characteristic of the molecule as a whole; they tell what is going on within the molecule. These types of absorbances are typically seen below 1500cm⁻¹ in the infrared spectrum. However, some functional groups will absorb in this region as well. As a result, this region of the spectrum is less reliable for identification, but the absence of a band is often more indicative than the presence of a band in this region (Hulkoti et al., 2014). FT-IR spectra were attained using Bruker-Tensor 27 in the range of 400-4000 cm⁻¹ (Xiong et al., 2006).

2.11 Biodiesel Synthesis

Selected non-edible feed stocks were converted to biodiesel using single step transesterification reactions.

2.11.1 Transesterification

Purified oil was pre heated and meanwhile, desired concentration of the selected catalyst was added to the known volume of methanol and heated at desired temperature for approximately 30 minutes. Then pre heated oil was transferred to it and the reaction of transesterification was carried out at appropriate reaction conditions. Optimum conditions of the transesterification reaction were obtained after performing a few reactions by varying one variable at a time and keeping other variables constant. The factors that can affect the process are reaction time, temperature, oil to methanol ratio and catalyst concentration. After reaction completion, the catalyst was recovered from the reaction media via centrifugation of the reaction mixture at 4000 rpm for approximately 10 minutes. Extra alcohol was evaporated using rotary evaporator. The resultant reaction mixture was moved to separating funnel to separate out glycerol from biodiesel via phase separation technique. And biodiesel yield was calculated using the following equation (Ezekannagha et al., 2017).

$$\text{Biodiesel yield} = \frac{\text{grams of biodiesel produced} \times 100}{\text{grams of oil used}} \quad \text{Equation 3}$$

2.12 Biodiesel Characterization

The produced biodiesel was characterized using the following techniques (analytical).

2.12.1 Fourier Transform Infrared Radiation (FT-IR) Spectroscopy

FT-IR is an analytical technique in which structures molecules are determined based on their molecular fingerprint i.e. molecule's characteristic absorption of infrared radiation. When sample molecules are exposed to the infrared radiation, they selectively absorb radiations of different wavelengths, causing change of dipole moment of sample molecules. Thus, the vibrational energy levels of the sample molecules change from ground to excited state. And the energy of the absorption peak is determined by the vibrational energy gap. The number of absorption peaks is directly related to the number of vibrational freedoms of the molecule. The intensity of absorption peaks is related to the change of dipole moment and the possibility of the transition of energy levels. Therefore, by analyzing the infrared spectrum, structure information of a molecule can easily be obtained (Voort et al., 2011). FT-IR spectrum of synthesized biodiesel was attained by Bruker-Tensor 27 (4000 cm^{-1} - 400 cm^{-1} range) to get the information about the functional groups and structural arrangement of FAMES (Fatty Acid Methyl Esters) (Mahamuni & Adewuyi, 2009).

2.12.2 Gas Chromatography-Mass Spectroscopy (GC-MS)

GC-MS combines the features of both gas-chromatography and mass-spectroscopy for identification of the components of the sample other advantages include; quantification of the analytes and identification of even trace impurities. For GC-MS sample can be of any nature i.e. liquid, solid or gaseous. GC/MS begins with the gas chromatograph, where the sample is volatilized. This effectively vaporizes the sample (the gas phase) and separates its various components using a capillary column

packed with a stationary (solid) phase. The compounds are propelled by an inert carrier gas such as argon, helium or nitrogen. As the components become separated, they elute from the column at different times, which is generally referred to as their retention times. Once the components leave the GC column, they are ionized by the mass spectrometer using electron or chemical ionization sources. Ionized molecules are then accelerated through the instrument's mass analyzer, which quite often is a quadrupole or ion trap. It is here that ions are separated based on their different mass-to-charge (m/z) ratios. The final steps of the process involve ion detection and analysis, with compound peaks appearing as a function of their m/z ratios. Peak heights, meanwhile, are proportional to the quantity of the corresponding compound. A complex sample will produce several different peaks, and the final readout will be a mass spectrum. Unknown compound and analytes can be identified using computer libraries of mass spectra for different compounds. GC is the separation technique of choice for smaller and volatile molecules such as benzenes, alcohols and aromatics, and simple molecules such as steroids, fatty acids and hormones. It is widely used for chemical analysis, and especially for drug and environmental contamination testing. When combined with MS, GC/MS can be used in both full scan MS or select ion monitoring (SIM) mode to cover either a wide range of m/z ratios or to gather data for specific masses of interest, respectively (Giera et al., 2012). The GC (6890N) joined with MS (5973 MSD) fitted with a DB-5MS capillary column of 30 to 0.32mm, and 0.25 μ m of Film thickness, was used for the credentials and description of methyl esters in PCBD. He gas with 1.5ml/min of flow rate and programmed column temp of 12°C–300°C (10°C/minute) was used (Tariq et al., 2011).

2.13 Determination of Fuel Properties

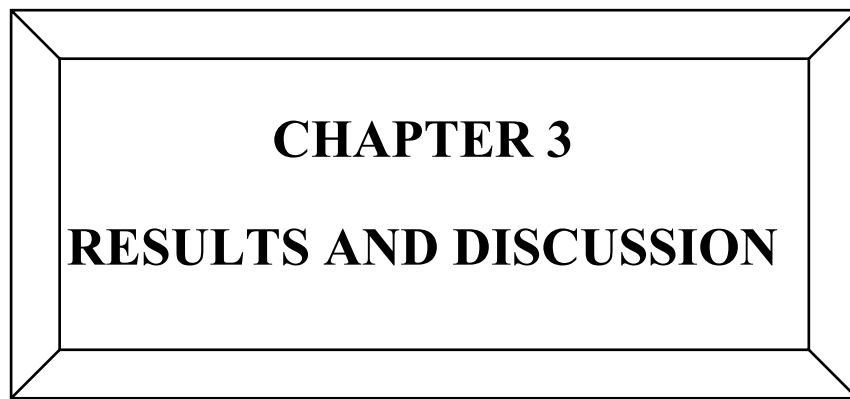
The fuel quality of produced biodiesel as well as its effects on diesel engines are essential to be examined. For this purpose, the physical properties (fuel properties) of the formed biodiesel were determined through PSO (Pakistan state oil). These fuel properties of synthesized biodiesel were then compared with international biodiesel standard i.e. American (ASTM D-6751), (ASTM D-951), European Union 14214, China GB/T 20828. These compared properties are Color, total acid no, kinematic viscosity, Sulfur amount, density, Cloud, Pour and flash points (Knothe, 2005).

2.14 Optimization study of Transesterification operational factors using Response Surface Methodology (RSM)

Different experiments were performed using variables with a factorial design, from which the results were analyzed with response surface methodology (RSM) to obtain optimized yield. A central composite design (CCD) was used to carry out experimental design during reaction. In this design four factor levels with six central point repetitions were used. Design of Experiments (DOE) software was used for optimizing transesterification reaction parameters and analyzing the data. Total of 30 experiments were used for optimization of transesterification process. The chosen extraction factors include, A: Catalyst (wt%), B: Time (min) and C: Temperature (0C) and D: oil (mol)-methanol. Moreover, randomization of the experiment was utilized to reduce the indescribable variation impacts in perceived reaction (response). After the completion of experiments, data was analyzed statistically by RSM to know the quadratic ploy method appear to be fitted using Design-Expb0ert 11 (Stat-Ease Inc, Minneapolis, USA). The reaction can be related by representing the dependent factor with y(yield) with investigational factors A (methanol oil), B(catalyst), C(temperature). The quadratic polynomial equation applied is as follows (Hasni et al., 2017).

$$Y = b_0 + \sum_{i=1}^k b_{ix}x_i + \sum_{i=1}^k b_{iix}x_i^2 + \sum_{i<j}^k b_{ijx}x_ix_j + e$$

where y = biodiesel yield and b₀ = intercept value (i= 1, 2, 3...k).



CHAPTER 3
RESULTS AND DISCUSSION

This chapter comprises of the four sections throwing light on various aspects i.e. LM and SEM based micro morphological identification of seeds of the non-edible feedstock, characterization of the three catalysts, their utilization in the synthesis of green based biodiesel from ten different non-edible oil yielding seeds. And lastly, comparison of their catalytic efficiencies.

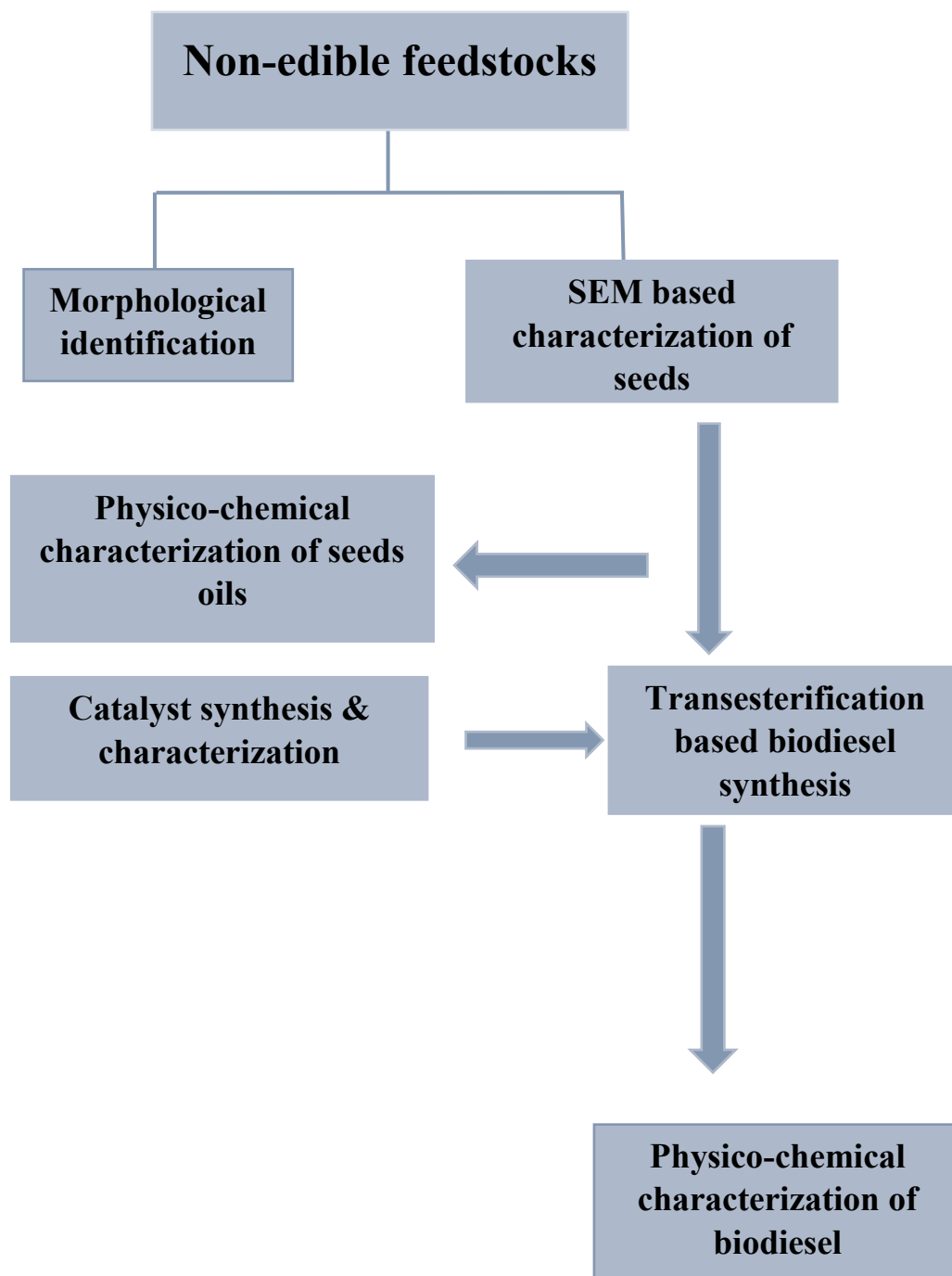
Section I: Morphological identification and Scanning Electron Micrography of seeds of non-edible feedstock

Section II: Catalysts characterization

Section III: Biodiesel synthesis from ten different non-edible oil yielding seeds

Section IV Comparison of Catalytic Efficiency of Catalysts

Flow sheet description of the whole chapter is presented on the next page.



Flow sheet 1: Steps Involved in Synthesis and Charaterization of Biodiesel

**Section I: Morphological identification and
Scanning Electron Micrographs of
seeds of non-edible feedstock**

This Section includes the morphological description of ten (10) novel non-edible oil yielding plants using light microscope along with in-depth examination of micro morphological features of seeds as energy crops utilizing SEM, Scanning electron microscopy. SEM is the recent technique and is used widely to resolve taxonomic puzzles by examining seeds ultra-morphological particulars which in turn aids in the species identification as well as validation of oil-bearing seeds (Harborne, 1977; Fatima et al., 2018;). Seeds micro morphological characters along with size and shape, act as the investigative tools for identification of diverse species (Luqman et al., 2018). These characters disclose the close association of unlike species of plants amongst each other at taxonomic level (Maciejewska-Rutkowska and Bednorz, 2004). Feedstock selection for biodiesel production highly relies on oil percentage, free fatty acid content and cost effectiveness. Thus, non-edible plant seeds prove themselves as a best candidate for renewable energy industry (Atabani et al., 2012). Hence, current study aims to introduce some new oil-bearing seeds together with their micro morphological particulars to the science as they have the potential to be utilized in the renewable energy sector as a feedstock for biodiesel industry. And seeds micro morphological characters thru LM and SEM are presented in Table 3.1.

3.3.1 *Brassica oleracea* L.

Brassica oleraceae L., commonly known as Chinese Kale or Kailan, appertain to family Brassicaceae. This family accommodates 350 genera and 3500 species (Nawaz et al., 2018). Most important genera of this family is Brassica which contain about 41 species (Gladis & Hammer, 1990). Most of species belonging to this genus have comprehensive importance due to their medicinal, nutritional, pharmaceutical and economic worth. Chinese Kale is named so because it was commenced in China (Issarakraisila et al., 2007). It grows extensively in China and South East Asia (Sun et al., 2011). It is most preferred vegetable consumed in Thailand (Leamsamrong et al., 2019). Different cultivars of Chinese Kale can grow in an extensive range of climatic conditions including both cold conditions and warm conditions. It can endure summer heat (Noichinda et al., 2007). Chinese Kale possess white flower, but some cultivars have yellow and red flowers (Okuda & Fujime, 1994). These races have tender rosette leaves with color ranging from light green to deep green (Okuda & Fujime, 1994) and contain bolting stems. Thin oval leaf blades, lengthy petioles, and lack of thickened

parts characterize this variety and these characters make them different from other varieties of *Brassica oleraceae* (Phelan & Vaughan, 1976). The bolting stem and rosette leaves serve as edible parts therefore they are immensely employed as leafy vegetables (Akram et al., 2019).

Brassica oleraceae L. seeds are Pitch black and rounded with glabrous surface, smallest seeds having size 3mm size (Plate 1; a, b, c, d). Anticlinal walls are identical. Seed wing are absent. Seed coat ornamentation having fabricated pattern with deep depression. Rift and wax-like pellicle of different size were observed on the surface of the seed (Table 3.1).



Plate1: (a) *Brassica oleraceae* L. Plant, (b) Seeds, (c,d) SEM of Seeds and Sculpturing

3.1.2 *Carthamus oxyacantha* M.Bieb.

Carthamus oxyacantha M.Bieb. belongs to family Asteraceae/Compositae and has sixteen identified species. Its commonly known as wild safflower and locally called as pholi/kandyari. It is an annual spiny-leaved herb that is up to 1.5 m tall. It is a xerophytic and harsh weed that grows in winter crops. Due to its spiny nature, it is not utilized by the animals thus, survives on grazing lands. Seed oil content ranges from 28% to 29% (non-edible). It is worldly distributed in India, Iraq, Kazakhstan, Pakistan, Turkey, Turkmenistan and Uzbekistan (Sheykhrou et al., 2012, Tariq et al., 2020).

Greyish elliptic-oblong achene with smooth surface, seed size 3.9mm. Anticlinical walls are thick. Seed surface cells were observed elongated with rough texture (Table 3.1). Seed ornamentation ruminant-gebulate. Each cell is identical with boundaries. (Plate; 2, c, d).

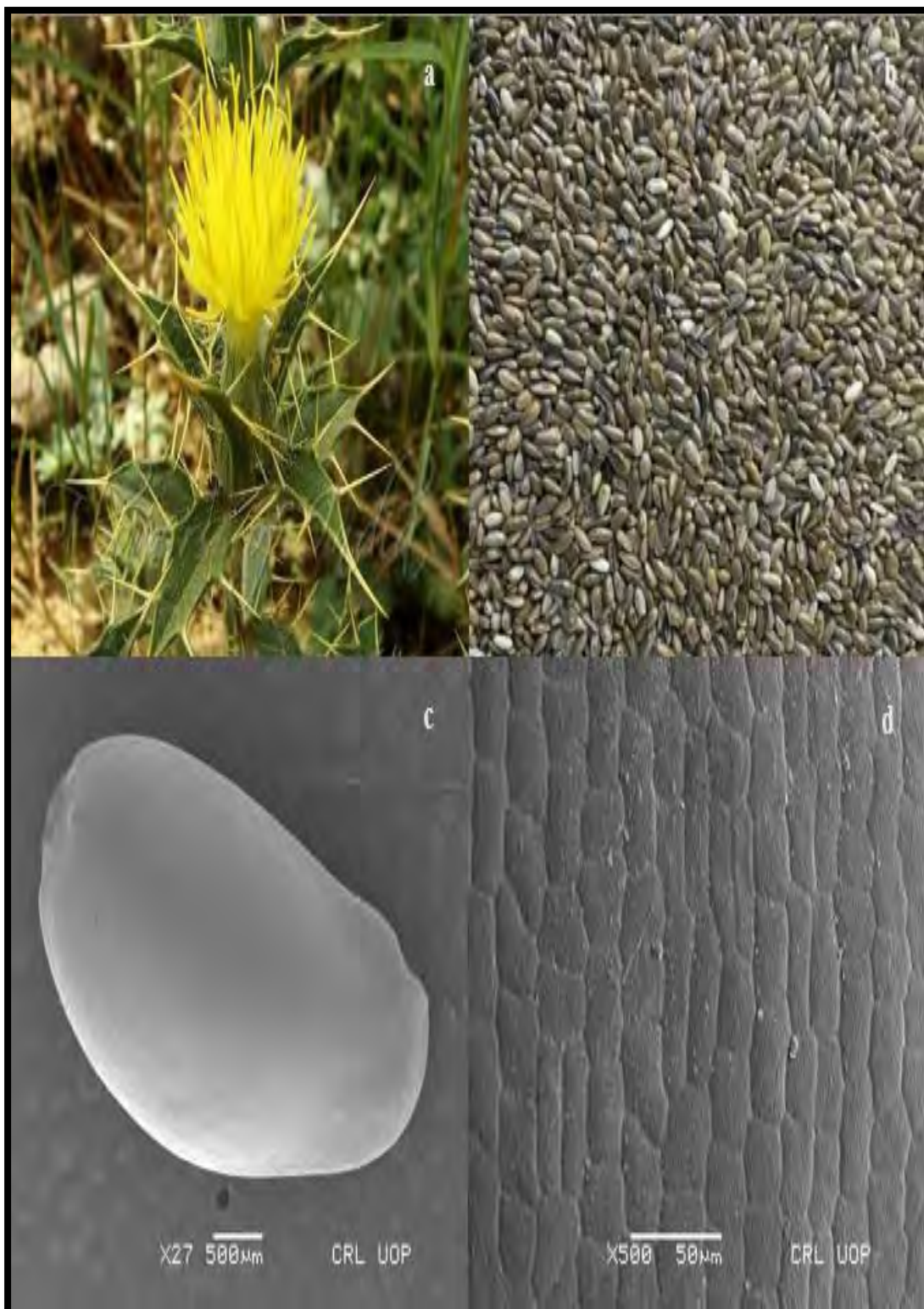


Plate2: (a) *Carthamus oxyacantha* M.Bieb. Plant, (b) Seeds, (c,d) SEM of Seeds and Sculpturing

3.1.3 *Carthamus tinctorius* L.

Carthamus tinctorius L. belongs to family Asteraceae/Compositae. It is a highly branched, herbaceous, thistle-like annual or winter annual, generally with several long sharp spines/leaves. Plant is usually 30-150 cm tall with capitula (globular flower heads) and bright yellow, orange or red flowers (Plate 3; a). Achenes are smooth, four-sided and generally lack pappus (Dajue & Mündel, 1996).

Yellowish white narrow obovate achene with shiny surface, seed size 35mm. Anticlinal walls are thin. Seed sculpture ornamentation observed fine variegated. Obovate hilum was noted in achene. (Plate; 3, b, c, d).



Plate3: (a) *Carthamus tinctorius* L. Plant, (b) Seeds, (c, d) SEM of Seeds and Sculpturing

3.1.4 *Beaumontia grandiflora* Wall

Beaumontia grandiflora Wall belongs to family Apocynaceae. It is vigorous, evergreen climbing shrub forming woody stems that can be up to 20 meters long vigorous, evergreen climbing shrub producing woody stems that can be up to 20 metres long Its stem is solid, leaves are opposite decussate, shape of the leaf apex is acuminate (El-Taher et al., 2019).

The largest seed size is measured in *B. grandiflora*. Seed and wing surface ornamentation having aculeate ornamentation while hilum surface show irregular Off white seed with flattened shape, seed size 20mm. According to the length and width ratio cells. Seed wing consist of round, thick to thin anticlinal wall. (Plate 4; a, c). Table 3.1.

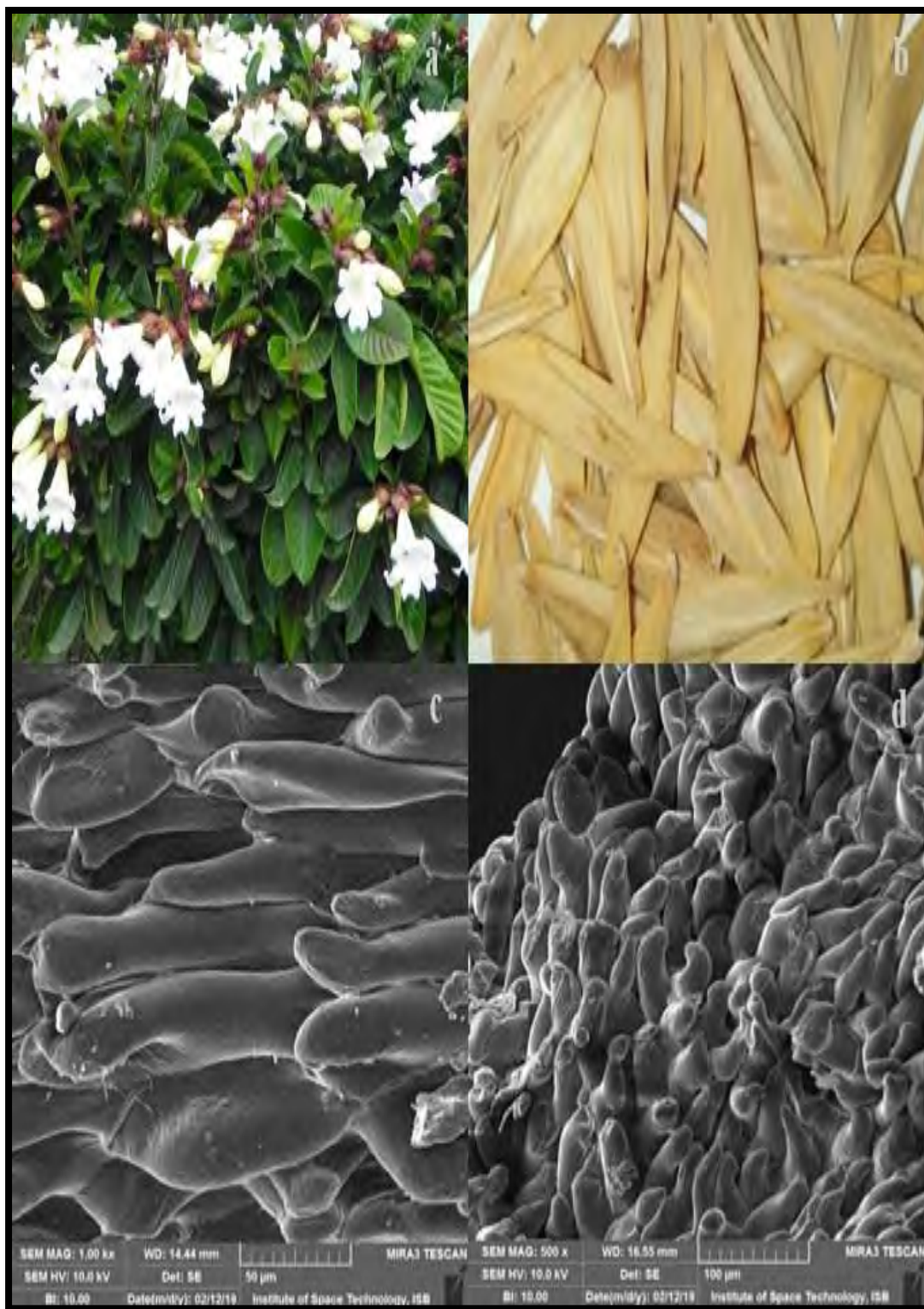


Plate 4: (a) *Beaumontia grandiflora* Wall Plant, (b) Seeds, (c, d) SEM of Seed Surface and Wing

3.1.5 *Celastrus paniculatus* Willd.

Celastrus paniculatus is commonly known as staff tree or black oil-plant. It belongs to family Celastraceae and is a woody climbing shrub (approximately 1250 m of height), wild, deciduous, with yellowish green flowers (April-June). It is 8-10 m large, have radish brown long slender and lenticulate stem with 18 to 20 cm diameter Fruit is capsule, globose, three valved with cells (3), enclosing 3-6 yellowish brown non-edible seeds in red arillus (Deodhar and Shinde, 2015). It is native to India and widely distributed in the foothill region of Himalaya, South China, and South. East Asia to Australia, Taiwan, Cambodia, Thailand, Malaysia, Vietnam, and many pacific islands (Bhanumathy et al., 2010).

The seeds were brownish (Plate 5, b), 1.3 -1.9 cm× 2.1- 2.9 cm, containing 55% oil, 0.98 FFA content yielding 89.42% biodiesel (Table 1). SEM of *Celastrus paniculatus* seeds (Plate 5, c & d) depict elongated, flattened, polygonal or elliptic shaped and asymmetric, with periclinal wall protuberance, walls smooth, reticulate irregular, polygonal surface, papillae absent, slightly projected outwards, cell margins are somewhat straight-angular, anticlinal wall is slightly deep while outer periclinal wall is flat to slightly concave (Table 3.1).



Plate 5: (a) *Celastrus paniculatus* Willd. Plant, (b) Seeds, (c, d) SEM of Seed Surface and Sculpturing

3.1.6 *Carthamus lanatus* L.

Carthamus lanatus L. belongs to family Asteraceae/Compositae. It is commonly known as Woolly distaff thistle, downy safflower or saffron thistle. It grows among rocks, in dry hills and unrefined land. Indigenous to the Mediterranean region and West Asia, as well as to many temperate regions of the world i.e. the United States of America, Argentina, Chile, New Zealand and Australia. An erect, somewhat hairy or occasionally woolly annual herb, growing about 1m or tall, but usually standing 40-90cm tall. The floral heads are yellow or cream colored (Plate 6; a). The fruit is four-sided, plane and 5-8 mm long. The fruit has a pappus of numerous rows of hard spines or scales having variable length on one side of the seed. Reproduction is carried out by the seeds (Plate 6; b). The plant itself is hardly ever eaten but then again, the seeds, have a high oil percentage and protein content, are source of food for sheep and birds. It usually dies in late autumn to early winter (Sheykhrou et al., 2012, Tariq et al., 2020).

Brownish narrow obovate seed with shiny surface, seed size 8 mm. Anticlinal walls are thin. Seed sculpture ornamentation was observed to be fine variegated. Obovate hilum was observed in the achene (Plate 6, c, d) (Table 3.1).

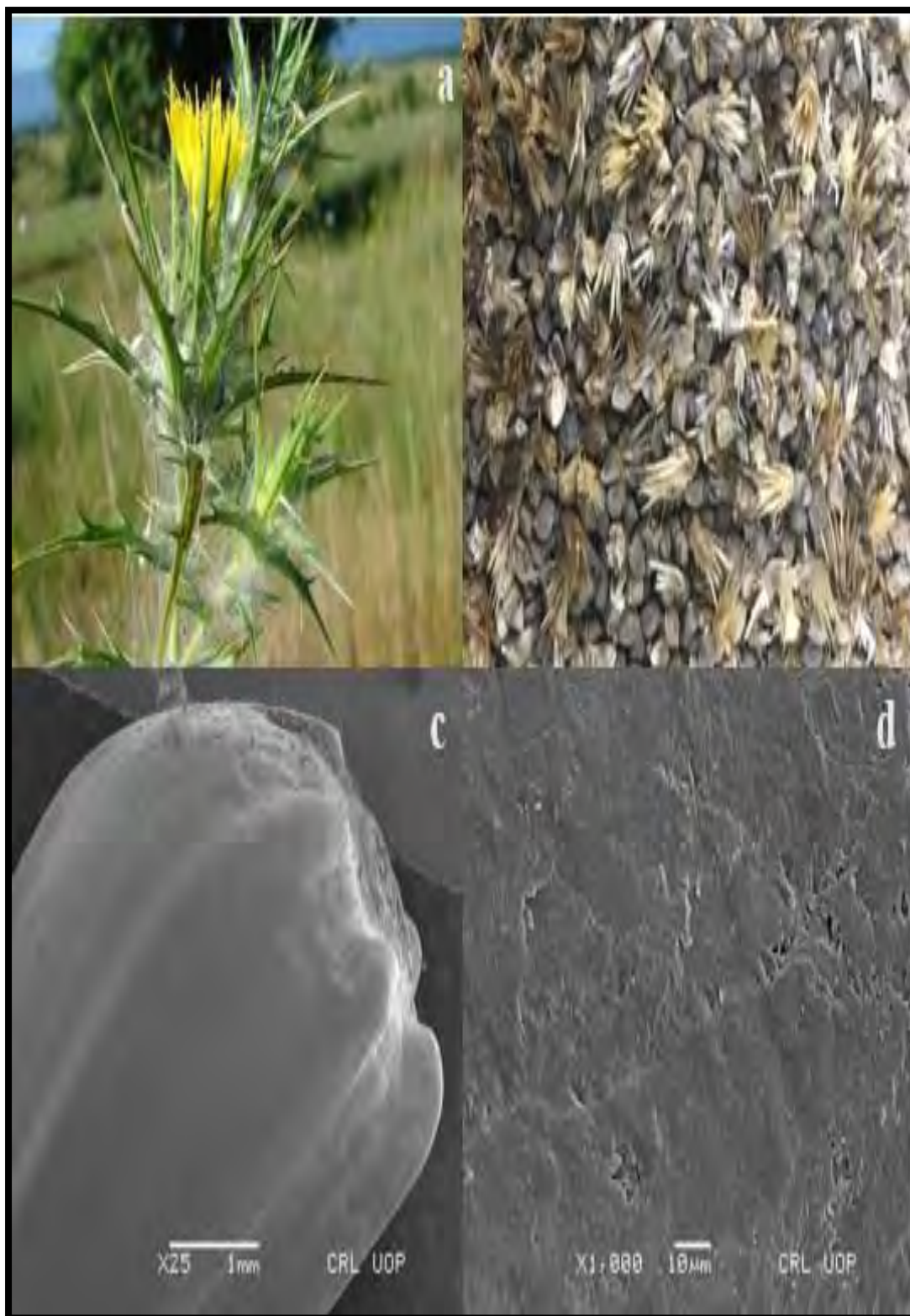


Plate 6: (a) *Carthamus lanatus* L. Plant, (b) Seeds, (c, d) SEM of Seed Surface and Sculpturing

3.1.7 *Acacia concinna* (Willd.) DC.

Acacia concinna (Willd.) DC. Belongs to family Fabaceae. It is natively known as sikakai. It is a climbing shrub. Its branches have brown flat stripes and thorny (thorns short, broad-based & flattened). Leaves present but early deciduous stipules not thorn-like; petiole is about 1 to 1.5 cm long with conspicuous gland in the middle; blade is bipinnate having 5-7 sets of pinae, the primary rachis is thorny, juvenile, the pinnae with 12 to 18 sets of pinnae; pinnae oblong-lanceolate having length of 3-10 mm, a crescent, acute and apiculate at the tip, diagonally rounded at the base, entire, glabrous. Inflorescences of 2/3 heads peduncled in the axils of the upper abridged leaves, look as if paniculate, peduncles are 1 to 2.5 cm in length, pubescent; heads approximately 1 cm in diameter at maturity. Flowers are pink colored, reduced subtending bracts may be present or absent; ovary is stipitate and glabrous. Pods are profuse, slightly compressed and stalked, are 8 cm in length, 15-18 mm in width. Seeds are present in the pods and there are usually 10-12 seeds per pod. The herb has antimicrobial and Antidermatophytic uses. In the Subcontinent it's used for hair care traditionally (Boatwright et al., 2015).

Reddish brown oblong achene, seed size 32 mm. Seed poles are rounded, Areole is linear oblong, surface pattern was irregularly reticulate-foveolate with thick anticlinal ridges (Plate 7) (Table 3.1).

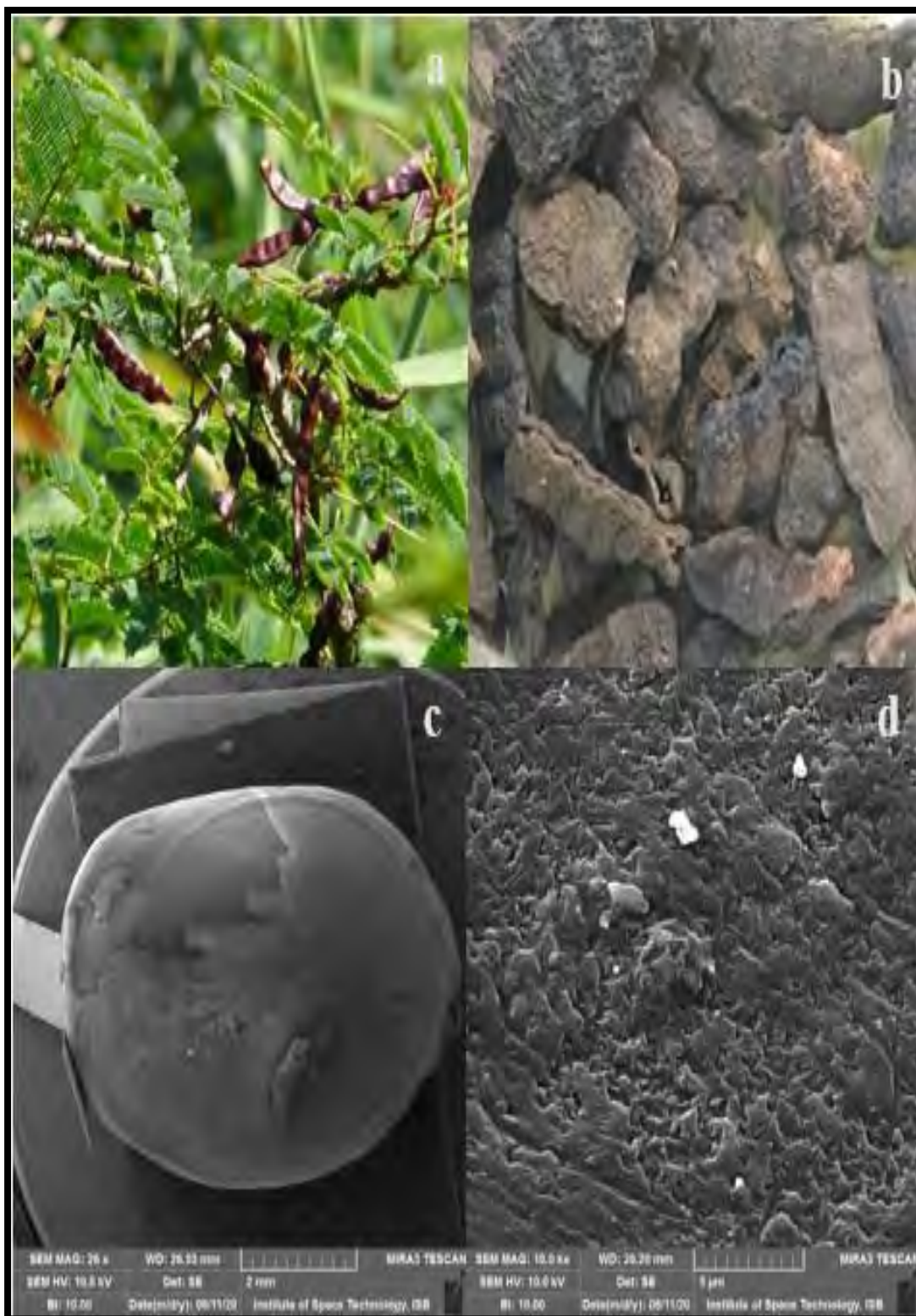


Plate 7: (a) *Acacia concinna* (Willd.) DC. Plant, (b) Seeds, (c, d) SEM of Seed Surface and Sculpturing

3.1.8 *Sapindus trifoliatus* L.

Sapindus trifoliatus L. belongs to family Sapindaceae. It is a large tree, up to 25 m in length, having compound leaves, 15 to 30 cm long. Leaflets are almost stalk less, 2 to 3 sets, 8 to 18 cm long, 5 to 7.5 cm broad, elliptic-lance shaped, flat, pointed at the tip, somewhat oblique at base, terminal pair is the longest. Flowers are of greenish-white color. Flower stalks are 3 mm in length, velvety in appearance. Sepals are 5 in number, to some extent fused at the base, 4 to 5 mm in length, ovate-oblong and appearance is velvety. Petals are 5 in number, free, 5 to 6 mm in length, lance-shaped to ovate. Disc is five lobed. Stamens are 8 in number, free, filaments are 2 to 3 mm in length. Ovary is three locular, ovoid and approximately 3 mm in length, velvety in appearance, having 1 ovule in each locule. Fruit is 2 to 3 lobed, length is 1.3 to 2 cm, velvety while young, hard and plane as mature. Each cell has a about 6 to 9 mm black and round seed, which is famous as a washing soap traditionally. Flowering period is from November to January (Naidu et al., 2000).

Pitch black seed with rounded shape, seed size 112mm. We examined that seed is the largest among other observed species in present findings. Seed coat ornamentation has been noticed as irregular polygons often triangular or pentagonal. Anticlinal and periclinal wall both are thick to thin (Plate 8).

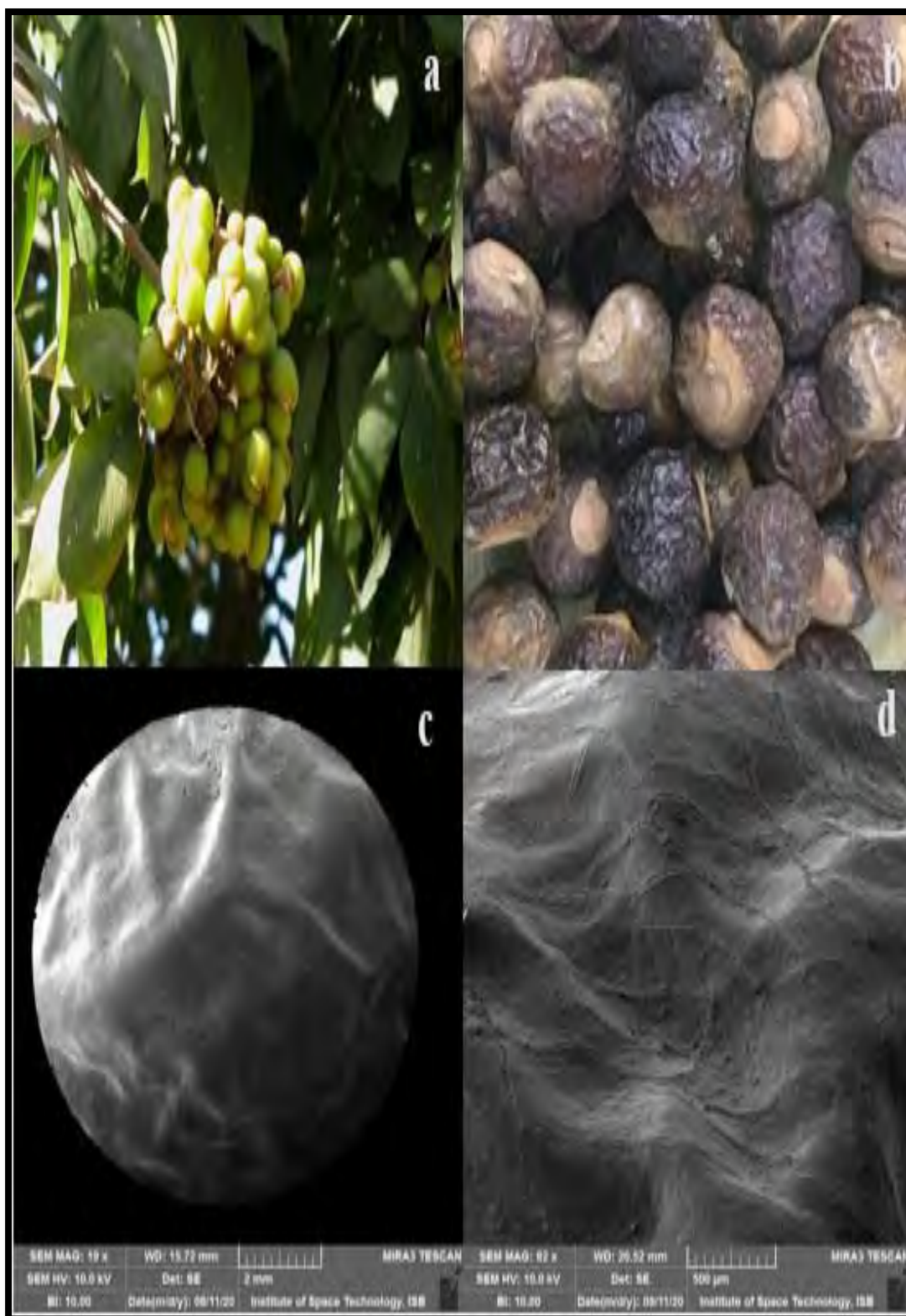


Plate 8: (a) *Sapindus trifoliatus* L. Plant, (b) Seeds, (c, d) SEM of Seed Surface and Sculpturing

3.1.9 *Sesamum indicum* L.

Sesamum indicum L. is an annual flowering plant of family Pedaliaceae. *Sesamum indicum* grows to 1 m (3ft 3in) by 0.5 m (1ft 8in). The flowers are gentle, and commonly of white, yellow, pink, pale blue or pale purple color having 5 to 10 petals. The fruit is a large and inflated capsule consisting of 3 to 7 united follicles, each having numerous seeds (Furat & Uzun, 2010).

The seeds are black colored, trigonus, angular, rugulose-tubercular, 3 mm in length (Plate 9; b, c). Thick periclinal wall is flat to convex. And seed surface is reticulate (Plate 9; d) (table 3.1).



Plate 9: (a) *Sesamum indicum* L. Plant, (b) Seeds, (c, d) SEM of Seed Surface and Sculpturing

3.1.10 *Ricinus communis* L.

Castor oil plant belonging to family Ranunculaceae, is a fast-growing, sucker and perennial shrub or seldom a soft wooded small tree approximately 6 m in length. Color of leaves is green or reddish, and generally 30 to 60 cm in diameter in length. The leaves contain 5 to 12 deep lobes with indelicately saw-like sections which are alternate and palmate. The stems are variable in pigment. The flowers are monoicous and roughly 30 to 60 cm in length. The seeds are variable in size and color. They are ovoid in shape, slightly compressed, 8 to 18 mm in length and 4 to 12 mm in width. The testa is smooth, thin and hard. Seeds have a caruncle, present typically at one end from which runs the raphe to terminate in a slightly raised chalaza at the opposite end of the seed (Nahar, 2013).

Reddish brown hexagonal seeds with shiny surface (Plate 10; b, c). Seed size is 60 mm. Prominent narrowly conical caruncle, sub stipitate, yellowish-white and pilose. And seed surface is Smooth, mottled (Plate 10; d).

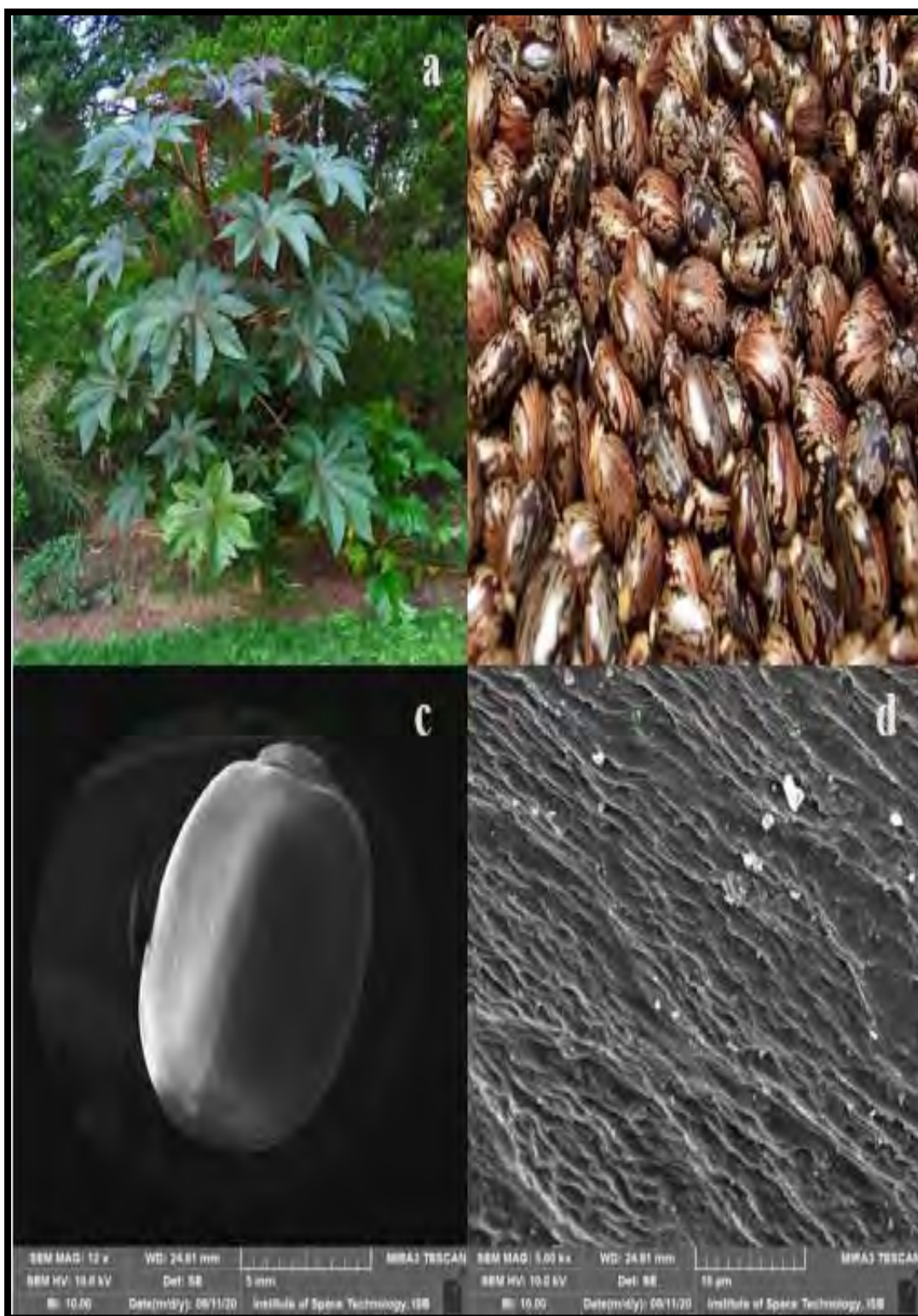


Plate 10: (a) *Ricinus communis* L. Plant, (b) Seeds, (c, d) SEM of Seed Surface and Sculpturing

Table 3.1: Micro morphological characteristics of oil yielding seeds determined via LM and SEM

PLANT	SEED COLOUR	SEED WEIGHT g	SEED LENGTH mm	SEED WIDTH mm	L/W RATIO	SEED SIZE(L×W) Mm	SEM DETERMINED MICROMORPHOLOGICAL FEATURES
<i>Brassica oleracea</i> L.	Pitch black	0.298	2	1.5	1.33	3	Rounded, glabrous surface, Anticlinal wall are identical. Seed wing are absent. Seed coat ornamentation having fabricated pattern with deep depression. Rift and wax-like pellicle of different size present on the surface of the seed
<i>Carthamus oxycantha</i>	Greenish grey	0.094	3.9	1	3.9	3.9	Greyish elliptic-oblong achene, smooth surface, Anticlinal walls are thick. Seed surface cells were elongated with rough texture. Seed ornamentation ruminant-gebulate. Each cell is identical with boundaries
<i>Carthamus tinctorius</i>	Yellowish white	0.024	7	5	1.4	35	Yellowish white narrow obovate achene with shiny surface, Anticlinal walls are thin. Seed sculpture ornamentation observed fine variegated. Obovate hilum was noted in achene.

<i>Carthamus lanatus</i>	Brown	0.02	4	2	2	8	Brownish narrow obovate seed with shiny surface, Anticlinal walls are thin. Seed sculpture ornamentation was observed to be fine variegated. Obovate hilum was observed in the achene
<i>Beaumontia grandiflora</i> Wall.	off-white						The largest seed size is measured in <i>B. grandiflora</i> . Seed and wing surface ornamentation have aculeate ornamentation while hilum surface show irregular Off white seed with flattened shape, Seed wing consist of round, thick to thin anticlinal wall
<i>Acasia concinna</i>	Brownish black	0.14	8	4	2	32	Reddish brown oblong achene, Seed poles are rounded, Areole is linear oblong, surface pattern was irregularly reticulate-foveolate with thick anticlinal ridges
<i>Sapindus trifoliatius</i>	Pitch black	1.78	14	8	1.75	112	Pitch black seed with rounded shape, Seed coat ornamentation has been noticed as irregular polygons often triangular or pentagonal. Anticlinal and periclinal wall both are thick to thin
<i>Sesamum indicum</i>	Black	0.41	3	1	3	3	The seeds are black colored, trigonus, angular, regulose-tubercular, Thick

							periclinal wall is flat to convex. And seed surface is reticulate
<i>Ricinus communis</i>	Light brown	0.24	12	5	2.4	60	Reddish brown hexagonal seeds with shiny surface, Prominent narrowly conical caruncle, sub stipitate, yellowish-white and pilose. And seed surface is Smooth, mottled
<i>Celastrus paniculatus</i>	Reddish brown	0.12	5	4	1.25	20	The seeds were brownish, elongated, flattened, polygonal or elliptic shaped and asymmetric, with periclinal wall protuberance, walls smooth, reticulate irregular, polygonal surface, papillae absent, slightly projected outwards, cell margins are somewhat straight-angular, anticlinal wall is slightly deep while outer periclinal wall is flat to slightly concave ¹

¹ Light microscope was used for the determination of the seed's length and width by placing the seeds under lens and then the L/W ratio and size (length x width) were calculated. The measurements of the L and W were repeated for approximately 10 times for each seed type. whereas seeds weight was calculated via measuring number of seeds per gram and then dividing it by hundred. However, seed colour was examined with naked eye.



Section II: Catalysts Characterization

Prepared single metal (Al), double metal (Na-Ag) and triple metal (Cu-Mg-Zn) montmorillonite clay catalysts were characterized using techniques like SEM, EDS, FTIR and XRD. Each of which are discussed in detail below.

3.2.1 Characterization of Al Montmorillonite Clay Catalyst

Inorganic clays (unmodified Mmt) have previously been used as a catalyst to carry out the transesterification of the edible oils to biodiesel. But showed less catalytic power when used unmodified as compared to modified ones. Manipulation of Montmorillonite Clay with Al metal through impregnation method at different temperatures showed high catalytic performance.

Therefore, single metal (Al-Mmt) montmorillonite clay catalyst was characterized using SEM, EDS, FRIT and XRD techniques to get the insight about its structure. Each of these are discussed in detail below.

3.2.1.1 Scanning Electron Microscopy of (Al) Montmorillonite Clay Catalyst

SEM is a technique widely used for the examination of the wide range of surfaces. The scanning electron micrograph of raw Mmt (uncalcined and unmodified) and calcined and modified Mmt clay catalyst with Al at 500°C temperature are shown in figure 3.2.1.1. The SEM image of raw Mmt clay shows its porous smooth surface having foliated constructions, giving frothy and fluffy appearance due to compact arrangement of flakes. SEM of the modified calcined clay shows agglomerated porous structures having multiple sites for reaction on the surface of large flakes (Figure 3.2.1.1 C & D). Difference of the morphology can easily be observed between raw and Al modified Mmt clay. The porous surface with significant number of available sites (Figure 3.2.1.1 d) added to the catalytic activity than the raw unmodified clay sample. This is reinforced by the fact that the catalytic efficiency of the Al-Mmt clay catalyst is significantly higher in transesterification of non-edible oils to biodiesel.

3.2.1.2 EDS Analysis of (Al) Montmorillonite Clay Catalyst

Energy Dispersive X-ray Spectroscopy was used to analyze the chemical composition of the Al modified Montmorillonite Clay Catalyst. The catalyst contained

34.27 wt% Pd, 23.96 wt% O, 12.38 wt% Si, 9.48 wt% Al, 8.58 wt% Fe, 5.52 wt% In, 4.48 wt% Sb, 1.82 wt% Ca, 1.61 wt% K. Presence of Aluminum confirms the formation of Al-Mmt clay catalyst (Figure 3.2.1.2).

3.2.1.3 FT-IR of Al-Mmt Clay Catalyst

FT-IR was used to analyze the different functional groups present on the surface of the Al modified Mmt clay catalyst (Figure 3.2.1.3). Basically FT-IR was done to obtain the information about the functional groups present on the surface of the catalyst. The peak at 997.25 cm^{-1} is due to the stretching vibrations in the plane of Si-O-Si present in the layered silicates. Furthermore, transmittance in the range of 778.16 cm^{-1} to 860 cm^{-1} are due to the stretching vibrations of Si-O-Al plane as reported previously in the literature. The transmittance peaks below 600 cm^{-1} reflect the presence of metal oxides (Figure 3.2.1.3).

3.2.1.4 XRD of Al-Mmt Clay Catalyst

X-ray diffraction technique at 40 Kv was used to examine the structure and morphology of synthesized Al-Mmt nanoparticles (Noor et al., 2018; Manyasree et al., 2018). $\text{CuK}\alpha$ radiation was used and pattern recorded at grazing incidence angle (3°) in 2θ range of 20° to 80° degree. XRD pattern of Al-Mmt indicate that it is in cubic shape. The peaks observed in the pattern expressively supported the formation of nanosized Al particles (Figure 3.2.1.4). The observed diffraction peaks and their intensities matches well with the reported values JCPDS file. XRD pattern of Al nanoparticle exhibited diffraction peaks at 2θ angles around 20° (100), 25° (101), 27° (110), 30° (102) and 46° (201). Average particle size was calculated and was found to be 83.50 nm. The lattice constant 0.614 using Debye Scherrer formula

$$D=0.9\lambda/\beta\cos\theta$$

Where, 0.9 is the shape factor, D is the crystalline size, λ is the wavelength of radiation, β is full width half maximum (FWHM) of the diffraction peak in radians and θ is Bragg's angle of X-ray diffraction peak (Farahmandjou and Golabiyani, 2015; Dhawale et al., 2018).

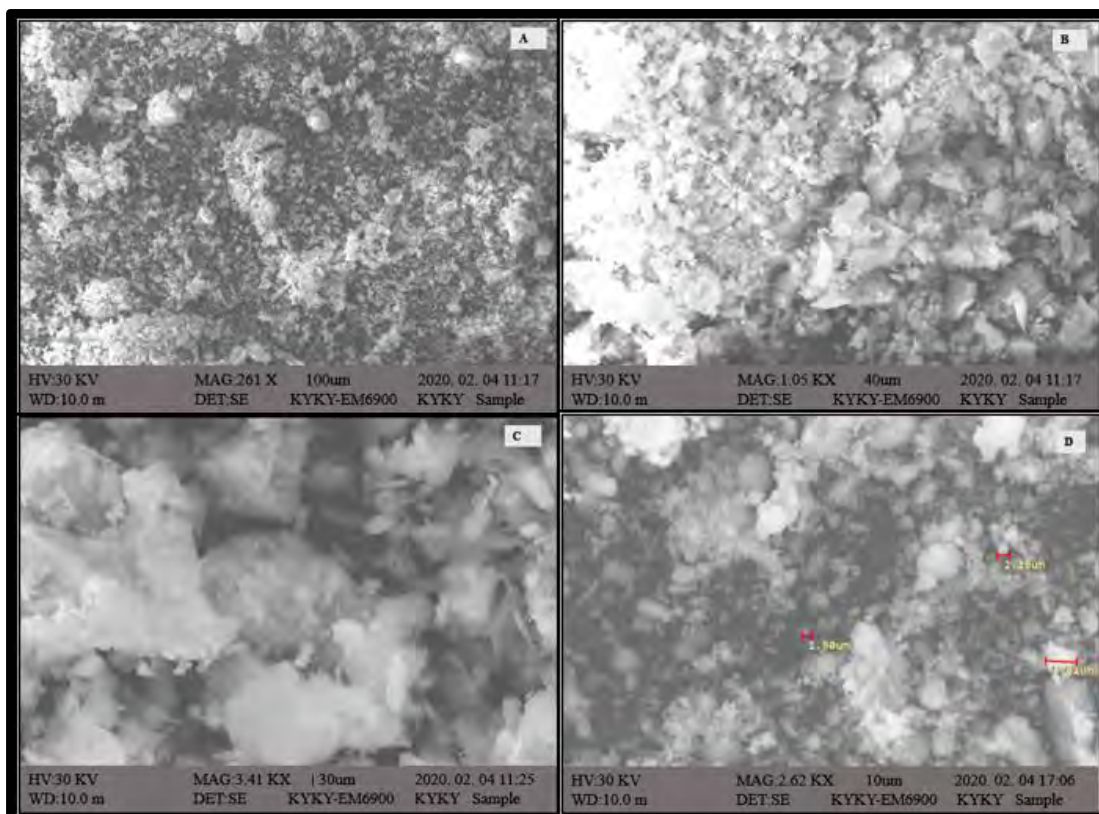


Figure 3.2.1.1: Scanning Electron Micrograph of Raw Mmt Clay (A), Scanning Electron Micrograph of Calcined Mmt Clay (B), Electron Micrograph of Al-Mmt Clay Catalyst at Different Resolutions (C, D)

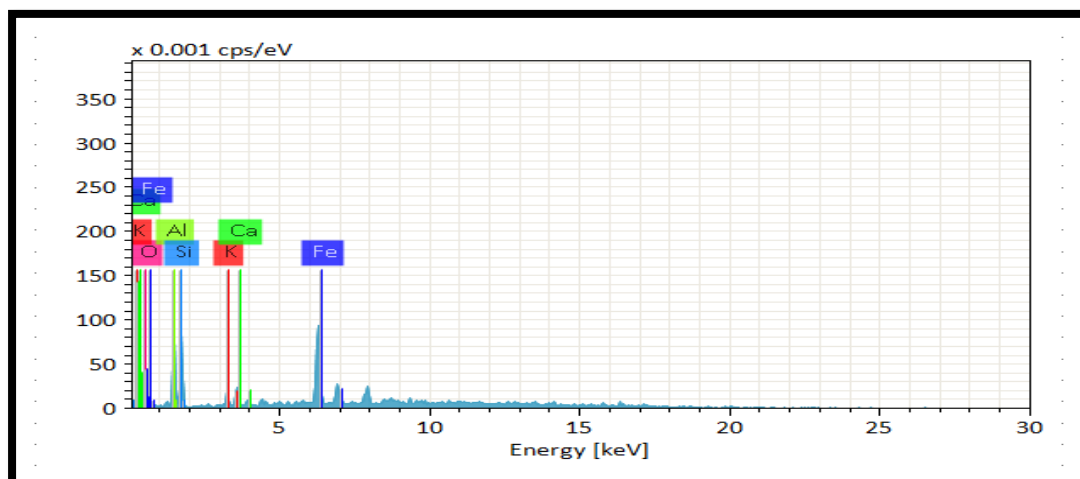


Figure 3.2.1.2: Energy Dispersive X-ray Spectroscopy of Al-Mmt Clay Catalyst

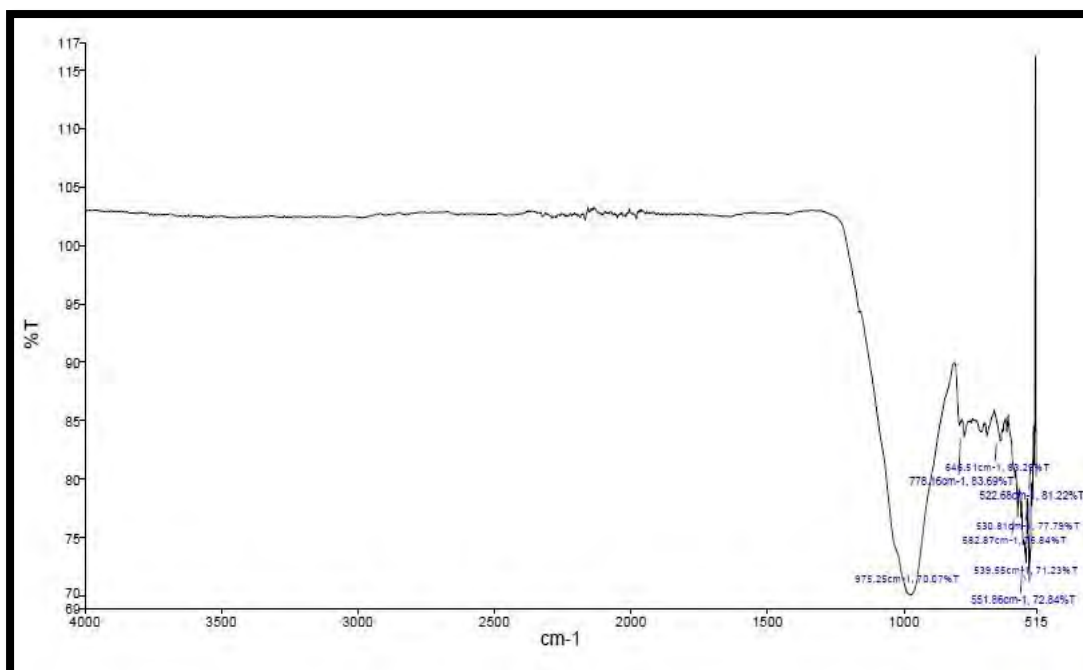


Figure 3.2.1.3: FT-IR Spectra of Al-Mmt Clay Catalyst (500°C calcination temperature) Showing Transmittance peaks at Different Wavelengths of IR Region

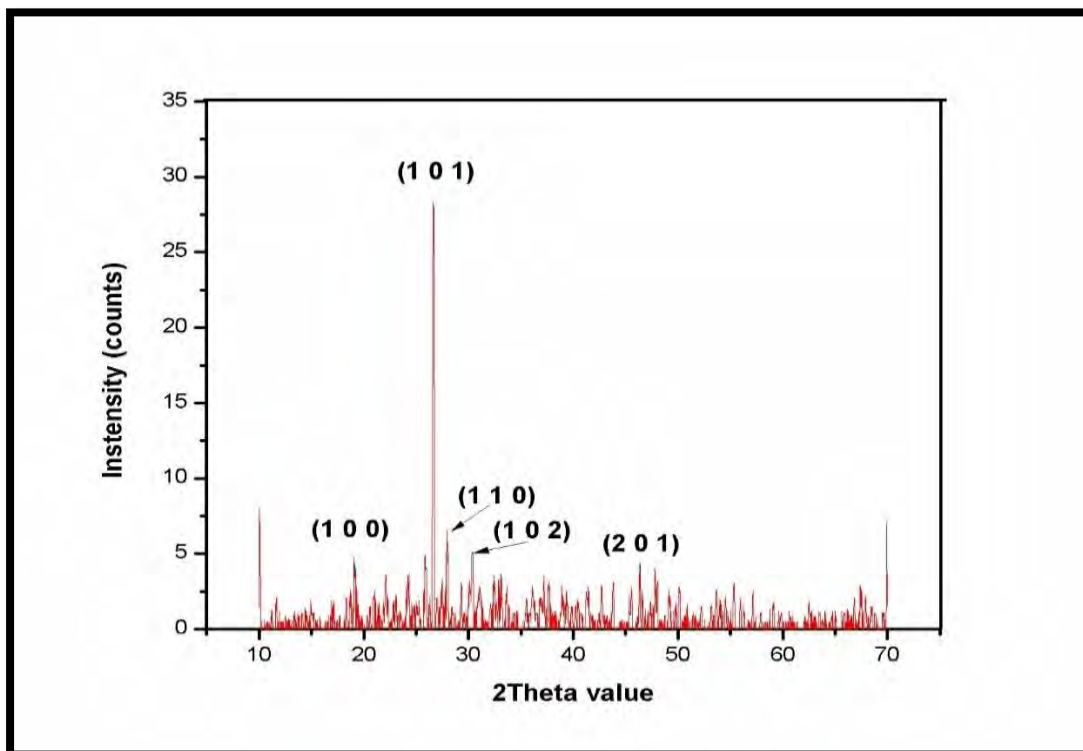


Figure 3.2.1.4: XRD Pattern of Al-Mmt Clay Catalyst

3.2.2 Characterization of Na-Ag Montmorillonite Clay Catalyst

Untreated Mmt clay, when modified with desired metals via impregnation and subsequent calcination gives promising results due to increase in the catalytic properties. Therefore, the Na-Ag- Mmt clay catalyst was synthesized and different techniques were used to get an insight about its structure and composition which are discussed below.

3.2.2.1 Scanning Electron Microscopy of Na-Ag Montmorillonite Clay Catalyst

SEM was used for the determination of the surface morphology of the raw Mmt (uncalcined and unmodified) and calcined and modified Mmt clay catalyst with Na-Ag at 500°C temperature are shown in figure 3.2.2.1. The SEM image of raw Mmt clay shows its porous smooth surface having foliated constructions, giving frothy and fluffy appearance due to compact arrangement of flakes manipulated clay catalyst. Unmodified Mmt clay has very compact structure having particles stacked over one another. However, Na-Ag-Mmt clay surface morphology obtained through SEM indicates it's to be more porous and smaller particles as compared to raw clay, providing more surface area (Figure 3.2.2.1, C, D). Thus, adding to the catalytic properties of the raw Mmt clay.

3.2.2.2 EDS Analysis of Na-Ag Montmorillonite Clay Catalyst

Elemental composition of the catalyst was determined using energy dispersive Xray spectroscopy (EDX) as shown in the figure 3.2.2.2. Catalyst was found to have 1.37% sodium (Na) and 2.08% silver (Ag). Fractions of other elements present in the Mmt clay catalyst included; C, O, Fe, Si, K. The modified clay catalyst significantly increases the rate of transesterification of seeds oils to biodiesel. Na-Ag-Mmt clay catalyst gave 90% yield of Acasia concinna biodiesel (ACB).

3.2.2.3 FT-IR of Na-Ag Montmorillonite Clay Catalyst

Functional group analysis of the Na-Ag-Mmt clay catalyst was done through FT-IR (Figure 3.2.2.3). It is a helpful technique as it gives information about both infra-red and finger-print region. Absorption bands of metals are generally below 1000 cm^{-1} . Furthermore, transmittance in the range of 927.14 cm^{-1} to 614.68 cm^{-1} are due to the

stretching vibrations of Si-O-Al plane as reported previously in the literature. The transmittance peaks below 600 cm^{-1} reflect the presence of metal oxides

3.2.2.4 XRD of Na-Ag Montmorillonite Clay Catalyst

The XRD pattern of prepared Na-Ag-Mmt was recorded by using Bruker d8 Advance X-ray diffractometer. $\text{CuK}\alpha$ was used as a radiation source, 40kV-40mA current range and $2\theta/\theta$ scanning mode were employed. Data was taken from the 2θ range of 20° to 80° degree. The diffractogram has been compared with JCPDS card (Shameli et al., 2012; Metha et al., 2017). Three peaks at 2θ of 26.18° , 33.10° , 46.40° have been identified due to silver and sodium metal could be attributed to (hkl) planes of (111), (200) and (220). Thus, the XRD pattern clearly illustrates that there are no impurities were found and no other phases were observed (Figure 3.2.2.4). The resultant particles in the prepared sample are Na-Ag-Mmt having hexagonal structure. The average particle size D was calculated by using Debye Scherrer equation. The average crystallite size of Na-Ag-Mmt particles at 24 hours of stirring are found to be 67.519 nm. Therefore, the XRD analysis confirmed that Na-Ag-Mmt nanoparticles with defined proportions can be synthesized by the reduction of metal ion.

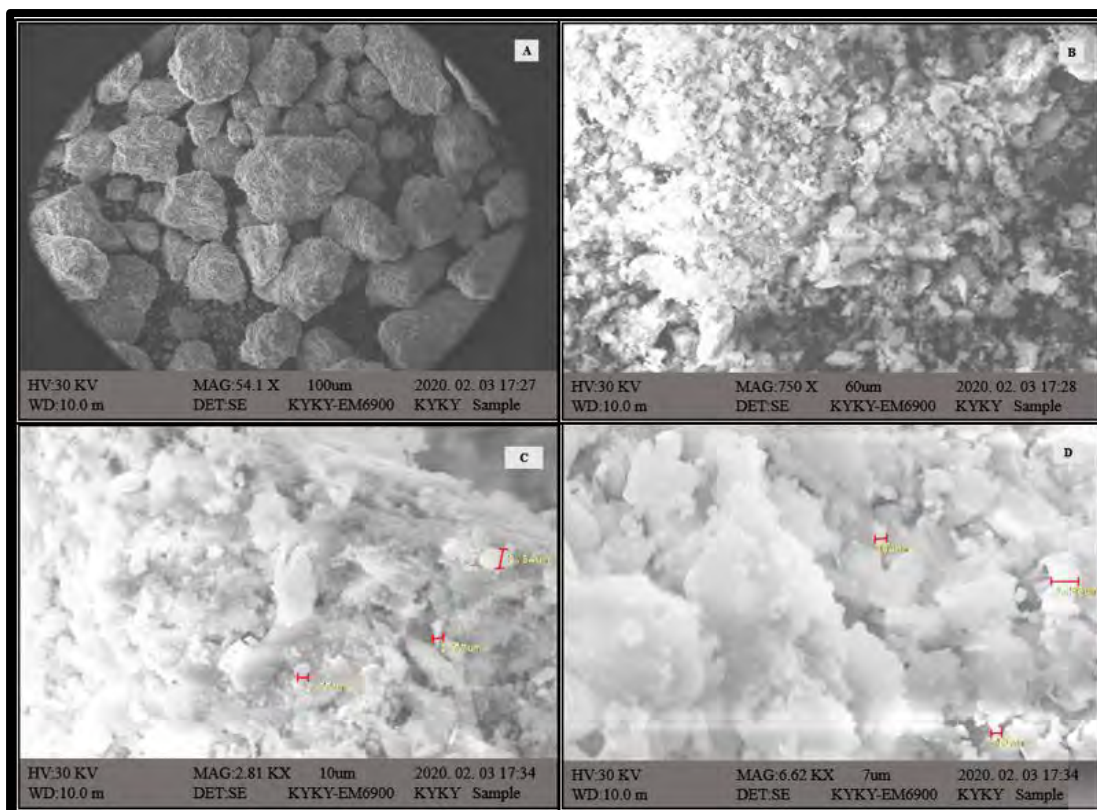


Figure 3.2.2.1: Scanning Electron Micrograph of Raw Mmt Clay (Raw) (A), Scanning Electron Micrograph of Calcined Mmt Clay (B), Scanning Electron Micrograph of Na-Ag-Mmt Clay Catalyst at Different Resolutions (C, D).

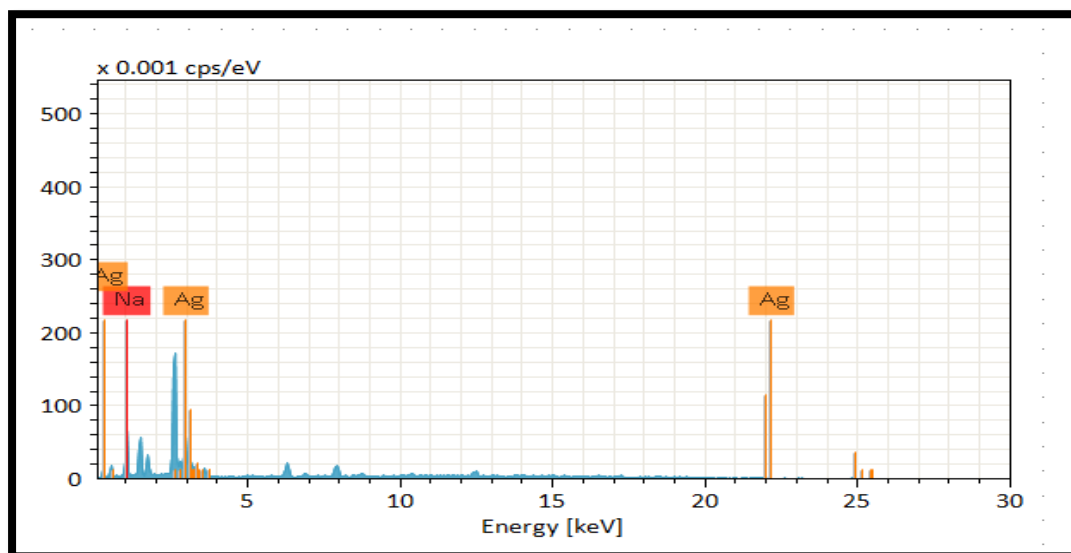


Figure 3.2.2.2: Energy Dispersive X-ray Spectroscopy of Na-Ag-Mmt Clay Catalyst

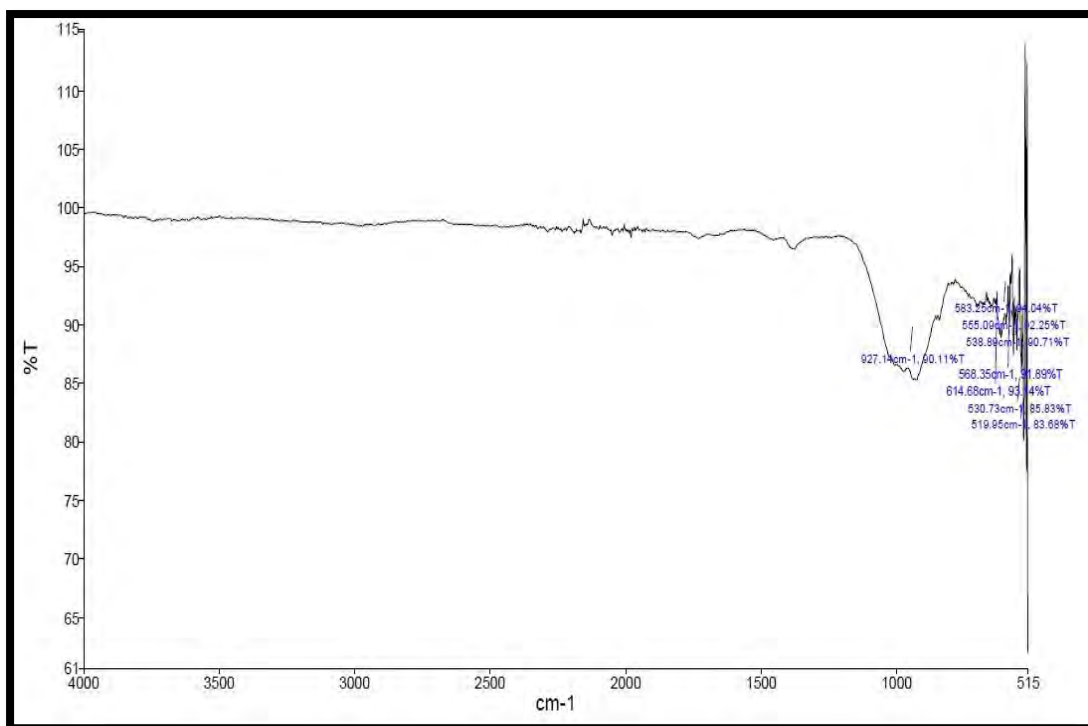


Figure 3.2.2.3: FT-IR Spectra of Na-Ag-Mmt Clay Catalyst (500°C calcination temperature) Showing Transmittance peaks at Different Wavelengths of IR Region

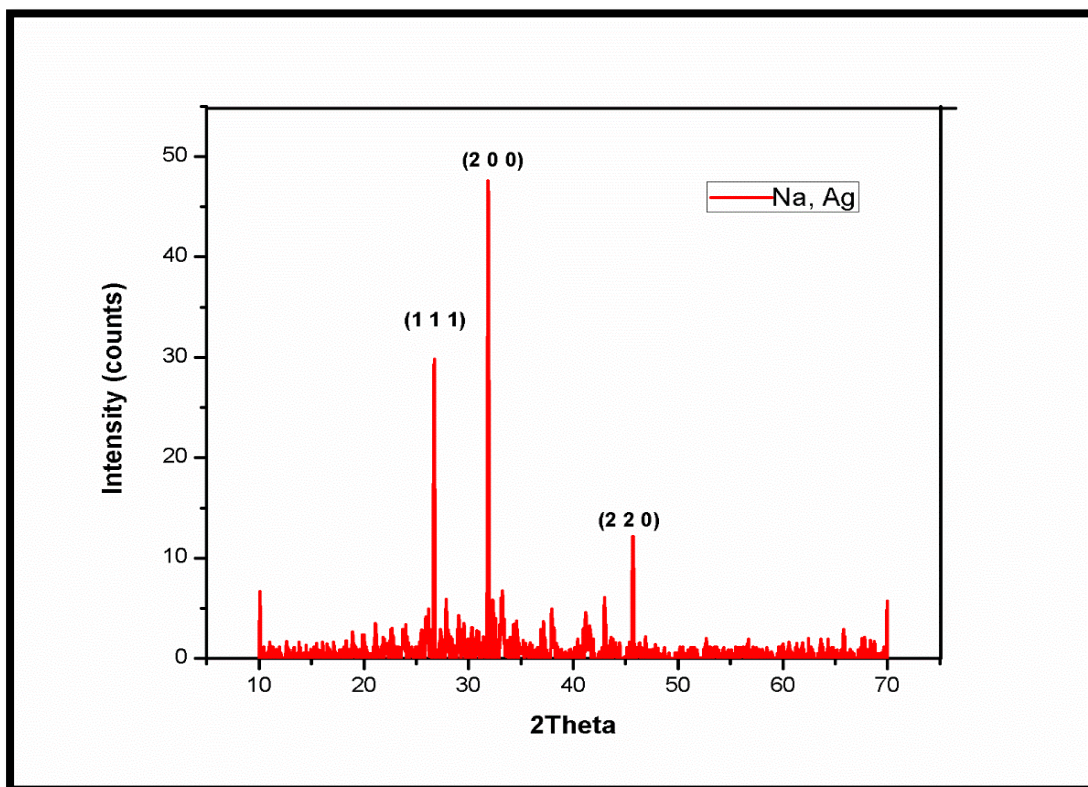


Figure 3.2.2.4: XRD Pattern of Na-Ag-Mmt Clay Catalyst

3.2.3 Characterization of Cu-Mg-Zn Montmorillonite Clay Catalyst

Cu-Mg-Zn-Mmt clay catalyst shows best catalytic results in the transesterification of the selected feed stocks to biodiesel. Details about its structure and composition are discussed below.

3.2.3.1 Scanning Electron Microscopy of Cu-Mg-Zn-Mmt Clay Catalyst

SEM was used for surface examination of the raw Mmt (uncalcined and unmodified) and calcined and modified Mmt clay catalyst with Na-Ag at 500°C temperature are shown in figure 3.2.3.1. The SEM image of raw Mmt clay indicates its spongy plane surface with foliated structures due to dense arrangement of flakes and particles stacked over one another (Figure 3.2.3.1 A, B). SEM was used for the characterization of the surface morphology of the montmorillonite triple metal (Cu-Mg, Zn) clay catalyst. The SEM images of calcined modified clay with Cu, Mg and Zn are shown in figure. 3.2.3.1 (C, D). It is observed that the modified calcined clay has big porous aggregates, probably due to providing sites for extra bonding that enables for agglomeration.

3.2.3.2 EDS of Cu-Mg-Zn Montmorillonite Clay Catalyst

EDX was used for stoichiometric analysis of the elemental composition of the catalyst. The Cu-Mg-Zn Mmt has 11.92% Zn, 3.44% Cu and 2.78% Mg alongside the other components of the montmorillonite clay i.e 2.49% O, 8.51% C, 5.81% Ag, 1.46% Ca, 0.81% Ba, 10.87% Si etc. presence of copper, magnesium and zinc in the clay confirms the formation of tri metallic montmorillonite clay catalyst (Figure 3.2.3.2).

3.2.3.3 FTIR of Cu-Mg-Zn Montmorillonite Clay Catalyst

FT-IR was used for functional group analysis. Absorption bands of metals are generally below 1000 cm^{-1} . The peak at 1438 shows bending of O-H group. The peak at 994.93 indicates the bending of C=C bond in alkane group. The peak at 779 shows the bending of C-H bond. The peak at 572.25 and 554.55 shows the strong stretching of halo compound (Figure 3.2.3.3). The transmission bands around 572 cm^{-1} and 535 cm^{-1} correspond to the vibration of Cu-O bond of CuO (Viter & Iatsunskyi, 2018,

Priscilla et al, 2017). The peak at 429 cm^{-1} represents the stretching vibrations of Mg-O bond (Mageshwari, 2013). The peaks in the range of 552 cm^{-1} to 417 cm^{-1} are due to the stretching of Zn-O bond (Labhane, 2015).

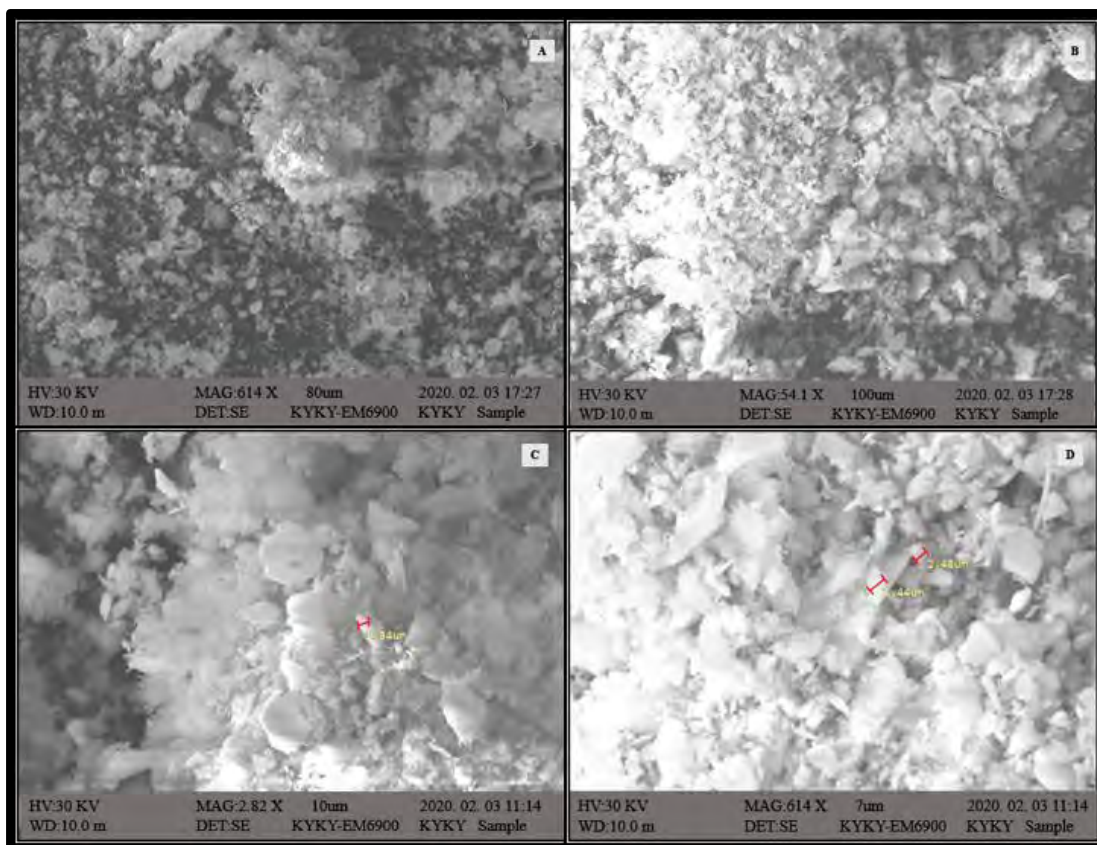


Figure 3.2.3.1: Scanning Electron Micrograph of Raw Mmt Clay (A), Scanning Electron Micrograph of Calcined Mmt Clay (B), Scanning Electron Micrograph of Cu-Mg-Zn-Mmt Clay Catalyst at Different Resolutions (C, D)

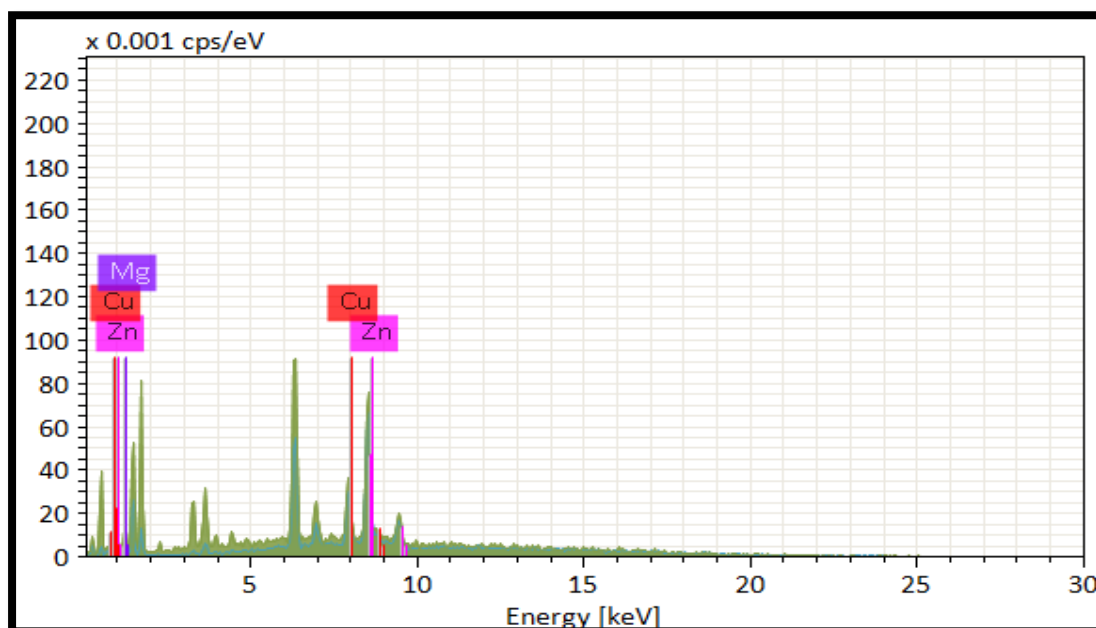


Figure 3.2.3.2: Energy Dispersive X-ray Spectroscopy of Cu-Mg-Zn-Mmt Clay Catalyst

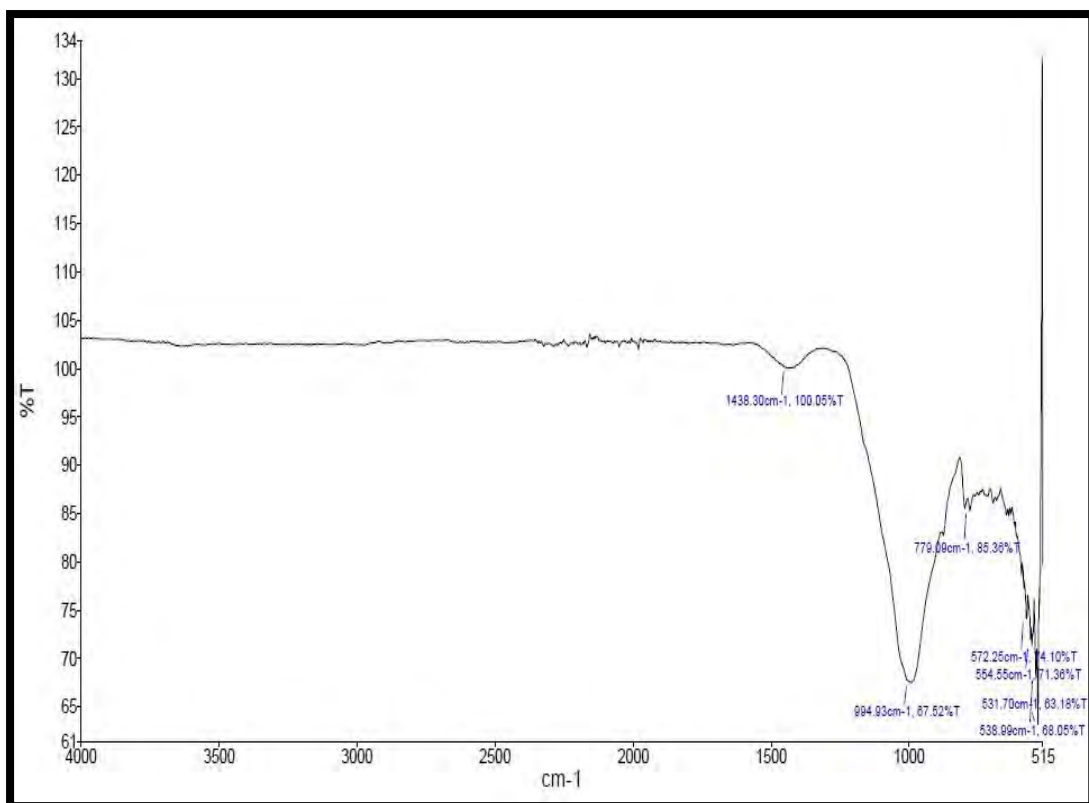


Figure 3.2.3.3: FT-IR Spectra of Cu-Mg-Zn-Mmt Clay Catalyst (500°C calcination temperature) Showing Transmittance peaks at Different Wavelengths of IR Region

**Section III: Biodiesel synthesis from ten
different non-edible oil yielding
seeds**

In this study ten non-edible seeds oils were used as potential biodiesel feed stock on laboratory scale. All the sources show promising results. Detail of biodiesel produced from each of these feedstocks is discussed in detail in this section. The oil content, FFA account of the under-discussion oil yielding seeds, biodiesel yield, FFA analysis and world distribution are discussed as well (Table 3.3.1). Of all the selected feed stock, *Brassica oleracea* L., *Carthamus lanatus* and *Beaumontia grandiflora* are explored for the very first time for the purpose of biodiesel synthesis. And are discussed in detail in the coming sections along with other non-edible feedstocks.

Table 3.3.1: Characteristics of oil yielding seeds

PLANT	FAMILY	ENGLISH NAME	OIL CONTENT	FFA (mg KOH/g)	FATTY ACID COMPOSITION OF OIL
<i>Brassica oleracea</i> L.	Brassicaceae	Broccolini	42.20%	0.329	C16:0, C18:0, C18:1, C18:2, C18:3, C20:1, C22:1 (Leonardo Velasco, Fernando D. Goffman & Heiko C. Becker, 1998)
<i>Carthamus oxycantha</i>	Asteraceae	Safflower	29.20%	0.219	C16:0, C18:0, C18:1, C18:2 (Carapetian, Jirair & Zarei, Gholamreza. 2005.)
<i>Carthamus tinctorius</i>	Asteraceae	Safflower	28.80%	0.264	C16:0, C18:0, C18:1, C18:2 (Umit et al., 2007)
<i>Carthamus lanatus</i>	Asteraceae	Safflower	22.40%	0.214	C16:0, C18:0, C18:1, C18:2, C18:3 (Sabzalian et al., 2008)
<i>Beaumontia grandiflora</i> wall	Apocynaceae		25.79%	0.352	C12:0, C14:1, C14:0, C15:0, C16:0, C16:1, C18:0, C18:2, C18:3, C19:0, C20:0, C22:0 (Abdelshafeek et al., 2010)
<i>Acasia concinna</i>	Fabaceae	Sekakai	22.00%	1.183	C16:0, C18:0, C18:1, C18:2, C18:3 (Saxena et al., 2019)

<i>Sapindus trifoliatus</i>	Sapindaceae	Soapnut	43%	1.071	C16:0, C18:0, C18:1, C18:2, C20:0, C20:1, C22:0 (Lovato et al., 2014)
<i>Sesamum indicum</i> L	Pedaliaceae	Black sesame seed	48%	0.028	C16:0, C18:0, C18:1, C18:2 (El Khieret al., 2008)
<i>Ricinus communis</i>	Ranunculaceae	castor oil	54%	0.637	C16:0, C18:0, C18:1, C18:2, C18:3 (Ogunniyi., 2006)
<i>Celastrus paniculatus</i>	Ranunculaceae	staff tree	55%	0.098	C14:0, C16:0, C18:0, C18:1, C18:2, C18:3 (Ramadan et al, 2009)

3.3.1 *Brassica oleracea* L. Biodiesel

3.3.1 *Brassica oleracea* L. Biodiesel

Brassica oleracea L. has 42% oil content and free fatty acid content is 0.329 which means it only requires one step transesterification to be converted into biodiesel. A series of transesterification reactions were carried out to get the optimum yield of the biodiesel produced from the seeds oil of *Brassica oleracea* L. The conditions at which optimum yield of the biodiesel from each of the seeds oil was obtained is given in table 3.3.1.1. All the three catalysts i.e. Al-Mmt clay catalyst, Na-Ag Mmt catalyst, Cu-Mg-Zn Mmt clay catalyst, were used in the transesterification of the seeds oil of *Brassica oleracea* L. to biodiesel but Al-Mmt clay catalyst gave the best yield among all.

3.3.1.1 Reaction Variables Affecting Transesterification of *Brassica Oleracea* L. Seeds Oil to Biodiesel

Transesterification is a reaction of an alcohol with a triglyceride molecule to form different types of esters in the presence or absence of a catalyst. And is the most common, easy and effective way of conversion of fatty acids into corresponding methyl esters. It is a reversible reaction and stoichiometric ratio of alcohol and triglyceride molecules is 3:1. Different factors which affect the rate of transesterification are; ratio of alcohol to oil, catalyst concentration, time and temperature of the reaction (Ferella et al., 2010).

A series of transesterification reactions were carried out to get the optimum yield of the *Brassica oleracea* L. biodiesel (BOB). The obtained biodiesel was separated from the glycerol and excess methanol via separating funnel. Afterwards, the resultant was washed, lukewarm water was added to the biodiesel and then centrifuged at 7000 rpm for 15 minutes (Atadashi et al., 2011). Then diesel layer was picked using micropipette and was saved in falcon tube for further analysis. The transesterification reactions were carried out using three variables i.e. oil to methanol molar ratio, catalyst concentration and reaction temperature. And their effect was noted to be as following:

3.3.1.1.1 Oil to Methanol Molar Ratio

One of the most important factors upon which the transesterification reaction depends is the oil to alcohol molar ratio. In the excess of alcohol, transesterification reaction follows pseudo first order in the forward and second order reaction kinetics in

the reverse direction. The stoichiometric ratio for FFAs conversion into esters requires 3 moles of alcohol and 1 mole of oil to produce 3 moles of fatty acid alkyl esters and 1 mole of glycerin (Meher et al, 2006). In the current scenario oil to methanol ratios of 1:3, 1:4, 1:5, 1:6, 1:7, 1:8, 1:9 and 1:10 were used keeping other reaction conditions constant i.e. reaction time, reaction temperature and catalyst concentration constant. The maximum conversion ratio was obtained at 1:7, 1:5 and 1:9 using Al-Mmt, Na-Ag-Mmt and Cu-Mg-Zn-mmt clay catalysts.

3.3.1.1.2 Catalyst Concentration

Another important factor which influences the yield of the fatty acid methyl esters (FAMES) is the type and concentration of the catalyst. Heterogeneous catalysts have many advantages over the homogeneous ones. As the catalyst is in different phase than the reaction mixture so catalyst is easily recovered after the reaction and reusability of the catalyst is enhanced significantly (Meher et al, 2006). Transesterification reaction for conversion of *Brassica Oleracea* seeds oil to FAMES, was carried out at different catalyst concentrations i.e. 0.1g, 0.2g, 0.3g, 0.4g, 0.5g, 0.6g and 0.7g and maximum yield of biodiesel was obtained at 0.3 g of Al-Mmt clay catalyst, 0.5g in case of Na-Ag-Mmt clay catalyst and 0.2g of Cu-Mg-Zn-Mmt clay catalyst gave best results.

3.3.1.1.3 Reaction Temperature (°C)

Temperature of the reaction and biodiesel yield are directly proportional i.e. increase in temperature results in the increase of the biodiesel yield up to the threshold point (>150°C) (Meher et al, 2006, Munir et al, 2019). A series of reactions were carried out at different reaction conditions keeping other factors constant i.e. methanol to oil molar ratio and catalyst concentration. Highest conversion ratio was achieved at 100 °C in case of Al-Mmt clay catalyst and 90 °C for Na-Ag-Mmt and Cu-Mg-Zn clay catalysts.

3.3.1.2 Chemical Characterization

3.3.1.2.1 GC-MS Analysis of *Brassica Oleracea* L. Biodiesel (BOB)

GC-MS analysis is broadly used technique to determine the chemical composition, type and structure of synthesized *Brassica Oleracea* FAMES. Mass spectrometer was set to scan in the range of m/z 2-600 and ionization potential 70V (Bu

et al., 2014; Zhang et al., 2014). Eight momentous peaks are observed and confirmed by Library match software (NO. NIST 11). Different FAMES were determined using the retention time by Mass Spectroscopic analysis (Dawood et al., 2018). Helium gas was used as a carrier with reaction temperature 300°C for 45 minutes. At peak 1 and 2, methyl alcohol (CH₃OH) were found. Methylenebutyronitrile at peak 3, 4,5-epithiovaleronitrile and Benzenepropanenitrile at 4 and 5, Hexadecanoic acid and 9, 12-Octadecadienal at 6 and 7 and Octadecanoic acid at peak 8, respectively as shown in Table. FAME's profile determines the suitability of feedstock for use in production of biodiesel fuel (Skoto et al., 2011). Results indicate that the abundantly present ester in *Brassica Oleracea* L. biodiesel is monounsaturated Methylene butyronitrile. This compound has propensity to give stability to methyl esters. High degree of unsaturation in biodiesel increase the polymerization tendency caused by peroxidation which reduces its uses as a fuel (Bamgboye & Hensen, 2008; Sokoto et al., 2011). High temperature accelerates the peroxidation reaction and combustion engine becomes gummed with polymerized FAMES. Hence the monounsaturated Methylene butyronitrile have not much affinity to oxygen that will lead to quick peroxidation. Nurdin et al., 2017 identified the different kind of methyl esters compound of biodiesel from crude palm oil. These are methyl hexadecanoate, methyl 9-octadecanoate, methyl octadecanoate and methyl 8,11-octadecadienoate (Table 3.3.1.2.1). The dominant ester compound was methyl 9-octadecanoate which confirms the formation of biodiesel (Nurdin et al., 2017). Qin et al., 2010 identified the main components in biodiesel from *Pistacia Chinensis* through GC-MS analysis. They are methyl palmitate, methyl linoleate, methyl oleate and methyl stearate which confirms the conversion of crude oil to biodiesel (Qin et al., 2010) (Figure 3.3.1.2.1).

3.3.1.2.2 FT-IR Analysis of *Brassica oleracea* L. Biodiesel

FT-IR is a faster analytical technique is used to identify the chemical bonds and explain its stretching and bending vibrations. It also determines the presence and absence of functional groups in chemical compounds (Shaheen et al., 2017). Figure 3.3.1.2.2 shows the FT-IR of *Brassica Oleracea* methyl esters. The alcohol (O-H) and aldehyde group were observed at 3007.62 cm⁻¹ and at 2922.07 cm⁻¹. A strong characteristic peak of alkane was observed at 2852.93 cm⁻¹. The ester group was found at 1743.67 cm⁻¹ and at 1710.28 cm⁻¹. The peak at 1458.49 cm⁻¹ shows the presence

of alkane (C-H) group whereas the peak at 1377.20 cm⁻¹, 1236.01 cm⁻¹, 1162.02 cm⁻¹ represents the presence of aliphatic amines (C-N) group. A strong ether group was found at peak 1099.06 cm⁻¹ whereas the bend of Alkanes (C-H) groups were present at 720.97 cm⁻¹. Rabelo et al., 2015 performed FT-IR analysis to confirm the presence of functional group in soybean biodiesel. The main spectrum region that differentiate between crude oil and its respective biodiesel is in the range of 1500-900 cm⁻¹. The peak at 1446 cm⁻¹ shows the asymmetric stretching of -CH₃ in biodiesel spectrum (Rabelo et al., 2015). Daniyan et al 2019 transesterified the palm oil. The FTIR also confirms the presence of ester carbonyl bond near the absorption band 1743.71 cm⁻¹ (Daniyan et al., 2019). Banik et al., 2018 performed FTIR analysis of neem biodiesel. It was found that the main functional groups carboxylic acid and alkanes were appeared at 1743.65 cm⁻¹ and 1462.04 cm⁻¹ respectively (Banik et al., 2018). Shah et al., 2016 examined the bio-oil obtained from fresh water alga (Spirogyra). FT-IR spectra indicates that (C-H) Alkane stretching at 2926.01 cm⁻¹ whereas alkane bending at 1384.89 cm⁻¹ occur and the peak intensity is variable. The strong intensity due to stretching vibration of ether group appears at 1273.02 cm⁻¹. The aromatic C=C stretching at 1537.27 cm⁻¹ which intensity is medium weak multiple band (Shah et al., 2016). Anisah et al., 2019 studied the effect of transesterification on the result of waste cooking oil conversion to biodiesel. FTIR analysis shows the Ester group at region 1300-1000 cm⁻¹ whereas C-H has a weak and sharp intensity peak at 2850-2750 cm⁻¹ (Anisah et al., 2019) (Table 3.3.1.2.2).

3.3.1.2.3 Fuel Properties of *Brassica oleracea* L. Biodiesel (BOB)

The fuel properties of synthesized *Brassica oleracea* L. biodiesel (BOB) were determined and compared with the ASTM standards (Table 3.3.1.2.3). Total acid number or acid value is the number of free fatty acids present in a fuel sample and expressed in mg KOH/gm. High acid value effects the engine efficiency (Akhtar et al., 2019).

The *Brassica oleracea* biodiesel (BOB) acid value (0.220mg KOH/gm) is well in range with international standards. The BOD density was 0.8544kg/L is also accordance with international standards. Fuel density has direct effect on fuel efficiency. Its greater value would cause corrosion in engine (Sultana et al., 2016). Kinematic viscosity shows the fuel stickiness. High viscosity fuel cause deposition in

engine and reduce its working (Gunstone & Hamilton, 2001). The kinematic viscosity of BOB was found 5.1 kg/L which is within the ASTM limits. The color of BOD is on visual 2 according to international standard. Flash point is an important property during fuel handling and transportation (Salaheldeen et al., 2015). It is the temperature at which fuel starts ignition. The flash point of BOB (81°C) was also in the range. Another important parameter is cold flow properties which includes Pour point and Cloud point of biodiesel (Akhtar et al., 2019). Pour point and cloud point value of BOB were -10°C and -13°C respectively. An ideal fuel has low sulfur content and is more operative for engine's life and environment (Candeia et al., 2009). The sulfur content in BOB was (0.00039ppm) by %weight.

3.3.1.3 Optimization Study of Transesterification Operational Factors Through Response Surface Methodology (RSM)

A Comprehensive experimental results of biodiesel yield, using four variables (oil methanol ratio, amount of catalysts, reaction temperature and time) are presented in Table 3.3.1.4. For optimization of transesterification process, four independent variables with maximum and minimum ranges i.e., Catalyst (A) 0.1-0.9 (Al-Mmt), Time (B) 1-7 hrs, Temperature (C) 60-120 °C and Oil to Methanol (D) 1:3-1:9 were chosen and 30 experiments were analyzed by RSM using the Box Behnken Design to test the fitness of Quadratic polynomial equation with the Design-Expert 11 (Stat Ease IncMinneapolis,USA). A coded model equation underneath representing Catalyst, Time, Temperature and oil to methanol ratio as A, B, C and D was used for studying the association among Input Variables as well as Output Response in terms of yield(Y).

$$Y = +10.96184 - 3.72735A + 0.016816B + 0.035001C - 3.11801D - 1.001065AB + 0.001247AC - 0.1793309AD + 4.16100E-07BC + 0.006211BD - 0.002336CD + 2.65398A^2 + 0.000095B^2 - 0.000181C^2 + 1.17505D^2$$

The quadratic surface response regression model as well as the regression coefficient produced via ANOVA results as presented in Table 3.3.1.4.1 help to maximize biodiesel (methyl esters) yield. The model F-value (69.67) and P-value (less than 1), depicting model significance for determining biodiesel yield. Moreover, The Lack of Fit F-value of 0.34 implies the Lack of Fit is not significant relative to the pure error. There is a 93.24% chance that a Lack of Fit F-value this large could occur due to

noise However, The Predicted R^2 of 0.9586 is in reasonable agreement with the Adjusted R^2 of 0.9707; i.e. the difference is less than 0.2, indicating the good correlation with the regression polynomial.. Adeq Precision measures the signal to noise ratio. A ratio greater than 4 is desirable. And ratio of 21.707 indicates an adequate signal. Thus, this model can be used to navigate the design space. Table 3.3.1.4, thus ensures the significance of the model terms like , (catalyst concentration) A, (process time) B, (process temperature) C, (methano oil ratio) D, (Catalyst and Time) AB, (Catalyst and temperature) AC, (Catalyst and methanol oil ratio) AD, (Time and oil to methanol ratio) BC, (Temperature and Oil to Methanol Ratio) BD, (process temperature and time) CD, (quadratic impact of Catalyst amount) A2, (quadratic impact of Time) B2, (quadratic impact of process temperature) C2, and (quadratic impact of Oil to Methanol Ratio) D2. These noteworthy model terms impact the yield of produced biodiesel.

3.3.1.4 Parametric characterization of transesterification process

The interactive effect of different variables on transesterification reaction was considered by drawing three-dimensional response curves versus every dual Independent variable whilst having other variable on pivotal point. The 3D response surface plot regarding the yield of the product was achieved using above equation and presented here in Figure 3.3.1.4 A, B, C, D, E & F. These plots help to comprehend different variables interactive effect, thus aid in locating optimal levels of every variable for the peak responses. Generally, it is expected that yield of biodiesel increases under optimum reaction conditions and sudden drop in yield was observed beyond the optimum level. The interactive effects of the transesterification process are explained in subsequent sub sections.

3.3.1.4.1 Interactive Impact of Catalyst Amount and Time

The combine influence of catalyst amount (wt%) and time (min) on biodiesel yield is presented in the Figure 3.3.1.4 A while keeping other parameters (oil: methanol ratio (1:7) and temperature (100°C)) constant. It is clear from the table that maximum BOBD (91.40%) obtained with the 0.3 wt% catalyst and steady rise in reaction time (60-120 min) owing to the more methoxy (-CH₃) species development by catalyst activity of and ultimately increased yield of biodiesel and equilibrium in the reaction. However, beyond the optimum values of catalyst concentration and reaction time,

sudden drop in yield was observed. This drop in yield might be linked to the shifting of reaction in opposite direction. Therefore, ANOVA results appears to be insignificant with Pvalue (0.5603) > 0.05 for time and catalyst on biodiesel yield.

3.3.1.4.2 Interactive Impact of Catalyst Amount and Temperature

The Figure 3.3.1.4 B represents the combined influence of catalyst concentration and temperature upon biodiesel yield. It is clear from the table that maximum FAMEs (91.40%) was obtained with the 0.3 wt% catalyst along with steady rise in temperature (80-100 °C) perhaps owing to more active site on the surface of catalyst to catalyze the reaction. However, lower conversion of FAMEs (77%) observed at 0.1% catalyst due to partial changeover of triglyceride to methyl ester, which is consistent with the previous study (García-Moreno et al., 2014). However, slight drop in BOB content was observed as the amount of catalyst increased beyond 0.87wt% up to 1wt%. This drop in FAMEs content might be due to reduced mass transfer and interaction between the reactant and catalyst. Therefore, it can be concluded from the results that the interactive outcome of these two parameters (time and catalyst amount) on biodiesel yields is in significant with Pvalue (0.5643) > 0.05.

3.3.1.4.3 Interactive Impact of Catalyst Amount and Oil: Methanol Ratio

The Figure 3.3.1.4 C represent three-dimensional surface plot showing collective effect of the catalyst and oil-methanol on yield of biodiesel based on the parameters set by Box-Behnken design experiment. It is observed that maximum biodiesel yield (91.40 %) is obtained with 1:7 oil: methanol ratio and 0.3 wt % catalyst. It is evident that there is a close agreement between these process parameters. Since both oil: methanol ratio and concentration of catalyst has the chief role for providing maximum biodiesel yield. The biodiesel yield increases considerably by increasing catalyst concentration from 0.1- 0.3% perhaps owing to more active site on the surface of catalyst to catalyze the reaction. However, lower conversion of 86 % FAMEs (0.9% catalyst) observed due to partial changeover of triglyceride to methyl ester, which is consistent with the previous study (García-Moreno et al., 2014). The slight drop in BOB content was observed as the amount of catalyst increased beyond 0.3wt% up to 1wt%. This drop in FAMEs content might be due to reduced mass transfer and interaction

between the reactant and catalyst, thus causing emulsification which would ultimately cause difficulty in separation of end products and contributing in decreased yield of FAMEs. However, ANOVA results depicts that oil: methanol and catalyst concentrations interactive effect are insignificant owing to their P-value ($P=0.7237$) which is > 0.05 .

3.3.1.4.4 Interactive impact of time and temperature

The time and temperature cooperative influence on the biodiesel yield is presented in the form of three-dimensional response surface plot in Figure 3.3.1.4 D based on the parameters set by Box-Behnken design experiment. It is clear from the data (Table 3.3.1.4.1) that a significant increase in yield (91.40%) was observed as the reaction time and temperature increases from 1 hrs-5 and 60-100 °C until a point where further increase in time (7 hrs) and temperature (>100 °C) show no significant changes in FAMEs content. This is so, as higher temperatures amenities ingenious dispersion of catalyst particle leading to mass transfer of reactor content. Higher temperatures also support the increased interaction among the protons which was produced by the interaction of mixed oxides catalysts and alcohol to the alkyl group present in triglycerides, making nucleophile, with subsequent reshuffle along with the transfer of proton, and hence, higher transition of oils to FAMEs. Conversely, temperature above the threshold level (> 100 °C) might initiates gasification of methanol leading to reduced FAME content. However, the short reaction time (1 hrs) and low temperature (70 °C) possibly do not allow the interaction of catalyst with oil leading to partially converted products. A slight decrease in FAMEs content at 4 hrs reaction time at 90 °C might be due to reserve transesterification reaction, making it unfavorable to obtain maximum FAMEs yield. The similar behavior was observed by (Ngamcharussrivichai et al., 2007; Olutoye et al., 2016), where higher FAMEs yield was found at higher reaction times (5hrs). The ANOVA results appears to be insignificant with P-value (0.9821) > 0.05 for time and temperature on biodiesel yield.

3.3.1.4.5 Interactive Impact of Time and Oil: Methanol Ratio

The time and oil: methanol collective impact on BOB yield is presented in the Figure 3.3.1.4 E while keeping other parameters like catalyst concentration (0.3wt%) and temperature (100°C) constant. The highest biodiesel yield (91.40%) is attained at

1:7 ratio of oil: methanol and 120 min time respectively. It is evident from the 3D plot that yield of biodiesel increases considerably by increasing the ratio of methanol. Therefore, determining the optimum ratios of these parameters is vital to amplify biodiesel yield. The two-sided mode of transesterification process thus necessitates the surplus alcohol to maintain the balance in reaction (higher conversion of oil to FAMES). Maximum BOB yield (91.40%) achieved at 1:7 oil to methanol and 5.5 reaction time due to increased interaction of excess methanol with oil. The low methanol ratio and short reaction time (1 hrs) and possibly do not permit the proper impregnation of modified clay with oil to achieve the equilibrium leading to partially converted products. In an earlier study on acorn kernel oil methyl esters and waste vegetable oil methyl esters, confirmed the strong influence of reaction time on product. However, decreased in BOB content was observed at the molar ratio of 1:9 related to the oils dilution effect thereby reducing the product yield. A slight decrease in FAMES content at 7 hrs reaction time might be due to reverse transesterification reaction, making it unfavorable to obtain FAMES yield. The similar behavior was observed by (Ngamcharussrivichai et al., 2007; Olutoye et al., 2016), where higher FAMES yield was found at higher reaction times (5hrs). Same trend was observed with 7 hrs reaction time with methanol ratio of 1:9, related to oil dilution effect that reduces end product yield. ANOVA results, however, proves their interactive outcome on final biodiesel yield appears to be insignificant with P-value (0.2745) > 0.05.

3.3.1.4.6 Interactive impact of oil: methanol ratio and temperature

The collective effect of the time and oil methanol collective impact on BOB yield is presented in Figure 3.3.1.4 F while keeping other parameters like catalyst represents the combined effect of oil:alcohol ratio and temperature on the biodiesel yield. Since, maximum biodiesel (91.04%) obtained with steady rise in temperature to 100 °C with 1:7 of oil to methanol. Conversely, temperature above the threshold level (> 100 °C) might initiates gasification of methanol leading to reduced FAMES content (Olutoye, Lee, & Hameed, 2011). This is so, as transesterification reaction is a three phase and endothermic so, an adequate amount of thermal energy is needed to overwhelm the dispersion of particles between these different phases (Oil, Methanol and catalyst). Therefore, it can be concluded from the results that combined impact of these parameters is insignificant with P-value > 0.05 (P=0.7198).

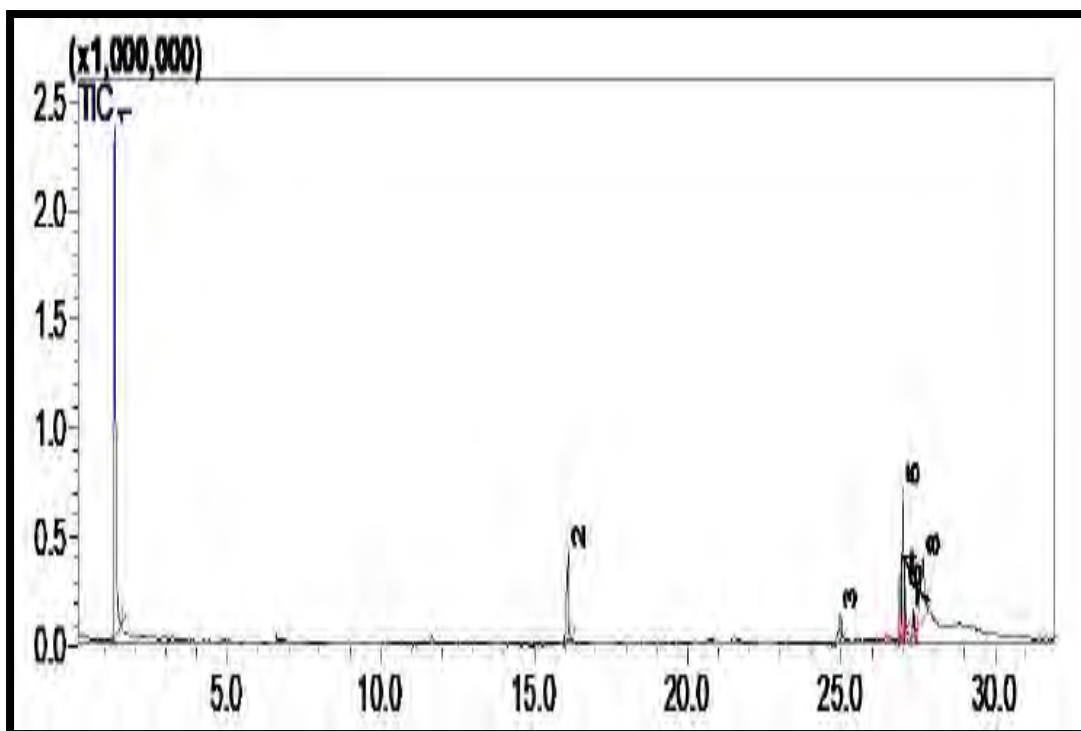


Figure 3.3.1.2.1: GCMS of *Brassica oleracea* L Biodiesel (BOB)

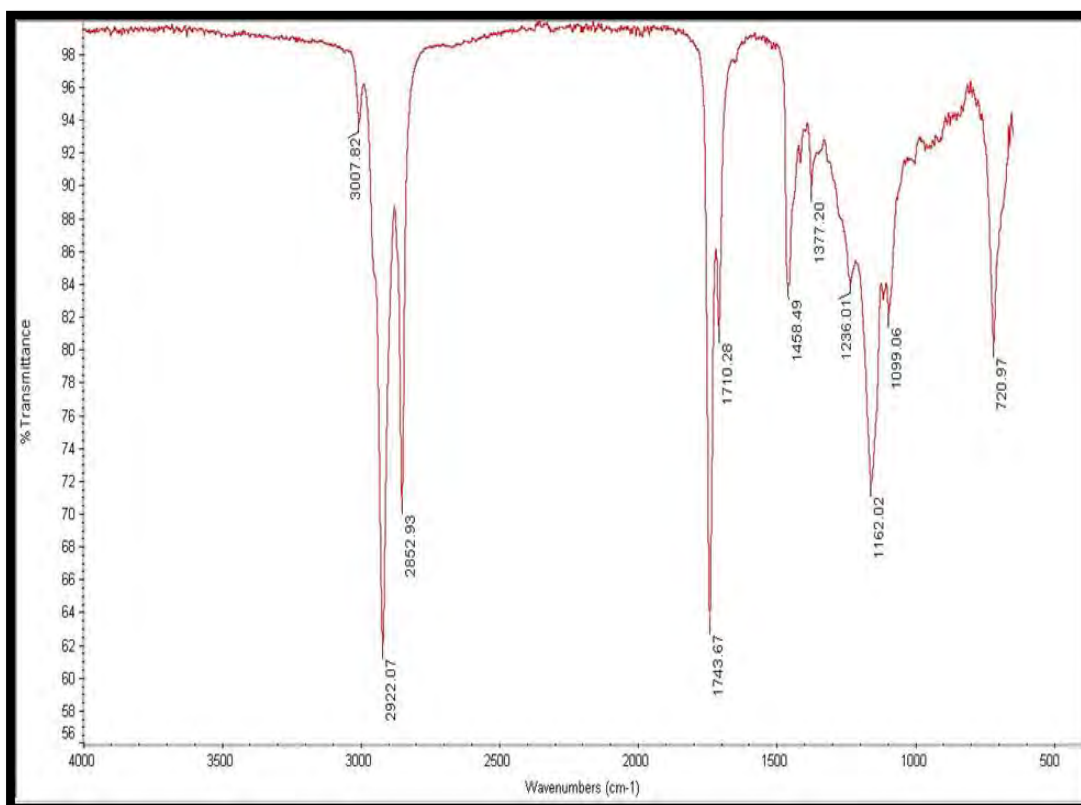


Figure 3.3.1.2.2: FTIR Spectrum of *Brassica oleracea* L. biodiesel (BOB)

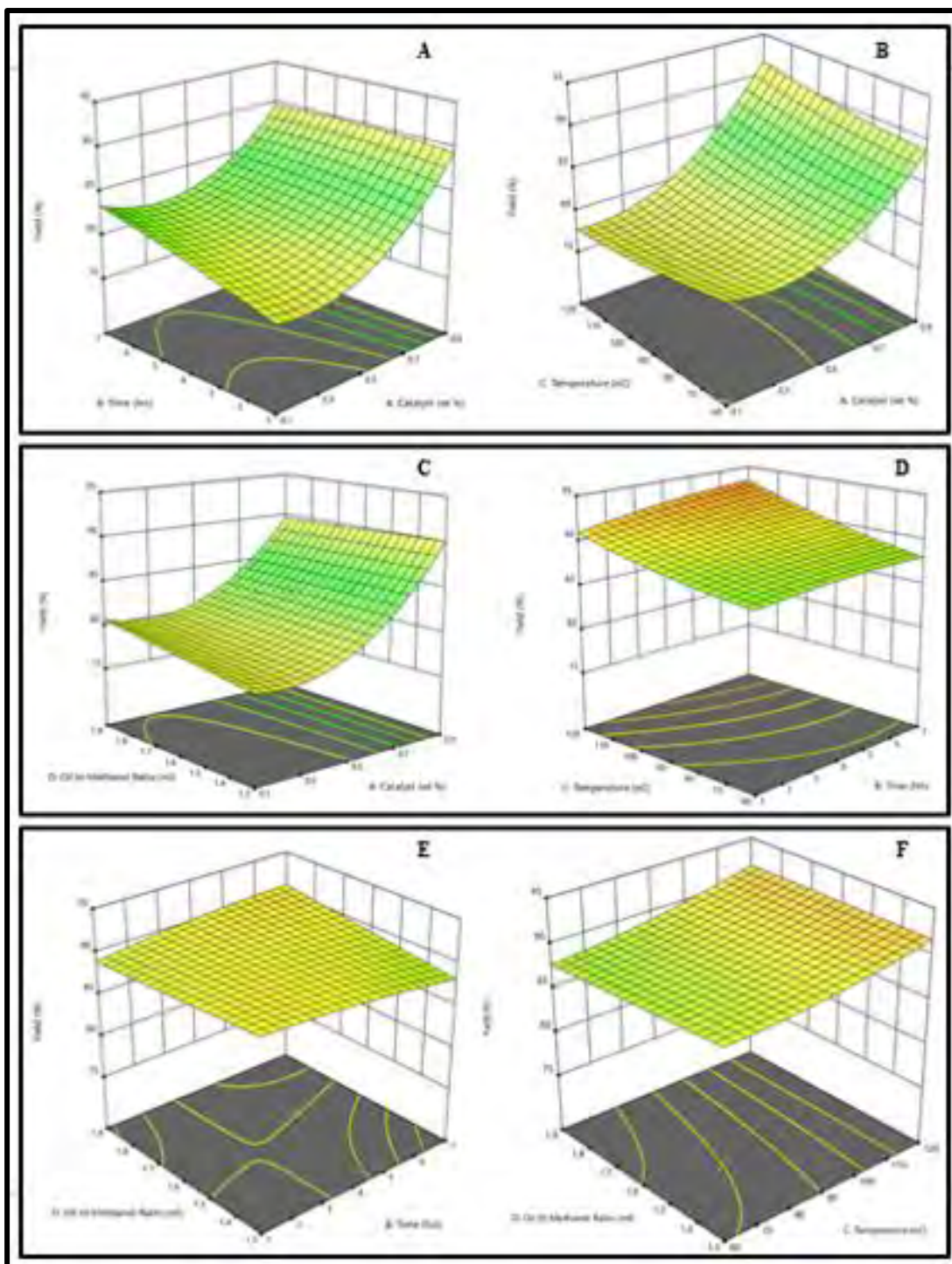


Figure 3.3.1.4: 3D surface Plots showing the impact of different parameters on *Brassica oleracea* L. biodiesel (BOB) yield

Table 3.3.1.1: Optimized Conditions for BOB Synthesis Using Na-Mmt, Na-Ag-Mmt, Cu-Mg-Zn-Mmt Clay Catalysts

Catalyst	Conc.(g)	Oil: Methanol	Time (hrs)	Temperature °C	Yield %
Al-Mmt	0.3	1:7	5.5	100	91.40
Na-Ag-Mmt	0.5	1:5	7	90	87
Cu-Mg-Zn-Mmt	0.2	1:9	5	90	91

Table 3.3.1.2.1: Identified Esters in *Brassica oleracea* L. Derived Biodiesel (BOB) Using GC-MS

Peak #	Identified Compound (FAMES)	Retention time	Molecular Formula
1	Methyl Alcohol	0.363 and 0.397	CH ₃ OH
2	Methyl Alcohol	0.397	CH ₃ OH
3	2-Methylenebutyronitrile	2.410	C ₆ H ₇ N
4	4,5-epithiovaleronitrile	9.329	C ₆ H ₇ NS
5	Benzenepropanenitrile	12.287	C ₉ H ₉ N
6	Hexadecanoic acid	29.409	C ₁₆ H ₃₂ O ₂
7	9, 12-Octadecadienal	33.035	C ₁₈ H ₃₂ O
8	Octadecanoic acid	33.210	C ₁₈ H ₃₆ O ₂

Table 3.3.1.2.2: FT-IR Spectrum of *Brassica oleracea* L. Biodiesel

Peaks (cm ⁻¹)	Frequency Range (Cm ⁻¹)	Bond	Functional Group	Characteristics of peak
3007.62	3200-3000	O-H stretch	Alcohol	Strong and Broad
2922.07	3000-2850	H-C=O: C-H stretch	Aldehyde	Medium to strong
2852.93	2870-2695	C-H stretch	Alkane	Medium to Strong
1743.67	1750-1700	RCOOH	Ester	Strong
1710.28	1750-1700	RCOOH	Ester	Strong
1458.49	1470-1450	C-H bend	Alkane	Variable
1377.20	1400-1360	C-N stretch	Amines	Medium
1236.01	1250-1220	C-N stretch	Amines	Medium
1162.02	1250-1020	C-N stretch	Amines	Medium
1099.06	1250-1020	C-O stretch	Ether	Strong/medium
720.97	725-720	C-Cl stretch	Alkyl Halide	Strong

Table 3.3.1.2.3: Fuel Properties of *Brassica oleracea* L. Biodiesel

TESTS	METHODS	ALM-B100
Colour	Visual	2
Flash Point °C (PMCC)	ASTM D-93	81
Density @ 15 °C Kg/L	ASTM D-1298	0.8544
K. Viscosity @ 40 °C Cst	ASTM D-445	5.1
Pour Point °C	ASTM D-97	-10
Cloud Point °C	ASTM D-2500	-13
Sulphur %wt	ASTM D-4294	0.00039
Total Acid No. mg KOH/gm	ASTM D-974	0.220

3.3.1.4 Experimental and Predicted yield of *Brassica oleracea* L. Biodiesel (BOB) using Box-Behnken Design

Std	Run	Catalyst (wt%)	Time (hrs)	Temperature (°C)	Oil: Methanol (ml)	Yield %
1	1	0.1	1	60	1.3	78
24	2	0.5	4	90	1.9	86
20	3	0.5	7	90	1.6	89
12	4	0.9	7	60	1.9	86
17	5	0.1	4	90	1.6	94
14	6	0.9	1	120	1.9	93
6	7	0.9	1	120	1.3	92
28	8	0.5	4	90	1.6	79
13	9	0.1	1	120	1.9	76
19	10	0.5	1	90	1.6	75
2	11	0.9	1	60	1.3	94
11	12	0.1	7	60	1.9	86
22	13	0.5	4	120	1.6	87
10	14	0.9	1	60	1.9	90
9	15	0.1	1	60	1.9	79
5	16	0.1	1	120	1.3	77
23	17	0.5	4	90	1.3	80
8	18	0.3	5.5	100	1.7	92.04
26	19	0.5	4	90	1.6	76
18	20	0.9	4	90	1.6	79
4	21	0.9	7	60	1.3	89
15	22	0.1	7	120	1.9	79
25	23	0.5	4	90	1.6	79
21	24	0.5	4	60	1.6	80
7	25	0.1	7	120	1.3	77
30	26	0.5	4	90	1.6	76
27	27	0.5	4	90	1.6	78
16	28	0.9	7	120	1.9	95
29	29	0.5	4	90	1.6	79
3	30	0.1	7	60	1.3	78

3.3.1.4.1 Analysis of Variance (ANOVA) from Achieved Results

Source	Sum of Squares	df	Mean Square	F-value	p-value	Remarks
Model	5.73	14	0.4095	69.67	< 0.0001	significant
A-Catalyst	4.84	1	4.84	822.98	< 0.0001	
B-Time	0.0009	1	0.0009	0.1464	0.7074	
C-Temperature	0.0009	1	0.0009	0.1483	0.7056	
D-Oil to Methanol Ratio	0.0008	1	0.0008	0.1380	0.7155	
AB	0.0033	1	0.0033	0.5603	0.4657	
AC	0.0033	1	0.0033	0.5643	0.4641	
AD	0.0008	1	0.0008	0.1297	0.7237	
BC	3.054E-06	1	3.054E-06	0.0005	0.9821	
BD	0.0076	1	0.0076	1.29	0.2745	
CD	0.0008	1	0.0008	0.1336	0.7198	
A ²	0.4010	1	0.4010	68.22	< 0.0001	
B ²	0.0125	1	0.0125	2.13	0.1652	
C ²	0.0689	1	0.0689	11.72	0.0038	
D ²	0.0004	1	0.0004	0.0609	0.8085	
Residual	0.0882	15	0.0059			
Lack of Fit	0.0355	10	0.0036	0.3374	0.9324	not significant
Pure Error	0.0526	5	0.0105			
Cor Total	5.82	29				

3.3.2 *Carthamus oxycantha* Biodiesel (COB)

3.3.2 *Carthamus oxycantha* Biodiesel (COB)

Carthamus oxycantha has 29.20% oil content and free fatty acid content is 0.219 thus, it only needs one step transesterification for conversion into biodiesel. Several transesterification reactions were done in order to get the optimal yield of the biodiesel produced from the seeds oil of *Carthamus oxycantha*. The conditions at which top yield of the COB from each of the synthesized catalyst was obtained is given in table 3.3.2. All the three catalysts i.e. Al-Mmt clay catalyst, Na-Ag Mmt catalyst, Cu-Mg-Zn Mmt clay catalyst, were used in the transesterification of the seeds oil of *Carthamus oxycantha*. to biodiesel but Cu-Mg-Zn-Mmt clay catalyst gave the best yield (91.8%) among all followed by Al-Mmt (90%) and Na-Ag-Mmt (89%).

3.3.2.1 Reaction Variables Affecting Transesterification of *Carthamus oxycantha* Seeds Oil to Biodiesel

The transesterification reactions were carried out using three variables i.e. oil to methanol molar ratio, catalyst concentration and reaction temperature. And their effect was noted to be as following:

3.3.2.1.1 Oil to Methanol Molar Ratio

The stoichiometric ratio for FFAs conversion into esters requires 3 moles of alcohol and 1 mole of oil to produce 3 moles of fatty acid alkyl esters and 1 mole of glycerin (Mehar et al, 2006). In the current scenario oil to methanol ratios of 1:3, 1:4, 1:5, 1:6, 1:7, 1:8, 1:9 and 1:10 were used keeping other reaction conditions constant i.e. reaction time, reaction temperature and catalyst concentration constant. The maximum conversion ratio was obtained at 1:5, 1:4 and 1:5 using Al-Mmt, Na-Ag-Mmt and Cu-Mg-Zn-mmt clay catalysts.

3.3.2.1.2 Catalyst Concentration

Catalyst plays a crucial role in the transesterification reaction as it lowers the activation energy required to start the reaction. Hetrogeneous catalyst is in different phase than the reaction mixture so catalyst recovery is easy after the reaction, thus, reusability of the catalyst is enhanced significantly (Mehar et al, 2006). Transesterification reaction for conversion of seeds oil to FAMES, was carried out at

different catalyst concentrations i.e. 0.1g, 0.2g, 0.3g, 0.4g, 0.5g, 0.6g and 0.7g and maximum yield of biodiesel was obtained at 0.3 g of Al-Mmt clay catalyst, 0.1g in case of Na-Ag-Mmt clay catalyst and 0.2g of Cu-Mg-Zn-Mmt clay catalyst gave best results.

3.3.2.1.3 Reaction Temperature (°C)

Another parameter which plays critical role in the conversion of FFAs to FAMES is Temperature and is directly related to the biodiesel yield (Mehar et al, 2006, Munir et al, 2019). A series of reactions were carried out at different reaction conditions keeping other factors constant i.e. methanol to oil molar ratio and catalyst concentration. Highest conversion ratio was achieved at 90 °C in case of Al-Mmt clay catalyst and 100 °C for Na-Ag-Mmt and Cu-Mg-Zn clay catalysts.

3.3.2.2 Chemical Characterization

3.3.2.2.1 GC-MS Analysis of *Carthamus oxycantha* Derived Biodiesel (COB)

GC-MS analysis is broadly used technique to determine the chemical composition, type and structure of synthesized FAMES. Mass spectrometer was set to scan in the range of m/z 2-600 and ionization potential 70V (Bu et al., 2014; Zhang et al., 2014). Six momentous peaks are observed and confirmed by Library match software (NO. NIST 11) (Table 3.3.2.2). Different FAMES were determined using the retention time by Mass Spectroscopic analysis (Dawood et al., 2018). Helium gas was used as a carrier with reaction temperature 300°C for 45 minutes. At peak 1 n-Hexadecanoic acid (C₁₆H₃₂O₂) was found. Octadecanoic acid (C₁₈H₃₆O₂) was present at second peak. At third peak (9Z)-octadec-9-enoic acid (C₁₈H₃₄O₂), at fourth (E)-octadec-9-enoic acid (C₁₈H₃₄O₂), at fifth Octadecadienoic acid (C₁₈H₃₂O₂) and 9,12,15-Octadecatrienoic acid (C₁₈H₃₀O₂) was present at sixth peak. Results indicate that the abundantly present ester in COB. Linoleic acid methyl ester. The dominant ester compound was Octadecadienoic acid confirming the formation of biodiesel (Figure 3.3.2.2.1).

3.3.2.2.2 FT-IR Analysis of *Carthamus oxycantha* Biodiesel (COB)

FT-IR is used for the identification of chemical bonds and explain their stretching and bending vibrations. It also detects the presence and absence of functional groups in chemical compounds (Shaheen et al., 2017). Figure 3.3.2.2.2 shows the FT-IR of *Carthamus oxycantha* methyl esters. The stretch in the C-H bond of alkane group was observed at 2980.82cm⁻¹. A strong peak at 2922.07 cm⁻¹ shows the presence of aldehyde group due to the stretch in the H-C=O and C-H bonds. A sharp peak found at 1743.59 cm⁻¹ showed the presence of esters. Subsequent variable to medium peaks at 1378.55 cm⁻¹, 1239.67 cm⁻¹ and 1162.02 cm⁻¹ indicate the presence of amines (C-N). Whereas, a strong peak at 1059.98 cm⁻¹ due to the stretching of C-H bond depict the presence of ether group. A strong peak at 956.32 cm⁻¹ shows the bending of C=C bond of alkenes. And peaks at 721.56 cm⁻¹ and 579.36 cm⁻¹ are due to the presence of alkyl halide group (Table 3.3.2.2.2).

3.3.2.2.3 Fuel Properties of *Carthamus oxycantha* Biodiesel (COB)

The fuel properties of produced *Carthamus oxycantha* Biodiesel (COB) were determined and compared with the ASTM standards (Table 3.3.2.2.3). These properties help in the determination of the quality of fuel and its effect on diesel engine. Total acid number or acid value is amount of the free fatty acid existent in a fuel sample and is determined in mg KOH/gm. If its value is higher in the sample that means engine efficiency will be affected in a negative way (Akhtar et al., 2019). *Carthamus oxycantha* Biodiesel (COB) acid value (0.173mg KOH/gm) is well in range of international standards.

Density of the COB is also in accordance with the international standards i.e. 0.8321 mg KOH/gm. Fuel density value is also crucial as its higher value causes engine corrosion and decreases its efficiency (Sultana et al., 2016). Kinematic viscosity is the determinant of the fuel thickness, higher value causes deposition in engine and reduces its working efficiency (Gunstone & Hamilton, 2001). COB's kinematic viscosity is in range of international standards (4.15 kg/L). The color of produced biodiesel is on visual 2 according to ASTM standards. Another important aspect is the Flash point of the diesel during fuel handling and transportation and fuels having flash point higher than 60°C are referred as safe (Salaheldeen et al., 2015). At this temperature fuel

ignition starts. Flash point of COB was found to be 72°C. Additional important parameter is cold flow properties which includes Pour point and Cloud point of biodiesel (Akhtar et al., 2019). Pour point and cloud point value of COB were -8°C and -13°C respectively. The sulfur contents in COB was (0.0002ppm) by %weight. An ideal fuel has low sulfur content and is more operative for engine's life and environment (Candeia et al., 2009).

3.3.2.3 Optimization Study of Transesterification Operational Factors Through Response Surface Methodology (RSM)

For optimization of transesterification process, four independent variables with maximum and minimum ranges as presented in Table 3.3.2.3 i.e., Catalyst amount 0.2-0.8 wt%(A), Time 1-7.5 hrs (B), Temperature 50-120 °C (C) and Oil to methanol ratio (D) 1:3-1:7 were chosen and RSM was applied using the Box Behnken Design was applied on 30 experiments to test the fitness of Quadratic polynomial equation with the Design-Expert 11 (Stat Ease IncMinneapolis,USA). A coded model equation underneath was used for studying the association among Input Variables, Catalyst (A), Time (B), Temperature (C) and Oil to methanol ratio (D) as well as Output Response in terms of yield (Y).

$$Y = +14.62682 - 2.34143A - 0.026433B - 0.012883C - 5.02980D + 0.003547AB - 0.003703AC + 0.367660AD - 0.000063BC + 0.023472BD - 0.001175CD + 0.286531A^2 + 0.000012B^2 + 0.000123C^2 + 1.19976D^2$$

ANOVA results as presented in Table 3.3.2.3.1 help to maximize the yield of (methyl esters) biodiesel. Model F-value and corresponding lack of fit has been used for determining the significance of the model. The Model F-value of 6.12 implies the model is significant. There is only a 0.06% chance that an F-value this large could occur due to noise. P-values less than 0.0500 indicate model terms are significant. In this case A is a significant model term. Values greater than 0.1000 indicate the model terms are not significant. The Lack of Fit F-value of 0.34 implies the Lack of Fit is not significant relative to the pure error. There is a 92.92% chance that a Lack of Fit F-value this large could occur due to noise. Non-significant lack of fit is good for the model to fit. The Predicted R² of 0.5385 is in reasonable agreement with the Adjusted R² of 0.7118; i.e. the difference is less than 0.2. Adeq Precision measures the signal to noise ratio. A ratio

greater than 4 is desirable. Ratio of 7.917 indicates an adequate signal. This model can be used to navigate the design space. Additionally, p value (Table 3.3.2.3.1) is less than 0.05 (0.0006), thus ensures the significance of the model terms like A :(Catalyst), B:(Time), C:(Temperature), D:(Oil:Methanol), AB:(catalyst amount and time), AC:(Catalyst amount and temperature), AD:(Catalyst amount and oil:methanol), BC:(time and temperature), BD:(time and oil:methanol), CD:(process temperature and oil:methanol), A2:(quadratic impact of catalyst amount), B2:(quadratic impact of time), C2:(quadratic impact of process temperature), and D2:(quadratic impact of oil:methanol).

3.3.2.4 Parametric characterization of transesterification process

The three-dimensional response curves (3D) presented here in Figure 3.3.2.4 A, B, C, D & F, plotted versus every dual Independent variable whilst having other variable on pivotal point. The interactive effects of transesterification reaction can be explained in the following sub sections.

3.3.2.4.1 Interactive Impact of Catalyst Amount and Time

The combine influence of catalyst amount and time on biodiesel yield is presented into Figure 3.3.2.4 A, while keeping other parameters (oil: methanol ratio (1:5) and temperature (100°C)) constant. Since maximum COB (91.8%) obtained with the catalyst loading of 0.2 wt% with steady increase in reaction time from 1-5 hrs owing to the formation of more methoxy species by the activity of catalyst. However, beyond the optimum values of catalyst concentration and reaction time, sudden drop in yield was observed (Onukwuli et al., 2017). Therefore, ANOVA results appears to be insignificant with P-value (0.5916) > 0.05.

3.3.2.4.2 Interactive Impact of Catalyst Amount and Temperature

The Figure 3.3.2.4 B represents the combined influence of temperature and catalyst concentration on the biodiesel yield. It is clear from the table that maximum COB (91.80%) obtained with the catalyst loading of 0.2 wt% with steady increase in reaction temperature from 80-100 °C. However, lower conversion of COB (72%) observed at 0.8% catalyst at 120 °C. This drop in FAMEs content is consistent with the previous study (Akia and Yazdani, 2015). Therefore, it can be concluded from the

results that the interactive outcome of (catalyst amount and time) on biodiesel yield is insignificant with P-value (0.5144) > 0.05.

3.3.2.4.3 Interactive Impact of Catalyst Amount and Oil: Methanol Ratio

The Figure 3.3.2.4 C represent three-dimensional surface plot showing collective effect of the catalyst and oil-methanol on yield of biodiesel. The maximum biodiesel yield (91.80 %) is obtained with 1:5 oil: methanol ratio and 0.2 wt % catalyst represented in 3D plot. Since both oil: methanol ratio and concentration of catalyst has the significant role for providing maximum biodiesel yield (Verma and Sharma, 2016b). The biodiesel yield increases considerably by increasing both methanol-oil ratio and catalyst concentration from 1:3-1:5 and 0.01-0.2% perhaps owing to more active site on the surface of catalyst to catalyze the reaction. However, lower conversion of 72.0 % COB was observed with 0.5% and 0.8wt% catalyst due to partial changeover of triglyceride to methyl ester, which is consistent with the previous study (Verma, Sharma & Dwivedi, 2016). However, ANOVA results depicts that oil: methanol and catalyst concentrations interactive effect are significant owing to their P-value (0.8596).

3.3.2.4.4 Interactive impact of time and temperature

Figure 3.3.2.4 D shows the combined effect of reaction time and temperature on the biodiesel yield. A significant increase in yield (91.80%) was observed as the reaction time and temperature increases from 1-5.5 min and 80-100 °C until a point where further increase in time 320 and temperature (>120 °C) show no significant changes in COB content. This is so, higher temperatures support the increased interaction among reactants to produced product. However, much higher temperature (> 120 °C) and time (7 hrs) might initiates gasification of methanol and reverse transesterification leading to reduced COB content (72 %). However, the short reaction time (1 hrs) and low temperature (85 °C) (30th run) possibly do not allow the interaction of catalyst with oil leading to partially converted products (Lee et al., 2011). however, ANOVA results for these parameters were insignificant with P-value (0.2713) > 0.05.

3.3.2.4.5 Interactive Impact of Time and Oil: Methanol Ratio

The Figure 3.3.2.4 E shows the time and oil: methanol collective impact on biodiesel yield while keeping other parameters like catalyst concentration (0.2 wt%) and temperature (100°C) constant. It is evident from the 3D plot that by increasing the ratio of oil: methanol and time the yield of biodiesel increases considerably. Maximum COB yield (91.8%) was obtained at 1:5 oil: methanol ratio at 5.5 hrs reaction time due to increased interaction of excess methanol with oil. The short reaction time of 1 hr and low methanol ratio (1:3) might initiate hydrolysis of oil (Naik et al., 2015). ANOVA results, however, proves that the interactive outcome of time and methanol oil ratio on final (biodiesel) yield is insignificant with P-value (0.2686) > 0.05.

3.3.2.4.6 Interactive impact of oil: methanol ratio and temperature

The combined effect of temperature along with oil:alcohol ratio upon biodiesel yield is presented in Figure 3.3.2.4 F. Since maximum biodiesel (91.8%) obtained with steady rise in temperature to 100 °C with 55 ml of methanol. This is so, higher temperature reduces the oil viscosity which in turn facilitates the mixing of oil and alcohol to produce biodiesel. Conversely, temperature above the threshold level (> 100 °C) might initiate gasification of methanol along with hydrolysis leading to reduced COB content (Talebian-Kiakalaieh et al., 2013). Therefore, it can be concluded from the results that combined effect these two parameters on the yield of biodiesel is insignificant with P-value (0.9413) > 0.05.

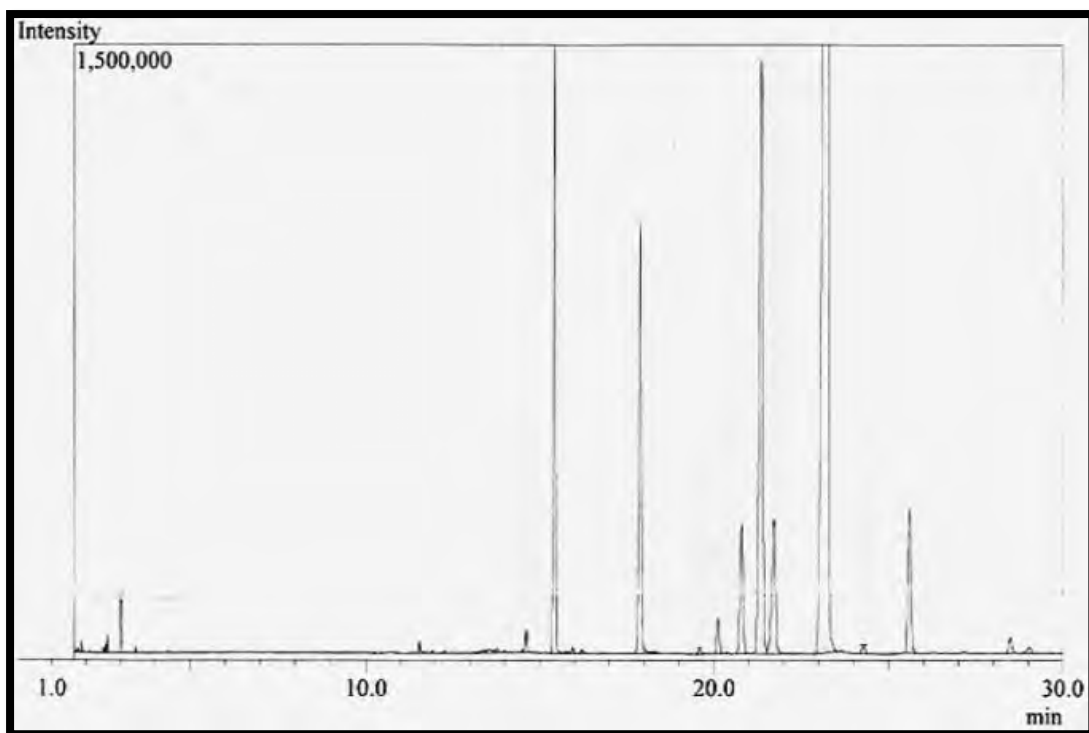


Figure 3.3.2.2.1: GCMS *Carthamus oxycantha* Biodiesel (COB)

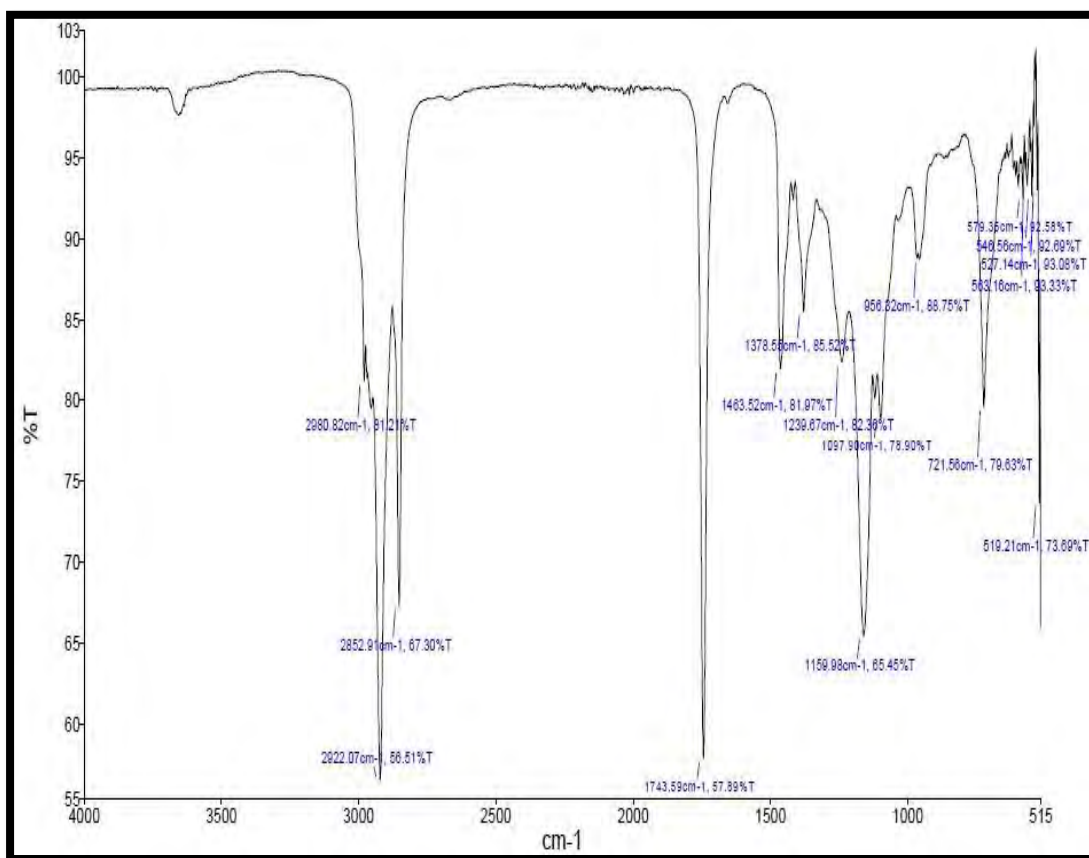


Figure 3.3.2.2.2: FTIR Spectrum of *Carthamus oxycantha* Biodiesel (COB)

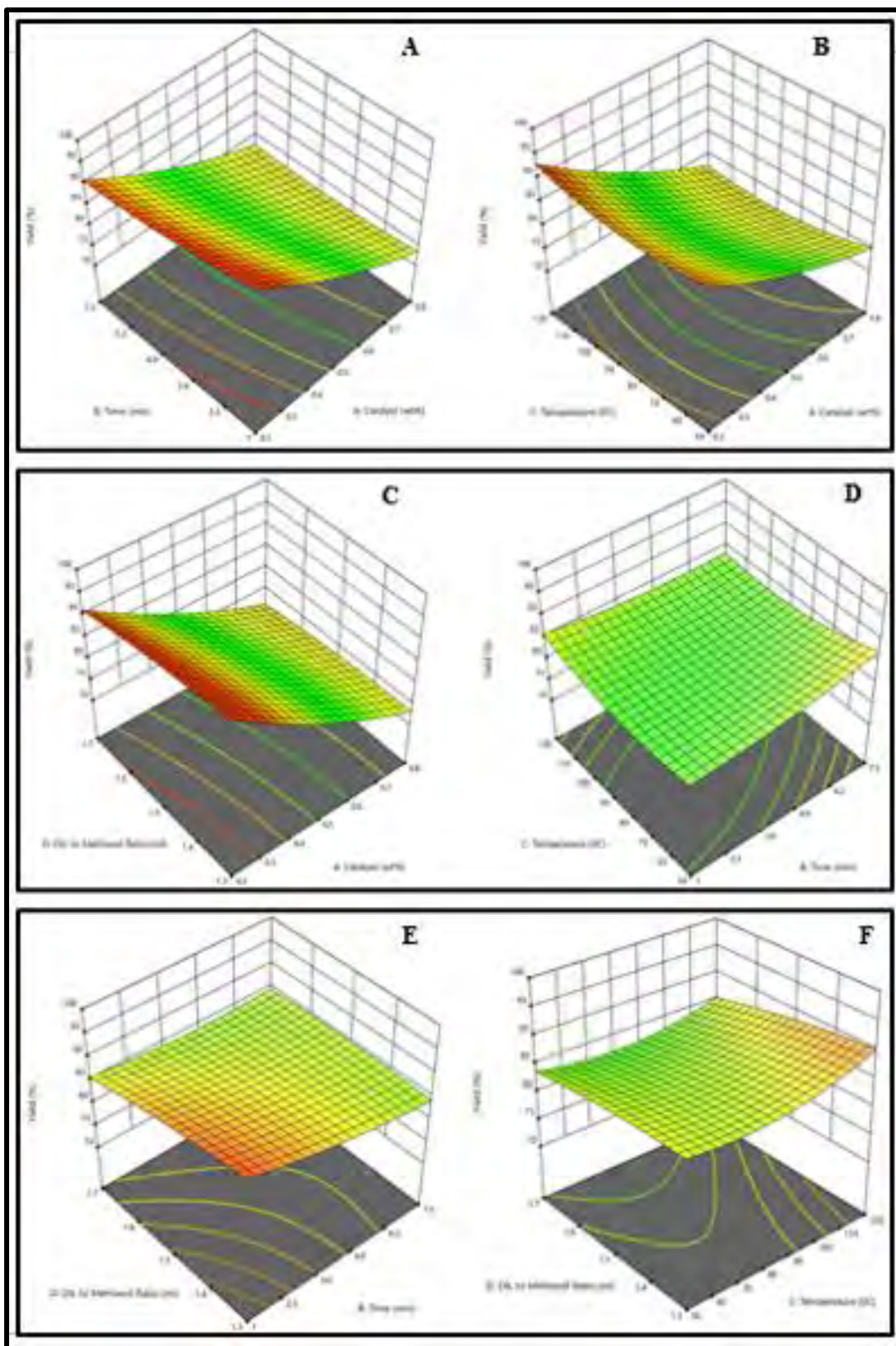


Figure 3.3.2.4: 3D surface Plots showing the impact of different parameters on *Carthamus oxycantha* biodiesel (COB) yield

Table 3.3.2: Optimized Conditions for COB Synthesis Using Na-Mmt, Na-Ag-Mmt, Cu-Mg-Zn-Mmt Clay Catalysts

Catalyst	Conc.(g)	Oil: Methanol	Time (hrs)	Temperature °C	Yield%
Al-Mmt	0.3	1:5	6	90	91
Na-Ag-Mmt	0.1	1:4	3.5	100	90
Cu-Mg-Zn-Mmt	0.2	1:5	5.5	100	91.8

Table 3.3.2.2.1: Identified Esters in *Carthamus oxycantha* Biodiesel (COB) Using GC-MS

Peak #	Identified Compound (FAMES)	Retention time	Molecular Formula
1	n-Hexadecanoic acid	14.35	C ₁₉ H ₃₄ O ₂
2	Octadecanoic acid	19.13	C ₁₈ H ₃₆ O ₂
3	(9Z)-octadec-9-enoic acid	20.17	C ₁₈ H ₃₄ O ₂
4	(E)-octadec-9-enoic acid	20.34	C ₁₈ H ₃₄ O ₂
5	Octadecadienoic acid	21.16	C ₁₈ H ₃₂ O ₂
6	9,12,15-Octadecatrienoic acid	20.27	C ₁₈ H ₃₀ O ₂

Table 3.3.2.2: FT-IR Spectrum of *Carthamus oxycantha* biodiesel (COB)

Peaks (cm ⁻¹)	Frequency Range (Cm ⁻¹)	Bond	Functional Group	Characteristics of peak
2980.82	3000-2500	C-H stretch	Alkane	Medium
2922.07	3000-2850	H-C=O: C-H stretch	Aldehyde	Medium to strong
2852.91	2870-2695	C-H stretch	Alkane	Medium to Strong
1743.59	1750-1700	RCOOH	Ester	Strong
1463.52	1470-1450	C-H bend	Alkane	Variable
1378.55	1400-1360	C-N stretch	Amines	Medium
1239.67	1250-1220	C-N stretch	Amines	Medium
1162.02	1250-1020	C-N stretch	Amines	Medium
1059.98	1250-1020	C-O stretch	Ether	Strong/medium
956.32	980-960	C=C bending	Alkene	Strong
721.56	725-720	C-Cl stretch	Alkyl Halide	Strong
579.36	600-500	C-I stretch	Alkyl Halide	Strong

Table 3.3.2.2.3: Fuel Properties of *Carthamus oxycantha* Biodiesel (COB)

TESTS	METHODS	ALM-B100
Colour	Visual	2
Flash Point °C (PMCC)	ASTM D-93	73
Density @ 15 °C Kg/L	ASTM D-1298	0.8321
K. Viscosity @ 40 °C Cst	ASTM D-445	4.15
Pour Point °C	ASTM D-97	-8
Cloud Point °C	ASTM D-2500	-13
Sulphur %wt	ASTM D-4294	0.0002
Total Acid No. mg KOH/gm	ASTM D-974	0.173

3.3.2.3 Experimental and Predicted yield of *Carthamus oxycantha* Biodiesel (COB) using Box-Behnken Design

Std	Run	Catalyst (wt%)	Time (hrs)	Temperature (°C)	Oil: Methanol (ml)	Yield (%)
16	1	0.8	7.5	120	1.7	72
10	2	0.8	1	50	1.7	70
5	3	0.2	5.5	100	1.5	92
23	4	0.5	4.25	85	1.3	83
18	5	0.8	4.25	85	1.5	72
29	6	0.5	6.7	85	1.5	84
8	7	0.8	7.5	120	1.3	72
11	8	0.2	7.5	50	1.7	92
19	9	0.5	1	85	1.5	83
6	10	0.8	1	120	1.3	73
7	11	0.2	7.5	120	1.3	89
17	12	0.2	4.25	85	1.5	90
9	13	0.2	1	50	1.7	90
25	14	0.5	4.25	85	1.5	80
26	15	0.5	4.25	85	1.5	80
27	16	0.5	4.25	85	1.5	80
1	17	0.2	1	50	1.3	91
4	18	0.8	7.5	50	1.3	73
28	19	0.5	4.25	85	1.5	70
13	20	0.2	1	120	1.7	92
3	21	0.2	7.5	50	1.3	92
2	22	0.8	1	50	1.3	75
20	23	0.5	7.5	85	1.5	78
14	24	0.8	1	120	1.7	73
22	25	0.5	4.25	120	1.5	83
21	26	0.5	4.25	50	1.5	83
15	27	0.2	5.5	100	1.5	92
12	28	0.8	7.5	50	1.7	83
24	29	0.5	4.25	85	1.7	78
30	30	0.5	4.25	85	1.5	72

3.3.2.3.1 Analysis of Variance (ANOVA) from Achieved Results

Source	Sum of Squares	df	Mean Square	F-value	p-value	Remarks
Model	4.65	14	0.3318	6.12	0.0006	significant
A-Catalyst	4.19	1	4.19	77.17	< 0.0001	
B-Time	0.0030	1	0.0030	0.0546	0.8184	
C-Temperature	0.0216	1	0.0216	0.3979	0.5377	
D-OIL to Methanol Ratio	0.0005	1	0.0005	0.0101	0.9213	
AB	0.0163	1	0.0163	0.3005	0.5916	
AC	0.0242	1	0.0242	0.4460	0.5144	
AD	0.0018	1	0.0018	0.0324	0.8596	
BC	0.0702	1	0.0702	1.29	0.2731	
BD	0.0716	1	0.0716	1.32	0.2686	
CD	0.0002	1	0.0002	0.0045	0.9474	
A ²	0.0017	1	0.0017	0.0318	0.8609	
B ²	0.0003	1	0.0003	0.0056	0.9413	
C ²	0.0584	1	0.0584	1.08	0.3158	
D ²	0.0003	1	0.0003	0.0056	0.9413	
Residual	0.8137	15	0.0542			
Lack of Fit	0.3314	10	0.0331	0.3436	0.9292	not significant
Pure Error	0.4822	5	0.0964			
Cor Total	5.46	29				

3.3.3 *Carthamus tinctorius* Biodiesel (CTB)

3.3.3 *Carthamus tinctorius* Biodiesel (CTB)

Carthamus tinctorius has 28.80% oil content and free fatty acid content (FFA) is 0.264 so, only single step transesterification is required to convert it to biodiesel (Table 3.3.1). Quite a few transesterification reactions were performed to obtain the top yield of the biodiesel from the seeds oil of *Carthamus tinctorius* (CTB). The conditions at which highest yield of the CTB from each of the synthesized catalyst was obtained is given in table 3.3.3. All of the 3 catalysts; Al-Mmt clay catalyst, Na-Ag Mmt catalyst, Cu-Mg-Zn Mmt clay catalyst, were utilized in the transesterification of the seeds oil of *Carthamus tinctorius*.(CTB) to biodiesel but Al-Mmt clay catalyst gave the best yield (95%) among all followed by Cu-Mg-Zn-Mmt (92%) and Na-Ag-Mmt (91%).

3.3.3.1 Reaction Variables Affecting Transesterification of *Carthamus tinctorius* Seeds Oil to Biodiesel

Affect of three variables on biodiesel yield in transesterification reaction is discussed below:

3.3.3.1.1 Oil to Methanol Molar Ratio

In the current scenario oil to methanol ratios of 1:3, 1:4, 1:5, 1:6, 1:7, 1:8, 1:9 and 1:10 were used keeping other reaction conditions constant i.e. reaction time, reaction temperature and catalyst concentration constant. The maximum conversion ratio was obtained at 1:7 by Al-Mmt, and 1:4 for both Na-Ag-Mmt and Cu-Mg-Zn-mmt clay catalysts.

3.3.3.1.2 Catalyst Concentration

Transesterification reaction for conversion of *Carthamus tinctorius* seeds oil to FAMES, was carried out at different catalyst concentrations i.e. 0.1g, 0.2g, 0.3g, 0.4g, 0.5g, 0.6g and 0.7g and maximum yield of biodiesel was obtained at 0.2 g of Al-Mmt clay catalyst, 0.1g in case of Na-Ag-Mmt clay catalyst and 0.2g of Cu-Mg-Zn-Mmt clay catalyst gave best results.

3.3.3.1.3 Reaction Temperature (°C)

Temperature of the reaction and biodiesel yield are directly proportional i.e. increase in temperature results in the increase of the biodiesel yield up to the threshold point (>150°C) (Mehar et al, 2006, Munir et al, 2019). A series of reactions were carried out at different reaction conditions keeping other factors constant i.e. methanol to oil molar ratio and catalyst concentration. Highest conversion ratio was achieved at 100 °C in case of all three; Al-Mmt, Na-Ag-Mmt and Cu-Mg-Zn clay catalysts.

3.3.3.2 Chemical Characterization

3.3.3.2.1 GC-MS of *Carthamus tinctorius* Biodiesel CTB

GC-MS analysis is broadly used technique to determine the chemical composition, type and structure of synthesized Fatty Acid Methyl Esters (FAMES). Mass spectrometer was set to scan in the range of m/z 2-600 and ionization potential 70V (Bu et al., 2014; Zhang et al., 2014). Different FAMES were determined using the retention time by Mass Spectroscopic analysis. Helium gas was used as a carrier with reaction temperature 300°C for 45 minutes. Six distinguishing peaks of *Carthamus tinctorius* Biodiesel CTB were observed as presented in figure 3.3.3.2.1. Hexadecanoic acid was present at first peak. Heptadecanoic acid, 6-Octadecenoic acid, 13-Octadecadien-1-ol, 7-Hexadecenoic acid and Ethyl 13-docosenoate were observed to be present at second, third, fourth, fifth and sixth peaks (Serin et al., 2013). Their molecular formulas along with retention time are mentioned in table 3.3.3.2.1.

3.3.3.2.2 FT-IR of *Carthamus tinctorius* Biodiesel CTB

FT-IR is used for the identification of chemical bonds and explain their stretching and bending vibrations. It also detects the presence and absence of functional groups in chemical compounds (Shaheen et al., 2017). Figure 33 shows the FT-IR of *Carthamus tinctorius* methyl esters. The stretch in the C-H bond of alkane group was observed at 2980.83cm⁻¹ and 2853.08 cm⁻¹. A peak at 1463.34 cm⁻¹ shows the bend of C-H bond of alkanes. A strong peak at 2923.28 cm⁻¹ shows the presence of aldehyde group due to the stretch in the H-C=O and C-H bonds. A sharp peak found at 1743.30 cm⁻¹ showed the presence of esters, confirming the formation of methyl esters of

biodiesel. Subsequent variable to medium peaks at 1378.60 cm^{-1} , 1239.46 cm^{-1} and 1149.48 cm^{-1} indicate the presence of amines (C-N). Whereas, a strong peak at 1097.64 cm^{-1} due to the stretching of C-H bond depict the presence of ether group. A strong peak at 956.69 cm^{-1} shows the bending of C=C bond of alkenes. And peaks at 721.56 cm^{-1} and 579.23 cm^{-1} are due to the presence of alkyl halide group (Table 3.3.3.2.2).

3.3.3.2.3 Fuel Properties of *Carthamus tinctorius* Biodiesel CTB

The fuel properties of produced *Carthamus tinctorius* Biodiesel (CTB) were determined and compared with the ASTM standards (Table 3.3.3.2.3). These properties help in the determination of the quality of fuel and its effect on diesel engine. Total acid number or acid value is amount of the free fatty acid existent in a fuel sample and is determined in mg KOH/gm. If its value is higher in the sample that means engine efficiency will be affected in a negative way (Akhtar et al., 2019). *Carthamus tinctorius* Biodiesel (CTB) acid value (0.203mg KOH/gm) is well in range of international standards. Density of the CTB is also in accordance with the international standards i.e. 0.8623 mg KOH/gm. Fuel density value is also crucial as its higher value causes engine corrosion and decreases its efficiency (Sultana et al., 2016). Kinematic viscosity is the determinant of the fuel thickness, higher value causes deposition in engine and reduces its working efficiency (Gunstone & Hamilton, 2001). CTB's kinematic viscosity is in range of international standards (5.32 kg/L). The color of produced biodiesel is on visual 2 according to ASTM standards. Another important aspect is the Flash point of the diesel during fuel handling and transportation and fuels having flash point higher than 60°C are referred as safe (Salaheldeen et al., 2015). At this temperature fuel ignition starts. Flash point of CTB was found to be 80°C. Additional important parameter is cold flow properties which includes Pour point and Cloud point of biodiesel (Akhtar et al., 2019). Pour point and cloud point value of COB were -9°C and -11°C respectively. The sulfur contents in CTB was (0.00041ppm) by %weight. An ideal fuel has low sulfur content and is more operative for engine's life and environment (Candeia et al., 2009).

3.3.3.2.4 Optimization study of Transesterification operational factors via response surface methodology (RSM)

For optimization of transesterification process, four independent variables with maximum and minimum ranges as presented in Table 3.3.3.4 i.e., (A) catalyst amount 1.5-5.0 %, Time (B) 1-7 h, reaction-temperature (C) 60-110 °C and methanol to Oil (D) 3:1- 9:1, were chosen and RSM was applied using the Box Behnken Design was applied on 30 experiments to test the fitness of Quadratic ploy-equation with the Design-Expert 11 (Stat Ease IncMinneapolis,USA). A coded model equation underneath was used for studying the association among Input Variables (Catalyst (A), Time (B), Temperature (C) and Methanol-oil (D)) as well as Output Response in terms of yield (Y).

$$Y = +8.15365-0.739282A+0.032987B-0.006767C+0.677858D-0.000728AB-0.000874AC+0.058552AD-8.73584E-06BC-0.000728BD-0.000874CD-0.624254A^2-0.000170B^2+0.000057C^2-0.202616D^2$$

Table 3.3.3.4.1 showing ANOVA results for transesterification process and helps to determine the fitness, significance and model precision. These can be identified by observing Model F-value and P-value. Here, F-value 39.56 (P-value= 0.0001 <1), is significance for determining biodiesel yield. However, F-value corresponding to the lake of fit is 0.4643 which appears to be not significant with the corresponding pure error, thus confirms the best fitness of model to experimental (trial) data. The Predicted R² of 0.9344 is in reasonable agreement with the Adjusted R² of 0.9490; i.e. the difference is less than 0.2, thus ensures the models reliability. Adequate Precision measures the signal to noise ratio. A ratio greater than 4 is desirable. And Adeq ratio of 18.278 indicates an adequate signal. This model can be used to navigate the design space. Moreover, small difference of (<0.2) between the adjusted R2 (R2=0.9490) and predicted R2 (R2=0.9344) values indicating the good correlation with the regression polynomial. Also, p value (Table 3.3.3.4) is less than 0.05, thus ensures the significance of the model terms like, A :(Catalyst), B:(Time), C:(Temperature), D:(Oil:Mathanol), AB:(catalyst amount and time), AC:(Catalyst amount and temperature), AD:(Catalyst amount and oil:methanol), BC:(time and temperature), BD:(time and oil:methanol), CD:(process temperature and oil:methanol), A2:(quadratic impact of catalyst amount),

B2:(quadratic impact of time), C2:(quadratic impact of process temperature), and D2:(quadratic impact of oil:methanol).

3.3.3.4 Parametric Characterization of Transesterification Process

The three-dimensional response curves (3D) presented here in Figure 3.3.3.4 A, B, C, D, E & F, plotted versus every dual Independent variable whilst having other variable on pivotal point. The interactive effects of transesterification reaction can be explained in the following sub sections.

3.3.3.4.1 Interactive Impact of Catalyst Amount and Time

The combine influence of catalyst amount and time on the CTB yield is shown in Figure 3.3.3.4 A. The maximum CTB (95%) was obtained with the catalyst loading of 0.2 wt% (Al-Mmt) with steady increase in reaction time from 1-5h. This is due to the formation of more methoxy species by the activity of catalyst and ultimately increased yield of biodiesel and equilibrium in the reaction (Hameed et al., 2009; Jahirul et al., 2014). However, beyond the optimum values of catalyst concentration and reaction time, sudden drop in yield (75%) was observed. This drop in yield might be linked to the shifting of reaction in opposite direction. Therefore, ANOVA results is insignificant with P-value (0.7456) > 0.05.

3.3.3.4.2 Interactive Impact of Catalyst Amount and Temperature

The Figure 3.3.3.4 B shows the combined influence of catalyst concentration and reaction temperature on the biodiesel yield. Maximum CTB (95%), obtained with the catalyst loading of 0.2 wt% (Al-Mmt) with steady increase in reaction temperature from 80-100 °C. However, lower conversion of CTB (75%) observed at 0.8 wt% catalyst and 110 °C due to partial changeover of triglyceride to methyl ester, which is consistent with the previous study (Uzun et al., 2012). However, slight drop in CTB content (85%) was observed as the amount of catalyst and temperature increased beyond 0.5wt% and 110 °C. This drop might be due to reduced mass transfer and interaction between the reactant and catalyst (Patil et al., 2011). Therefore, it can be concluded from the results that interactive outcome of these two parameters (time and catalyst amount) on biodiesel yield is insignificant with P-value (0.7456) > 0.05.

3.3.3.4.3 Interactive Impact of Catalyst Amount and Oil: Methanol Ratio

The three-dimensional surface plot (3D) showing collective effect of the catalyst and oil-methanol on yield of biodiesel is shown in Figure 3.3.3.4 C. The maximum biodiesel yield (95 %) is obtained at 1:7 oil: methanol ratio and 0.2 wt % catalyst as represented in the 3D plot. Likewise, the high yield of biodiesel (92 %) is achieved with 1:3 oil: methanol ratio and 0.2% catalyst concentration respectively. It is evident that there is a close agreement between these process parameters. Since both oil: methanol ratio and concentration of catalyst has the leading role for providing maximum biodiesel yield. The biodiesel yield increases considerably by increasing both catalyst concentration and oil-methanol ratio from 0.1-0.3% to 1:7 owing to availability of more active site on the surface of catalyst (Muppaneni et al., 2013). However, as the catalyst amount is reduced to 0.1% together with low oil methanol ratio of 1:3 lower conversions of 75 % CTB (0.1% catalyst) observed. Similar trend was observed with higher amounts of amount of catalyst and methanol ratio (0.8wt%, 1:9) owing to emulsification which would ultimately cause difficulty in separation of end products and contributing in decreased yield of FAMEs (Muppaneni et al., 2012). However, ANOVA results depicts that oil: methanol and catalyst concentrations interactive effect are insignificant owing to their P-value (0.7940) > 0.05.

3.3.3.4.4 Interactive impact of time and temperature

The reaction time and temperature combine effect on the CTB yield is shown Figure 3.3.3.4 D. A significant increase in CTB yield (95%) was observed as the reaction time and temperature increases from 1h-5h and 80-100 °C. The increased CTB yield might be linked to the ingenious dispersion of catalyst particle being facilitated by higher temperature (Jeong and Park, 2009). Where as, there is drop in CTB yield (75 %) due to gasification of methanol which is facilitated as the temperature increased above the threshold level (> 110 °C). similar trend in reduced CTB yield is observed with 6h reaction time at 110 °C due to reverse transesterification reaction (Shin et al., 2012; Tiwari et al., 2007). The ANOVA results is insignificant with P-value (0.7456) >0.05.

3.3.3.4.5 Interactive Impact of Time and Oil: Methanol Ratio

The time and oil: methanol collective impact on biodiesel yield is presented in Figure 3.3.3.4 E. The highest biodiesel (CTB) yield (95%) is attained at 1:7 oil: methanol ratio and reaction time of 5h respectively. It is evident from the 3D plot that by increasing the ratio of oil: methanol and reaction time the yield of biodiesel increases considerably owing to the two sided mode of transesterification process that necessitates the surplus alcohol to maintain the balance in reaction (higher conversion of oil to FAMES). The short reaction time of 1h and low methanol ratio (3) possibly decreases CTB yield due to partially converted products. The similar behaviour was observed by (Omar and Amin, 2011; Verma and Sharma, 2016a). Decreased CTB content (75%) is observed with 7h reaction time at the molar ratio of 1:9, related to the oil's dilution effect (Du et al., 2004) which contributes the reduced CTB yield. Thus, ANOVA results appears to be insignificant with P-value (0.7456) > 0.05.

3.3.3.4.6 Interactive impact of oil: methanol ratio and temperature

The Figure 3.3.3.4 F represents the combined effect of temperature along with oil:alcohol ratio upon CTB yield. Since maximum biodiesel (95%) obtained with steady rise in temperature (80-100 °C with 1:7 oil to methanol). On the contrary, higher temperature (> 100 °C) might initiates gasification of methanol leading to reduced FAMES content (Ghoreishi and Moein, 2013). Therefore, it can be concluded from results that combined effect of these two parameters on the yield of biodiesel is insignificant with Pvalue (0.7456) > 0.05.

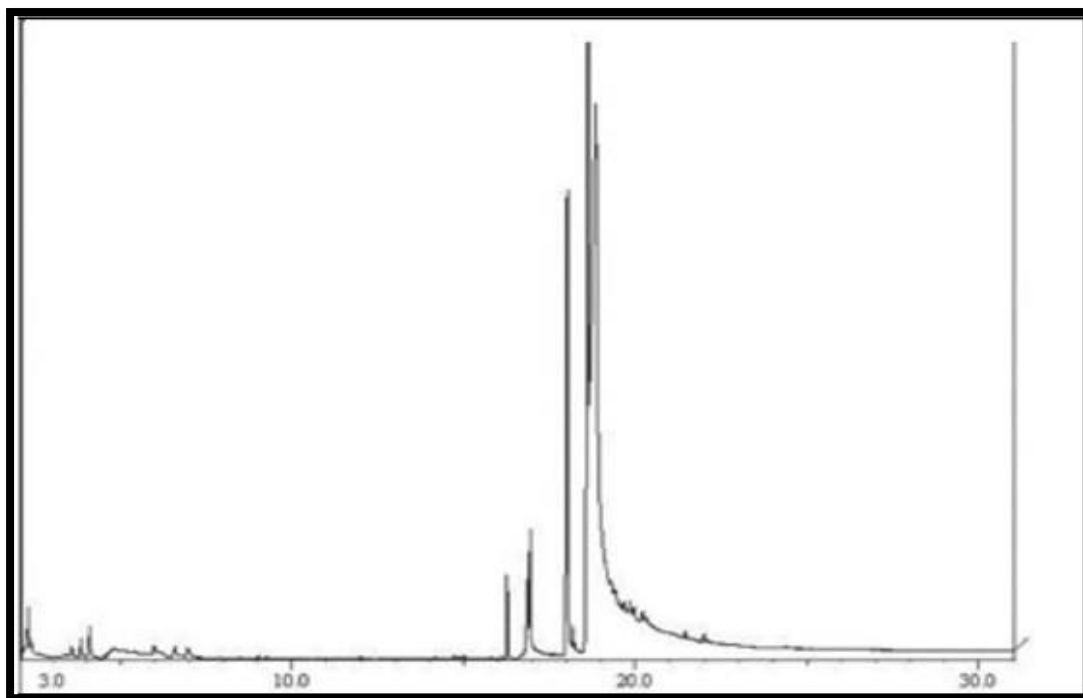


Figure 3.3.3.2.1: GCMS of *Carthamus tinctorius* Biodiesel (CTB)

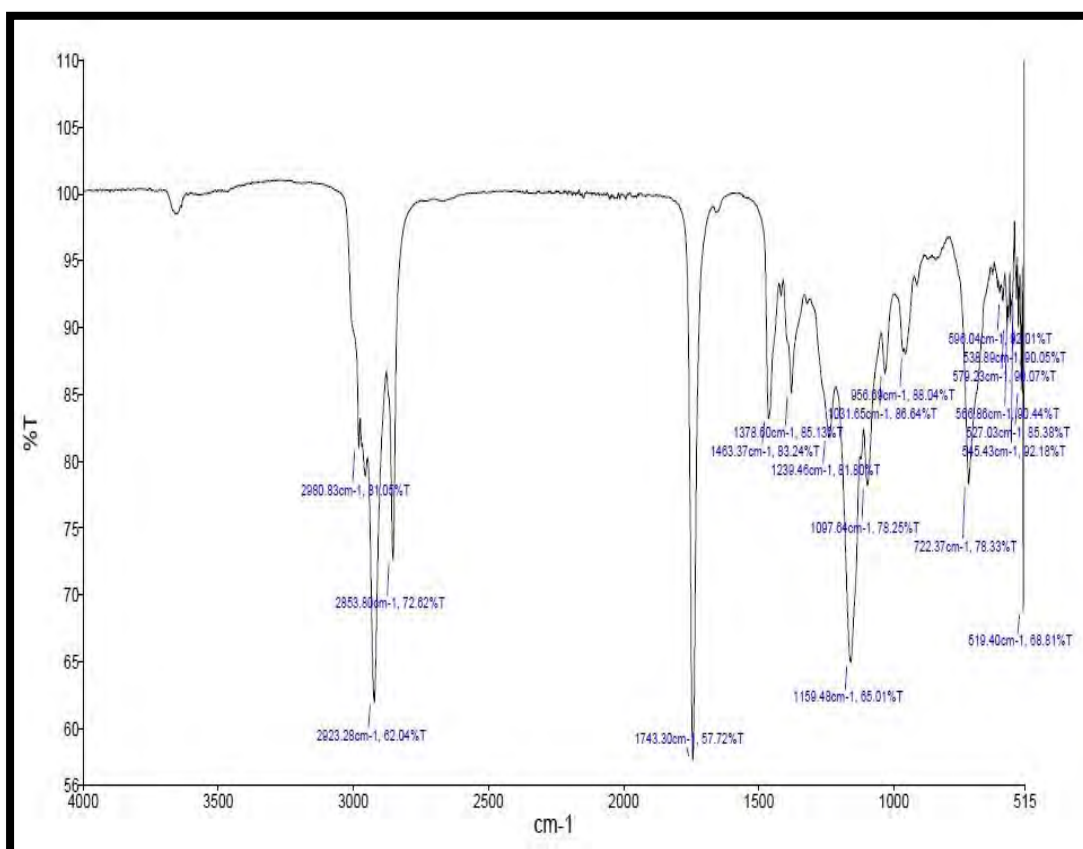


Figure 3.3.3.2.2: FT-IR of *Carthamus tinctorius* Biodiesel (CTB)

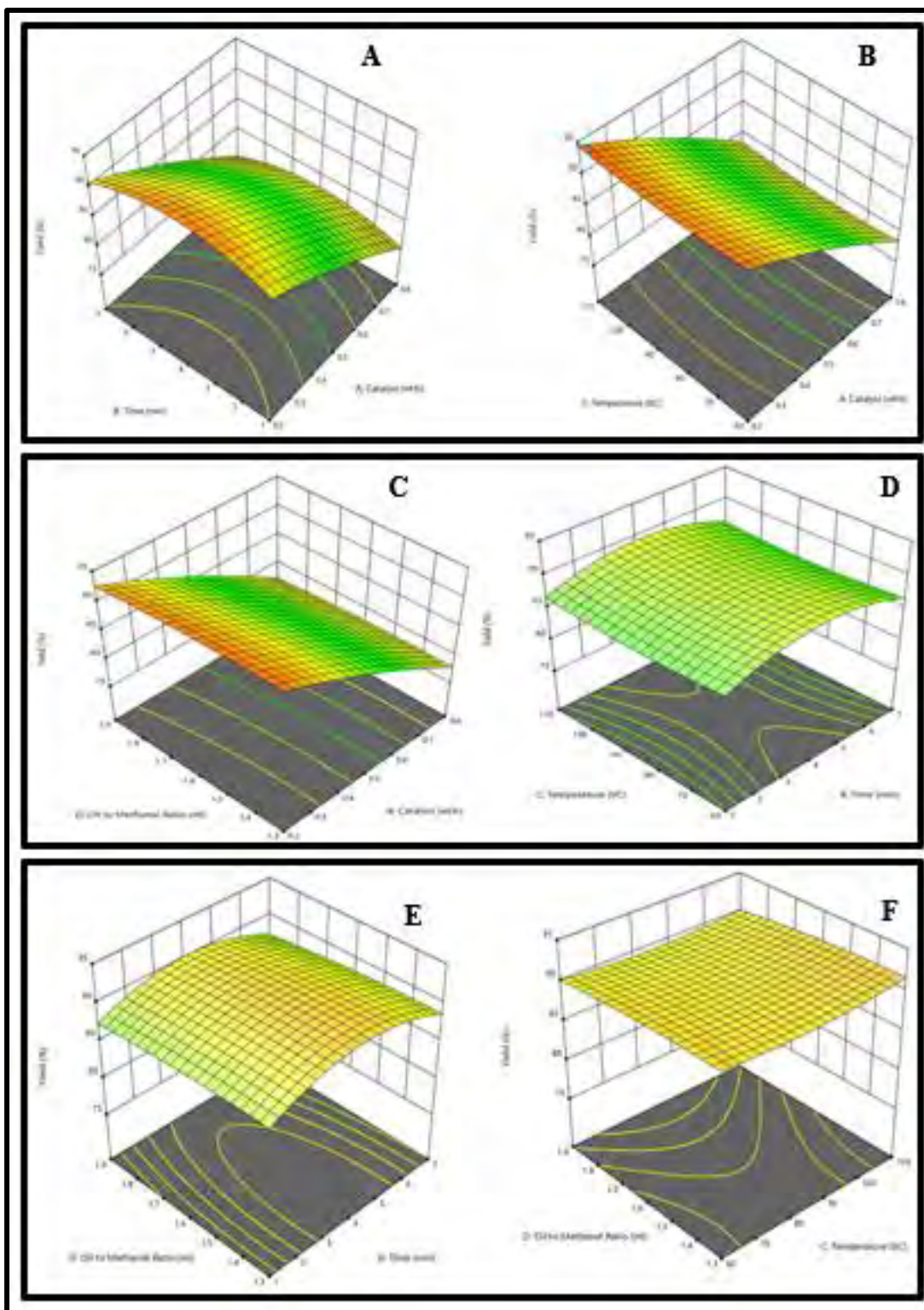


Figure 3.3.3.4 surface Plots showing the impact of different parameters on *Carthamus tinctorius* biodiesel (CTB) yield.

Table 3.3.3: Optimized Conditions for CTB Synthesis Using Na-Mmt, Na-Ag-Mmt, Cu-Mg-Zn-Mmt Clay Catalysts

Catalyst	Conc.(g)	Oil:Methanol	Time (hrs)	Temperature °C	Yield%
Al-Mmt	0.2	1:7	5	100	95
Na-Ag-Mmt	0.1	1:4	3.5	100	91
Cu-Mg-Zn-Mmt	0.2	1:4	3	100	92

Table 3.3.3.2.1: Identified Esters in *Carthamus tinctorius* Biodiesel (CTB) Using GC-MS

Peak #	Identified Compound (FAMES)	Retention time	Molecular Formula
1	Hexadecanoic acid	16.94	C ₁₆ H ₃₂ O ₂
2	Heptadecanoic acid	17.21	C ₁₇ H ₃₄ O ₂
3	6-Octadecenoic acid	18.01	C ₁₈ H ₃₄ O ₂
4	13-Octadecadien-1-ol	18.61	C ₁₈ H ₃₄ O
5	7-Hexadecenoic acid	21.44	C ₁₆ H ₃₀ O ₂
6	Ethyl 13-docosenoate	22.02	C ₂₄ H ₄₆ O ₂

Table 3.3.3.2.2: FT-IR Spectrum of *Carthamus tinctorius* Biodiesel (CTB)

Peaks (cm ⁻¹)	Frequency Range (Cm ⁻¹)	Bond	Functional Group	Characteristics of peak
2980.83	3000-2500	C-H stretch	Alkane	Medium
2923.28	3000-2850	H-C=O: C-H stretch	Aldehyde	Medium to strong
2853.80	2870-2695	C-H stretch	Alkane	Medium to Strong
1743.30	1750-1700	RCOOH	Ester	Strong
1463.37	1470-1450	C-H bend	Alkane	Variable
1378.60	1400-1360	C-N stretch	Amines	Medium
1239.46	1250-1220	C-N stretch	Amines	Medium
1159.48	1250-1020	C-N stretch	Amines	Medium
1097.64	1250-1020	C-O stretch	Ether	Strong/medium
956.69	980-960	C=C bending	Alkene	Strong
722.37	725-720	C-Cl stretch	Alkyl Halide	Strong
579.23	600-500	C-I stretch	Alkyl Halide	Strong

Table 3.3.3.2.3: Fuel Properties of *Carthamus tinctorius* Biodiesel (CTB)

TESTS	METHODS	ALM-B100
Colour	Visual	2
Flash Point °C (PMCC)	ASTM D-93	80
Density @ 15 °C Kg/L	ASTM D-1298	0.8623
K.Viscosity @ 40 °C cST	ASTM D-445	5.32
Pour Point °C	ASTM D-97	-9
Cloud Point °C	ASTM D-2500	-11
Sulphur %wt	ASTM D-4294	0.00041
Total Acid No. mg KOH/gm	ASTM D-974	0.203

3.3.3.4 Experimental and Pridicted yield of *Carthamus tinctorius* Biodiesel (CTB) using Box-Behnken Design

Std	Run	Catalyst (wt%)	Time (hrs)	Temperature (°C)	Oil: Methanol (ml)	Yield %
12	1	0.8	7	110	1.9	75
5	2	0.2	1	90	1.3	92
3	3	0.2	7	90	1.3	92
27	4	0.5	4	85	1.6	84
26	5	0.5	4	85	1.6	88
7	6	0.2	7	110	1.3	92
24	7	0.5	4	85	1.9	88
2	8	0.8	1	60	1.3	76
13	9	0.2	1	110	1.9	90
16	10	0.8	7	110	1.9	75
22	11	0.5	4	110	1.6	88
6	12	0.8	1	110	1.3	76
25	13	0.5	4	85	1.6	84
19	14	0.5	1	85	1.6	85
9	15	0.2	1	60	1.9	90
20	16	0.5	7	85	1.6	84
30	17	0.5	4	85	1.6	85
14	18	0.8	1	110	1.9	75
18	19	0.8	4	85	1.6	78
17	20	0.2	5	100	1.7	95
8	21	0.8	7	110	1.3	76
28	22	0.5	4	85	1.6	86
15	23	0.2	7	110	1.9	90
23	24	0.5	4	85	1.3	86
1	25	0.2	1	60	1.3	90
29	26	0.5	4	85	1.6	88
21	27	0.5	4	60	1.6	88
4	28	0.8	7	60	1.3	76
11	29	0.2	7	60	1.9	90
10	30	0.8	1	60	1.9	75

3.3.3.4.1 Analysis of Variance (ANOVA) from Achieved Results

Source	Sum of Squares	df	Mean Square	F-value	p-value	Remarks
Model	3.48	14	0.2488	39.56	< 0.0001	significant
A-Catalyst	3.22	1	3.22	511.87	< 0.0001	
B-Time	0.0001	1	0.0001	0.0225	0.8828	
C-Temperature	0.0006	1	0.0006	0.0971	0.7596	
D-Oil to Methanol Ratio	0.0106	1	0.0106	1.69	0.2132	
AB	0.0007	1	0.0007	0.1092	0.7456	
AC	0.0007	1	0.0007	0.1092	0.7456	
AD	0.0004	1	0.0004	0.0707	0.7940	
BC	0.0007	1	0.0007	0.1092	0.7456	
BD	0.0007	1	0.0007	0.1092	0.7456	
CD	0.0007	1	0.0007	0.1092	0.7456	
A ²	0.0082	1	0.0082	1.30	0.2720	
B ²	0.0607	1	0.0607	9.66	0.0072	
C ²	0.0032	1	0.0032	0.5154	0.4838	
D ²	0.0009	1	0.0009	0.1370	0.7165	
Residual	0.0943	15	0.0063			
Lack of Fit	0.0454	10	0.0045	0.4643	0.8587	not significant
Pure Error	0.0489	5	0.0098			
Cor Total	3.58	29				

3.3.4 *Carthamus lanatus* Biodiesel (CLB)

3.3.4 *Carthamus lanatus* Biodiesel (CLB)

Carthamus lanatus has 22.40% oil content and free fatty acid content (FFA) is 0.214. Single step transesterification is required to convert it to biodiesel (Table 3.3.1). Quite a few transesterification reactions were performed to obtain the top yield of the biodiesel from the seeds oil of *Carthamus lanatus* (CLB). The conditions at which maximum yield of the CLB from each of the synthesized catalyst was obtained is given in table 3.3.4. All of the 3 catalysts; Al-Mmt clay catalyst, Na-Ag Mmt catalyst, Cu-Mg-Zn Mmt clay catalyst, were utilized in the transesterification of the seeds oil of *Carthamus lanatus* to biodiesel but Cu-Mg-Zn-Mmt clay catalyst gave the best yield (90%) among all followed by Na-Ag-Mmt (89%) and Al-Mmt (87%).

3.3.4.1 Reaction Variables Affecting Transesterification of *Carthamus lanatus* Seeds Oil to Biodiesel

Three variables i.e. oil to methanol molar ratio, catalyst concentration and reaction temperature, affecting transesterification reaction efficiency are discussed below:

3.3.4.1.1 Oil to Methanol Molar Ratio

Oil to methanol ratios of 1:3, 1:4, 1:5, 1:6, 1:7, 1:8, 1:9 and 1:10 were used keeping other reaction conditions constant i.e. reaction time, reaction temperature and catalyst concentration constant. The maximum conversion ratio was obtained at 1:7 by Al-Mmt, 1:6 for Na-Ag-Mmt and 1:4 for Cu-Mg-Zn-mmt clay catalysts.

3.3.4.1.2 Catalyst Concentration

Another important factor which influences the yield of the fatty acid methyl esters (FAMES) is the type and concentration of the catalyst. Heterogeneous catalysts have many advantages over the homogeneous ones. As the catalyst is in different phase than the reaction mixture so catalyst is easily recovered after the reaction and reusability of the catalyst is enhanced significantly (Mehar et al, 2006). Transesterification reaction for conversion of *Carthamus lanatus* seeds oil to FAMES, was carried out at different catalyst concentrations i.e. 0.1g, 0.2g, 0.3g, 0.4g, 0.5g, 0.6g and 0.7g and maximum

yield of biodiesel was obtained at 0.4 g of Al-Mmt clay catalyst, 0.1g in case of Na-Ag-Mmt clay catalyst and 0.2g of Cu-Mg-Zn-Mmt clay catalyst gave best results.

3.3.4.1.3 Reaction Temperature (°C)

Temperature of the reaction and biodiesel yield are directly proportional i.e. increase in temperature results in the increase of the biodiesel yield up to the threshold point ($>150^{\circ}\text{C}$) (Mehtar et al, 2006, Munir et al, 2019). A series of reactions were carried out at different reaction conditions keeping other factors constant i.e. methanol to oil molar ratio and catalyst concentration. Highest conversion ratio was achieved at 95°C , 100°C and 90°C in case of Al-Mmt, Na-Ag-Mmt and Cu-Mg-Zn clay catalysts.

3.3.4.2 Chemical Characterization

3.3.4.2.1 GC-MS of *Carthamus lanatus* Biodiesel (CLB)

GC-MS analysis is broadly used technique to determine the chemical composition, type and structure of synthesized Fatty Acid Methyl Esters (FAMES). Mass spectrometer was set to scan in the range of m/z 2-600 and ionization potential 70V (Bu et al., 2014; Zhang et al., 2014). Different FAMES were determined using the retention time by Mass Spectroscopic analysis. Helium gas was used as a carrier with reaction temperature 300°C for 45 minutes. Six distinguishing peaks of *Carthamus lanatus* Biodiesel CLB were observed as presented in figure 3.3.4.2.1. n-Hexadecanoic acid ($\text{C}_{19}\text{H}_{34}\text{O}_2$) was present at first peak. Heptadecanoic acid ($\text{C}_{16}\text{H}_{32}\text{O}_2$), Ethyl hexadecanoate ($\text{C}_{18}\text{H}_{36}\text{O}_2$), Oleic acid methyl ester ($\text{C}_{19}\text{H}_{36}\text{O}_2$), Ethyl Oleate ($\text{C}_{20}\text{H}_{38}\text{O}_2$) and 9,12-Octadecadienoic acid ($\text{C}_{18}\text{H}_{32}\text{O}_2$) were observed to be present at second, third, fourth, fifth and sixth peaks. Their molecular formulas along with retention time are mentioned in table 3.3.4.2.1 (Serin et al., 2013).

3.3.4.2.2 FT-IR of *Carthamus lanatus* Biodiesel (CLB)

FT-IR is used for the identification of chemical bonds and explain their stretching and bending vibrations. It also detects the presence and absence of functional groups in chemical compounds (Shaheen et al., 2017). Figure 3.3.4.2.2 shows the FT-IR of *Carthamus lanatus* methyl esters. The stretch in the C-H bond of alkane group was observed at 2852.90 cm^{-1} . A peak at 1463.74 cm^{-1} shows the bend of C-H bond of

alkanes. A strong peak at 2922.06 cm^{-1} shows the presence of aldehyde group due to the stretch in the H-C=O and C-H bonds. A sharp peak found at 1743.63 cm^{-1} showed the presence of esters, confirming the formation of methyl esters of biodiesel. Subsequent variable to medium peaks at 1378.19 cm^{-1} , 1239.12 cm^{-1} and 1159.32 cm^{-1} indicate the presence of amines (C-N). Whereas, a strong peak at 1098.43 cm^{-1} due to the stretching of C-H bond depict the presence of ether group. And peaks at 721.70 cm^{-1} and 581.95 cm^{-1} are due to the presence of alkyl halide group (Table 3.3.4.2.2).

3.3.4.2.3 Fuel Properties of *Carthamus lanatus* Biodiesel (CLB)

The fuel properties of produced *Carthamus lanatus* Biodiesel (CLB) were determined and compared with the ASTM standards (Table 3.3.4.2.3). These properties help in the determination of the quality of fuel and its effect on diesel engine. Total acid number or acid value is amount of the free fatty acid existent in a fuel sample and is determined in mg KOH/gm. If its value is higher in the sample that means engine efficiency will be affected in a negative way (Akhtar et al., 2019). *Carthamus lanatus* Biodiesel (CLB) acid value (0.171mg KOH/gm) is well in range of international standards. Density of the CLB is also in accordance with the international standards i.e. 0.8304 mg KOH/gm. Fuel density value is also crucial as its higher value causes engine corrosion and decreases its efficiency (Sultana et al., 2016). Kinematic viscosity is the determinant of the fuel thickness, higher value causes deposition in engine and reduces its working efficiency (Gunstone & Hamilton, 2001). CLB's kinematic viscosity is in range of international standards (4.11 kg/L). The color of produced biodiesel is on visual 2 according to ASTM standards. Another important aspect is the Flash point of the diesel during fuel handling and transportation and fuels having flash point higher than 60°C are referred as safe (Salaheldeen et al., 2015). At this temperature fuel ignition starts. Flash point of CLB was found to be 74°C. Additional important parameter is cold flow properties which includes Pour point and Cloud point of biodiesel (Akhtar et al., 2019). Pour point and cloud point value of CLB were -8°C and -11°C respectively. The sulfur content in CLB was (0.0002ppm) by %weight. An ideal fuel has low sulfur content and is more operative for engine's life and environment (Candeia et al., 2009).

3.3.4.3 Optimization Study of Transesterification Operational Factors Through Response Surface Methodology (RSM)

Response surface methodology (RSM) was used to find out the parametric impact of four independent variables with maximum and minimum ranges i.e., Catalyst amount 0.2 wt% (Cu-Mg-Zn-Mmt)(A), Time 4 hrs (B), Temperature 90 °C(C), Oil to methanol ratio 1:4 ml (D). Total of 30 experiments have been chosen to test the fitness of Quadratic polynomial equation with the Design-Expert 11 (Stat Ease Inc Minneapolis, USA). A coded model equation underneath representing catalyst (A), Time (B), Temperature (C) and Methanol: oil (D) was used for studying the association among Input Variables as well as Output Response in terms of yield (Y).

$$Y = +8.44045-1.85871A+0.071673B+0.006789C+1.41445D-0.046858AB+0.003875AC+1.68097AD-0.000138BC-0.062647BD+0.004192CD-2.15401A^2+0.005868B^2-0.000078C^2-0.773175D^2$$

ANOVA results as presented in Table 3.3.4.3.1. helps to maximize (methyl esters) the yield of biodiesel. Model F-value 105.25 (P-value = 0.0001 > 1), depicting the models significance while F-value corresponding to the lack of fit is 1.88 which appears to be insignificant with the corresponding pure error, thus confirms the best fitness of model to experimental (trial) data. The Predicted R² of 0.9549 is in reasonable agreement with the Adjusted R² of 0.9805; i.e. the difference is less than 0.2. Adequate Precision measures the signal to noise ratio. A ratio greater than 4 is desirable. Model ratio of 28.889 indicates an adequate signal. This model can be used to navigate the design space. Table 3.3.4.3.1, thus ensures the significance of the model terms like , (catalyst concentration) A, (process time) B, (process temperature) C, (methano oil ratio) D, (Catalyst and Time) AB, (Catalyst and temperature) AC, (Catalyst and methanol oil ratio) AD, (Time and oil to methanol ratio) BC, (Temperature and Oil to Methanol Ratio) BD, (process temperature and time) CD, (quadratic impact of Catalyst amount) A², (quadratic impact of Time) B², (quadratic impact of process temperature) C², and (quadratic impact of Oil to Methanol Ratio) D². These noteworthy model terms impact the yield of produced biodiesel.

3.3.4.4 Parametric characterization of transesterification process

The 3D response surface plot regarding the yield of the product was achieved using polynomial equation and presented here in Figure 3.3.4.4 A, B, C, D, E & F. The interactive effects of transesterification reaction can be explained in the following sub sections.

3.3.4.4.1 Interactive Impact of Catalyst Amount and Time

The combine influence of catalyst amount and time on CLB yield is presented in Figure 3.3.4.4 A. Maximum CLB (90 %) obtained with the catalyst loading of 0.2 wt% with steady increase in reaction time from 1-4 hrs. This high CLB yield is linked to the formation of more methoxy species by the activity of catalyst and equilibrium in the reaction (Lee et al., 2011). However, beyond the optimum values of catalyst concentration and reaction time (0.4 wt%, 5 hrs) sudden drop in CLB yield (86%) was observed. This drop in yield might be linked to the shifting of reaction in opposite direction (Hasni et al., 2017). However, ANOVA results appears to be insignificant with P-value (0.2694) > 0.05.

3.3.4.4.2 Interactive Impact of Catalyst Amount and Temperature

The Figure 3.3.4.4 B illustrates the combined influence of catalyst concentration and reaction temperature on the biodiesel yield. Since maximum CLB (90%) obtained with the catalyst loading of 0.2 wt% with steady increase in reaction temperature from 70- 90 °C. However, lower conversion of CLB (76%) observed at 0.7 % catalyst due to partial changeover of triglyceride to methyl ester, which is consistent with the previous study (Ghoreishi and Moein, 2013). However, slight drop in CLB content (86%) was observed as the amount of catalyst and temperature increased beyond 0.45-0.7wt% and 80-100 °C. This drop in CLB content might be due to the oil decomposition (Maran and Priya, 2015a). Therefore, it can be concluded from the results that the interactive outcome of these two parameters (time and catalyst amount) on biodiesel yield is insignificant with P-value (0.2694) > 0.05.

3.3.4.4.3 Interactive Impact of Catalyst Amount and Oil: Methanol Ratio

The Figure 3.3.4.4 C represent collective effect of the catalyst and oil methanol ratio on yield of biodiesel in form of 3D surface plot. The maximum CLB yield (90 %) is obtained at 1:4 oil: methanol ratio and 0.2 wt % catalyst. Since both oil: methanol ratio and concentration of catalyst has leading role for providing maximum biodiesel yield. The biodiesel yield increases considerably by increasing catalyst concentration and methanol ratio from 0.1-0.2% to 1:4. This is so as the catalyst concentration and methanol ratio increases; more active sites will be available on catalyst surface to catalyse the reaction in forward direction (Rashid et al., 2011). The slight drop in CLB content was observed as the amount of catalyst and methanol ratio increased beyond 0.45wt% and 1:7 might be due emulsification which would ultimately cause difficulty in separation of end products, and contributing in decreased yield of CLB (Betiku and Adepoju, 2013). However, ANOVA results depicts that oil: methanol and catalyst concentrations interactive effect are highly significant P-value (0.0003) < 0.05.

3.3.3.4.4 Interactive impact of time and temperature

The time and temperature cooperative influence on the CLB yield is presented in the form of three-dimensional response surface plot in Figure 3.3.4.4 D significant increase in yield (90%) was observed as the reaction time and temperature increases from 1h-4h and 70-90 °C (Table 3.3.4.4). This is so, as higher temperatures amenities effective scattering of catalyst particle that in turn facilitates the increased interaction among the protons and hence, higher transition of oils to FAMEs (CLB) (Chen et al., 2008). Also, much higher temperature (> 100 °C) and more time (5 hrs) leading to reduced CLB content (85 %) is due to reserve transesterification reaction. While, the short reaction time (1hrs) and low temperature (50 °C) possibly do not allow the interaction of catalyst with oil leading to partially converted products. The similar trend was observed by (Silva et al., 2011; Dwivedi and Sharma, 2015). The ANOVA results appears insignificant with P-value (0.7695) > 0.05.

3.3.4.4.5 Interactive Impact of Time and Oil: Methanol Ratio

The time and oil methanol collective impact on CLB yield is presented in Figure 3.3.4.4 E while keeping other parameters like catalyst concentration (0.2%) and temperature (90°C) constant. The highest biodiesel yield (90.0%) is attained at 1:4 oil: methanol ratio and reaction time of 4h respectively. It is evident from the 3D plot that by increasing the ratio of oil: methanol the yield of biodiesel increases considerably. The two-sided mode of transesterification process thus necessitates the surplus alcohol to maintain the balance in reaction (higher conversion of oil to FAMES). The short reaction time of 1hrs possibly do not permit the proper impregnation of catalyst with oil leading to partially converted products. A slight decrease in CLB content at 6h reaction time with 1:7 ml methanol might be due oil dilution effect that cause reverse transesterification reaction, making it unfavourable to obtain FAMES yield. The similar behaviour was observed by (Agarry and Ogunleye, 2012; Fan et al., 2011). ANOVA result, however, is insignificant with P-value (0.4317) >0.05.

3.3.4.4.6 Interactive impact of oil: methanol ratio and temperature

The combined effect of temperature along with oil:alcohol ratio upon CLB yield is shown in Figure 3.3.4.4 F. Since maximum biodiesel (90.0%) obtained with steady rise in temperature (90%) as the temperature increased to 90 °C with 1:4 methanol. However much higher temperature (> 100 °C) cause reduced CLB yield that is linked to the gasification of methanol (Yuan et al., 2008). Therefore, it can be concluded from ANOVA results that combined effect of these two parameters on the yield of biodiesel is insignificant with P-value (0.6006) >0.05.

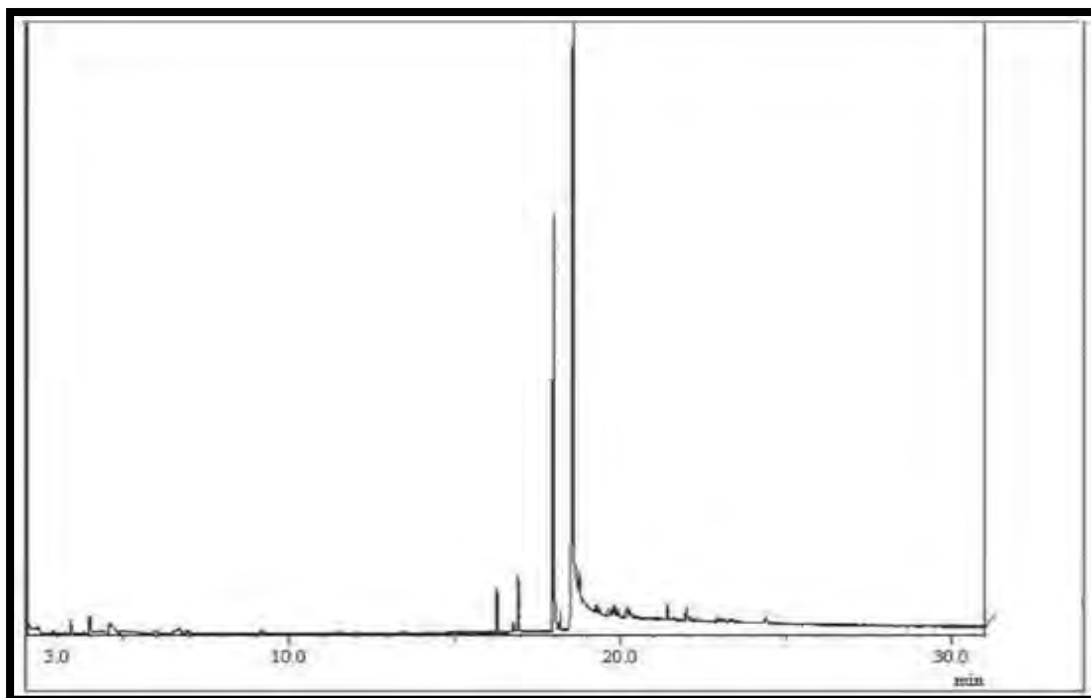


Figure 3.3.4.2.1: GC-MS of *Carthamus lanatus* Biodiesel (CLB)

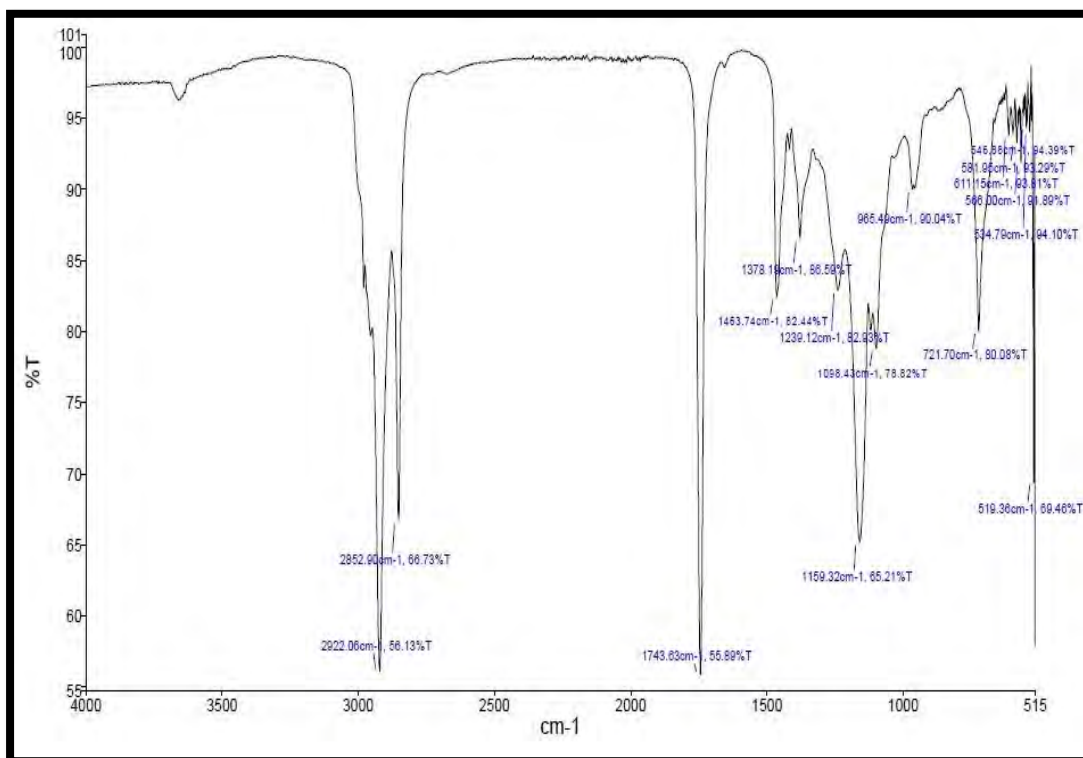


Figure 3.3.4.2.2: FT-IR of *Carthamus lanatus* Biodiesel (CLB)

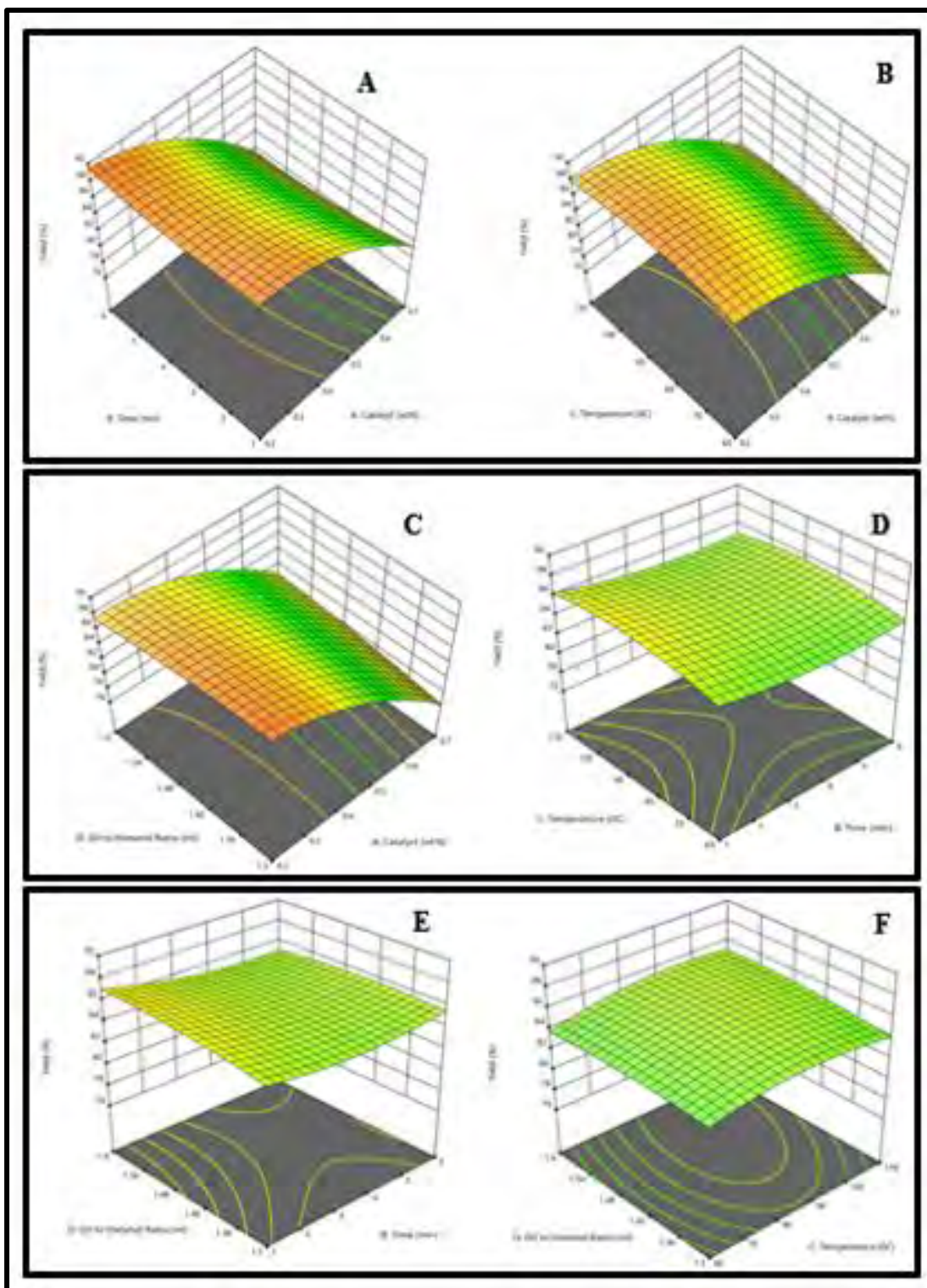


Figure 3.3.4.4: 3D surface Plots showing the impact of different parameters on *Carthamus lanatus* biodiesel (CLB) yield

Table 3.3.4: Optimized Conditions for CLB Synthesis Using Na-Mmt, Na-Ag-Mmt, Cu-Mg-Zn-Mmt Clay Catalysts

Catalyst	Conc.(g)	Oil:Methanol	Time (hrs)	Temperature °C	Yield%
Al-Mmt	0.4	1:7	5	95	87
Na-Ag-Mmt	0.1	1:6	4	100	89
Cu-Mg-Zn-Mmt	0.2	1:4	4	90	90

Table 3.3.4.2.1: Identified Esters in *Carthamus lanatus* Biodiesel (CLB) Using GC-MS

Peak #	Identified Compound (FAMES)	Retention time	Molecular Formula
1	n-Hexadecanoic acid	14.35	C ₁₉ H ₃₄ O ₂
2	Hexadecanoic acid	16.25	C ₁₆ H ₃₂ O ₂
3	Ethyl hexadecanoate	16.29	C ₁₈ H ₃₆ O ₂
4	Oleic acid methyl ester	18.02	C ₁₉ H ₃₆ O ₂
5	Ethyl Oleate	18.23	C ₂₀ H ₃₈ O ₂
6	9,12-Octadecadienoic acid	18.53	C ₁₈ H ₃₂ O ₂

Table 3.3.4.2.2: FT-IR Spectrum of *Carthamus lanatus* Biodiesel (CLB)

Peaks (cm ⁻¹)	Frequency Range (Cm ⁻¹)	Bond	Functional Group	Characteristics of peak
2922.06	3000-2850	H-C=O: C-H stretch	Aldehyde	Medium to strong
2852.90	2870-2695	C-H stretch	Alkane	Medium to Strong
1743.63	1750-1700	RCOOH	Ester	Strong
1463.74	1470-1450	C-H bend	Alkane	Variable
1378.19	1400-1360	C-N stretch	Amines	Medium
1239.12	1250-1220	C-N stretch	Amines	Medium
1159.32	1250-1020	C-N stretch	Amines	Medium
1098.43	1250-1020	C-O stretch	Ether	Strong/medium
721.70	725-720	C-Cl stretch	Alkyl Halide	Strong
581.95	600-500	C-Cl stretch	Alkyl Halide	Strong

Table 3.3.4.2.3: Fuel Properties of *Carthamus lanatus* Biodiesel (CLB)

TESTS	METHODS	ALM-B100
Colour	Visual	2
Flash Point °C (PMCC)	ASTM D-93	74
Density @ 15 °C Kg/L	ASTM D-1298	0.8304
K.Viscosity @ 40 °C cST	ASTM D-445	4.11
Pour Point °C	ASTM D-97	-8
Cloud Point °C	ASTM D-2500	-11
Sulphur %wt	ASTM D-4294	0.0002
Total Acid No. mg KOH/gm	ASTM D-974	0.171

3.3.4.4 Experimental and Predicted yield of *Carthamus lanatus* Biodiesel(CLB) using Box-Behnken Design

Std	Run	Catalyst (wt%)	Time (min)	Temperature (°C)	Oil: Methanol (ml)	Yield %
30	1	0.45	3.5	85	1.45	86
11	2	0.2	6	60	1.6	87
8	3	0.7	6	110	1.3	76
4	4	0.7	6	60	1.3	76
9	5	0.7	1	101.667	1.6	87
17	6	0.2	4	90	1.4	90
6	7	0.7	1	110	1.3	77
26	8	0.45	3.5	85	1.45	86
19	9	0.45	1	85	1.45	86
21	10	0.45	3.5	60	1.45	86
7	11	0.2	6	110	1.3	89
1	12	0.2	1	60	1.3	89
20	13	0.45	6	85	1.45	86
18	14	0.7	3.5	85	1.45	76
12	15	0.7	6	60	1.6	76
15	16	0.2	6	110	1.6	87
27	17	0.45	3.5	85	1.45	85
29	18	0.45	3.5	85	1.45	85
23	19	0.45	3.5	85	1.3	85
25	20	0.45	3.5	85	1.45	85
10	21	0.7	1	60	1.6	78
14	22	0.7	1	110	1.6	78
16	23	0.7	6	110	1.6	78
24	24	0.45	3.5	85	1.6	85
13	25	0.2	1	110	1.6	87
22	26	0.45	3.5	110	1.45	86
28	27	0.45	3.5	85	1.45	86
3	28	0.2	6	60	1.3	89
5	29	0.2	1	110	1.3	89
2	30	0.7	1	60	1.3	76

3.3.4.4.1 Analysis of Variance (ANOVA) from Achieved Results

Source	Sum of Squares	df	Mean Square	F-value	p-value	Remarks
Model	2.05	14	0.1465	105.25	< 0.0001	significant
A-Catalyst	1.79	1	1.79	1284.89	< 0.0001	
B-Time	0.0016	1	0.0016	1.17	0.2966	
C-Temperature	0.0016	1	0.0016	1.17	0.2966	
D-Oil to Metanol Ratio	0.0011	1	0.0011	0.8015	0.3848	
AB	0.0018	1	0.0018	1.32	0.2694	
AC	0.0018	1	0.0018	1.32	0.2694	
AD	0.0316	1	0.0316	22.71	0.0003	
BC	0.0002	1	0.0002	0.1449	0.7088	
BD	0.0002	1	0.0002	0.1449	0.7088	
CD	0.0002	1	0.0002	0.1449	0.7088	
A ²	0.0661	1	0.0661	47.52	< 0.0001	
B ²	0.0003	1	0.0003	0.2484	0.6254	
C ²	0.0003	1	0.0003	0.2484	0.6254	
D ²	0.0047	1	0.0047	3.37	0.0864	
Residual	0.0209	15	0.0014			
Lack of Fit	0.0165	10	0.0016	1.88	0.2520	not significant
Pure Error	0.0044	5	0.0009			
Cor Total	2.07	29				

3.3.5 *Beaumontia grandiflora* Wall Biodiesel
(BGB)

3.3.5 *Beaumontia grandiflora* Wall Derived Biodiesel (BGB)

Beaumontia grandiflora Wall has 25.79% oil content and free fatty acid (FFA) content is 0.352 which means it only requires one step transesterification to be converted into biodiesel (Table 3.3.1). A series of transesterification reactions were carried out to get the optimum yield of the biodiesel produced from the seeds oil of *Beaumontia grandiflora* Wall. The conditions at which optimum yield of the biodiesel from each of the catalysts was obtained is given in table 3.3.5. All the three catalysts i.e. Al-Mmt clay catalyst, Na-Ag Mmt catalyst, Cu-Mg-Zn Mmt clay catalyst, were used in the transesterification of the seeds oil of *Beaumontia grandiflora* Wall to biodiesel but Cu-Mg-Zn-Mmt clay catalyst gave the best yield among all i.e. 88.52% biodiesel yield (Table 3.3.5).

3.3.5.1 Reaction Variables Affecting Transesterification of *Beaumontia grandiflora* Wall Seeds Oil to Biodiesel

Transesterification reaction is dependent on the variables discussed below:

3.3.5.1.1 Oil to Methanol Molar Ratio

Oil to methanol ratios of 1:3, 1:4, 1:5, 1:6, 1:7, 1:8, 1:9 and 1:10 were used keeping other reaction conditions constant i.e. reaction time, reaction temperature and catalyst concentration constant. The maximum conversion ratio was obtained at 1:7 by Al-Mmt, 1:9 for both Na-Ag-Mmt and Cu-Mg-Zn-mmt clay catalysts.

3.3.5.1.2 Catalyst Concentration

Transesterification reaction for conversion of *Beaumontia grandiflora* seeds oil to FAMES, was carried out at different catalyst concentrations i.e. 0.1g, 0.2g, 0.3g, 0.4g, 0.5g, 0.6g and 0.7g and maximum yield of biodiesel was obtained at 0.6 g of Al-Mmt clay catalyst, 0.3 g in case of Na-Ag-Mmt clay catalyst and 0.3 g of Cu-Mg-Zn-Mmt clay catalyst gave best results.

3.3.5.1.3 Reaction Temperature (°C)

Temperature of the reaction and biodiesel yield are directly proportional i.e. increase in temperature results in the increase of the biodiesel yield up to the threshold point (>150°C) (Mehar et al, 2006, Munir et al, 2019). A series of reactions were carried out at different reaction conditions keeping other factors constant i.e. methanol to oil molar ratio and catalyst concentration. Highest conversion ratio was achieved at 95 °C in case of Al-Mmt and 100 °C for Na-Ag-Mmt and Cu-Mg-Zn clay catalysts.

3.3.5.2 Chemical Characterization

3.3.5.2.1 GC-MS Analysis of *Beaumontia grandiflora* Wall Biodiesel (BGB)

GC-MS analysis is broadly used technique to determine the chemical composition, type and structure of synthesized Fatty Acid Methyl Esters (FAMES). Mass spectrometer was set to scan in the range of m/z 2-600 and ionization potential 70V (Bu et al., 2014; Zhang et al., 2014). Different FAMES were determined using the retention time by Mass Spectroscopic analysis. Helium gas was used as a carrier with reaction temperature 300°C for 45 minutes. Ten distinguishing peaks of *Beaumontia grandiflora* Wall biodiesel were observed as presented in figure 3.3.5.2.1. At peak 1, Isopropyl alcohol (C₃H₈O) was present. 2,4-Decadienal (E,E) having molecular formula of C₁₀H₁₆O was present at second peak. Third peak identified n-Hexadecanoic acid (C₁₆H₃₂O) in the biodiesel sample. Fourth, fifth, sixth, seventh, eighth, ninth and tenth indicate the presence of Octadecadienoic acid (Z,Z),methyl ester (C₁₉H₃₄O), 9-Octadecenoic acid, methyl ester (C₁₉H₃₆O₂), Oleic Acid (C₁₈H₃₄O₂), Octadecanoic acid (C₁₈H₃₆O₂), Oleoyl chloride (C₁₈H₃₃ClO), cyclododecyne (C₁₂H₂₄) and 9-Octadecenoic acid, 1,2,3-propanetriyl ester (C₅₇H₁₀₄O₆) respectively. The dominant ester compound was methyl 9-octadecanoate which confirms the formation of biodiesel (Table 3.3.5.2.1).

3.3.5.2.2 FT-IR of *Beaumontia grandiflora* Wall Biodiesel (BGB)

FT-IR is a modern analytical method for fast and easy detection of Fatty acid methyl esters due to its capability as “finger-print technique” which aid in recognition

of chemical bonds and functional groups in oils, fats and biodiesel samples. Figure 3.3.5.2.2 represents the FT-IR spectrum of *Beaumontia grandiflora* Wall Biodiesel. The alcohol (O-H) and aldehyde group were observed at 2980.83 cm^{-1} . The medium to strong characteristic peaks of alkane was observed at 2922.05 cm^{-1} to 2852.93 cm^{-1} . Characteristic peak (strong) of the ester group was found at 1743.58 cm^{-1} . A medium peak of alkane was observed at 1463.62 cm^{-1} due to bending of the plane of C-H bond. Whereas the peaks at 1378.51 cm^{-1} , 1239.77 cm^{-1} and 1159.26 cm^{-1} depict the presence of aliphatic amines (C-N) group. A strong ether group was found at peak 1098.57 cm^{-1} . However, peaks at 956.36 cm^{-1} and 721.74 cm^{-1} show the bending of C=C plane in case of alkene and a strong stretch in C-Cl bond in case of alkyl halide respectively. The main spectrum region which distinguishes between crude oil and its respective biodiesel is in the range of $1500\text{-}900\text{ cm}^{-1}$. The FTIR confirms the presence of ester carbonyl bond near the absorption band 1743.71 cm^{-1} (Daniyan et al., 2019). Presence of above-mentioned peaks in the FT-IR spectra confirms the biodiesel synthesis (Table 3.3.5.2.2).

3.3.5.2.3 Fuel Properties of *Beaumontia grandiflora* Wall Biodiesel (BGB)

The fuel properties of synthesized *Beaumontia grandiflora* Wall Biodiesel were determined and compared with the ASTM standards (Table 3.3.5.2.3). These properties help in the determination of the quality of fuel and its effect on diesel engine. Total acid number or acid value is amount of the free fatty acids existent in a fuel sample and is determined in mg KOH/gm. If its value is higher in the sample that means engine efficiency will be affected in a negative way (Akhtar et al., 2019). *Beaumontia grandiflora* Wall Biodiesel's acid value (0.172 mg KOH/gm) is well in range of international standards. Density of the BGB is also in accordance with the international standards i.e. 0.8312 mg KOH/gm . Fuel density value is also crucial as its higher value causes engine corrosion and decreases its efficiency (Sultana et al., 2016). Kinematic viscosity is the determinant of the fuel thickness, higher value causes deposition in engine and reduces its working efficiency (Gunstone & Hamilton, 2001). *Beaumontia grandiflora* Wall Biodiesel's kinematic viscosity is in range of international standards (4.21 kg/L). The color of produced biodiesel is on visual 2 according to ASTM standards. Another important aspect is the Flash point of the diesel during fuel handling

and transportation and fuels having flash point higher than 60°C are referred as safe (Salaheldeen et al., 2015). At this temperature fuel ignition starts. Flash point of *Beaumontia grandiflora* Wall Biodiesel was found to be 72°C. Additional important parameter is cold flow properties which includes Pour point and Cloud point of biodiesel (Akhtar et al., 2019). Pour point and cloud point value of BGB were -8°C and -9°C respectively. The sulfur content of BGB was (0.0002ppm) by %weight. An ideal fuel has low sulfur content and is more operative for engine's life and environment (Candeia et al., 2009).

3.3.5.3 Optimization Study of Transesterification Operational Factors Through Response Surface Methodology (RSM)

The response surface methodology (RSM) using the Box Behnken Design for transesterification of BGO using four variables with maximum and minimum ranges i.e., Catalyst (A) 0.3-0.7 (Cu-Mg-Zn-Mmt), Time (B) 1-7 hrs, Temperature (C) 50-110 °C and Oil to Methanol (D) 1:4-1:9 for 30 experiments are presented in Table 3.3.5.4. A coded model equation underneath was used for studying the association among Input Variables as well as Output Response in terms of yield (Y).

$$Y = +7.00925+0.451829A+0.001590B-0.003001C+2.49968D+9.68399E-06AB-0.006698AC+0.002399AD+7.40218E-06BC+0.001110BD+0.001104CD-0.025068A^2-1.11414E-06B^2+0.000029C^2-0.697075D^2$$

The ANOVA results as presented in Table 3.3.5.4.1 depicting models significance with Fvalue 7.24 (P-value = 0.0002<1) and F-value corresponding to the lack of fit is 4.88. The Model F-value of 7.24 implies the model is significant. There is only a 0.02% chance that an F-value this large could occur due to noise. The Lack of Fit F-value of 4.88 implies the Lack of Fit is significant. There is only a 4.71% chance that a Lack of Fit F-value this large could occur due to noise. Significant lack of fit is bad, and we want the model to fit. Predicted R² is -0.2718 and adjusted R² is 0.7507, negative Predicted R² implies that the overall mean may be a better predictor of the response than the current model. In some cases, a higher order model may also predict better. Adequate Precision measures the signal to noise ratio. A ratio greater than 4 is desirable. model ratio of 15.438 indicates an adequate signal. This model can be used to navigate the design space.

3.3.5.4 Parametric characterization of transesterification process

The interactive effect of different variables on transesterification reaction were considered by drawing three-dimensional response curves versus every dual Independent variable and are presented here in Figure 3.3.5.4 A, B, C, D, E & F. These can be explained in the following sub sections.

3.3.5.4.1 Interactive Impact of Catalyst Amount and Time

The combine influence of catalyst amount and time on biodiesel yield is presented into Figure 3.3.5.4 A, while keeping other parameters I.e. catalyst amount 0.3 (Cu-Mg-Zn-Mmt), time 7 hrs, temperature 100 °C and oil: methanol ratio (1:9) constant. Since optimum time and catalyst amount (7 hrs and 0.3 wt%) favours the maximum BGB yield (88.52%) which is linked to the system equilibrium that is attained via formation of more methoxy species by the activity of catalyst (Hebbar et al., 2018) with the BGO. However, beyond the optimum values of catalyst concentration and reaction time, sudden drop in yield (85%) was observed (Table 3.3.5.4) due to the backward reaction (Fauzi & Amin, 2013). ANOVA results, therefore, is insignificant with Pvalue (0.4798) > 0.05 for time and catalyst amount.

3.3.5.4.2 Interactive Impact of Catalyst Amount and Temperature

The Figure 3.3.5.4 B represents the combined influence of temperature and catalyst concentration on the BGB yield. Maximum BGB (88.52%) was obtained with the catalyst loading of 0.3 wt% and reaction temperature of 100 °C. However, lower conversion of BGB (85%) observed at 0.7% catalyst (Table 3.3.5.4.) due to partial changeover of triglyceride to methyl ester, which is consistent with the previous study (Chakraborty and Sahu, 2014). And 80% BGB content was observed as the amount of catalyst and temperature increased beyond 0.8 wt% and 100-120 °C due to the less interaction between the reactant and catalyst. Therefore, it can be concluded from the ANOVA results that the interactive outcome of these parameters (time and catalyst amount) on biodiesel yield is highly significant with P-value (0.0034) < 0.05.

3.3.5.4.3 Interactive Impact of Catalyst Amount and Oil: Methanol Ratio

The Figure 3.3.5.4 C showing collective effect of the catalyst and oil methanol on yield of biodiesel. The high yield of BGB (88.52%) is achieved with 1:9 oil: methanol ratio and 0.3% catalyst concentration respectively. Both oil: methanol ratio and concentration of catalyst has the foremost role for providing maximum biodiesel yield. The biodiesel yield increases considerably by increasing both the catalyst concentration and methanol amount from 0.1-0.3% and 1:3-1:9. However, lower conversion of 80 % BGB observed with 1% catalyst and 1:7 ml oil to methanol due to partial changeover of triglyceride to methyl ester, which is consistent with the previous study (Tan et al., 2010). The slight drop in BGB content was observed as the amount of catalyst and methanol increased beyond 1 wt% and 1:7. Our results are in line with the reported work (Tan et al., 2017). However, ANOVA results depicts that oil: methanol and catalyst concentrations interactive effect are insignificant owing to their P-value (0.6398) > 0.05.

3.3.5.4.4 Interactive impact of time and temperature

The cooperative influence of time and temperature on BGB yield is presented in Figure 3.3.5.4 D. Significant BGB yield (88.52%) was observed as the reaction time and temperature increases from 1-7 hrs and 80-100 °C. This is so, higher temperatures facilitates the well diffusion of catalyst particle with BGO thus enhances the increased interaction among the protons which in turn supports the higher transition of BGO to BGB. On the other hand, methanol gasification would result if the temperature raised above the above (> 110 °C) leading to reduced BGB content (80 %). A slight decrease in BGB content was thus observed at 6 hrs reaction time at 110 °C. The similar trend was observed by (Li et al., 2010). The ANOVA results is insignificant for these parameters owing to P-value (0.9923) > 0.05.

3.3.5.4.5 Interactive Impact of Time and Oil: Methanol Ratio

The time on and oil methanol interactive impact on BGB yield is presented in the Figure 3.3.5.4 E while keeping other parameters like catalyst concentration (0.3%) and temperature (100°C) constant. The 1:9 oil: methanol ratio and reaction time of 7

hrs favours the highest BGB yield (88.52%). It is evident from the 3D plot that there is a direct relation between ratio of oil: methanol and BGB yield. Therefore, determining the optimum value of these parameters is essential for maximizing the BGB yield. The two-sided mode of transesterification process thus necessitates the surplus alcohol to maintain the balance in reaction (higher conversion of oil to BGB). The little reaction time of 1h and low methanol ratio (1:3) possibly do not permit the proper impregnation of modified clay with oil to achieve the equilibrium leading to partially converted products. A slight decrease in BGB content at 6h with 1:7 oil methanol ratio might be due to reserve transesterification reaction, making it unfavourable to obtain BGB yield. Same trend was observed with 6 hrs reaction time at the molar ratio of 1:7 with decreased in BGB content (80%), related to the oil's dilution effect (Xue, 2013). The ANOVA results for the combined effect of these parameters on the yield of biodiesel is insignificant with Pvalue (0.3004) > 0.05.

3.3.5.4.6 Interactive impact of oil: methanol ratio and temperature

The Figure 3.3.5.4 F represents the combined effect of oil:alcohol ratio and temperature on the BGB yield. Maximum BGB (88.52%) obtained as the temperature increased to 100 °C with 1:9 oil to methanol ratio. Conversely, temperature above the threshold level (> 100 °C) reduced bgb content (Shin et al., 2012). Therefore, it can be concluded from results that combined effect of these two parameters on the yield of biodiesel is insignificant with P-value (0.3004) > 0.05.

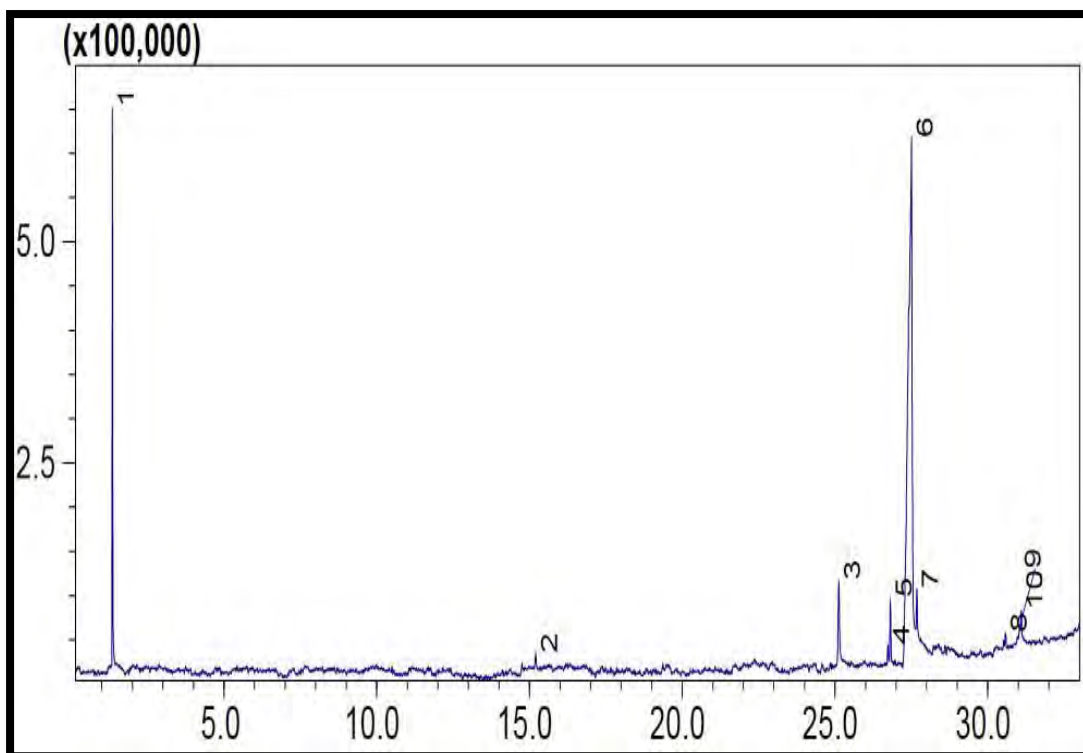


Figure 3.3.5.2.1: GC-MS of *Beaumontia grandiflora* Wall Biodiesel (BGB)

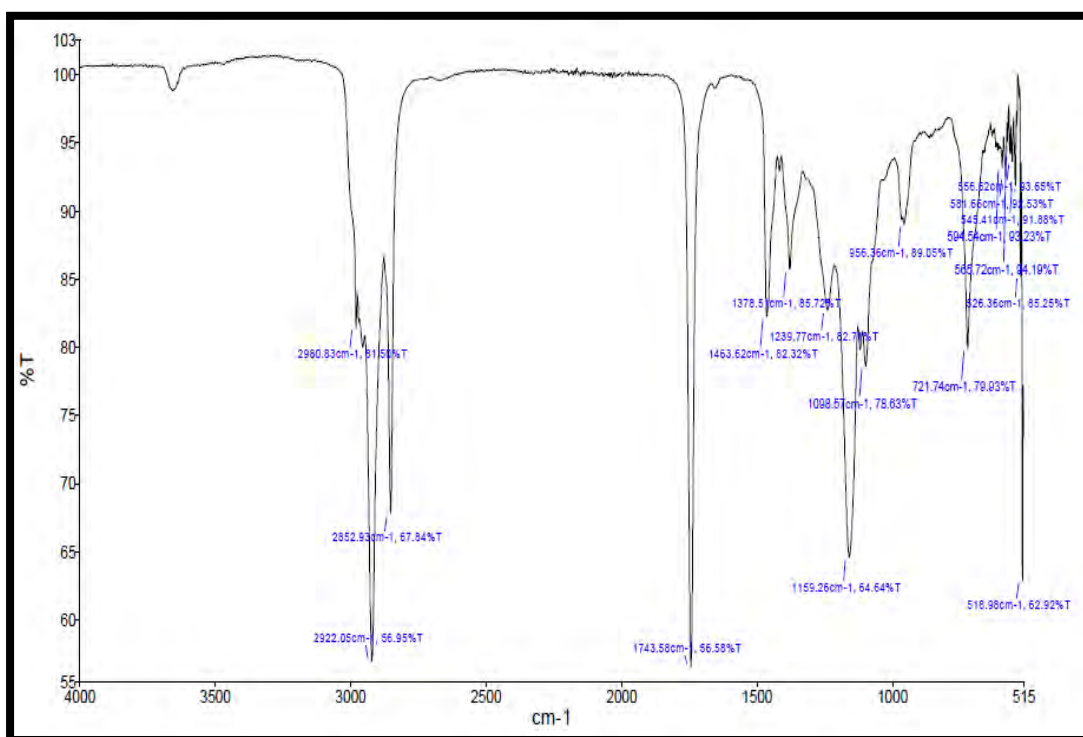


Figure 3.3.5.2.2: FT-IR of *Beaumontia grandiflora* Wall Biodiesel (BGB)

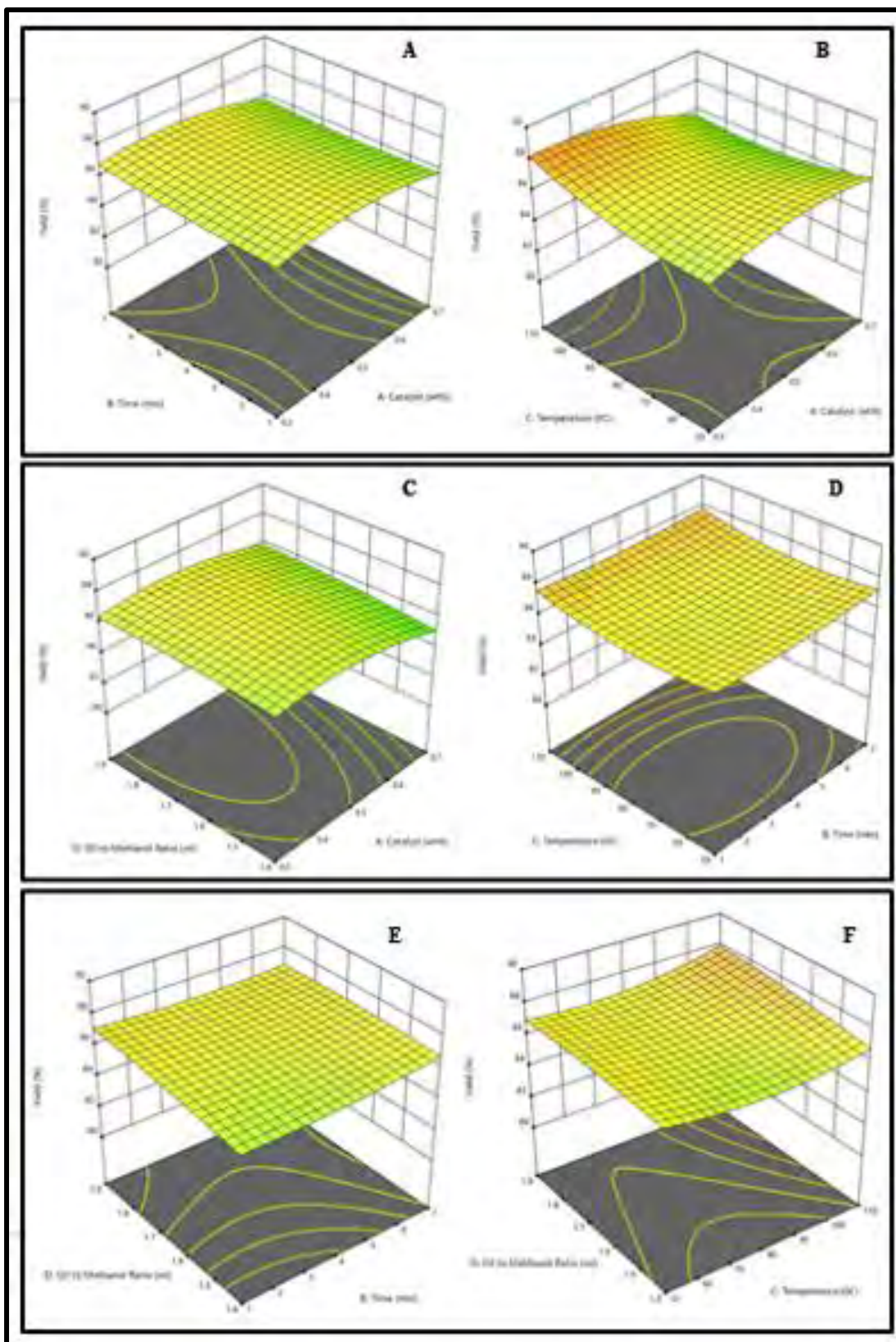


Figure 3.3.5.4: 3D surface Plots showing the impact of different parameters on *Beaumontia grandiflora* Wall biodiesel (BGB) yield

Table 3.3.5: Optimized Conditions for BGB Synthesis Using Na-Mmt, Na-Ag-Mmt, Cu-Mg-Zn-Mmt Clay Catalysts

Catalyst	Conc.(g)	Oil:Methanol	Time (hrs)	Temperature °C	Yield%
Al-Mmt	0.6	1:7	8	95	85
Na-Ag-Mmt	0.5	1:9	6.5	100	87
Cu-Mg-Zn-Mmt	0.3	1:9	7	100	88.52

Table 3.3.5.2.1: Identified Esters in. *Beaumontia grandiflora* Wall Biodiesel (BGB) Using GC-MS

Peak #	Identified Compound (FAMES)	Retention time	Molecular Formula
1	Isopropyl alcohol	1.345	C ₃ H ₈ O
2	2,4-Decadienal-(E,E)	15.203	C ₁₀ H ₁₆ O
3	n-Hexadecanoic acid	25.127	C ₁₆ H ₃₂ O ₂
4	9,12-Octadecadienoic acid-(Z,Z), methyl ester	26.732	C ₁₉ H ₃₄ O
5	9-Octadecenoic acid, methyl ester	26.732	C ₁₉ H ₃₆ O ₂
6	Oleic Acid	27.506	C ₁₈ H ₃₄ O ₂
7	Octadecanoic acid	27.679	C ₁₈ H ₃₆ O ₂
8	Oleoyl chloride	30.580	C ₁₈ H ₃₃ ClO
9	Cyclododecyne	31.040	C ₁₂ H ₂₄
10	9-Octadecenoic acid, 1,2,3-propanetriyl ester	31.098	C ₅₇ H ₁₀₄ O ₆

Table 3.3.5.2.2: FT-IR of *Beaumontia grandiflora* Wall (BGB) biodiesel

Peaks (cm ⁻¹)	Frequency Range (Cm ⁻¹)	Bond	Functional Group	Characteristics of peak
2980.83	3000-2850	H-C=O: C-H stretch	Aldehyde	Medium to strong
2922.05	3000-2500	C-H stretch	Alkane	Medium
2852.93	2870-2695	C-H stretch	Alkane	Medium to Strong
1743.58	1750-1700	RCOOH	Ester	Strong
1463.62	1470-1450	C-H bend	Alkane	Medium
1378.51	1400-1360	C-N stretch	Amines	Medium
1239.77	1250-1220	C-N stretch	Amines	Medium
1159.26	1250-1020	C-N stretch	Amines	Medium
1098.57	1250-1020	C-O stretch	Ether	Strong/medium
956.36	1000-650	C=C bend	Alkene	Strong
721.74	725-720	C-Cl stretch	Alkyl Halide	Strong

Table 3.3.5.2.3: Fuel Properties of *Beaumontia grandiflora* Wall Biodiesel (BGB)

TESTS	METHODS	ALM-B100
Colour	Visual	2
Flash Point °C (PMCC)	ASTM D-93	72
Density @ 15 °C Kg/L	ASTM D-1298	0.8312
K.Viscosity @ 40 °C cST	ASTM D-445	4.21
Pour Point °C	ASTM D-97	-8
Cloud Point °C	ASTM D-2500	-9
Sulphur %wt	ASTM D-4294	0.0002
Total Acid No. mg KOH/gm	ASTM D-974	0.172

3.3.1.4 Experimental and Predicted yield of *Beaumontia grandiflora* Wall Biodiesel (BGB) using Box-Behnken Design

Std	Run	Catalyst (wt%)	Time (hrs)	Temperature (°C)	Oil: Methanol (ml)	Yield %
7	1	0.3	7	110	1.4	88
27	2	0.5	4	80	1.65	87
16	3	0.7	7	110	1.9	87
23	4	0.5	4	80	1.4	86
29	5	0.5	4	80	1.65	87
15	6	0.3	7	100	1.9	88.52
20	7	0.5	7	80	1.65	87
25	8	0.5	4	80	1.65	87
18	9	0.7	4	80	1.65	86
21	10	0.5	4	50	1.65	87
10	11	0.7	1	50	1.9	88
9	12	0.3	1	50	1.9	86
26	13	0.5	4	80	1.65	86
5	14	0.3	1	110	1.4	87
6	15	0.7	1	110	1.4	86
14	16	0.7	1	110	1.9	85
13	17	0.3	1	110	1.9	89
19	18	0.5	1	80	1.65	86
24	19	0.5	4	80	1.9	86
28	20	0.5	4	80	1.65	87
22	21	0.5	4	110	1.65	87
11	22	0.3	7	50	1.9	86
1	23	0.3	1	50	1.4	86
12	24	0.7	7	50	1.9	86
17	25	0.3	4	80	1.65	87
2	26	0.7	1	50	1.4	85
3	27	1	7	110	1.7	80
8	28	0.7	7	110	1.4	85
30	29	0.5	4	80	1.65	87
4	30	0.7	7	50	1.4	87

3.3.5.4.1 Analysis of Variance (ANOVA) from Achieved Results

Source	Sum of Squares	df	Mean Square	F-value	p-value	Remarks
Model	5.73	14	0.4095	69.67	< 0.0001	Significant
A-Catalyst	4.84	1	4.84	822.98	< 0.0001	
B-Time	0.0009	1	0.0009	0.1464	0.7074	
C-Temperature	0.0009	1	0.0009	0.1483	0.7056	
D-Oil to Methanol Ratio	0.0008	1	0.0008	0.1380	0.7155	
AB	0.0033	1	0.0033	0.5603	0.4657	
AC	0.0033	1	0.0033	0.5643	0.4641	
AD	0.0008	1	0.0008	0.1297	0.7237	
BC	3.054E-06	1	3.054E-06	0.0005	0.9821	
BD	0.0076	1	0.0076	1.29	0.2745	
CD	0.0008	1	0.0008	0.1336	0.7198	
A ²	0.4010	1	0.4010	68.22	< 0.0001	
B ²	0.0125	1	0.0125	2.13	0.1652	
C ²	0.0689	1	0.0689	11.72	0.0038	
D ²	0.0004	1	0.0004	0.0609	0.8085	
Residual	0.0882	15	0.0059			
Lack of Fit	0.0355	10	0.0036	0.3374	0.9324	not significant
Pure Error	0.0526	5	0.0105			
Cor Total	5.82	29				

3.3.6 *Acasia concinna* Biodiesel (ACB)

3.3.6 *Acasia concinna* Biodiesel (ACB)

Acasia concinna has 22% oil content and free fatty acid (FFA) content is 1.183 which means it only requires one step transesterification to be converted into biodiesel (Table 3.3.1). A series of transesterification reactions were carried out to get the optimum yield of the biodiesel produced from the seeds oil of *Acasia concinna* biodiesel (ACB) using all three catalysts. The conditions at which optimum yield of the biodiesel from each of the catalysts was obtained is given in table 3.3.6. All the three catalysts i.e. Al-Mmt clay catalyst, Na-Ag Mmt catalyst, Cu-Mg-Zn Mmt clay catalyst, were used in the transesterification of the seeds oil of *Acasia concinna*.to biodiesel but Na-Ag-Mmt clay catalyst gave the best yield among all i.e. 90%, Cu-Mg-Zn-Mmt clay catalyst gave 87% yield whereas Al-Mmt clay catalyst gave biodiesel yield of 89%.

3.3.6.1 Reaction Variables Affecting Transesterification of *Acasia concinna* Seeds Oil to Biodiesel

Following factors affect biodiesel yield in the transesterification of fatty acids in the presence of alcohol in a catalyzed reaction.

3.3.6.1.1 Oil to Methanol Molar Ratio

Oil to methanol ratios of 1:3, 1:4, 1:5, 1:6, 1:7, 1:8, 1:9 and 1:10 were used keeping other reaction conditions constant i.e. reaction time, reaction temperature and catalyst concentration constant. The maximum conversion ratio was obtained at 1:7 by Al-Mmt and Cu-Mg-Zn-mmt clay catalysts, 1:6 for Na-Ag-Mmt clay catalyst.

3.3.6.1.2 Catalyst Concentration

Transesterification reaction for conversion of *Acasia concinna* seeds oil to FAMES, was carried out at different catalyst concentrations i.e. 0.1g, 0.2g, 0.3g, 0.4g, 0.5g, 0.6g and 0.7g and maximum yield of biodiesel was obtained at 0.5 g of Al-Mmt clay catalyst, 0.3 g in case of Na-Ag-Mmt clay catalyst and 0.4 g of Cu-Mg-Zn-Mmt clay catalyst gave best results.

3.3.6.1.3 Reaction Temperature (°C)

Temperature of the reaction and biodiesel yield are directly proportional i.e. increase in temperature results in the increase of the biodiesel yield up to the threshold point ($>150^{\circ}\text{C}$) (Mehar et al, 2006, Munir et al, 2019). A series of reactions were carried out at different reaction conditions keeping other factors constant i.e. methanol to oil molar ratio and catalyst concentration. Highest conversion ratio was achieved at 90°C in case of Both Al-Mmt and Na-Ag-Mmt and 100°C for Cu-Mg-Zn clay catalysts.

3.3.6.2 Chemical Characterization

3.3.6.2.1 GC-MS Analysis of *Acasia concinna* Biodiesel (ACB)

GC-MS analysis is widely used technique to determine the chemical composition, type and structure of synthesized Fatty Acid Methyl Esters (FAMES). Mass spectrometer was set to scan in the range of m/z 2-600 and ionization potential 70V (Bu et al., 2014; Zhang et al., 2014). Different FAMES were determined using the retention time by Mass Spectroscopic analysis. Helium gas was used as a carrier with reaction temperature 300°C for 45 minutes. Seven characteristic peaks of *Acasia concinna* biodiesel (ACB) were observed as presented in figure 3.3.6.2.1. At peak 1, Tetradecanoic acid ($\text{C}_{14}\text{H}_{28}\text{O}_2$) was observed. Whereas, 6-Octadecenoic acid ($\text{C}_{18}\text{H}_{34}\text{O}_2$), 9-Hexadecenal ($\text{C}_{16}\text{H}_{30}\text{O}$), 10-Hydroxydecanoic acid ($\text{C}_{10}\text{H}_{20}\text{O}_3$), n-Hexadecanoic acid ($\text{C}_{19}\text{H}_{34}\text{O}_2$), Octadecanoic acid ($\text{C}_{18}\text{H}_{36}\text{O}_2$), Octadecadienoic acid ($\text{C}_{18}\text{H}_{32}\text{O}_2$) were found at second, third, fourth, fifth, sixth and seventh position. Their retention times along with molecular formulas are given in the table 3.3.6.2.1.

3.3.6.2.2 FT-IR Analysis of *Acasia concinna* Biodiesel (ACB)

FT-IR is used for the identification of chemical bonds and explain their stretching and bending vibrations. It also detects the presence and absence of functional groups in chemical compounds (Shaheen et al., 2017). Figure 3.3.6.2.2 shows the FT-IR of *Acasia concinna* methyl esters. A strong peak at 2922.35 cm^{-1} shows the presence of aldehyde group due to the stretch in the H-C=O and C-H bonds. A sharp peak found at 1743.35 cm^{-1} showed the presence of esters. Whereas, peaks at 2853.10 cm^{-1} and 1464.09 cm^{-1} show the presence of alkanes in the sample. Subsequent variable to

medium peaks at 1377.91 cm^{-1} , 1238.52 cm^{-1} and 1160.11 cm^{-1} indicate the presence of amines (C-N). Whereas, a strong peak at 1097.87 cm^{-1} due to the stretching of C-H bond depict the presence of ether group. And peaks at 721.93 cm^{-1} and 595.25 cm^{-1} are due to the presence of alkyl halide group (Table 3.3.6.2.2).

3.3.6.2.3 Fuel Properties of *Acasia concinna* Biodiesel (ACB)

The fuel properties of synthesized *Acasia concinna* Biodiesel (ACB) were determined and compared with the ASTM standards (Table 3.3.6.2.3). These properties help in the determination of the quality of fuel and its effect on diesel engine. Total acid number or acid value is amount of the free fatty acid existent in a fuel sample and is determined in mg KOH/gm. If its value is higher in the sample that means engine efficiency will be affected in a negative way (Akhtar et al., 2019). ACB's acid value (0.175 mg KOH/gm) is well in range of international standards. Density of the ACB is also in accordance with the international standards i.e. 0.921 mg KOH/gm . Fuel density value is also crucial as its higher value causes engine corrosion and decreases its efficiency (Sultana et al., 2016). Kinematic viscosity is the determinant of the fuel thickness, higher value causes deposition in engine and reduces its working efficiency (Gunstone & Hamilton, 2001). ACB's kinematic viscosity is in range of international standards (4.22 kg/L). The color of produced biodiesel is on visual 2 according to ASTM standards. Another important aspect is the Flash point of the diesel during fuel handling and transportation and fuels hving flash point higher than 60°C are referred as safe (Salaheldeen et al., 2015). At this temperature fuel ignition starts. Flash point of *Acasia concinna* Biodiesel (ACB) was found to be 80°C . Additional important parameter is cold flow properties which includes Pour point and Cloud point of biodiesel (Akhtar et al., 2019). Pour point and cloud point value of ACB were -9°C and -12°C respectively. The sulfur content in ACB was (0.0011 ppm) by %weight. An ideal fuel has low sulfur content and is more operative for engine's life and environment (Candeia et al., 2009).

3.3.6.3 Optimization Study of Transesterification Operational Factors Through Response Surface Methodology (RSM)

Table 3.3.6.3 shows the thorough experimental results of ACB yield, using four independent variables with maximum and minimum ranges i.e., Catalyst (A) 0.1-0.3 (Na-Ag-Mmt), Time (B) 1-5 hrs, Temperature (C) 70-90 °C and Oil to Methanol (D) 1:3-1:6 were chosen and 30 experiments were analyzed by RSM using the Box Behnken Design to test the fitness of Quadratic polynomial equation with the Design-Expert 11 (Stat Ease Inc Minneapolis, USA). A coded model equation for studying the association among Input Variables as well as Output Response in terms of yield (Y) is.

$$Y = +14.48646 - 6.545548A + 0.000716B + 0.033675C - 5.42981D + 0.003000AB - 0.001571AC + 1.45793AD - 0.000019BC - 0.003763BD - 0.003737CD + 2.84439A^2 + 0.000036B^2 - 0.000148C^2 + 1.45164D^2$$

Table 3.3.6.4 shows the ANOVA results, with significance models F-value 4 (Pvalue = 0.0058 < 1) while F-value corresponding to the lack of fit is not significant (0.1471), thus confirms the best fitness of model to experimental (trial) data. However, The Predicted R² of 0.5847 is in reasonable agreement with the Adjusted R² of 0.5919; i.e. the difference is less than 0.2. Adeq Precision measures the signal to noise ratio. A ratio greater than 4 is desirable. The ratio of 7.238 indicates an adequate signal. This model can be used to navigate the design space.

3.3.6.4 Parametric characterization of transesterification process

The interactive effect of different variables as presented in Figure 3.3.6.4 A, B, C, D, E, & F can be explained in the following sub sections.

3.3.6.4.1 Interactive Impact of Catalyst Amount and Time

The combine influence of catalyst amount and time on ACB yield is presented into Figure 3.3.6.4 A, while keeping other parameters (oil: methanol ratio (1:6) and temperature (90°C)) constant. 90% ACB obtained with the catalyst loading of 0.3 wt% 5 hr time. This increased yield is being facilitated by abundant methoxy species by the activity of catalyst which establish equilibrium in the reaction (Silitonga et al., 2017). However, beyond the optimum values of catalyst concentration and reaction time,

sudden drop in yield (77%) was observed. This drop in yield might be linked to the shifting of reaction in opposite direction (Dias et al., 2012). Therefore, ANOVA results proves to be insignificant with Pvalue (0.5783) > 0.05 for these parameters.

3.3.6.4.2 Interactive Impact of Catalyst Amount and Temperature

The Figure 3.3.6.4 B shows the combined influence of catalyst concentration and reaction temperature on the ACB yield. Maximum ACB yield (90%) obtained with the catalyst loading of 0.3wt% and reaction temperature from 90°C. However, only 77% ACB was obtained at 0.7% catalyst and 1:6 of oil to methanol, which is similar with the reported work (Sreedhar, 2014). However, as the amount of catalyst and temperature increased beyond 1wt% and 90 °C slight drop in ACB content (77%) was observed. These parameters were found insignificant with P-value (0.7702) > 0.05 as indicated by ANOVA results.

3.3.6.4.3 Interactive Impact of Catalyst Amount and Oil: Methanol Ratio

The Figure 3.3.6.4 C represent three-dimensional surface plot showing collective effect of the catalyst and oil: methanol on yield of biodiesel. The high yield of biodiesel (90 %) is achieved with 1:6 oil: methanol ratio and 0.3% catalyst (Na-Ag-Mmt) concentration respectively. It is evident that there is a close agreement between these process parameters thus helping in attaining maximum ACB yield. The biodiesel yield increases considerably by increasing catalyst concentration and methanol amount from 0.1-0.3% to 60 ml. This will facilities the increased interaction of catalyst with reactant (Worapun et al., 2012). However, lower conversion of 77 % ACB is observed with 0.7% catalyst and low methanol ratio. This low ACB yield is linked to the incomplete changeover of triglyceride to methyl ester, which is coherent with the previous study (Muthukumaran et al., 2017). Same trend is observed with higher catalyst amount and methanol ratio, which favours the emulsification which would ultimately cause difficulty in separation of end products and contributing in decreased yield ACB. However, ANOVA results depicts that oil: methanol and catalyst concentrations interactive effect are insignificant with P-value (0.1876) > 0.05.

3.3.6.4.4 Interactive impact of time and temperature

The cooperative influence of time and temperature on the ACB yield is presented in Figure 3.3.6.4 D. Table 3.3.6.4 shows the 90% ACB yield as time and temperature increases from 1h-5h and 70-90 °C. Since, higher temperatures favour the through dispersion of catalyst particle which in turn support the increased interaction among the protons, and hence, higher transition of oils to ACB. Likewise, temperature above the threshold level (> 90 °C) leads to reduced ACB content (77 %). A slight decrease in ACB content at 6h reaction time at 100 °C might be due to reverse transesterification reaction (Kansedo et al., 2009), making it unfavourable to obtain higher ACB yield. Therefore, ANOVA results for time and temperature on the biodiesel yield is insignificant with P-value (0.5913) > 0.05 .

3.3.6.4.5 Interactive Impact of Time and Oil: Methanol Ratio

The time and oil: methanol collective impact on ACB yield is presented in Figure 3.3.6.4 E. The highest biodiesel yield (90%) is attained at 1:6 oil: methanol ratio and reaction time of 5h respectively. It is obvious that as the ratio of oil: methanol and time increases the yield of biodiesel increases considerably. Therefore, it is vital to determine the optimum value of these parameters in order to maximize the yield of biodiesel. Owing to the two-sided mode of transesterification process, surplus alcohol is needed to maintain the balance in reaction (Saqib et al., 2012) thus giving 90% ACB yield due to increased interaction of excess methanol with oil. ACB yield decreases considerably with 1 hr time and low methanol ratio (1:3) which is linked to partially converted products (Verma and Sharma, 2016a). The same is true as the time and oil methanol ratio increases (6 h, 1:9) due to reverse transesterification reaction, which also contributes the reduced ACB yield (77%). ANOVA results is insignificant for these parameters with P-value equal to 0.6008.

3.3.6.4.6 Interactive impact of oil: methanol ratio and temperature

The combined effect of oil:alcohol ratio and temperature on the ACB yield is presented in Figure 3.3.6.4 F. Maximum ACB (90%) is obtained as the temperature is increased to 90 °C with 60 ml methanol. However, as the temperature raised above 110 °C, ACB yield decreases owing to gasification of methanol (Fan et al., 2010).

Therefore, the combine impact of these parameters as indicated by ANOVA is insignificant with P-value (0.6032) > 0.05.

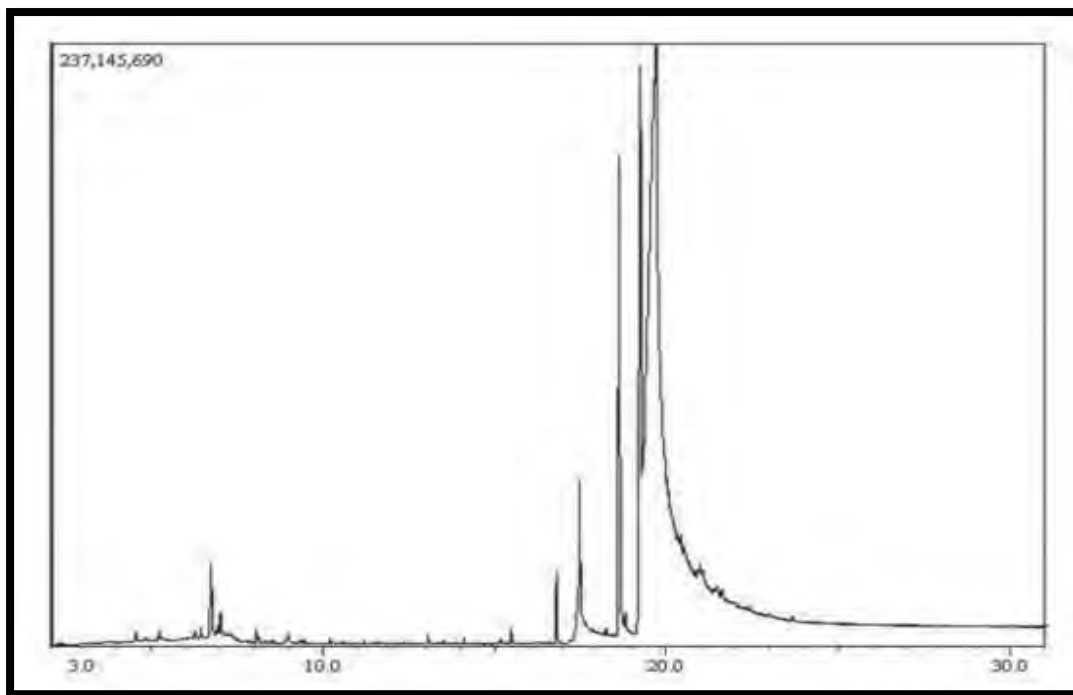


Figure 3.3.6.2.1: GC-MS of *Acasia concinna* Biodiesel (ACB)

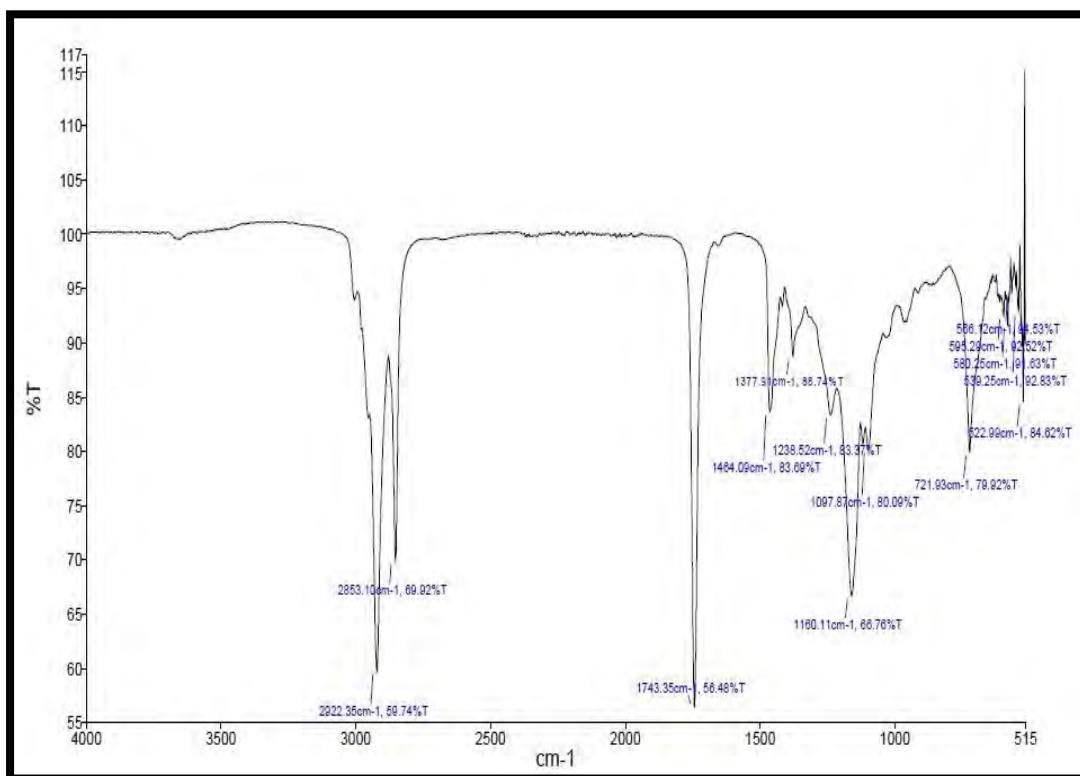


Figure 3.3.6.2.2: FT-IR of *Acasia concinna* Biodiesel (ACB)

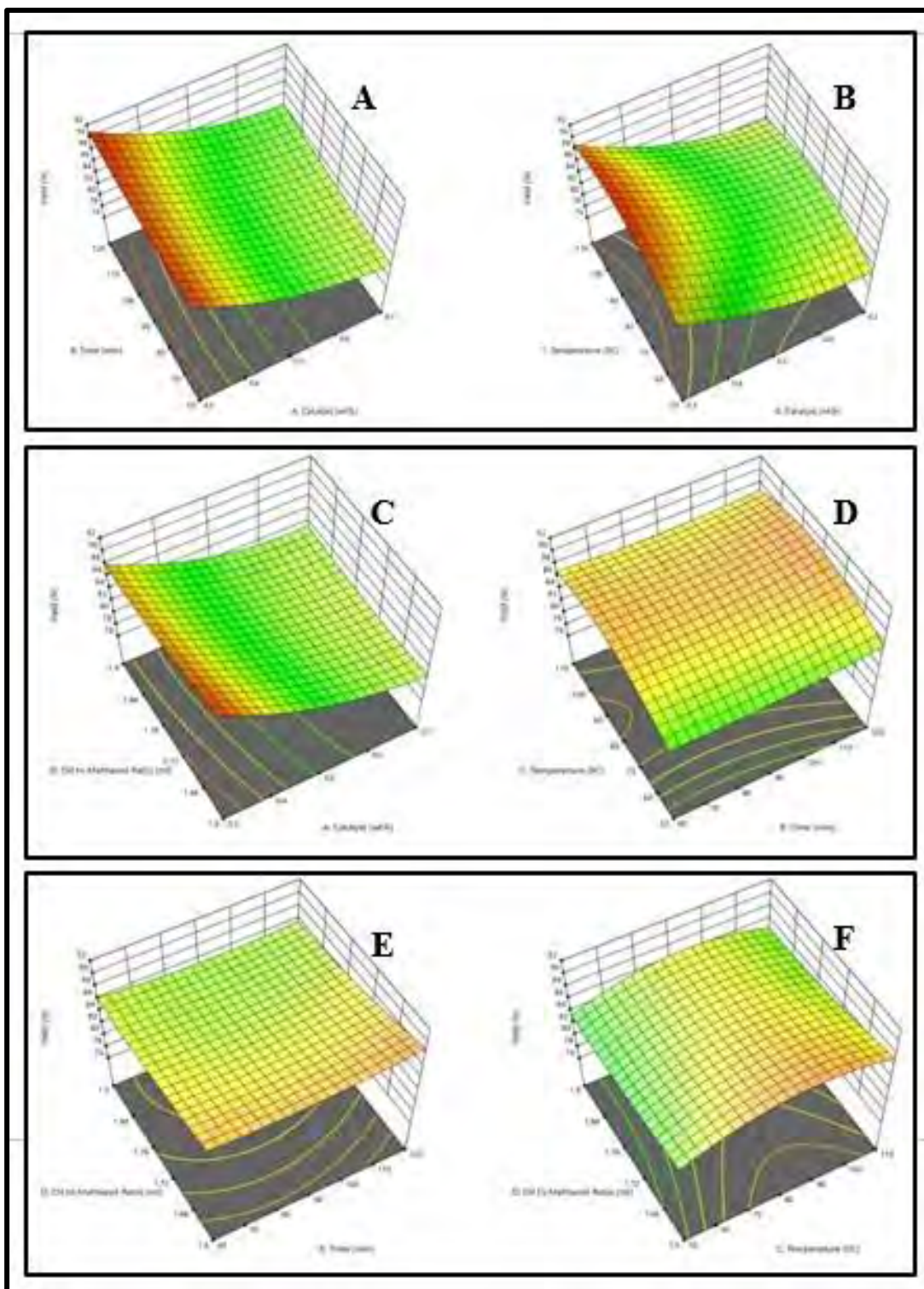


Figure 3.3.6.4: 3D surface Plots showing the impact of different parameters on *Acasia concinna* biodiesel (ACB) yield

Table 3.3.6: Optimized Conditions for ACB Synthesis Using Na-Mmt, Na-Ag-Mmt, Cu-Mg-Zn-Mmt Clay Catalysts

Catalyst	Conc.(g)	Oil:Methanol	Time (hrs)	Temperature°C	Yield%
Al-Mmt	0.5	1:7	6	90	89
Na-Ag-Mmt	0.3	1:6	5	90	90
Cu-Mg-Zn-Mmt	0.4	1:7	5	100	87

Table 3.3.6.2.1: Identified Ester in. *Acasia concinna* Biodiesel (ACB) Using GC-MS

Peak #	Identified Compound (FAMES)	Retention time	Molecular Formula
1	Tetradecanoic acid	13.64	C ₁₄ H ₂₈ O ₂
2	6-Octadecenoic acid	18.00	C ₁₈ H ₃₄ O ₂
3	9-Hexadecenal	18.71	C ₁₆ H ₃₀ O
4	10-Hydroxydecanoic acid	16.21	C ₁₀ H ₂₀ O ₃
5	n-Hexadecanoic acid	14.35	C ₁₉ H ₃₄ O ₂
6	Octadecanoic acid	19.13	C ₁₈ H ₃₆ O ₂
7	Octadecadienoic acid	20.14	C ₁₈ H ₃₂ O ₂

Table 3.3.6.2.2: FT-IR of *Acasia concinna* Biodiesel (ACB)

Peaks (cm ⁻¹)	Frequency Range (Cm ⁻¹)	Bond	Functional Group	Characteristics of peak
2922.35	3000-2850	H-C=O: C-H stretch	Aldehyde	Medium to strong
2853.10	2870-2695	C-H stretch	Alkane	Medium to Strong
1743.35	1750-1700	RCOOH	Ester	Strong
1464.09	1470-1450	C-H bend	Alkane	Variable
1377.91	1400-1360	C-N stretch	Amines	Medium
1238.52	1250-1220	C-N stretch	Amines	Medium
1160.11	1250-1020	C-N stretch	Amines	Medium
1097.87	1250-1020	C-O stretch	Ether	Strong/medium
721.93	725-720	C-Cl stretch	Alkyl Halide	Strong
595.25	600-500	C-Cl stretch	Alkyl Halide	Strong

Table 3.3.6.2.3: Fuel Properties of *Acasia concinna* Biodiesel (ACB)

TESTS	METHODS	ALM-B100
Colour	Visual	2
Flash Point °C (PMCC)	ASTM D-93	80
Density @ 15 °C Kg/L	ASTM D-1298	0.921
K. Viscosity @ 40 °C cST	ASTM D-445	4.22
Pour Point °C	ASTM D-97	-9
Cloud Point °C	ASTM D-2500	-12
Sulphur %wt	ASTM D-4294	0.0011
Total Acid No. mg KOH/gm	ASTM D-974	0.175

3.3.6.4 Experimental and Predicted yield of *Acacia concinna* Biodiesel (ACB) using Box-Behnken Design

Std	Run	Catalyst (wt%)	Time (hrs)	Temperature (°C)	Oil: Methanol (ml)	Yield %
19	1	0.5	1	80	1.75	85
12	2	0.7	6	50	1.9	80
26	3	0.5	4	80	1.75	85
11	4	0.3	6	50	1.9	85
24	5	0.5	3	80	1.9	82
1	6	0.3	6	50	1.6	86
21	7	0.5	3	50	1.75	80
4	8	0.7	4	50	1.6	80
18	9	0.7	4	80	1.75	82
5	10	0.3	1	110	1.6	89
8	11	0.7	3	110	1.6	80
28	12	0.5	5	80	1.75	85
17	13	0.3	5.5	80	1.75	87
2	14	0.7	3	50	1.6	77
16	15	0.7	1	110	1.9	80
30	16	0.5	3	80	1.75	79
7	17	0.3	5	110	1.6	90
15	18	0.3	6	110	1.9	85
6	19	0.7	4	110	1.6	79
29	20	0.5	7	80	1.75	85
20	21	0.5	4	80	1.75	81
13	22	0.3	5	110	1.9	86
22	23	0.5	4	110	1.75	80
27	24	0.5	3	80	1.75	78
9	25	0.3	4	50	1.9	85
3	26	0.3	6	50	1.6	88
10	27	0.7	3	50	1.9	78
25	28	0.5	3.5	80	1.75	79
14	29	0.7	4	110	1.9	79
23	30	0.5	4.5	80	1.6	84

3.3.6.4.1 Analysis of Variance (ANOVA) from Achieved Results

Source	Sum of Squares	df	Mean Square	F-value	p-value	Remarks
Model	0.8998	14	0.0643	4.00	0.0058	significant
A-Catalyst	0.7277	1	0.7277	45.33	< 0.0001	
B-Time	0.0044	1	0.0044	0.2721	0.6095	
C-Temperature	0.0133	1	0.0133	0.8313	0.3763	
D-Oil to Methanol Ratio	0.0269	1	0.0269	1.68	0.2150	
AB	0.0052	1	0.0052	0.3229	0.5783	
AC	0.0014	1	0.0014	0.0885	0.7702	
AD	0.0306	1	0.0306	1.91	0.1876	
BC	0.0048	1	0.0048	0.3011	0.5913	
BD	0.0046	1	0.0046	0.2858	0.6008	
CD	0.0045	1	0.0045	0.2819	0.6032	
A ²	0.0335	1	0.0335	2.09	0.1689	
B ²	0.0027	1	0.0027	0.1670	0.6886	
C ²	0.0461	1	0.0461	2.87	0.1109	
D ²	0.0028	1	0.0028	0.1722	0.6841	
Residual	0.2408	15	0.0161			
Lack of Fit	0.0548	10	0.0055	0.1471	0.9948	not significant
Pure Error	0.1860	5	0.0372			
Cor Total	1.14	29				

3.3.7 *Sapindus trifoliatus* Biodiesel (STB)

3.3.7 *Sapindus trifoliatus* Biodiesel (STB)

Sapindus trifoliatus has 43% oil content and free fatty acid (FFA) content is 1.071. It only requires one step transesterification to be converted into biodiesel (table 3.2). A series of transesterification reactions were carried out to get the optimum yield of the biodiesel produced from the seeds oil of *Sapindus trifoliatus* biodiesel (STB) using all three catalysts. The conditions at which optimum yield of the biodiesel from each of the catalysts was obtained is given in table 3.3.7. All the three catalysts i.e. Al-Mmt clay catalyst, Na-Ag Mmt catalyst, Cu-Mg-Zn Mmt clay catalyst, were used in the transesterification of the seeds oil of *Sapindus trifoliatus* to biodiesel but Cu-Mg-Zn-Mmt clay catalyst gave the best yield among all i.e. 95%, Na-Ag-Mmt clay catalyst gave 93% yield. Whereas Al-Mmt clay catalyst gave biodiesel yield of 90%.

3.3.7.1 Reaction Variables Affecting Transesterification of *Sapindus trifoliatus* Seeds Oil to Biodiesel

Following are the reaction variables for transesterification of fatty acids to FAMES:

3.3.7.1.1 Oil to Methanol Molar Ratio

In the current setup oil to methanol ratios of 1:3, 1:4, 1:5, 1:6, 1:7, 1:8, 1:9 and 1:10 were used keeping other reaction conditions constant i.e. reaction time, reaction temperature and catalyst concentration constant. The maximum conversion ratio was 1:4 by all three Mmt clay catalysts.

3.3.7.1.2 Catalyst Concentration

Another important factor which influences the yield of the fatty acid methyl esters (FAMES) is the type and concentration of the catalyst. Transesterification reaction for conversion of *Sapindus trifoliatus* seeds oil to FAMES, was carried out at different catalyst concentrations i.e. 0.1g, 0.2g, 0.3g, 0.4g, 0.5g, 0.6g and 0.7g and maximum yield of biodiesel was obtained at 0.4 g of Al-Mmt clay catalyst, 0.1 g in case of Na-Ag-Mmt clay catalyst and 0.2 g of Cu-Mg-Zn-Mmt clay catalyst gave best results.

3.3.7.1.3 Reaction Temperature (°C)

A series of reactions were carried out at different reaction conditions keeping other factors constant i.e. methanol to oil molar ratio and catalyst concentration. Highest conversion ratio was achieved at 100 °C in all, Al-Mmt, Na-Ag-Mmt and Cu-Mg-Zn-Mmt clay catalysts.

3.3.7.2 Chemical Characterization

3.3.7.2.1 GC-MS Analysis of *Sapindus trifoliatus* Biodiesel (STB)

GC-MS analysis is widely used technique to determine the chemical composition, type and structure of synthesized Fatty Acid Methyl Esters (FAMES). Mass spectrometer was set to scan in the range of m/z 2-600 and ionization potential 70V (Bu et al., 2014; Zhang et al., 2014). Different FAMES were determined using the retention time by Mass Spectroscopic analysis. Helium gas was used as a carrier with reaction temperature 300°C for 45 minutes. Seven characteristic peaks of fatty acid methyl esters of *Sapindus trifoliatus* Biodiesel (STD) were observed as presented in figure 3.3.7.2.1. Three out of these seven methyl esters are unsaturated and remaining are saturated ones. At peak 1, Hexadecanoic acid (C₁₇H₃₄O₂) was observed. Whereas, Methyl linoleate (C₂₁H₄₀O₂), Methyl oleate (C₁₉H₃₆O₂), Methyl stearate (C₁₉H₃₈O₂), 11-Eicosenoic acid (C₂₁H₄₀O₂), Methyl arachidate (C₂₁H₄₂O₂) and Docosanoic acid (C₂₃H₄₆O₂) were found at second, third, fourth, fifth, sixth and seventh position. Their retention times along with molecular formulas are given in the table 3.3.7.2.1.

3.3.7.2.2 FT-IR Analysis of *Sapindus trifoliatus* Biodiesel (STB)

FT-IR is used for the identification of chemical bonds and explain their stretching and bending vibrations. It also detects the presence and absence of functional groups in chemical compounds (Shaheen et al., 2017). Figure 3.3.7.2.2 shows the FT-IR of *Sapindus trifoliatus* methyl esters. A strong peak at 2922.30 cm⁻¹ shows the presence of aldehyde group due to the stretch in the H-C=O and C-H bonds. A sharp peak found at 1743.39 cm⁻¹ showed the presence of esters. Whereas, peaks at 2853.06 cm⁻¹ and 1464.37 cm⁻¹ show the presence of alkanes in the sample. Successive variable to medium peaks at 1377.78 cm⁻¹, 1238.46 cm⁻¹ and 1160.10 cm⁻¹ confirm the presence

of amines (C-N). Whereas, a strong peak at 1096.75 cm^{-1} due to the stretching of C-H bond depict the presence of ether group. And peaks at 722.63 cm^{-1} and 581.60 cm^{-1} are due to the presence of alkyl halide group (table 3.3.7.2.2).

3.3.7.2.3 Fuel Properties of *Sapindus trifoliatius* Biodiesel (STB)

The fuel properties of synthesized *Sapindus trifoliatius* Biodiesel (STB) were determined and compared with the ASTM standards (table 3.3.6.2.3). These properties help in the determination of the quality of fuel and its effect on diesel engine. Total acid number or acid value is amount of the free fatty acids existent in a fuel sample and is determined in mg KOH/gm. If its value is higher in the sample that means engine efficiency will be affected in a negative way (Akhtar et al., 2019). *Sapindus trifoliatius* Biodiesel's acid value (0.200mg KOH/gm) is well in range of international standards. Density of the STB is also in accordance with the international standards i.e. 0.8611 mg KOH/gm . Fuel density value is also crucial as its higher value causes engine corrosion and decreases its efficiency (Sultana et al., 2016). Kinematic viscosity is the determinant of the fuel thickness, higher value causes deposition in engine and reduces its working efficiency (Gunstone and Hamilton, 2001). *Sapindus trifoliatius* Biodiesel's kinematic viscosity is in range of international standards (5.32 kg/L). The color of produced *Sapindus trifoliatius* biodiesel is on visual 2 according to ASTM standards. Another important aspect is the Flash point of the diesel during fuel handling and transportation and fuels having flash point higher than 60°C are referred as safe (Salaheldeen et al., 2015). At this temperature fuel ignition starts. Flash point of Flash point of *Sapindus trifoliatius* Biodiesel (STB) was found to be 80°C . Other main parameter is cold flow properties which includes Pour point and Cloud point of biodiesel (Akhtar et al., 2019). Pour point and cloud point value of STB were -9°C and -11°C respectively. The sulfur contents in STB was (0.0004ppm) by %weight. An ideal fuel has low sulfur content and is more operative for engine's life and environment (Candeia et al., 2009).

3.3.7.3 Optimization Study of Transesterification Operational Factors Through Response Surface Methodology (RSM)

The optimization of transesterification process was performed by choosing four independent variables (Table 3.3.7.4) with maximum and minimum ranges i.e., Catalyst (A) 0.2-0.5 (Cu-Mg-Zn-Mmt), Time (B) 1-7 hrs, Temperature (C) 50-100 °C and Oil to Methanol (D) 1:4-1:6 and RSM build on Box Behnken Design was applied on 30 experiments to test the fitness of Quadratic ploy-equation with the Design-Expert 11 (Stat Ease IncMinneapolis,USA). A coded model equation used for studying the association among Input Variables as well as Output Response in terms of yield (Y) is

$$Y = +10.90290-0.909007A+0.006890B+0.021432C-3.33332D-0.002889AB-0.003408AC-0.007067AD-8.99960E-06BC+0.002213BD-0.007857CD+1.71822A^2-0.000045B^2-0.000023C^2+1.25244D^2$$

ANOVA results as presented in Table 3.3.7.4 depicts that model F-value (7.67) is significant. There is only a 0.02% chance that an F-value this large could occur due to noise. P-values less than 0.0500 indicate model terms are significant. In this case A, C are significant model terms. Values greater than 0.1000 indicate the model terms are not significant (P-value = 0.0002 <1). The Lack of Fit F-value of 0.54 implies the Lack of Fit is not significant relative to the pure error. There is a 81.27% chance that a Lack of Fit F-value this large could occur due to noise. Non-significant lack of fit is good, and we want the model to fit. The adequate precision (22.02) is greater than 4, so ensures the adequateness of the model to circumnavigate via space thus predicting the yield of biodiesel. Moreover, the adjusted R² (R²=0.914632) and predicted R² (R²=0.745663) values difference (<0.2) indicating the good correlation with the regression polynomial.

3.3.7.4 Parametric characterization of transesterification process

Figure 3.3.7.4 A, B, C, D, E & F shows the interactive effect of different variables on transesterification reaction in form of 3D response surface plot which can be explained in the following sub sections.

3.3.7.4.1 Interactive Impact of Catalyst Amount and Time

The combine influence of catalyst amount and time on biodiesel yield is presented into the Figure 3.3.7.4.A, while keeping other parameters (oil: methanol ratio (1:4) and temperature (100°C)) constant. At optimal levels of catalyst loading and process time (0.2% and 3.5 hrs) maximum 95% STB yield achieved owing to the equilibrium in the reaction. However, beyond the optimum values of catalyst concentration and reaction time, sudden drop in yield (88%) was observed which is similar with the reported work (Wong et al., 2015). These parameters are insignificant with P-value (0.2929)>0.05 for the transesterification reaction.

3.3.7.4.2 Interactive Impact of Catalyst Amount and Temperature

The combined influence of temperature and catalyst concentration on the STB yield is shown in Figure 3.3.7.2 B. Maximum STB yield of 95% is obtained with the catalyst loading of 1.2 wt% at 100 °C. However, lower conversion of STB (88%) observed with 0.5% catalyst due to partial changeover of triglyceride to methyl ester, which is consistent with the previous study (García-Moreno et al., 2014; Sarve et al., 2015). The same behaviour is noticeable with 88% STB yield as the amount of catalyst and temperature increased beyond 0.5wt% and 110 °C. Our findings are in line with the reported work elsewhere (Ferella et al., 2010). Therefore, based on ANOVA results, the interactive outcome of catalyst concentration and time on the biodiesel yield is insignificant with Pvalue (0.3008) < 0.05.

3.3.7.4.3 Interactive Impact of Catalyst Amount and Oil: Methanol Ratio

The Figure 3.3.7.4 C represents three-dimensional surface plot showing collective effect of the catalyst and oil: methanol on yield of biodiesel yield based on the parameters set by Box-Behnken design experiment. It is observed that maximum biodiesel yield (95 %) is obtained at 1:4 oil: methanol ratio and 0.2 wt % catalyst. The methanol-oil ratio is the significant parameters pushing the biodiesel yield. Stoichiometrically, 3 moles of methanol needed for the transesterification of oil (1 mole) yielding glycerol (1 mole) and biodiesel (3 moles). Since transesterification is a double-sided reaction so, an additional amount of methanol is needed for pushing the

reaction onward. For maximum FAME yield, 1:6 oil-methanol ratio is sufficient (Chuah et al., 2015). The biodiesel yield increases considerably by increasing methanol ratio and catalyst concentration from 0.1-0.2% and 40ml perhaps owing to more active site on the surface of catalyst to catalyze the reaction. However, lower conversion of 88 % FAME was observed due to partial changeover of triglyceride to methyl ester, which is consistent with the previous study (Obadiah et al., 2012). The slight drop in STB content was observed as the amount of catalyst and methanol ratio increased beyond 0.7wt% and 60 ml. However, ANOVA results depicts that oil: methanol and catalyst concentrations interactive effect are insignificant with P-value (0.9930) > 0.05.

3.3.7.4.4 Interactive impact of time and temperature

The time and temperature cooperative impact on the biodiesel yield is presented in Figure 3.3.7.4 D. It is evident that biodiesel yield (95 %) increases significantly as temperature (100°C) and catalyst amount (0.2 wt.%) (Cu-Mg-Zn-Mmt) increases and any further increase in temperature (110°C) would cause a decline in yield (88%) possibly due to saponification (Vicente et al., 2007). Arrhenius equation could explain it, stating an increasing process temperature may steadily increase the reaction rate and yield of biodiesel. Our findings agreed with the reported work (Olutoye et al., 2016) revealing that yield increases up to 100°C temperature afterward a substantial decline in bio-diesel yield was observed. Thus, the maximum yield of biodiesel (95%) was achieved on 100°C with 3.5 hr owing to the thorough mingling of oil and the methanol followed by easy separation of glycerol and end product (Verma et al., 2017). However higher temperature and time may facilitate hydrolysis of alkyl esters to generate acids along with the polarity of methanol (Verma et al., 2017) thereby decreasing biodiesel yield (Dwivedi and Sharma, 2015). Therefore, the combined impact of time and temperature on final yield is insignificant with P-value (0.5798) > 0.05.

3.3.7.4.5 Interactive Impact of Time and Oil: Methanol Ratio

The time and oil: methanol collective impact on STB yield is shown in Figure 3.3.7.4 E while keeping other parameters like catalyst concentration (0.2%) and temperature (100°C) constant. Highest biodiesel yield (95%) is attained at 1:4 oil: methanol ratio and reaction time of 3.5h due to increased interaction of excess methanol with oil (Singh et al., 2018). The short reaction time of 1h and low methanol ratio (2)

possibly do not permit the proper impregnation of modified clay with oil to achieve the equilibrium leading to partially converted products which contributes to the reduced STB yield. In an earlier study on castor oil methyl esters, confirmed the strong influence of reaction time on end product (Baskar et al., 2018). A slight decrease in FAME content (88 %) at 7h with 1:6 oil methanol ratio might be due related to the oil's dilution effect and reverse transesterification reaction, making it unfavourable to obtain desired STB yield. The similar behavior was observed by (Baskar and Soumiya, 2016; Ngamcharussrivichai et al., 2007; Olutoye et al., 2016. ANOVA results declare these parameters insignificant with P-value (0.5859) > 0.05.

3.3.7.4.6 Interactive impact of oil: methanol ratio and temperature

The Figure 3.3.7.4 F displays the combined effect of oil:alcohol ratio and temperature upon biodiesel yield. 95% STB yield was obtained as the temperature increased to 100 °C with 40 ml methanol. However, as the temperature rises above the threshold level (> 110 °C) STB yield decreases significantly. Therefore, it can be concluded from results that combined effect of these two parameters on the yield of biodiesel is insignificant with Pvalue (0.1203) > 0.05 which are in consistence with the reported work elsewhere (Gu et al., 2015).

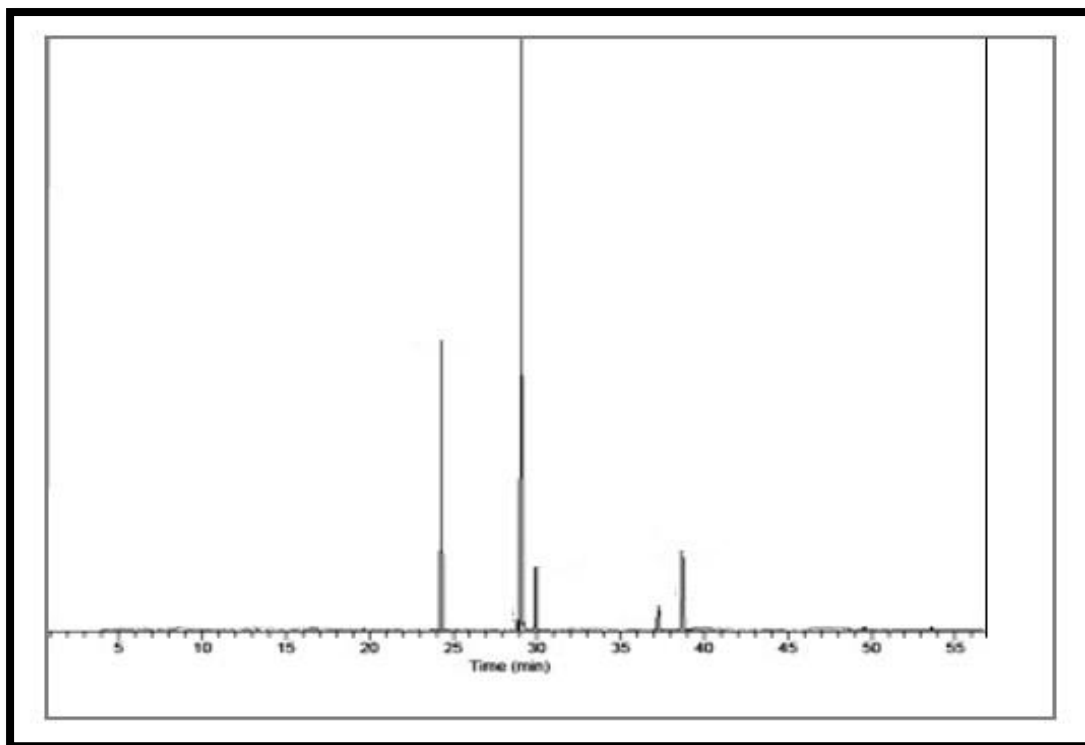


Figure 3.3.7.2.1: GC-MS of *Sapindus trifoliatum* Biodiesel (STB)

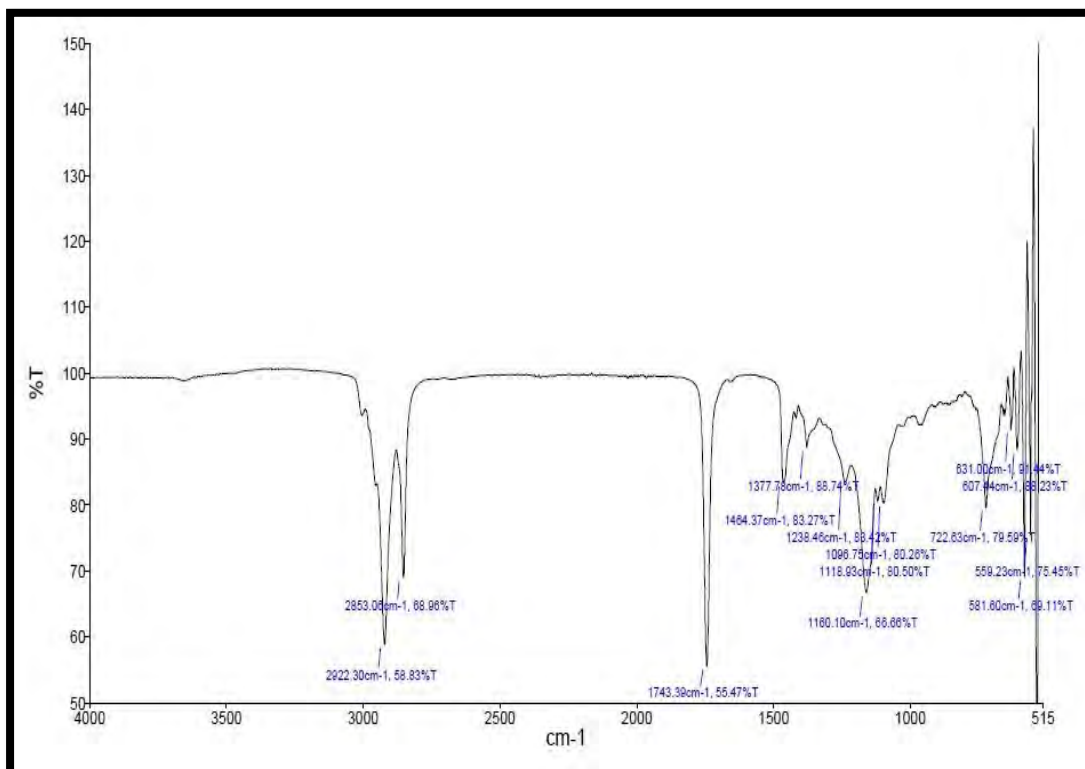


Figure 3.3.7.2.2: FT-IR of *Sapindus trifoliatum* Biodiesel (STB)

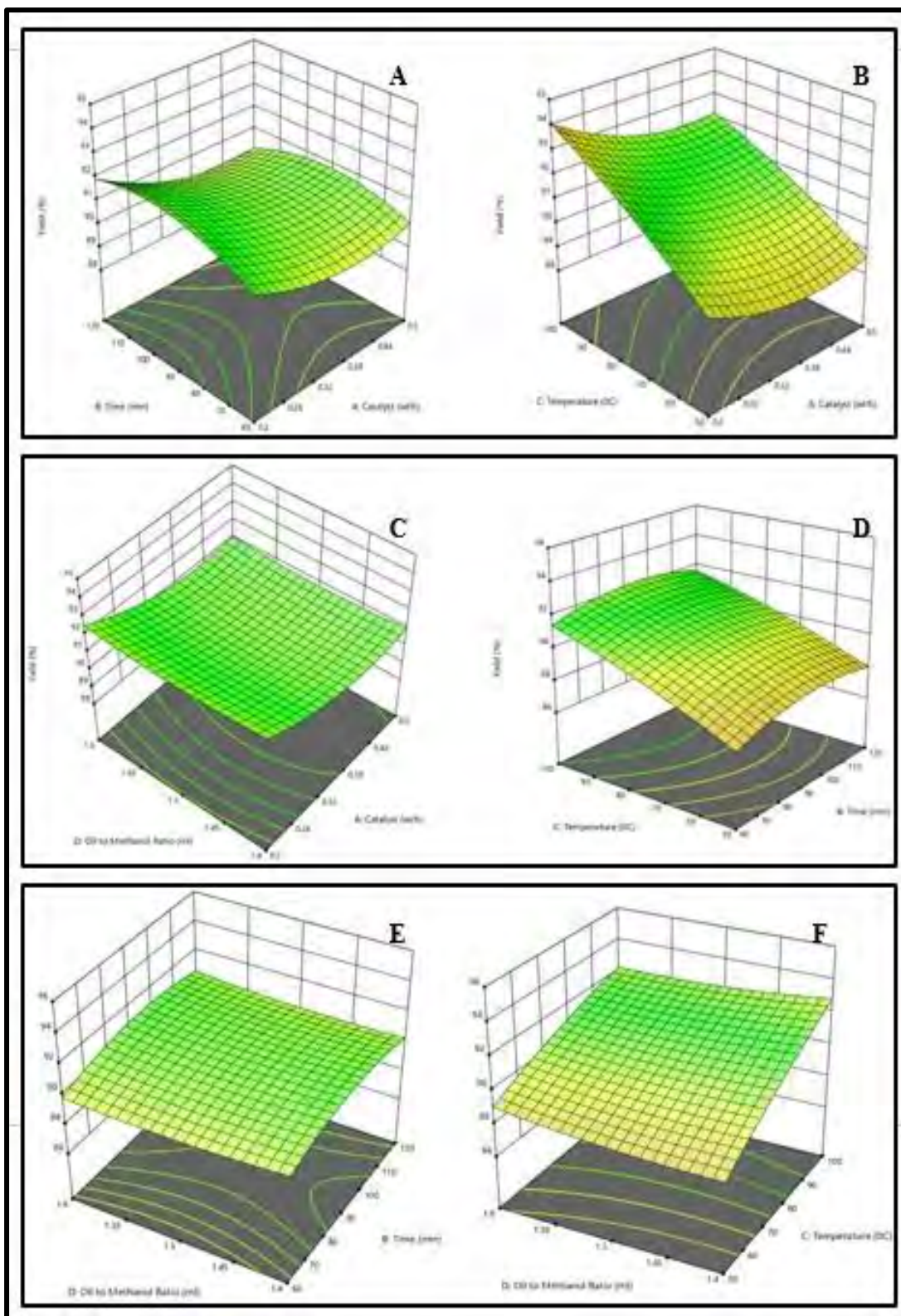


Figure 3.3.7.4: 3D surface Plots showing the impact of different parameters on *Sapindus trifoliatum* biodiesel (STB) yield

Table 3.3.7: Optimized Conditions for STB Synthesis Using Na-Mmt, Na-Ag-Mmt, Cu-Mg-Zn-Mmt Clay Catalysts

Catalyst	Conc.(g)	Oil: Methanol	Time (hrs)	Temperature°C	Yield%
Al-Mmt	0.4	1:4	4	100	90
Na-Ag-Mmt	0.1	1:4	3	100	93
Cu-Mg-Zn-Mmt	0.2	1:4	3.5	100	95

Table 3.3.7.2.1: Identified Esters in. *Sapindus trifoliatu*s Biodiesel (STB) Using GC-MS

Peak #	Identified Compound (FAMES)	Retention time	Molecular Formula
1	Hexadecanoic acid	24.25	C ₁₇ H ₃₄ O ₂
2	Methyl linoleate	28.79	C ₁₉ H ₃₄ O ₂
3	Methyl oleate	29.06	C ₁₉ H ₃₆ O ₂
4	Methyl stearate	29.89	C ₁₉ H ₃₈ O ₂
5	11-Eicosenoic acid	37.26	C ₂₁ H ₄₀ O ₂
6	Methyl arachidate	38.70	C ₂₁ H ₄₂ O ₂
7	Docosanoic acid	46.52	C ₂₃ H ₄₆ O ₂

Table 3.3.7.2.2: FT-IR of *Sapindus trifoliatu*s Biodiesel (STB)

Peaks (cm ⁻¹)	Frequency Range (Cm ⁻¹)	Bond	Functional Group	Characteristics of peak
2922.30	3000-2850	H-C=O: C-H stretch	Aldehyde	Medium to strong
2853.06	2853-065	C-H stretch	Alkane	Medium to Strong
1743.39	1750-1700	RCOOH	Ester	Strong
1464.37	1470-1450	C-H bend	Alkane	Variable
1377.78	1400-1360	C-N stretch	Amines	Medium
1238.46	1250-1220	C-N stretch	Amines	Medium
1160.10	1250-1020	C-N stretch	Amines	Medium
1096.75	1250-1020	C-O stretch	Ether	Strong/medium
722.63	725-720	C-Cl stretch	Alkyl Halide	Strong

581.60	600-500	C-Cl stretch	Alkyl Halide	Strong
--------	---------	--------------	--------------	--------

Table 3.3.7.2.3: Fuel Properties of *Sapindus trifoliatus* Biodiesel (STB)

TESTS	METHODS	ALM-B100
Colour	Visual	2
Flash Point °C (PMCC)	ASTM D-93	80
Density @ 15 °C Kg/L	ASTM D-1298	0.8611
K.Viscosity @ 40 °C Cst	ASTM D-445	5.32
Pour Point °C	ASTM D-97	-9
Cloud Point °C	ASTM D-2500	-11
Sulphur %wt	ASTM D-4294	0.00045
Total Acid No. mg KOH/gm	ASTM D-974	0.200

3.3.7.4 Experimental and Predicted yield of *Brassica oleracea* L. Biodiesel (BOB) using Box-Behnken Design

Std	Run	Catalyst (wt%)	Time (hrs)	Temperature (°C)	Oil: Methanol (ml)	Yield%
8	1	0.5	3	100	1.4	91
14	2	0.5	4	100	1.6	91
5	3	0.2	3	100	1.4	93
28	4	0.35	3.2	75	1.5	90
13	5	0.2	3	100	1.6	93
12	6	0.5	4	50	1.6	89
24	7	0.35	4	75	1.6	91
15	8	0.2	3	100	1.6	93
11	9	0.2	3.25	50	1.6	90
30	10	0.35	3	75	1.5	90
19	11	0.35	5	75	1.5	89
16	12	0.5	4	100	1.6	92
3	13	0.2	4.5	50	1.4	89
21	14	0.35	5	50	1.5	88
29	15	0.35	4	75	1.5	90
20	16	0.35	4	75	1.5	90
22	17	0.35	3	100	1.5	92
4	18	0.5	5.5	50	1.4	88
18	19	0.5	4	75	1.5	90
1	20	0.2	6.3	50	1.4	88
2	21	0.5	7	110	1.4	88
25	22	0.35	3	75	1.5	92
27	23	0.35	3	75	1.5	92
6	24	0.5	3.2	100	1.4	93
23	25	0.35	4	75	1.4	90
7	26	0.2	3.5	100	1.4	95
9	27	0.2	5	50	1.6	89
26	28	0.35	4	75	1.5	92
17	29	0.2	4	75	1.5	92
10	30	0.5	7	110	1.6	88

3.3.7.4.1 Analysis of Variance (ANOVA) from Achieved Results

Source	Sum of Squares	df	Mean Square	F-value	p-value	Remarks
Model	0.2444	14	0.0175	7.67	0.0002	significant
A-Catalyst	0.0219	1	0.0219	9.62	0.0073	
B-Time	0.0038	1	0.0038	1.69	0.2131	
C-Temperature	0.1986	1	0.1986	87.26	< 0.0001	
D-Oil to Methanol Ratio	0.0002	1	0.0002	0.0781	0.7836	
AB	0.0027	1	0.0027	1.19	0.2929	
AC	0.0026	1	0.0026	1.15	0.3008	
AD	1.798E-07	1	1.798E-07	0.0001	0.9930	
BC	0.0007	1	0.0007	0.3203	0.5798	
BD	0.0007	1	0.0007	0.3100	0.5859	
CD	0.0062	1	0.0062	2.71	0.1203	
A ²	0.0039	1	0.0039	1.70	0.2117	
B ²	0.0042	1	0.0042	1.84	0.1952	
C ²	0.0005	1	0.0005	0.2341	0.6355	
D ²	0.0004	1	0.0004	0.1786	0.6786	
Residual	0.0341	15	0.0023			
Lack of Fit	0.0177	10	0.0018	0.5354	0.8127	not significant
Pure Error	0.0165	5	0.0033			
Cor Total	0.2785	29				

3.3.7 *Sapindus trifoliatus* Biodiesel (STD)

3.3.8 *Sesamum indicum* Biodiesel (SIB)

Sesamum indicum has 48% oil content and FFA (free fatty acid) content is 0.028 which means it can be converted into biodiesel thru single step transesterification. A series of transesterification reactions were carried out to get the optimal yield of the biodiesel produced from the seeds oil of *Sesamum indicum*. The conditions at which optimum yield of the biodiesel from each of the seeds oil was obtained is given in table 3.3.8. All the three catalysts i.e. Al-Mmt clay catalyst, Na-Ag Mmt catalyst, Cu-Mg-Zn Mmt clay catalyst, were used in the transesterification of the seeds oil of *Sesamum indicum*.to biodiesel but Cu-Mg-Zn-Mmt clay catalyst gave the best yield (93%) among all followed by Al-Mmt clay catalyst (91%) and Na-Ag-Mmt clay catalyst (90%).

3.3.8.1 Reaction Variables Affecting Transesterification of *Sesamum indicum* Seeds Oil to Biodiesel

The transesterification reactions were carried out using three variables i.e. oil to methanol molar ratio, catalyst concentration and reaction temperature. And their effect was noted to be as following:

3.3.8.1.1 Oil to Methanol Molar Ratio

In a series of reactions for optimization of biodiesel synthesis, oil to methanol ratios of 1:3, 1:4, 1:5, 1:6, 1:7, 1:8, 1:9 and 1:10 were used keeping other reaction conditions constant i.e. reaction time, reaction temperature and catalyst concentration constant. The maximum conversion ratio was 1:3 by all three Mmt clay catalysts.

3.3.8.1.2 Catalyst Concentration

Transesterification reaction for conversion of *Sesamum indicum* seeds oil to FAMES, was carried out at different catalyst concentrations i.e. 0.1g, 0.2g, 0.3g, 0.4g, 0.5g, 0.6g and 0.7g and maximum yield of biodiesel was obtained at 0.5 g of Al-Mmt clay catalyst, 0.2 g of Na-Ag-Mmt clay catalyst and Cu-Mg-Zn-Mmt clay catalyst gave best results.

3.3.8.1.3 Reaction Temperature (°C)

Temperature of the reaction and biodiesel yield are directly proportional i.e. increase in temperature results in the increase of the biodiesel yield up to the threshold point ($>150^{\circ}\text{C}$) (Mehar et al, 2006, Munir et al, 2019). A series of reactions were carried out at different reaction conditions keeping other factors constant i.e. methanol to oil molar ratio and catalyst concentration. Highest conversion ratio was achieved at 90°C in all, Al-Mmt, Na-Ag-Mmt and Cu-Mg-Zn-Mmt clay catalysts.

3.3.8.2 Chemical Characterization

3.3.8.2.1 GC-MS Analysis of *Sesamum indicum* Biodiesel (SIB)

GC-MS analysis is broadly used technique to determine the chemical composition, type and structure of synthesized FAMES. Mass spectrometer was set to scan in the range of m/z 2-600 and ionization potential 70V (Bu et al., 2014; Zhang et al., 2014). Eleven monumental peaks representing methyl esters of the corresponding fatty acid were observed and confirmed by Library match software (NO. NIST 11). Different FAMES were determined using the retention time by Mass Spectroscopic analysis (Figure 3.3.8.2.1). Helium gas was used as a carrier with reaction temperature 300°C for 45 minutes. Peak 1 and 2 represent the methyl esters of Tetradecanoic acid ($\text{C}_{15}\text{H}_{30}\text{O}_2$) and 9-Hexadecenoic acid ($\text{C}_{16}\text{H}_{30}\text{O}_2$). Whereas methyl esters of n-Hexadecanoic acid ($\text{C}_{19}\text{H}_{34}\text{O}_2$), 9-Octadecenoic acid ($\text{C}_{19}\text{H}_{36}\text{O}_2$), Octadecanoic acid ($\text{C}_{18}\text{H}_{36}\text{O}_2$), 11-Eicosenoic acid ($\text{C}_{21}\text{H}_{40}\text{O}_2$), Eicosanoic acid ($\text{C}_{21}\text{H}_{42}\text{O}_2$), 13-Docosenoic acid ($\text{C}_{23}\text{H}_{44}\text{O}_2$), Docosanoic acid ($\text{C}_{23}\text{H}_{46}\text{O}_2$) and Tetracosanoic acid ($\text{C}_{25}\text{H}_{50}\text{O}_2$) are represented by peak number 3,4,5,6,7,8,9,10 and 11 respectively (Table 3.3.8.2.1). FAME's profile determines the suitability of feedstock for use in production of biodiesel fuel (Skoto et al., 2011).

3.3.8.2.2 FT-IR Analysis of *Sesamum indicum* Biodiesel (SIB)

FT-IR is a modern analytical method for fast and easy detection of Fatty acid methyl esters due to its capability as “finger-print technique” which aid in recognition of chemical bonds and functional groups in oils, fats and biodiesel samples. Figure 3.3.8.2.2 represents the FT-IR spectrum of *Sesamum indicum* Biodiesel (SIB).

Appearance of peak at 2922.75 cm^{-1} shows the presence of aldehyde compounds in the biodiesel sample. Presence of alkanes was determined by two spate peaks at 2853.37 cm^{-1} and other at 1463.95 cm^{-1} , first one showing the stretching of C-H bond whereas second one indicating a bend in the C-H plane. A characteristic peak of esters was appeared at 1743.28 cm^{-1} . The congestive peaks at 1377.89 cm^{-1} , 1238.68 cm^{-1} and 1160.21 cm^{-1} show the presence of amines in the sample. The stretch in the C-O bond of ether was explained by the peak at 1097.89 cm^{-1} . Bending of C=C bond of alkene was observed at 964.15 cm^{-1} . And peaks at 722.18 cm^{-1} and 579.36 cm^{-1} depict the presence of alkyl halides.

The FTIR confirms the presence of ester carbonyl bond near the absorption band 1743.71 cm^{-1} (Daniyan et al., 2019). Presence of above-mentioned peaks in the FT-IR spectra confirms the biodiesel synthesis.

3.3.8.2.3 Fuel Properties of *Sesamum indicum* Biodiesel (SIB)

The fuel properties of synthesized *Sesamum indicum* Biodiesel (SIB) were determined and found well in accordance with the ASTM standards (Table 3.3.8.2.3). These properties help in the estimation of the fuel quality and its efficiency in the diesel engine. Total acid number or acid value is amount of the free fatty acids existent in a fuel sample and is determined in mg KOH/gm. If its value is higher in the sample that means engine efficiency will be affected in a negative way (Akhtar et al., 2019). SIB's acid value (0.170 mg KOH/gm) is well in range of international standards. Density of the SIB is also in accordance with the international standards i.e. 0.844 mg KOH/gm . Fuel density value is also crucial as its higher value causes engine corrosion and decreases its efficiency (Sultana et al., 2016). Kinematic viscosity is the determinant of the fuel thickness, higher value causes deposition in engine and reduces its working efficiency (Gunstone and Hamilton, 2001). SIB's kinematic viscosity is in range of international standards (4.77 kg/L). The color of produced biodiesel is on visual 2 according to ASTM standards. Another important aspect is the Flash point of the diesel during fuel handling and transportation and fuels having flash point higher than 60°C are referred as safe (Salaheldeen et al., 2015). At this temperature fuel ignition starts. Flash point of *Sesamum indicum* Biodiesel (SIB) was found to be 74°C . Additional important parameter is cold flow properties which includes Pour point and Cloud point of biodiesel (Akhtar et al., 2019). Pour point and cloud point value of SIB were -6°C

and -10°C respectively. The sulfur contents in SIB was (0.0012ppm) by %weight. An ideal fuel has low sulfur content and is more operative for engine's life and environment (Candeia et al., 2009).

3.3.8.3 Optimization Study of Transesterification Operational Factors Through Response Surface Methodology (RSM)

For optimization of transesterification process, four independent variables with maximum and minimum ranges (Table 3.3.8.4) i.e., Catalyst (A) 0.2-0.6 (Cu-Mg-Zn-Mmt), Time (B) 2-6 hrs, Temperature (C) 50-100 °C and Oil to Methanol (D) 1:3-1:8 were chosen and 30 experiments were analyzed by RSM using the Box Behnken Design to test the fitness of Quadratic ploy-equation with the Design-Expert 11 (Stat Ease IncMinneapolis,USA). A coded model equation used for studying the association among Input Variables as well as Output Response in terms of yield (Y) is

$$Y = +13.14736 - 2.78642A + 0.341644B + 0.041730C - 7.06900D + 0.058464AB - 0.000971AC + 0.791984AD - 0.000235BC - 0.081250BD - 0.011111CD + 0.466023A^2 - 0.029140B^2 - 0.000152C^2 + 2.54282D^2$$

The ANOVA results as presented in Table 3.3.8.4.1 gives insight about the model significance. Model F-value (4.32 (P-value = 0.0040 < 1)) shows that model is significant while Fvalue corresponding to the lake of fit is 0.8129 which appears to be not significant with the corresponding pure error, thus confirms the best fitness of model to experimental (trial) data. The Predicted R² of 0.0168 is not as close to the Adjusted R² of 0.6158 as one might normally expect, i.e. the difference is more than 0.2. Adeq Precision measures the signal to noise ratio. A ratio greater than 4 is desirable. The ratio of 7.437 indicates an adequate signal.

3.3.8.4 Parametric characterization of transesterification process

The interactive effect of different variables on transesterification reaction are presented here in Figure 3.3.8.4 A, B, C, D, E & F and can be explained in the following sub sections.

3.3.8.4.1 Interactive Impact of Catalyst Amount and Time

The combine influence of catalyst amount and time on biodiesel yield is shown into Figure 3.3.8.4 A, while keeping other parameters (oil: methanol ratio (1:3) and temperature (90°C)) constant. Maximum SIB yield (93%) obtained with the catalyst loading of 0.2 wt% for 3 hrs reaction time. These optimum conditions would permit the formation of extra methoxy species by the activity of catalyst and ultimately increased yield of biodiesel and equilibrium in the reaction. However, beyond the optimum values of catalyst concentration and reaction time, sudden drop in yield (78%) was observed. This drop in yield might be linked to the shifting of reaction in opposite direction (Mahesh et al., 2015). However, ANOVA results are insignificant for time and catalyst on yield with P-value (0.5477) > 0.05.

3.3.8.4.2 Interactive Impact of Catalyst Amount and Temperature

The Figure 3.3.8.4 B represents the combined influence of temperature and catalyst concentration on the yield of biodiesel. Maximum SIB (93%) obtained with the catalyst loading of 0.2 wt% with steady increase in reaction temperature to 90°C. However, lower conversion of SIB (78%) observed at 0.4% catalyst due to partial changeover of triglyceride to methyl ester, which is consistent with the previous study (Lee et al., 2011). Same is true with higher amounts of catalyst and temperature as indicated in run 19th with 75% SIB yield due to lessened interaction between the reactant and catalyst (Dhingra et al., 2014). This shows the insignificant of these parameters on final biodiesel yield with P-value (0.9057) > 0.05.

3.3.8.4.3 Interactive Impact of Catalyst Amount and Oil: Methanol Ratio

The three-dimensional response surface plot in Figure 3.3.8.4 C shows the collective effect of catalyst and oil: methanol on the yield of biodiesel. As maximum biodiesel yield (93 %) is obtained at 1:3 oil: methanol ratio and 0.2 wt % catalyst. Both oil: methanol ratio and concentration of catalyst has the dominant role for providing maximum biodiesel yield. Thus, biodiesel yield increases substantially by increasing catalyst concentration and methanol amount from 0.1-0.2% to 30ml. This increased SIB yield is linked with generation of more active site on the surface of catalyst to catalyse

the reaction. However, as the amount of catalyst and methanol decreases or increased further beyond optimum level there is sudden drop in SIB yield like 75 % PBD (0.6% catalyst, 30ml methanol) and 88% PBD yield (0.4% catalyst, 55ml methanol). This drop is linked to the partial changeover of triglyceride to methyl ester and emulsification, which is consistent with the previous study (Omar and Amin, 2011; Wan et al., 2015). However, ANOVA results for these factors is insignificant owing to their Pvalue (0.3363) > 0.05.

3.3.8.4.4 Interactive impact of time and temperature

The time and temperature cooperative influence on the biodiesel yield is presented in the form of three-dimensional response surface plot in Figure 3.3.8.4 D. Maximum SIB yield (93%) with 3 hrs reaction time at 90°C. This is so, as higher time temperatures allow the well dispersion of catalyst particle leading to mass transfer of reactor content (Avramović et al., 2015) which ultimately supports the increased interaction among the catalyst and SIO and hence, higher transition of oils to SIB. and any further increase in temperature (100°C) would cause a decline in yield (80%) possibly due to saponification (Vicente et al., 2007). Arrhenius equation could explain it, stating an increasing process temperature may steadily increase the reaction rate and yield of biodiesel. Our findings agreed with the reported work (Noshadi et al., 2012). These parameters are insignificant as indicated by ANOVA with P-value (0.7708) > 0.05.

3.3.8.4.5 Interactive Impact of Time and Oil: Methanol Ratio

The time and oil: methanol collective impact on SIB yield is presented in Figure 3.3.8.4 E while keeping other parameters like catalyst concentration (0.2%) and temperature (90°C) constant. The highest biodiesel yield (93%) is attained at 1:3 oil: methanol ratio and reaction time of 3h. There is a direct dependence of SIB yield and ratio of oil: methanol. Stoichiometrically, 3 moles of methanol needed for the transesterification of oil (1 mole) yielding glycerol (1 mole) and biodiesel (3 moles). The reversible mode of transesterification process thus necessitates the surplus alcohol to maintain the balance in reaction (higher conversion of oil to biodiesel) (Mubarak et al., 2016). The short reaction time of 1h and low methanol ratio (30 ml) possibly do not permit the proper impregnation of modified clay with oil to achieve the equilibrium

leading to partially converted products (75%) (Dharma et al., 2016). A slight decrease in SIB content (88%) at 4h with 1:55 oil methanol ratio might be due to reverse transesterification reaction, making it unfavourable to obtain desired SIB yield (Mumtaz et al., 2014). ANOVA results is insignificant for these factors with P-value (0.3155) > 0.05.

3.3.8.4.6 Interactive impact of oil: methanol ratio and temperature

The combined effect of temperature along with oil:alcohol ratio upon SIB (biodiesel) yield is presented in Figure 3.3.8.4 F. 93% SIB yield is obtained at 90 °C with 30 ml methanol. But an abrupt drop in SIB yield is observed as the temperature raised above the threshold level (> 90 °C) which might initiate gasification of methanol leading to reduced SIB content (Y. Li et al., 2013). These two parameters have insignificant effect on biodiesel yield with P-value (0.1015) > 0.05.

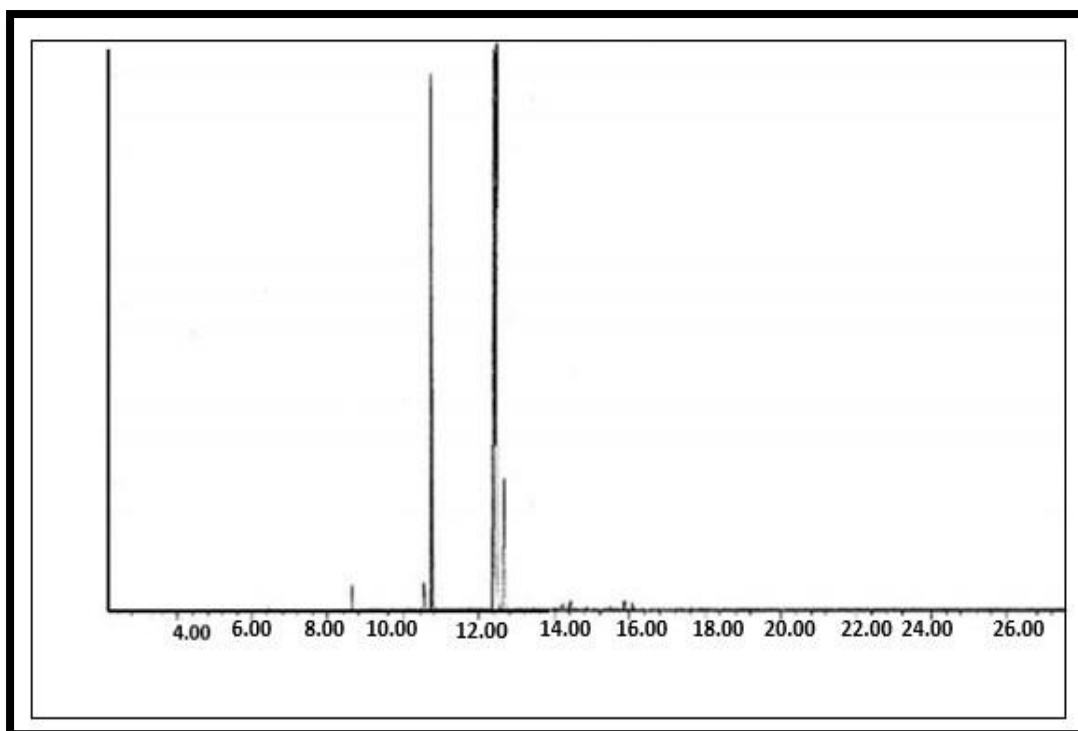


Figure 3.3.8.2.1: GC-MS of *Sesamum indicum* Biodiesel (SIB)

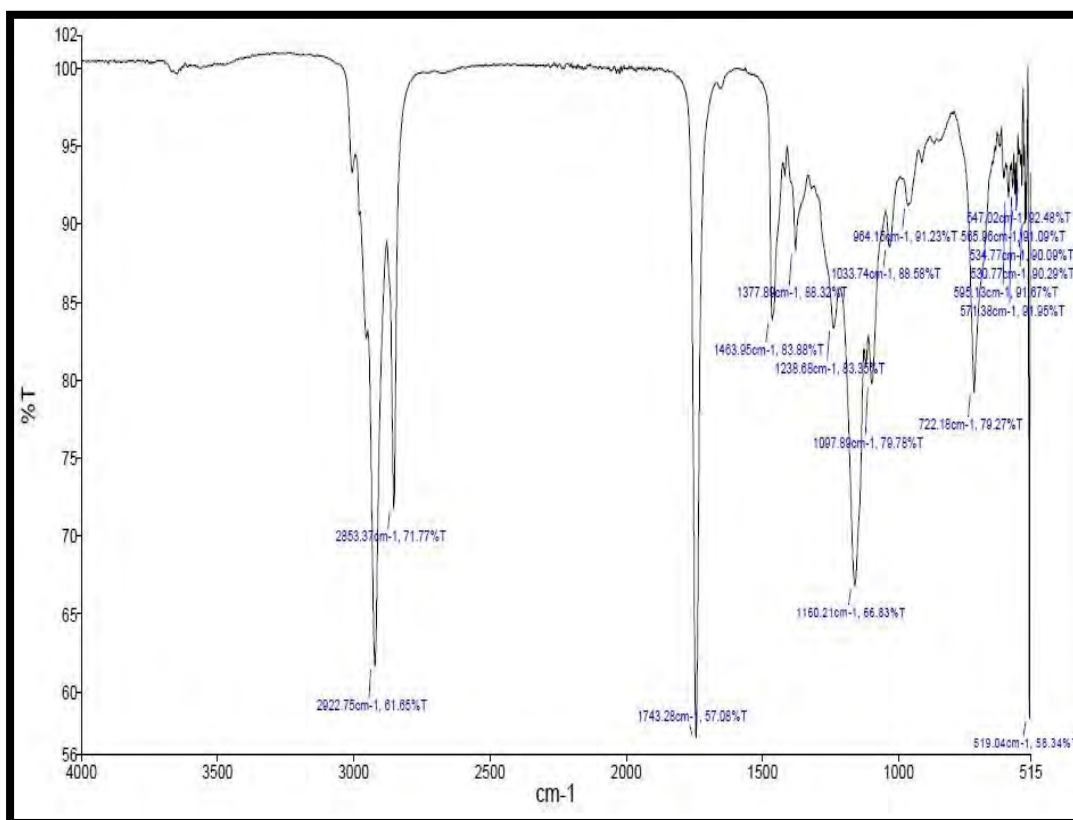


Figure 3.3.8.2.2: FT-IR of *Sesamum indicum* Biodiesel (SIB)

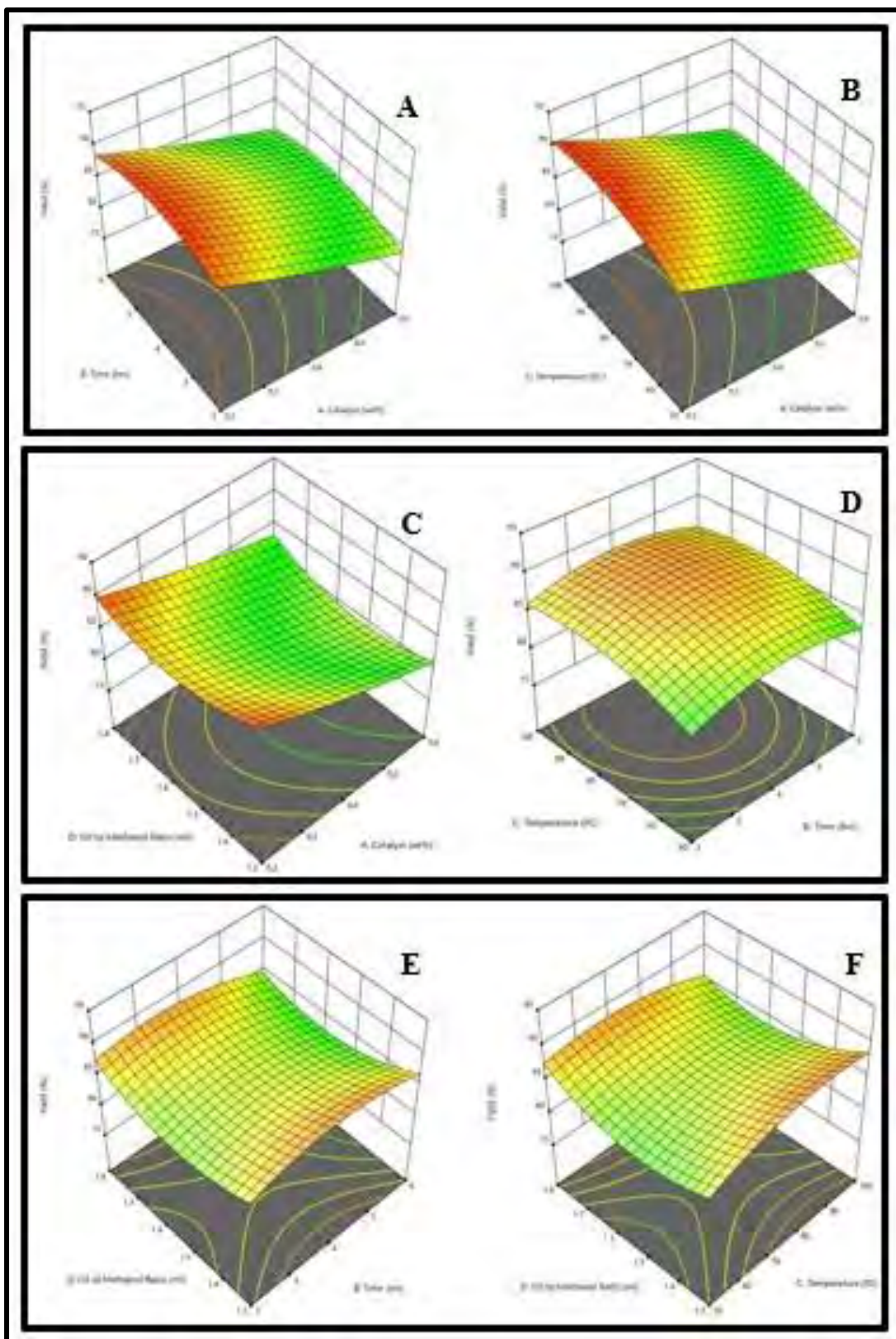


Figure 3.3.8.4: 3D surface Plots showing the impact of different parameters on *Sesamum indicum* biodiesel (SIB) yield

Table 3.3.8: Optimized Conditions for SIB Synthesis Using Na-Mmt, Na-Ag-Mmt, Cu-Mg-Zn-Mmt Clay Catalysts

Catalyst	Conc.(g)	Oil:Methanol	Time (hrs)	Temperature°C	Yield%
Al-Mmt	0.5	1:3	3.5	90	91
Na-Ag-Mmt	0.2	1:3	3.5	90	90
Cu-Mg-Zn-Mmt	0.2	1:3	3	90	93

Table 3.3.8.2.1: Identified Esters in. *Sesamum indicum* Biodiesel (SIB) Using GC-MS

Peak #	Identified Compound (FAMES)	Retention time	Molecular Formula
1	Tetradecanoic acid, methyl ester	8.63	C ₁₅ H ₃₀ O ₂
2	9-Hexadecenoic acid, methyl ester	10.32	C ₁₆ H ₃₀ O ₂
3	n-Hexadecanoic acid, methyl ester	10.81	C ₁₉ H ₃₄ O ₂
4	8,11-Octadecadienoic acid, methyl ester	11.94	C ₁₉ H ₃₄ O ₂
5	9-Octadecenoic acid, methyl ester	12.36	C ₁₉ H ₃₆ O ₂
6	Octadecanoic acid, methyl ester	12.13	C ₁₈ H ₃₆ O ₂
7	11-Eicosenoic acid, methyl ester	14.08	C ₂₁ H ₄₀ O ₂
8	Eicosanoic acid, methyl ester	14.43	C ₂₁ H ₄₂ O ₂
9	13-Docosenoic acid methyl ester	15.84	C ₂₃ H ₄₄ O ₂

10	Docosanoic acid, methyl ester	16.03	C ₂₃ H ₄₆ O ₂
11	Tetracosanoic acid, methyl ester	17.54	C ₂₅ H ₅₀ O ₂

Table 3.3.8.2.2: FT-IR of *Sesamum indicum* Biodiesel (SIB)

Peaks (cm ⁻¹)	Frequency Range (Cm ⁻¹)	Bond	Functional Group	Characteristics of peak
2922.75	3000-2850	H-C=O: C-H stretch	Aldehyde	Medium to strong
2853.37	2870-2695	C-H stretch	Alkane	Medium to Strong
1743.28	1750-1700	RCOOH	Ester	Strong
1463.95	1470-1450	C-H bend	Alkane	Variable
1377.89	1400-1360	C-N stretch	Amines	Medium
1238.68	1250-1220	C-N stretch	Amines	Medium
1160.21	1250-1020	C-N stretch	Amines	Medium
1097.89	1250-1020	C-O stretch	Ether	Strong/medium
964.15	980-960	C=C bending	Alkene	Strong
722.18	725-720	C-Cl stretch	Alkyl Halide	Strong
579.36	600-500	C-Cl stretch	Alkyl Halide	Strong

Table 3.3.8.2.3: Fuel Properties of *Sesamum indicum* Biodiesel (SIB)

TESTS	METHODS	ALM-B100
Colour	Visual	2
Flash Point °C (PMCC)	ASTM D-93	74
Density @ 15 °C Kg/L	ASTM D-1298	0.844
K.Viscosity @ 40 °C cST	ASTM D-445	4.77
Pour Point °C	ASTM D-97	-6
Cloud Point °C	ASTM D-2500	-10
Sulphur %wt	ASTM D-4294	0.0012
Total Acid No. mg KOH/gm	ASTM D-974	0.170

3.3.8.4 Experimental and Predicted yield of *Sesamum indicum* Biodiesel (SIB) using Box-Behnken Design

Std	Run	Catalyst (wt%)	Time (hrs)	Temperature (0C)	Oil: Methanol (ml)	Yield %
13	1	0.2	2	100	1.8	87
30	2	0.4	4	75	1.55	85
12	3	0.6	6	50	1.8	79
24	4	0.4	4	75	1.8	86
20	5	0.4	6	75	1.55	78
4	6	0.6	6	50	1.3	79
7	7	0.2	3	90	1.3	93
3	8	0.2	6	50	1.3	85
11	9	0.2	6	50	1.8	86
29	10	0.4	4	75	1.55	85
21	11	0.4	4	50	1.55	84
28	12	0.4	4	75	1.55	86
23	13	0.4	4	75	1.3	85
19	14	0.4	2	75	1.55	83
10	15	0.6	2	50	1.8	82
5	16	0.2	2	100	1.3	89
27	17	0.4	4	75	1.55	78
18	18	0.6	4	75	1.55	78
2	19	0.6	2	50	1.3	75
17	20	0.4	4	75	1.55	88
6	21	0.6	2	100	1.3	80
8	22	0.6	6	100	1.3	81
16	23	0.6	6	100	1.8	79
25	24	0.4	4	75	1.55	85
14	25	0.6	2	100	1.8	79
26	26	0.4	4	75	1.55	85
9	27	0.2	2	50	1.8	86
22	28	0.4	4	100	1.55	78
1	29	0.2	2	90	1.3	90
15	30	0.2	6	100	1.3	89

3.3.8.4.1 Analysis of Variance (ANOVA) from Achieved Results

Source	Sum of Squares	df	Mean Square	F-value	p-value	Remarks
Model	1.21	14	0.0861	4.32	0.0040	significant
A-Catalyst	0.6474	1	0.6474	32.47	< 0.0001	
B-Time	0.0086	1	0.0086	0.4302	0.5218	
C-Temperature	0.0018	1	0.0018	0.0891	0.7694	
D-Oil to Methanol Ratio	0.0007	1	0.0007	0.0350	0.8541	
AB	0.0075	1	0.0075	0.3784	0.5477	
AC	0.0003	1	0.0003	0.0145	0.9057	
AD	0.0197	1	0.0197	0.9868	0.3363	
BC	0.0018	1	0.0018	0.0880	0.7708	
BD	0.0215	1	0.0215	1.08	0.3155	
CD	0.0593	1	0.0593	2.98	0.1051	
A ²	0.0009	1	0.0009	0.0456	0.8337	
B ²	0.0356	1	0.0356	1.78	0.2016	
C ²	0.0248	1	0.0248	1.25	0.2819	
D ²	0.0661	1	0.0661	3.32	0.0886	
Residual	0.2990	15	0.0199			
Lack of Fit	0.1643	9	0.0183	0.8129	0.6258	not significant
Pure Error	0.1347	6	0.0225			
Cor Total	1.50	29				

3.3.9 *Ricinus communis* Biodiesel (RCB)

3.3.9 *Ricinus communis* Biodiesel (RCB)

Ricinus communis has 54% oil content and free fatty acid (FFA) content is 0.637. One step transesterification is needed for *Ricinus communis* oil to be converted into biodiesel (Table 3.3.1). A series of transesterification reactions were carried out to get the optimum yield of the biodiesel produced from the seeds oil of *Ricinus communis* biodiesel (RCB) using all three catalysts. The conditions at which optimum yield of the biodiesel from each of the catalysts was obtained is given in table 3.3.9. All the three catalysts i.e. Al-Mmt clay catalyst, Na-Ag Mmt catalyst, Cu-Mg-Zn Mmt clay catalyst, were used in the transesterification of the seeds oil of *Ricinus communis*.to biodiesel but Cu-Mg-Zn-Mmt clay catalyst gave the best yield among all i.e. 89%, Al-Mmt clay catalyst gave biodiesel yield of 85.37% and Na-Ag-Mmt clay catalyst gave 85% yield.

3.3.9.1 Reaction Variables Affecting Transesterification of *Ricinus communis* Seeds Oil to RCB

Effect of three reaction variables was noted to be as following:

3.3.9.1.1 Oil to Methanol Molar Ratio

Various reactions were carried out to get the maximum yield of TCB. And oil to methanol ratios of 1:3, 1:4, 1:5, 1:6, 1:7, 1:8, 1:9 and 1:10 were used keeping other reaction conditions constant i.e. reaction time, reaction temperature and catalyst concentration constant. The maximum conversion ratio was 1:3 by all three Mmt clay catalysts.

3.3.9.1.2 Catalyst Concentration

Transesterification reaction for conversion of *Ricinus communis* seeds oil to FAMES, was carried out at different catalyst concentrations i.e. 0.1g, 0.2g, 0.3g, 0.4g, 0.5g, 0.6g and 0.7g and maximum yield of biodiesel was obtained at 2.0 g of Al-Mmt clay catalyst, 3.0 g of Na-Ag-Mmt clay catalyst and 2.3 g Cu-Mg-Zn-Mmt clay catalyst gave best results.

3.3.9.1.3 Reaction Temperature °C

A series of reactions were carried out at different reaction conditions keeping other factors constant i.e. methanol to oil molar ratio and catalyst concentration. Highest conversion ratio was achieved at 115 °C in Al-Mmt, 110 °C for Na-Ag-Mmt and Cu-Mg-Zn-Mmt clay catalysts.

3.3.9.2 Chemical Characterization

3.3.9.2.1 GC-MS Analysis of *Ricinus communis* Biodiesel (RCB)

GC-MS analysis is broadly used technique to determine the chemical composition, type and structure of synthesized FAMES. Mass spectrometer was set to scan in the range of m/z 2-600 and ionization potential 70V (Bu et al., 2014; Zhang et al., 2014). Seven monumental peaks representing methyl esters of the corresponding fatty acid were observed and confirmed by Library match software (NO. NIST 11). Different FAMES were determined using the retention time by Mass Spectroscopic analysis (Figure 3.3.9.2.1). Helium was used as a carrier gas. Peak 1 and 2 represent the methyl esters of Hexadecanoic acid (C₁₇H₃₄O₂) and Methyl linoleate (C₁₉H₃₄O₂). Whereas methyl esters of (9Z)-9-Octadecenoic acid (C₁₉H₃₆O₂), Octadecanoic acid (C₁₉H₃₈O₂), Methyl ricinoleate (C₁₉H₃₆O₃), 11,14-Eicosadienoic acid (C₂₁H₃₈O₂) and Erucic acid (C₂₃H₄₄O₂) are represented by peak number 3,4,5,6 and 7 respectively (table 3.3.9.2.1). FAME's profile determines the suitability of feedstock for use in production of biodiesel fuel (Skoto et al., 2011). Ricinoleic acid (C18:1) was found to be abundantly present fatty acid methyl ester in the RCB FAMES.

3.3.9.2.2 FT-IR Analysis of *Ricinus communis* Biodiesel (RCB)

FT-IR is a modern analytical method for fast and easy detection of Fatty acid methyl esters due to its capability as “finger-print technique” which aid in recognition of chemical bonds and functional groups in oils, fats and biodiesel samples. Figure 3.3.9.2.2 gives the insight about the FT-IR spectrum of *Ricinus communis* Biodiesel (RCB).

Appearance of peak at the 3405.11 cm⁻¹ shows the stretching of O-H bond of alcohol group. Whereas presence of peak at 2924.06 cm⁻¹ shows the presence of

aldehyde compounds in the biodiesel sample. Presence of alkanes was determined by two separate peaks at 2853.96 cm^{-1} and other at 1458.08 cm^{-1} , first one showing the stretching of C-H bond whereas second one indicating a bend in the C-H plane. A characteristic peak of esters was appeared at 1742.77 cm^{-1} . The congestive peaks at 1377.71 cm^{-1} , 1239.94 cm^{-1} and 1162.17 cm^{-1} show the presence of amines in the sample. The stretch in the C-O bond of ether was explained by the peak at 1096.08 cm^{-1} . And peaks at 723.45 cm^{-1} and 566.21 cm^{-1} depict the presence of alkyl halides in the biodiesel sample (Table 3.3.9.2.2).

3.3.9.2.3 Fuel Properties of *Ricinus communis* Biodiesel (RCB)

The fuel properties of synthesized *Ricinus communis* Biodiesel (RCB) were determined and found well in accordance with the ASTM standards (Table 3.3.9.2.3). These properties help in the estimation of the fuel quality and its efficiency in the diesel engine. Total acid number or acid value is amount of the free fatty acid existent in a fuel sample and is determined in mg KOH/gm. If its value is higher in the sample that means engine efficiency will be affected in a negative way (Akhtar et al., 2019). RCB's acid value (0.200 mg KOH/gm) is well in range of international standards. Density of the RCB is also in accordance with the international standards i.e. 0.878 mg KOH/gm . Fuel density value is also crucial as its higher value causes engine corrosion and decreases its efficiency (Sultana et al., 2016). Kinematic viscosity is the determinant of the fuel thickness, higher value causes deposition in engine and reduces its working efficiency (Gunstone & Hamilton, 2001). RCB's kinematic viscosity is in range of international standards (5.11 kg/L). The color of produced *Ricinus communis* biodiesel is on visual 2 according to ASTM standards. Another important aspect is the Flash point of the diesel during fuel handling and transportation and fuels having flash point higher than 60°C are referred as safe (Salaheldeen et al., 2015). At this temperature fuel ignition starts. Flash point of *Ricinus communis* Biodiesel (RCB) was found to be 78°C . Additionally important parameter is cold flow properties which includes Pour point and Cloud point of biodiesel (Akhtar et al., 2019). Pour point and cloud point value of RCB were -8°C and -10°C respectively. The sulfur contents in RCB was found to be (0.00041 ppm) by %weight. An ideal fuel has low sulfur content and is more operative for engine's life and environment (Candeia et al., 2009).

3.3.9.3 Optimization Study of Transesterification Operational Factors Through Response Surface Methodology (RSM)

Response Surface Methodology (RSM) built upon Box Behnken Design has been used to optimize the transesterification process, using four independent variables (Table 3.3.9.4) with maximum and minimum ranges i.e., Catalyst (A) 0.2-4.0 (Cu-Mg-Zn-Mnt), Time (B) 1-9 hrs, Temperature (C) 60-110 °C and Oil to Methanol (D) 1:3-1:7 for 30 experiments. A coded model equation representing Catalyst, Time, Temperature and oil: methanol as A, B, C and D used for studying the association among Input Variables as well as Output Response in terms of yield (Y) is

$$Y = +13.92786 - 0.949550A + 0.087773B + 0.025291C - 5.91404D - 0.000554AB - 0.000085AC + 0.058236AD - 0.000242BC - 0.029051BD - 0.002293CD + 0.106878A^2 - 0.001994B^2 - 0.000095C^2 + 1.96770D^2$$

The Table 3.3.9.4.1 shows the ANOVA results depicting that the Model F-value of 16.83 implies that model is significant. There is only a 0.01% chance that an F-value this large could occur due to noise. Pvalue is 0.0001 (<1) and is significant for determining biodiesel yield. However, F-value corresponding to the lack of fit is (3.14) not significant with the corresponding pure error, thus confirms the best fitness of model to experimental (trial) data. The Predicted R² of 0.5915 is not as close to the Adjusted R² of 0.8843 as one might normally expect, i.e. the difference is more than 0.2. Adeq Precision measures the signal to noise ratio. A ratio greater than 4 is desirable. Your ratio of 14.723 indicates an adequate signal.

3.3.9.4 Parametric characterization of transesterification process

The interactive effect of different variables on transesterification reaction were considered by drawing three-dimensional response curves versus every dual Independent variable presented in Figure 3.3.9.4 A, B, C, D, E & F and can be explained in the following sub sections.

3.3.9.4.1 Interactive Impact of Catalyst Amount and Time

The combine influence of catalyst amount and time on biodiesel yield is presented into the Figure 3.3.9.4 A, while keeping other parameters (oil: methanol ratio

(1:3) and temperature (110°C)) constant. It is clear from the table that maximum RCB (89%) obtained with the catalyst loading of 2.3 wt% 7 hrs time. However, beyond the optimum values of catalyst concentration and reaction time, sudden drop in yield (80%) was observed. This drop in yield might be linked to the shifting of reaction in opposite direction (Verma and Sharma, 2016a). Since methanol and oil are immiscible, so the addition of catalyst during transesterification reaction helps to increase the final yield. However, soap formation would occur when too high catalyst concentration was employed, making separation of glycerol and end product difficult thus lowering biodiesel yield (due to incomplete reaction) (Rajan et al., 2016). Therefore, the results of the present study were in agreement with reported work elsewhere (Verma et al., 2017). The ANOVA result is insignificant for these factors with P-value (0.9125) > 0.05.

3.3.9.4.2 Interactive Impact of Catalyst Amount and Temperature

The Figure 3.3.9.4 B displays the combined influence of temperature and catalyst concentration on the yield of biodiesel. Maximum of 89 % RCB yield is obtained with the catalyst loading of 2.3 wt% at 110 °C. However, lower conversion of RCB (80%) observed at 3.15% catalyst is consistent with the previous study (Chakraborty et al., 2011). Similarly, a slight drop in RDB content (82%) was observed as the amount of catalyst and temperature increased beyond 2.5wt% and 110 °C. This drop in RCB content might be due to lowered interaction between the reactant and catalyst (Mahesh et al., 2015). Therefore, the interactive outcome of these two parameters on biodiesel yield is insignificant with P-value (0.9152) > 0.05.

3.3.9.4.3 Interactive Impact of Catalyst Amount and Oil: Methanol Ratio

The 3D plot (Figure 3.3.9.4 C) were made using experimental data defined by Box-Behnken matrix and represent the effect of different parameters on RCB yield keeping further parameter on the central point. As maximum biodiesel yield (89 %) is obtained at 1:3 oil: methanol ratio and 2.3 wt %. However, lower conversion of 80 % RCB (3.15% catalyst) observed due to partial changeover of triglyceride to methyl ester, which is consistent with the previous study (Lee et al., 2011). The slight drop in RCB content was observed as the amount of catalyst increased beyond 2.3wt% and

might be due to reduced interaction (Najafi et al., 2018) between the RCO and catalyst, thus causing emulsification and contributing in decreased yield of RCB (80%) in 28th run. However, ANOVA results depicts that oil: methanol and catalyst concentrations interactive effect are insignificant with P-value (0.5606) > 0.05.

3.3.9.4.4 Interactive impact of time and temperature

The time and temperature impact on the biodiesel yield are presented in Figure 3.3.9.4 D. It is evident that RCB yield (89%) increases significantly as temperature (110°C) and catalyst amount (2.3 wt.%) increases and any further increase in temperature (120°C) would cause a decline in yield (83%) possibly due to saponification (Rashtizadeh et al., 2014; Vicente et al., 2007). However, the short reaction time (1hrs) and low temperature (60 °C) possibly do not allow the interaction of catalyst with oil leading to partially converted products (80%) (Silva et al., 2011). Therefore, their combine impact on biodiesel yield is insignificant with P-value (0.1670) > 0.05.

3.3.9.4.5 Interactive Impact of Time and Oil: Methanol Ratio

The time and oil: methanol collective impact on SABD yield is presented into the Figure 3.3.9.4 E while keeping other parameters like catalyst concentration (2.3%) and temperature (110°C) constant. The highest biodiesel yield (89%) is attained at 1:3 oil: methanol ratio and reaction time of 7hrs. The literature survey indicates that oil: methanol ratio has a main role in providing maximum the yield of biodiesel. Therefore, determining the optimum value of these parameters is necessary. The two-sided mode of transesterification process thus forces the surplus alcohol to maintain the balance in reaction (higher conversion of oil (RCO) to FAMES (RCB)) (Pradhan et al., 2012). Thus, maximum RCB yield (89%) was obtained at 1:3 oil: methanol ratio and 7 h reaction time due to increased interaction of excess methanol with RCO. On the other hand, short and prolonged reaction time and methanol ratio (1 hr and 60 ml methanol; 9 hrs and 90 ml methanol) possibly do not permit the proper impregnation of catalyst with oil to achieve the equilibrium (Maran and Priya, 2015b) leading to reduced RCB yield (81%, 78%). The similar behaviour was observed by (Mahesh et al., 2015). ANOVA results is insignificant for these parameters with P-value (0.1827) > 0.05.

3.3.9.4.6 Interactive impact of oil: methanol ratio and temperature

The Figure 3.3.9.4 F represents the combined effect of temperature along with oil:alcohol ratio upon RCB yield. 89% RCB is obtained at 110 °C with 30 ml methanol. Conversely, temperature above the threshold level (> 110 °C) might initiates gasification of methanol, which would not permit the reaction among the methanol and RCO thus leads to reduced RCB yield (Liu et al., 2015). Therefore, these parameters have direct impact on biodiesel yield and are insignificant with P-value $(0.5063) > 0.05$.

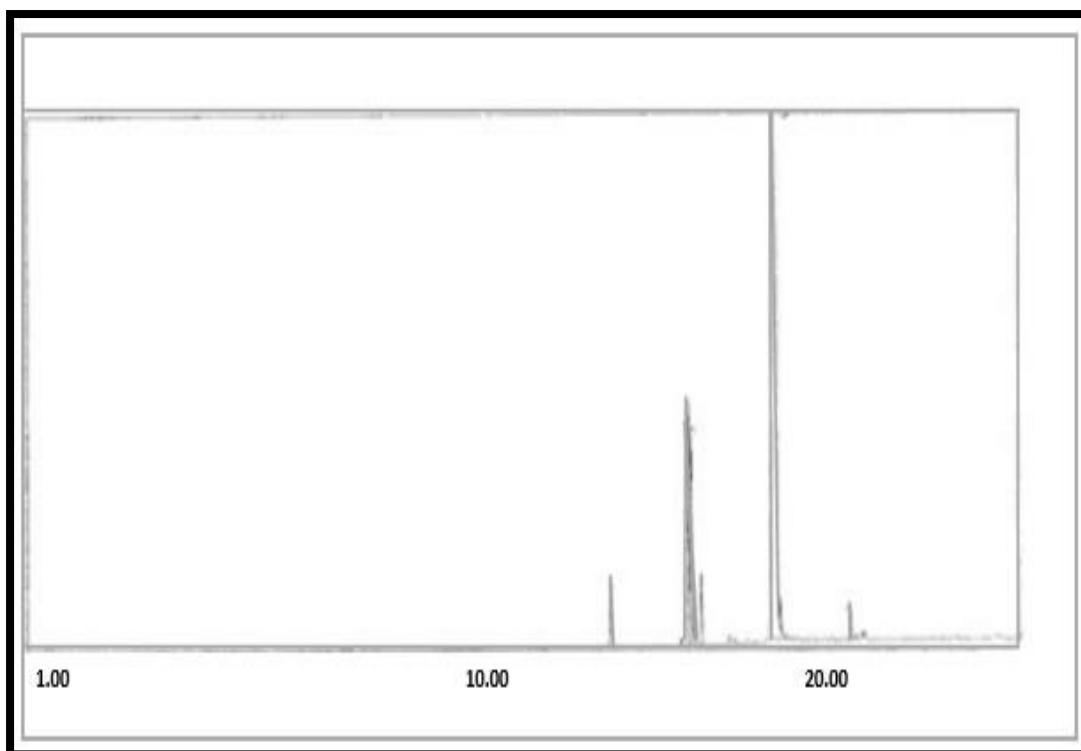


Figure 3.3.9.2.1: GC-MS Spectrum of *Ricinus communis* Biodiesel (RCB)

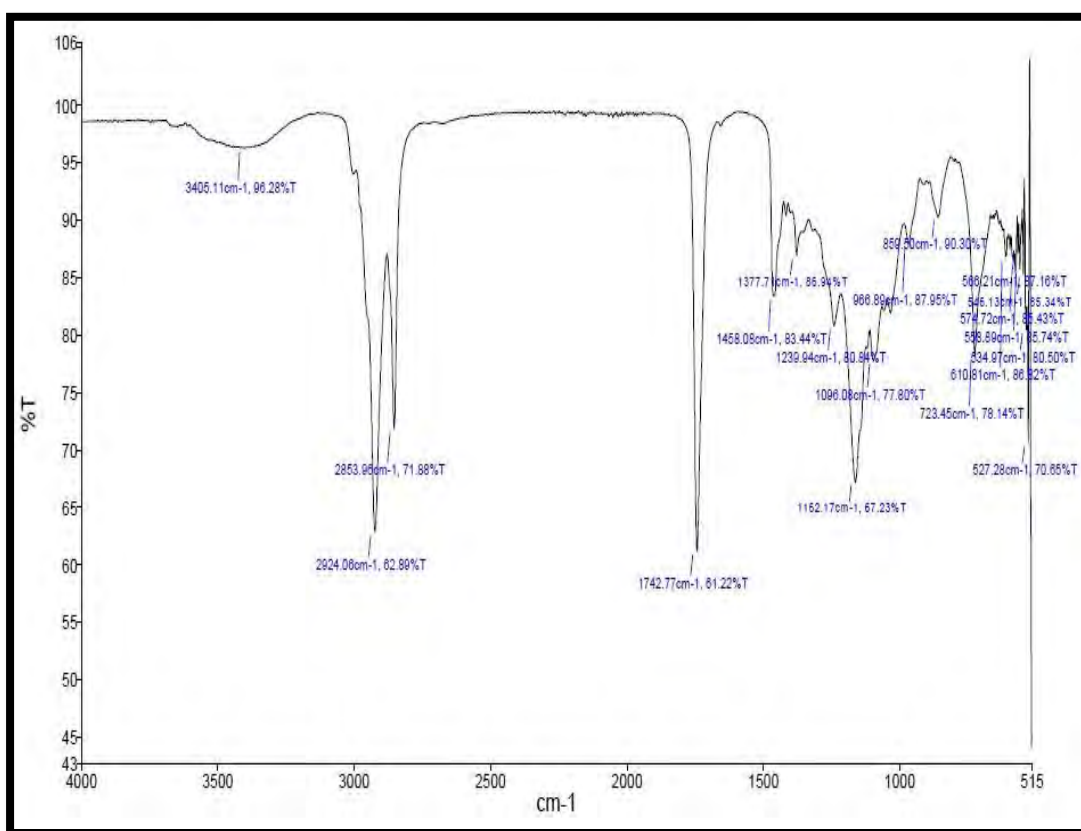


Figure 3.3.9.1.2: FT-IR of *Ricinus communis* Biodiesel (RCB)

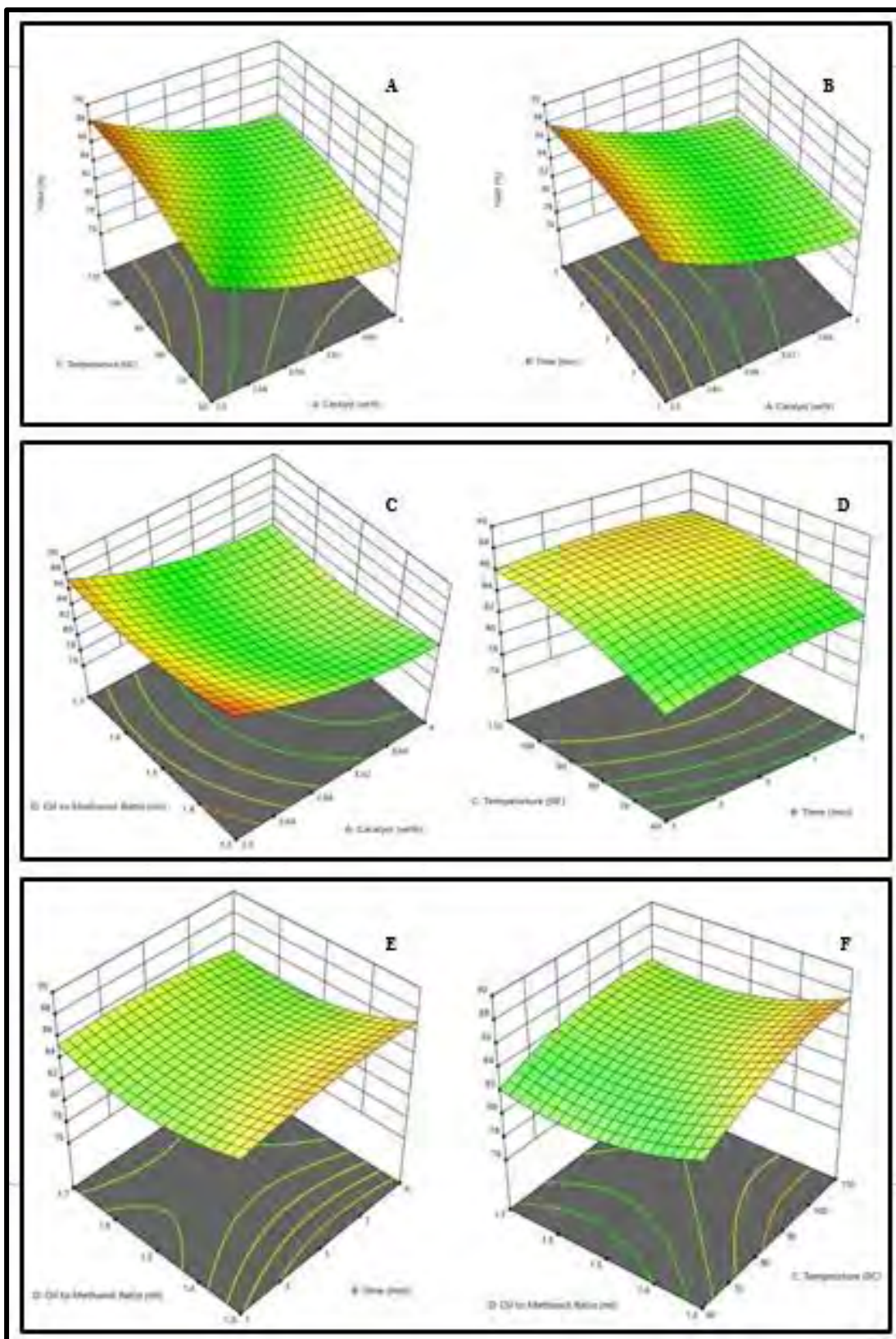


Figure 3.3.9.4: 3D surface Plots showing the impact of different parameters on *Ricinus communis* biodiesel (RCB) yield

Table 3.3.9: Optimized Conditions for RCB Synthesis Using Na-Mmt, Na-Ag-Mmt, Cu-Mg-Zn-Mmt Clay Catalysts

Catalyst	Conc.(g)	Oil: Methanol	Time (hrs)	Temperature°C	Yield%
Al-Mmt	2.0	1:3	6.5	115	85.37
Na-Ag-Mmt	3.0	1:3	6	110	85
Cu-Mg-Zn-Mmt	2.3	1:3	7	110	89

Table 3.3.9.2.1: Identified Esters in. *Ricinus communis* Biodiesel (RCB) Using GC-MS

Peak #	Identified Compound (FAMES)	Retention time	Molecular Formula
1	Hexadecanoic acid	23.43	C ₁₇ H ₃₄ O ₂
2	Methyl linoleate	25.5	C ₁₉ H ₃₄ O ₂
3	(9Z)-9-Octadecenoic acid	25.46	C ₁₉ H ₃₆ O ₂
4	Octadecanoic acid	25.07	C ₁₉ H ₃₈ O ₂
5	Methyl ricinoleate	22.78	C ₁₉ H ₃₆ O ₃
6	11,14-Eicosadienoic acid	25.13	C ₂₁ H ₃₈ O ₂
7	Erucic acid	29.54	C ₂₃ H ₄₄ O ₂

Table 3.3.9.2.2: FT-IR of *Ricinus communis* Biodiesel (RCB)

Peaks (cm ⁻¹)	Frequency Range (Cm ⁻¹)	Bond	Functional Group	Characteristics of peak
3405.11	4000-3000	O-H stretch	Alcohol	Medium
2924.06	3000-2850	H-C=O: C-H stretch	Aldehyde	Medium to strong
2853.96	2870-2695	C-H stretch	Alkane	Medium to Strong
1742.77	1750-1700	RCOOH	Ester	Strong
1458.08	1470-1450	C-H bend	Alkane	Medium
1377.71	1400-1360	C-N stretch	Amines	Medium
1239.94	1250-1220	C-N stretch	Amines	Medium
1162.17	1250-1020	C-N stretch	Amines	Medium
1096.08	1250-1020	C-O stretch	Ether	Strong/medium
723.45	725-720	C-Cl stretch	Alkyl Halide	Strong
566.21	600-500	C-Cl stretch	Alkyl Halide	Strong

Table 3.3.9.2.3: Fuel Properties of *Ricinus communis* Biodiesel (RCB)

TESTS	METHODS	ALM-B100
Colour	Visual	2
Flash Point °C (PMCC)	ASTM D-93	78
Density @ 15 °C Kg/L	ASTM D-1298	0.878
K.Viscosity @ 40 °C cST	ASTM D-445	5.11
Pour Point °C	ASTM D-97	-8
Cloud Point °C	ASTM D-2500	-10
Sulphur %wt	ASTM D-4294	0.00041
Total Acid No. mg KOH/gm	ASTM D-974	0.200

3.3.9.4 Experimental and Predicted yield of *Ricinus communis* Biodiesel (RCB) using Box-Behnken Design

Std	Run	Catalyst (wt%)	Time (hrs)	Temperature (°C)	Oil: Methanol (ml)	Yield %
28	1	3.15	5	85	1.5	82
9	2	2.3	1	110	1.3	89
14	3	4	1	110	1.7	81
15	4	2.3	9	110	1.7	86
5	5	2.3	1	110	1.3	89
19	6	3.15	1	85	1.5	82
22	7	3.15	5	110	1.5	81
7	8	2.3	9	110	1.3	89
16	9	4	9	110	1.7	81
6	10	4	1	110	1.3	82
12	11	4	9	60	1.7	78
1	12	2.3	1	60	1.3	82
26	13	3.15	5	85	1.5	82
8	14	4	9	110	1.3	83
2	15	4	1	60	1.3	78
18	16	4	5	85	1.5	80
4	17	4	9	60	1.3	78
11	18	2.3	9	60	1.7	83
17	19	2.3	5	85	1.5	86
3	20	2.3	9	60	1.3	87
25	21	3.15	5	85	1.5	82
21	22	3.15	5	60	1.5	80
27	23	3.15	5	85	1.5	80
10	24	4	1	60	1.7	77
24	25	3.15	5	85	1.7	83
30	26	3.15	5	85	1.5	82
13	27	2.3	1	110	1.7	88
20	28	3.15	9	85	1.5	80
23	29	3.15	5	85	1.3	83
29	30	3.15	5	85	1.5	82

3.3.9.4.1 Analysis of Variance (ANOVA) from Achieved Results

Source	Sum of Squares	df	Mean Square	F-value	p-value	Remarks
Model	0.9229	14	0.0659	16.83	< 0.0001	Significant
A-Catalyst	0.4507	1	0.4507	115.09	< 0.0001	
B-Time	0.0010	1	0.0010	0.2532	0.6222	
C-Temperature	0.1751	1	0.1751	44.72	< 0.0001	
D-Oil to Methanol Ratio	0.0181	1	0.0181	4.63	0.0481	
AB	0.0000	1	0.0000	0.0125	0.9125	
AC	0.0000	1	0.0000	0.0117	0.9152	
AD	0.0014	1	0.0014	0.3542	0.5606	
BC	0.0083	1	0.0083	2.11	0.1670	
BD	0.0076	1	0.0076	1.95	0.1827	
CD	0.0018	1	0.0018	0.4637	0.5063	
A ²	0.0154	1	0.0154	3.94	0.0658	
B ²	0.0026	1	0.0026	0.6717	0.4253	
C ²	0.0092	1	0.0092	2.34	0.1466	
D ²	0.0160	1	0.0160	4.09	0.0613	
Residual	0.0587	15	0.0039			
Lack of Fit	0.0485	9	0.0054	3.14	0.0886	not significant
Pure Error	0.0103	6	0.0017			
Cor Total	0.9817	29				

3.3.10 *Celastrus paniculatus* Biodiesel (CPB)

3.3.10 *Celastrus paniculatus* Biodiesel (CPB)

Celastrus paniculatus has 55% oil content and free fatty acid (FFA) content is 0.098 which means it only requires one step transesterification to be converted into biodiesel (Table 3.3.1). A series of transesterification reactions were carried out to get the optimum yield of the biodiesel produced from the seeds oil of *Celastrus paniculatus* biodiesel (CPB) using all three catalysts. The conditions at which optimum yield of the biodiesel from each of the catalysts was obtained is given in table 3.3.10. All the three catalysts i.e. Al-Mmt clay catalyst, Na-Ag Mmt catalyst, Cu-Mg-Zn Mmt clay catalyst, were used in the transesterification of the seeds oil of *Celastrus paniculatus*.to biodiesel but Cu-Mg-Zn-Mmt clay catalyst gave the best yield among all i.e. 92%, Na-Ag-Mmt clay catalyst gave 87% yield whereas Al-Mmt clay catalyst gave biodiesel yield of 85%.

3.3.10.1 Reaction Variables Affecting Transesterification of *Celastrus paniculatus* Seeds Oil to Biodiesel

Biodiesel yield is affected by three variables i.e. oil to methanol molar ratio, catalyst concentration and reaction temperature, in transesterification. And their effect is as following:

3.3.10.1.1 Oil to Methanol Molar Ratio

The stoichiometric ratio for FFAs conversion into esters requires 3 moles of alcohol and 1 mole of oil to produce 3 moles of fatty acid alkyl esters and 1 mole of glycerin (Mehar et al, 2006). In the current scenario oil to methanol ratios of 1:3, 1:4, 1:5, 1:6, 1:7, 1:8, 1:9 and 1:10 were used keeping other reaction conditions constant i.e. reaction time, reaction temperature and catalyst concentration constant. The maximum conversion ratio was 1:6 by all three Mmt clay catalysts.

3.3.10.1.2 Catalyst Concentration

Transesterification reaction for conversion of *Celastrus paniculatus* seeds oil to FAMES, was carried out at different catalyst concentrations i.e. 0.1g, 0.2g, 0.3g, 0.4g, 0.5g, 0.6g and 0.7g and maximum yield of biodiesel was obtained at 0.5 g of Al-Mmt

clay catalyst, 0.2 g of Na-Ag-Mmt clay catalyst and Cu-Mg-Zn-Mmt clay catalyst gave best results.

3.3.10.1.3 Reaction Temperature (°C)

A series of reactions were carried out at different reaction conditions keeping other factors constant i.e. methanol to oil molar ratio and catalyst concentration. Highest conversion ratio was achieved at 75 °C in Al-Mmt, 70 °C for Na-Ag-Mmt and 90 °C Cu-Mg-Zn-Mmt clay catalysts.

3.3.10.2 Chemical Characterization

3.3.10.2.1 GC-MS Analysis of *Celastrus paniculatus* Biodiesel (CPB)

GC-MS analysis is broadly used technique to determine the chemical composition, type and structure of synthesized FAMES. Mass spectrometer was set to scan in the range of m/z 2-600 and ionization potential 70V (Bu et al., 2014; Zhang et al., 2014). Five monumental peaks representing methyl esters of the corresponding fatty acid were observed and confirmed by Library match software (NO. NIST 11). Different FAMES were determined using the retention time by Mass Spectroscopic analysis (Figure 3.3.10.2.1). Helium gas was used as a carrier with reaction temperature 300°C for 45 minutes. Peak 1 and 2 represent the methyl esters of 10-octadecenoic acid (C₁₈H₃₄O₂) and Methyl tetradecanoate (C₁₅H₃₀O₂). Whereas methyl esters of Methyl hexadecanoate (C₁₇H₃₄O₂), (7Z)-10-Methyl-hexadec-7-enoate (C₁₇H₃₁O₂) and Methyl 9-octadecenoate (C₁₉H₃₆O₂) are represented by peak 3,4 and 5 respectively (Table 3.3.10.2.1). 10-octadecenoic acid (C₁₈H₃₄O₂) was the major methyl ester found in the CPD. FAME's profile determines the suitability of feedstock for use in production of biodiesel fuel (Skoto et al., 2011).

3.3.10.2.2 FT-IR Analysis of *Celastrus paniculatus* Biodiesel (CPB)

FT-IR is a modern analytical method for fast and easy detection of Fatty acid methyl esters due to its capability as “finger-print technique” which aid in recognition of chemical bonds and functional groups in oils, fats and biodiesel samples. Figure 3.3.10.2.2 represents the FT-IR spectrum of *Celastrus paniculatus* Biodiesel (CPB).

Appearance of peak at 2922.78 cm^{-1} shows the presence of aldehyde compounds in the biodiesel sample. Presence of alkanes was determined by two spate peaks at 2853.35 cm^{-1} and other at 1464.15 cm^{-1} , first one showing the stretching of C-H bond whereas second one indicating a bend in the C-H plane. A characteristic peak of esters was appeared at 1743.22 cm^{-1} . The congestive peaks at 1377.87 cm^{-1} , 1238.50 cm^{-1} and 1160.09 cm^{-1} show the presence of amines in the sample. The stretch in the C-O bond of ether was explained by the peak at 1098.36 cm^{-1} . And peaks at 722.14 cm^{-1} and 580.09 cm^{-1} depict the presence of alkyl halides (Table 3.3.10.2.2).

The FTIR confirms the presence of ester carbonyl bond near the absorption band 1743.71 cm^{-1} (Daniyan et al., 2019). Presence of above-mentioned peaks in the FT-IR spectra confirms the biodiesel synthesis.

3.3.10.2.3 Fuel Properties of *Celastrus paniculatus* Biodiesel (CPB)

The fuel properties of synthesized *Celastrus paniculatus* Biodiesel (CPB) were determined and found well in accordance with the ASTM standards (Table 3.3.10.2.3). These properties help in the estimation of the fuel quality and its efficiency in the diesel engine. Total acid number or acid value is amount of the free fatty acid existent in a fuel sample and is determined in mg KOH/gm. If its value is higher in the sample that means engine efficiency will be affected in a negative way (Akhtar et al., 2019). CPB's acid value (0.173 mg KOH/gm) is well in range of international standards. Density of the CPB is also in accordance with the international standards i.e. 0.832 mg KOH/gm . Fuel density value is also crucial as its higher value causes engine corrosion and decreases its efficiency (Sultana et al., 2016). Kinematic viscosity is the determinant of the fuel thickness, higher value causes deposition in engine and reduces its working efficiency (Gunstone & Hamilton, 2001). CPB's kinematic viscosity is in range of international standards (4.15 kg/L). The color of produced biodiesel is on visual 2 according to ASTM standards. Another important aspect is the Flash point of the diesel during fuel handling and transportation and fuels having flash point higher than 60°C are referred as safe (Salaheldeen et al., 2015). At this temperature fuel ignition starts. Flash point of *Celastrus paniculatus* Biodiesel (CPB) was found to be 73°C . Additional important parameter is cold flow properties which includes Pour point and Cloud point of biodiesel (Akhtar et al., 2019). Pour point and cloud point value of CPB were -8°C and -13°C respectively. The sulfur contents in CPB were (0.0002 ppm) by %weight. An

ideal fuel has low sulfur content and is more operative for engine's life and environment (Candeia et al., 2009).

3.3.10.3 Optimization Study of Transesterification Operational Factors Through Response Surface Methodology (RSM)

The optimization of transesterification process was performed by choosing four independent variables (Table 3.3.10.4) with maximum and minimum ranges i.e., Catalyst (A) 0.2-0.8 (Cu-Mg-Zn-Mmt), Time (B) 1-8 hrs, Temperature (C) 50-90 °C and Oil to Methanol (D) 1:3-1:6 and RSM build on Box Behnken Design was applied on 30 experiments to test the fitness of Quadratic ploy-equation with the Design-Expert 11 (Stat Ease IncMinneapolis,USA). A coded model equation used for studying the association among Input Variables as well as Output Response in terms of yield (Y) is

$$Y = +25.80239 - 1.19184A - 0.001553B + 0.033612C - 24.47227D + 0.032788AB - 0.000638AC + 0.471817AD + 0.000382BC + 0.052526BD + 0.018015CD - 0.448649A^2 - 0.011925B^2 - 0.000380C^2 + 7.96506D^2$$

ANOVA results as presented in Table 3.3.10.4.1 depicts that The Model F-value of 5.98 implies the model is significant. There is only a 0.07% chance that an F-value this large could occur due to noise. P-value <1, while the Lack of Fit F-value of 1.13 implies the Lack of Fit is not significant relative to the pure error. There is a 47.61% chance that a Lack of Fit F-value this large could occur due to noise. Non-significant lack of fit is good for the model to fit, thus confirms the best fitness of model to experimental (trial) data. These values thus depict the closeness of predicted values of biodiesel yield with the experimental Box-Behnken designs. The adequate precision (9.140) is greater than 4, so ensures the adequateness of the model to circumnavigate via space thus predicting the yield of biodiesel. Moreover, the adjusted R2 (R2=0.7061) and predicted R2 (R2=0.3797) values difference (>0.2) indicating the good correlation with the regression polynomial.

3.3.10.4 Parametric characterization of transesterification process

Figure 3.3.10.4 A, B, C, D, E & F shows the interactive effect of different variables on transesterification reaction in form of 3D response surface plot which can be explained in the following sub sections.

3.3.10.4.1 Interactive Impact of Catalyst Amount and Time

The combine influence of catalyst amount and time on biodiesel yield is presented into the Figure 3.3.10.4 A, while keeping other parameters (oil: methanol ratio (1:6) and temperature (90°C)) constant. At optimal levels of catalyst loading and process time (0.2% and 6 hrs) maximum 92% CPB yield achieved owing to the equilibrium in the reaction. However, beyond the optimum values of catalyst concentration and reaction time, sudden drop in yield (76%) was observed (Run 5 and 30) which is similar with the reported work (Wong et al., 2015). These parameters are insignificant with P-value (0.3971) > 0.05 for the transesterification reaction.

3.3.10.4.2 Interactive Impact of Catalyst Amount and Temperature

The combined influence of temperature and catalyst concentration on the CPB yield is shown in Figure 3.3.10.4 B. Maximum CPB yield of 92% is obtained with the catalyst loading of 0.2 wt% at 90 °C. However, lower conversion of CPB (76%) observed with 0.5% catalyst due to partial changeover of triglyceride to methyl ester, which is consistent with the previous study (García-Moreno et al., 2014; Sarve et al., 2015). The same behaviour is noticeable with 79% CPB yield as the amount of catalyst and temperature increased beyond 0.2wt% and 90 °C. Our findings are in line with the reported work elsewhere (Ferella et al., 2010). Therefore, based on ANOVA results, the interactive outcome of catalyst concentration and time on the biodiesel yield is highly significant with Pvalue (0.001) < 0.05.

3.3.10.4.3 Interactive Impact of Catalyst Amount and Oil: Methanol Ratio

The Figure 3.3.10.4 C represent 3D surface plot showing collective effect of the catalyst and oil: methanol on yield of biodiesel yield based on the parameters set by Box-Behnken design experiment. It is observed that maximum biodiesel yield (92 %) is obtained at 1:6 oil: methanol ratio and 0.2 wt % catalyst. The methanol-oil ratio is the significant parameters pushing the biodiesel yield. Stoichiometrically, 3 moles of methanol needed for the transesterification of oil (1 mole) yielding glycerol (1 mole) and biodiesel (3 moles). Since transesterification is a double-sided reaction so, an additional amount of methanol is needed for pushing the reaction onward. For

maximum FAME yield, 6:1 oil-methanol ratio is sufficient (Chuah et al., 2015). However, lower conversion of 76 % FAME (30th) observed due to partial changeover of triglyceride to methyl ester, which is consistent with the previous study (Obadiah et al., 2012). The slight drop in CPB content was observed as the amount of catalyst and methanol ratio increased beyond 0.2wt% and 60 ml. However, ANOVA results depicts that oil: methanol and catalyst concentrations interactive effect are insignificant with P-value (0.5087) > 0.05.

3.3.10.4.4 Interactive impact of time and temperature

The time and temperature cooperative impact on the biodiesel yield is presented in Figure 3.3.10.4 D. It is evident that biodiesel yield (92 %) increases significantly as temperature (90°C) and catalyst amount (0.2 wt.%) increases and any further increase in temperature would cause a decline in yield possibly due to saponification (Vicente et al., 2007). Arrhenius equation could explain it, stating an increasing process temperature may steadily increase the reaction rate and yield of biodiesel. Our findings agreed with the reported work (Olutoye et al., 2016) revealing that yield increases up to 90°C temperature afterward a substantial decline in bio-diesel yield was observed. Thus, the maximum yield of biodiesel (92%) was achieved on 90°C with 6 hr owing to the thorough mingling of oil and the methanol followed by easy separation of glycerol and end product (Verma et al., 2017). However higher temperature and time may facilitate hydrolysis of alkyl esters to generate acids along with the polarity of methanol (Verma et al., 2017) thereby decreasing biodiesel yield (Dwivedi and Sharma, 2015). Therefore, the combined impact of time and temperature on final yield is significant with P-value (0.014) < 0.05.

3.3.10.4.5 Interactive Impact of Time and Oil: Methanol Ratio

The time and oil: methanol collective impact on CPB yield is shown in Figure 3.3.10.4 E while keeping other parameters like catalyst concentration (0.2%) and temperature (90°C) constant. Highest biodiesel yield (92%) is attained at 1:6 oil: methanol ratio and reaction time of 6 h due to increased interaction of excess methanol with oil (Singh et al., 2018). The short reaction time of 1h and low methanol ratio (3) possibly do not permit the proper impregnation of modified clay with oil to achieve the equilibrium leading to partially converted products which contributes to the reduced CPB yield. In an earlier study on castor oil methyl esters, confirmed the strong influence of reaction time on end product (Baskar et al., 2018). A slight decrease in FAME content (76 %) at 4.5 hrs with 1:45 oil

methanol ratio in run 30 might be due related to the oil's dilution effect and reserve transesterification reaction, making it unfavourable to obtain desired CPB yield. ANOVA results declare these parameters insignificant with P-value (0.4957) > 0.05.

3.3.10.4.6 Interactive impact of oil: methanol ratio and temperature

The Figure 3.3.10.4.F displays the combined effect of oil:alcohol ratio and temperature upon biodiesel yield. 92% CPB yield was obtained as the temperature increased to 90 °C with 60 ml methanol. However, as the temperature rises above the threshold level (>90 °C) CPB yield decreases significantly. Therefore, it can be concluded from results that combined effect of these two parameters on the yield of biodiesel is insignificant with Pvalue (0.1914) > 0.05 which are in consistence with the reported work elsewhere (Gu et al., 2015).

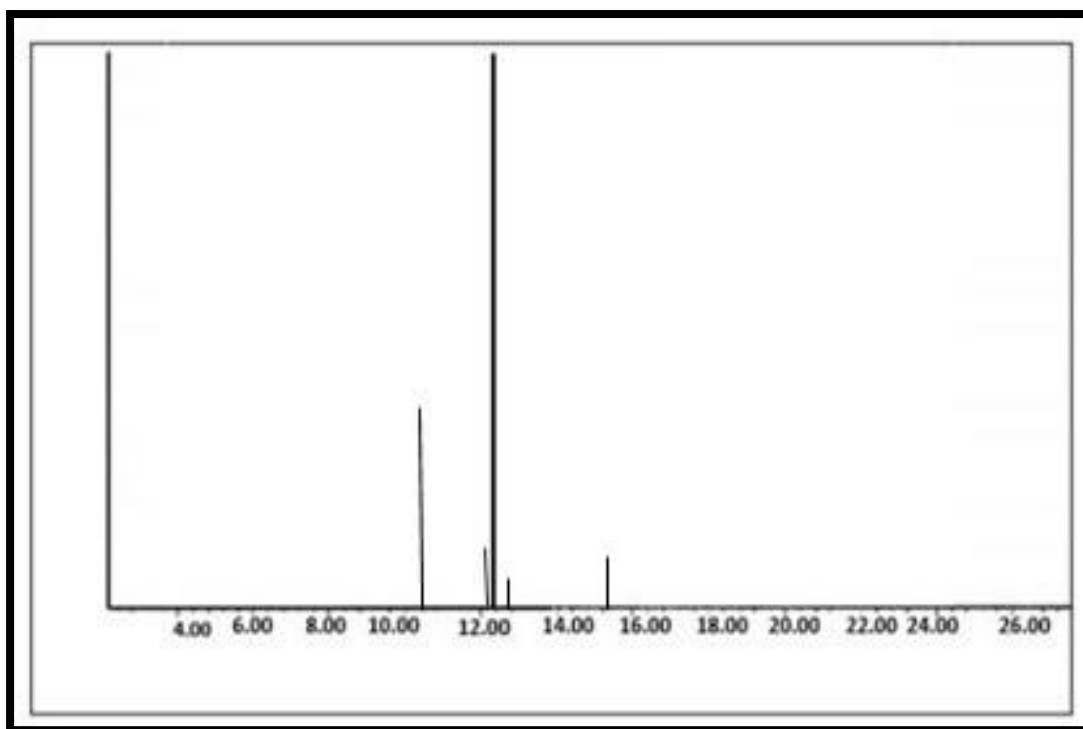


Figure 3.3.10.2.1: GC-MS of *Celastrus paniculatus* Biodiesel (CPB)

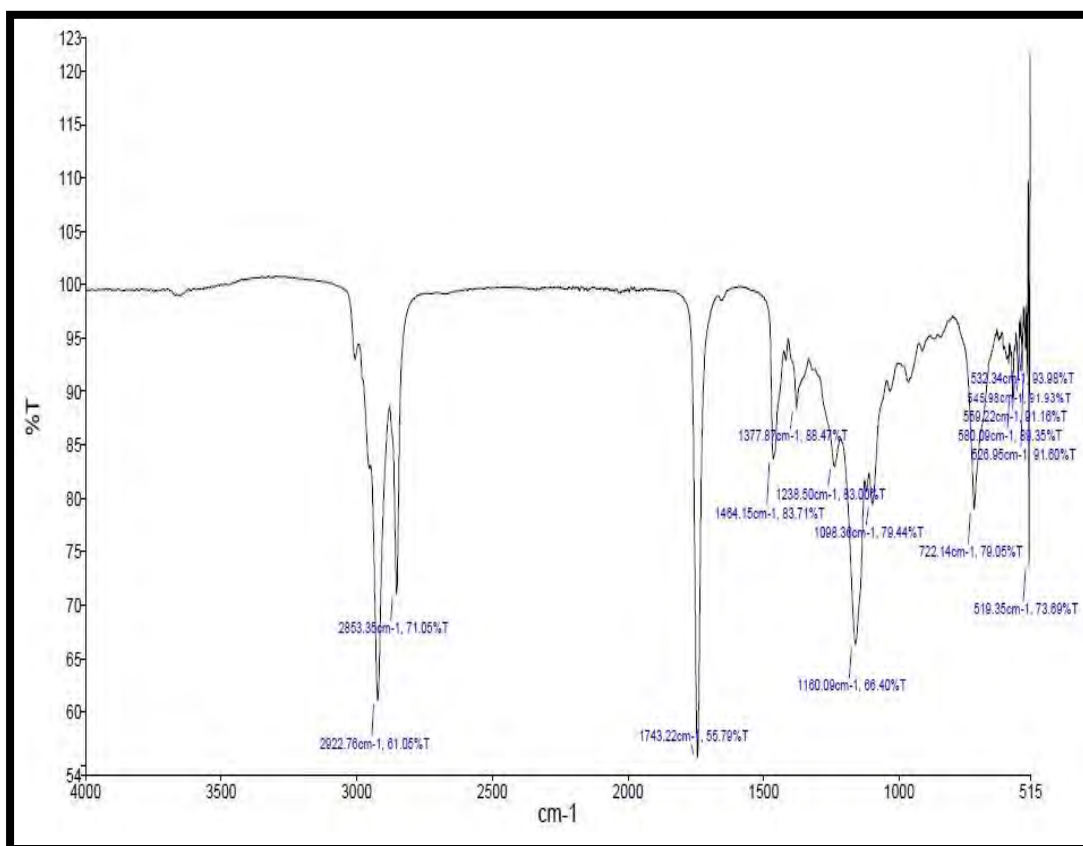


Figure 3.3.10.2.2: FT-IR of *Celastrus paniculatus* Biodiesel (CPB)

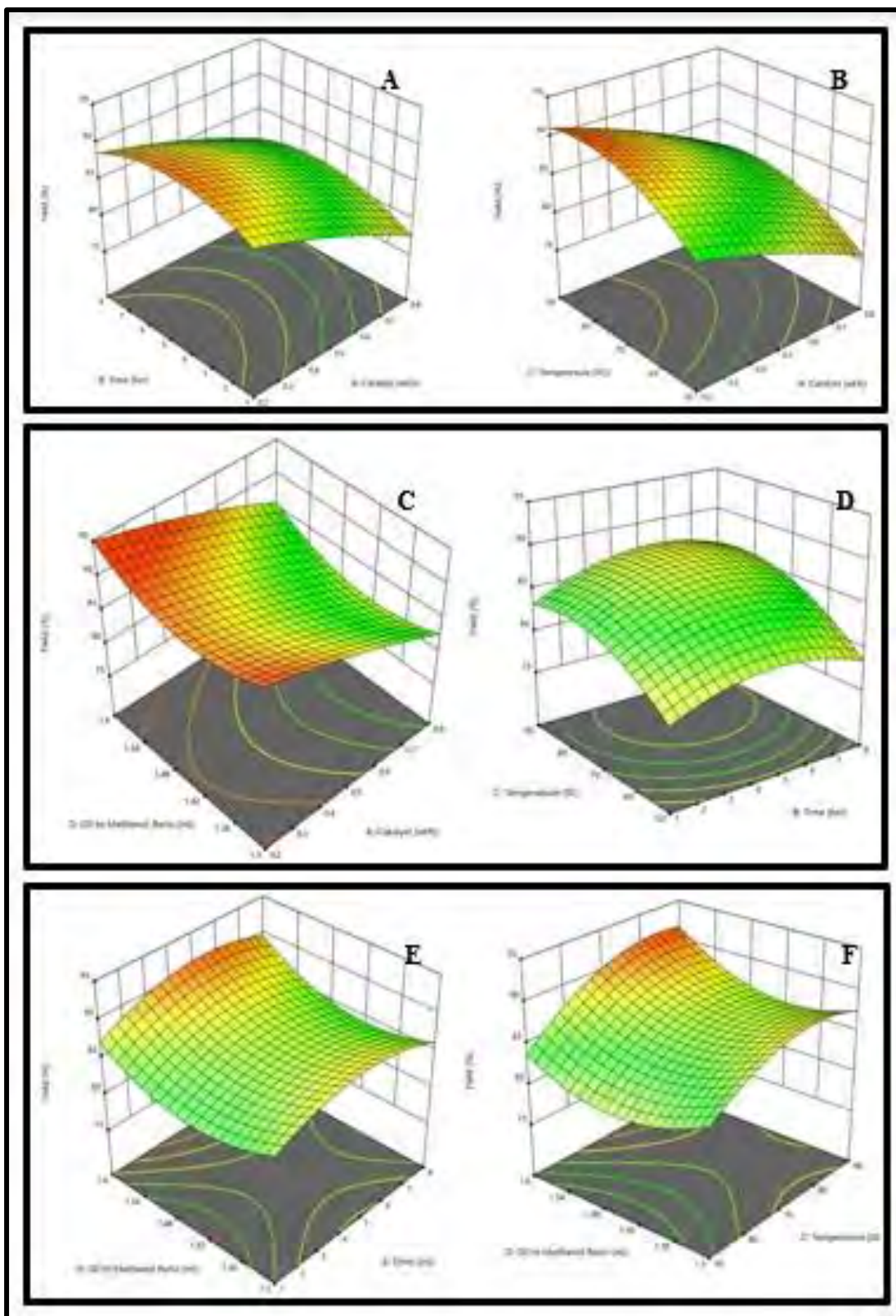


Figure 3.3.10.4: 3D surface Plots showing the impact of different parameters on *Celastrus paniculatus* biodiesel (CPB) yield

Table 3.3.10: Optimized Conditions for CPB Synthesis Using Na-Mmt, Na-Ag-Mmt, Cu-Mg-Zn-Mmt Clay Catalysts

Catalyst	Conc.(g)	Oil:Methanol	Time (hrs)	Temperature °C	Yield%
Al-Mmt	0.5	1:6	5	75	85
Na-Ag-Mmt	0.2	1:6	5	70	87
Cu-Mg-Zn-Mmt	0.2	1:6	6	90	92

Table 3.3.10.2.1: Identified Esters in. *Celastrus paniculatus* Biodiesel (CPB) Using GC-MS

Peak #	Identified Compound (FAMES)	Retention time	Molecular Formula
1	10-octadecenoic acid	19.13	C ₁₈ H ₃₄ O ₂
2	Methyl tetradecanoate	13.64	C ₁₅ H ₃₀ O ₂
3	Methyl hexadecanoate	14.35	C ₁₇ H ₃₄ O ₂
4	(7Z)-10-Methyl-hexadec-7-enoate	12.58	C ₁₇ H ₃₁ O ₂
5	Methyl 9-octadecenoate	20.04	C ₁₉ H ₃₆ O ₂

Table 3.3.10.2.2: FT-IR of *Celastrus paniculatus* Biodiesel (CPB)

Peaks (cm ⁻¹)	Frequency Range (Cm ⁻¹)	Bond	Functional Group	Characteristics of peak
2922.78	3000-2850	H-C=O: C-H stretch	Aldehyde	Medium to strong
2853.35	2870-2695	C-H stretch	Alkane	Medium to Strong
1743.22	1750-1700	RCOOH	Ester	Strong
1464.15	1470-1450	C-H bend	Alkane	Variable
1377.87	1400-1360	C-N stretch	Amines	Medium
1238.50	1250-1220	C-N stretch	Amines	Medium
1160.09	1250-1020	C-N stretch	Amines	Medium
1098.36	1250-1020	C-O stretch	Ether	Strong/medium
722.14	725-720	C-Cl stretch	Alkyl Halide	Strong
580.09	600-500	C-Cl stretch	Alkyl Halide	Strong

Table 3.3.10.2.3: Fuel Properties of *Celastrus paniculatus* Biodiesel (CPB)

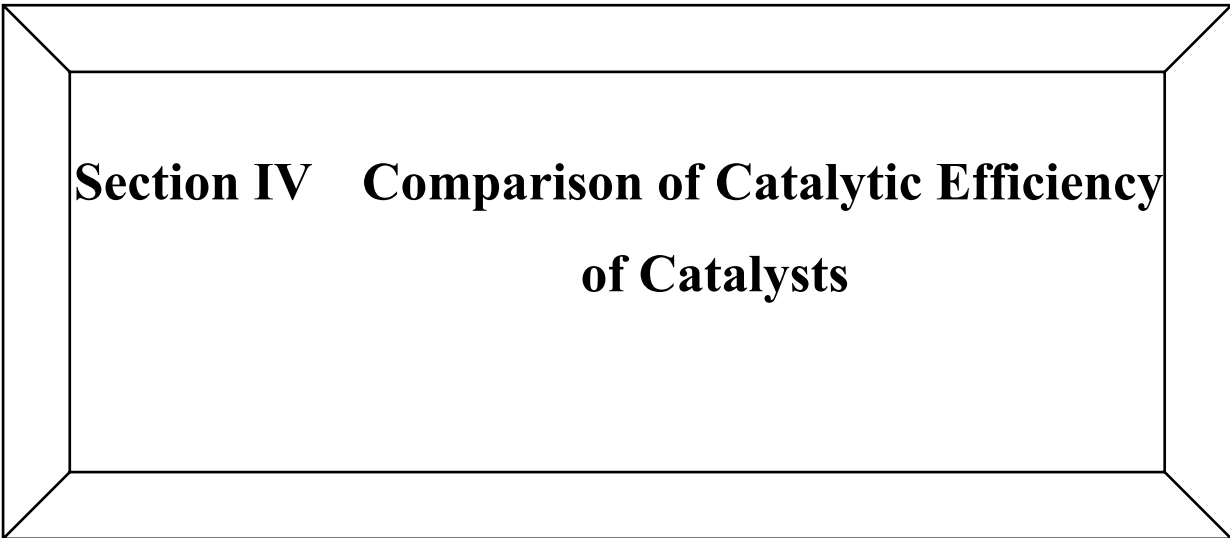
TESTS	METHODS	ALM-B100
Colour	Visual	2
Flash Point °C (PMCC)	ASTM D-93	73
Density @ 15 °C Kg/L	ASTM D-1298	0.832
K.Viscosity @ 40 °C cST	ASTM D-445	4.15
Pour Point °C	ASTM D-97	-8
Cloud Point °C	ASTM D-2500	-13
Sulphur %wt	ASTM D-4294	0.0002
Total Acid No. mg KOH/gm	ASTM D-974	0.173

3.3.10.4 Experimental and Pridicted yield of *Celastrus paniculatus* Biodiesel (BOB) using Box-Behnken Design

Std	Run	Catalyst (wt%)	Time (hrs)	Temperature (°C)	Oil: Methanol (ml)	Yield %
19	1	0.5	1	70	1.45	82
5	2	0.2	1	90	1.3	89
17	3	0.2	4.5	70	1.45	89
18	4	0.8	4.5	70	1.45	79
2	5	0.8	1	50	1.3	76
20	6	0.5	8	70	1.45	82
4	7	0.8	8	50	1.3	77
13	8	0.2	1	90	1.6	92
16	9	0.8	8	90	1.6	89
28	10	0.5	4.5	70	1.45	82
10	11	0.8	1	50	1.6	76
25	12	0.5	4.5	70	1.45	89
29	13	0.5	4.5	70	1.45	89
8	14	0.8	8	90	1.3	78
30	15	0.5	4.5	70	1.45	89
7	16	0.2	8	90	1.3	90
6	17	0.8	1	90	1.3	79
9	18	0.2	1	50	1.6	86
15	19	0.2	8	90	1.6	92
22	20	0.5	4.5	90	1.45	88
24	21	0.5	4.5	70	1.6	89
27	22	0.5	4.5	70	1.45	89
23	23	0.5	4.5	70	1.3	87
14	24	0.8	1	90	1.6	79
11	25	0.2	8	50	1.6	85
26	26	0.5	4.5	70	1.45	88
12	27	0.8	8	50	1.6	77
1	28	0.2	1	50	1.3	85
3	29	0.2	8	50	1.3	86
21	30	0.5	4.5	50	1.45	76

3.3.10.4.1 Analysis of Variance (ANOVA) from Achieved Results

Source	Sum of Squares	df	Mean Square	F-value	p-value	Remarks
Model	2.09	14	0.1492	5.98	0.0007	significant
A-Catalyst	1.18	1	1.18	47.27	< 0.0001	
B-Time	0.0239	1	0.0239	0.9594	0.3429	
C-Temperature	0.4473	1	0.4473	17.92	0.0007	
D-Oil to Methanol Ratio	0.0524	1	0.0524	2.10	0.1679	
AB	0.0190	1	0.0190	0.7597	0.3971	
AC	0.0002	1	0.0094	16.29261	0.0012	
AD	0.0072	1	0.0072	0.2890	0.5988	
BC	0.0114	1	0.0114	2.962081	0.0141	
BD	0.0122	1	0.0122	0.4875	0.4957	
CD	0.0467	1	0.0467	1.87	0.1914	
A ²	0.0042	1	0.0042	0.1692	0.6866	
B ²	0.0553	1	0.0553	2.22	0.1574	
C ²	0.0600	1	0.0600	2.40	0.1419	
D ²	0.0832	1	0.0832	3.33	0.0878	
Residual	0.3744	15	0.0250			
Lack of Fit	0.2593	10	0.0259	1.13	0.4761	not significant
Pure Error	0.1151	5	0.0230			
Cor Total	2.46	29				



**Section IV Comparison of Catalytic Efficiency
of Catalysts**

In the current study three different types of catalysts were synthesized and used in the transesterification of the selected feed stock to the biodiesel. All of these three catalysts showed good catalytic power. Catalytic behavior of these catalysts is discussed below.

3.4.1 Catalytic Efficiency of Al-Mmt Clay Catalyst

Al-Mmt Clay Catalyst was used in the transesterification of all the selected feed stock i.e. *Brassica oleracea* L., *Carthamus lanatus*, *Carthamus tinctorius*, *Carthamus oxycantha*, *Beaumontia grandiflora*, *Acacia concinna*, *Sapindus trifoliatus*, *Sesamum indicum*, *Ricinus communis* and *Celastrus paniculatus*. Overall, it showed good catalytic strength, giving 91.40% biodiesel yield in conversion of *Brassica oleracea* L seeds oil to biodiesel and 95 % *Carthamus tinctorius* biodiesel yield. Both feed stock gave best of their yield when reacted with methanol in the presence of Al-Mmt clay catalyst as compared to other catalysts i.e. Na-Ag-Mmt and Cu-Mg-Zn-Mmt catalyst. However, against *Carthamus lanatus*, *Carthamus oxycantha*, *Beaumontia grandiflora*, *Acacia concinna*, *Sapindus trifoliatus*, *Sesamum indicum*, *Ricinus communis* and *Celastrus paniculatus*.it gave % biodiesel yield of 87%, 91%, 85%, 89%, 90%, 91%, 85.4% and 85% respectively. Least biodiesel yield (85%) was recorded in case of and *Celastrus paniculatus*.

3.4.1.1 Reusability of Al-Mmt Clay Catalyst

The feasibility and usability of Al-Mmt clay catalyst during the transesterification reaction can be examined by the investigation of the catalyst reusability on biodiesel yield under optimized reaction conditions (0.2g catalyst, 1:7 oil to methanol ratio, 5 hrs, 100°C). Same catalyst was used in seven reactions repeatedly. At the end of every reaction, catalyst was washed with methanol and dried in the oven (100°C) for up to 3 hours. The treated and washed catalyst was found to be active and was efficiently used in five repeated reactions with no halt in the catalytic power (Figure 3.4.1.1). However, a notable drop in efficiency was recorded after fifth cycle probably due to deactivation of active site.

3.4.2 Catalytic Efficiency of Na-Ag-Mmt Clay Catalyst

Bi metallic Na-Ag-Mmt clay catalyst, when used in the transesterification of the *Brassica oleracea* L., *Carthamus lanatus*, *Carthamus tinctorius*, *Carthamus oxycantha*, *Beaumontia grandiflora*, *Acacia concinna*, *Sapindus trifoliatus*, *Sesamum indicum*, *Ricinus communis* and *Celastrus paniculatus*, gave biodiesel yield of 87%, 89%, 91%, 90%, 87%, 90%, 93%, 90%, 85% and 87% respectively. *Beaumontia grandiflora* and *Acacia concinna* showed optimum yield (87% and 90% respectively) against Al-Mmt catalyst. However, it showed best efficiency in the transesterification of *Sapindus trifoliatus* (93%).

3.4.2.1 Reusability of Na-Ag-Mmt Clay Catalyst

The viability and reusability of Na-Ag-Mmt clay catalyst during the transesterification reaction of biodiesel synthesis can be examined by the study of the catalyst reusability in biodiesel yield under optimal reaction conditions (0.1g catalyst, 1:4 oil to methanol ratio, 3 hrs, 100°C). Same catalyst was used in seven reactions repeatedly. Catalyst was treated with methanol and dried in the oven (100°C) for up to 3 hours after reaction completion. The treated and washed catalyst was found to be active and was efficiently used in three repeated reactions with no fall in the catalytic properties (Figure 3.4.2.1). However, a notable drop in efficiency was recorded after third cycle perhaps due to deactivation of active site.

3.4.3 Catalytic Efficiency of Cu-Mg-Zn-Mmt Clay Catalyst

Tri metallic Mmt clay hybrid catalyst (Cu-Mg-Zn) was found to be most effective of all the catalysts used for the transesterification of oils to biodiesel. Six out of ten feed stock i.e. *Carthamus oxycantha*, *Carthamus lanatus*, *Sapindus trifoliatus*, *Sesamum indicum*, *Ricinus communis* and *Celastrus paniculatus*, gave optimal yield against this catalyst. However, among these the best results were shown by *Sapindus trifoliatus* i.e. 95% yield of biodiesel.

3.4.3.1 Reusability of Cu-Mg-Zn-Mmt Clay Catalyst

The viability and reusability of Cu-Mg-Zn-Mmt clay catalyst during the transesterification reaction of biodiesel synthesis can be examined by the study of the

catalyst reusability in biodiesel yield under optimal reaction conditions (0.2g catalyst, 1:4 oil to methanol ratio, 3.5 hrs, 100°C). Catalyst was used in seven reactions repetitively. And was treated with methanol and dried in the oven (100°C) for up to 3 hours at the end of each reaction. The treated and washed catalyst was found to be active and was efficiently used in four repeated reactions with no halt in the catalytic properties (Figure 3.4.3.1). Though, a remarkable decrease in efficiency was recorded after fourth cycle possibly because of the deactivation of active site.

All three catalysts show good catalysis during transesterification. However, among these, Cu-Mg-Zn-Mmt showed best results in maximum number of reactions, making it most effective catalyst of the three. Moreover, reusability of the catalyst is also promising, it can be reused for three times without any decrease in the catalytic efficiency. Na-Ag-Mmt and Al-Mmt clay catalyst also show auspicious results in the transesterification of oils to biodiesel (Figure 3.4). Sustainability of these catalysts is also remarkable i.e. Al-Mmt can be used five times and Na-Ag-Mmt for three times without any halt in the catalytic strength. Plants along with the best yield obtained by the catalyst are given in the table 3.4.

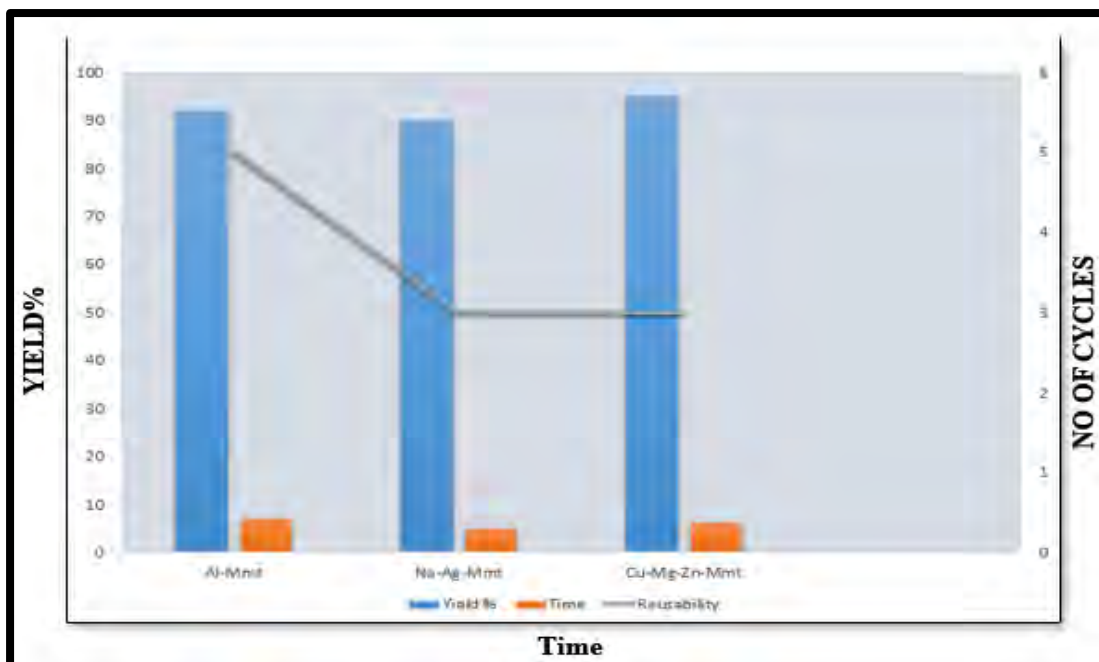


Figure 3.4: Comparison of Catalytic Efficiencies of Catalysts, Al-Mmt, Na-Ag-Mmt & Cu-Mg-Zn-Mmt (from Left to Right Respectively), Time and Their Reusability in Six Consecutive Experiments

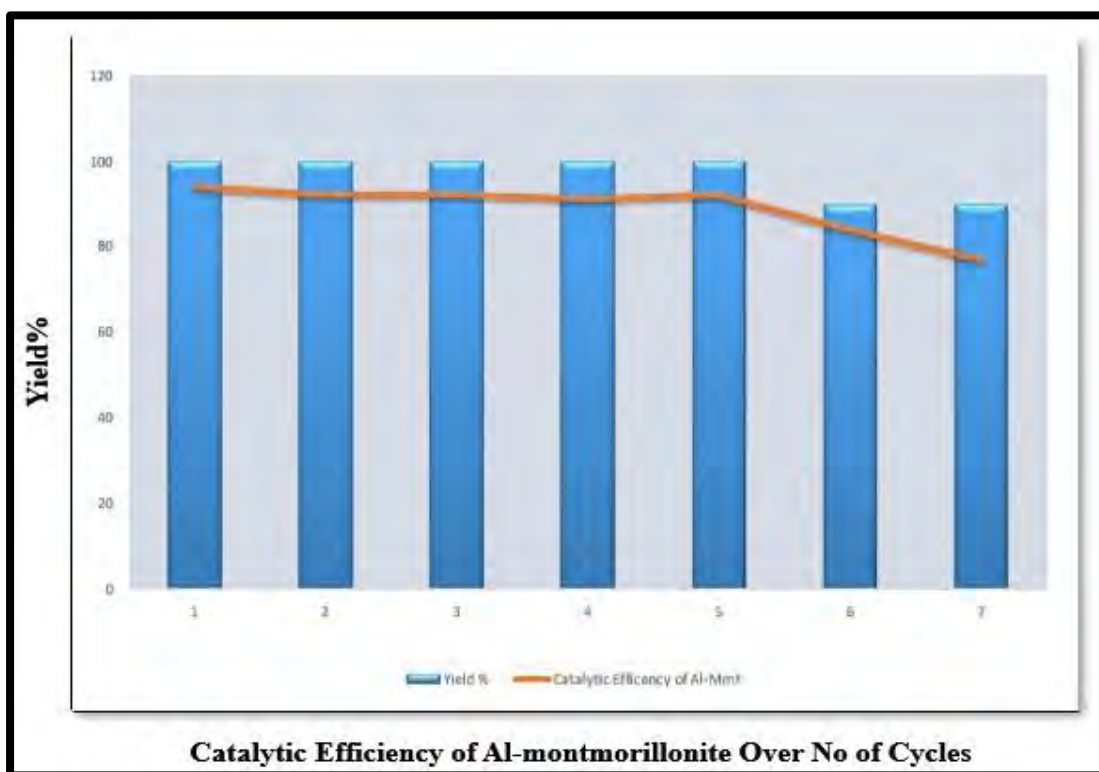


Figure 3.4.1.1: Reusability of Al-Mmt Catalyst in Transesterification Reaction (blue bars are representing biodiesel yield) in Seven Consecutive Experiments

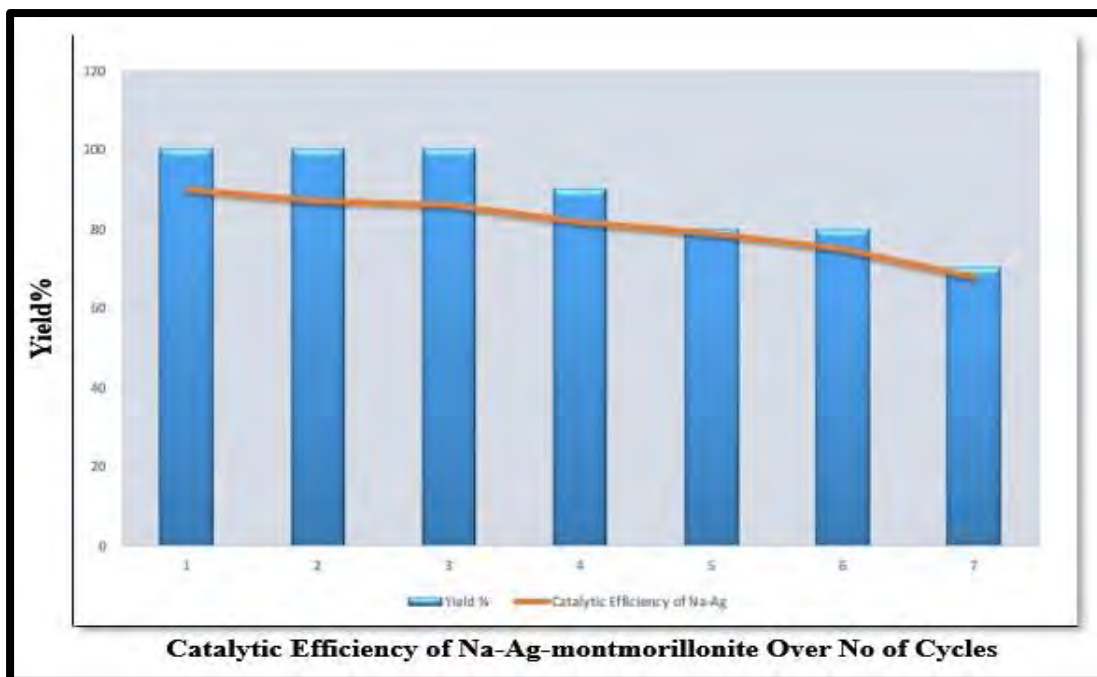


Figure 3.4.2.1: Reusability of Na-Ag-Mmt Catalyst in Transesterification Reaction (blue bars are representing biodiesel yield) in Seven Consecutive Experiments

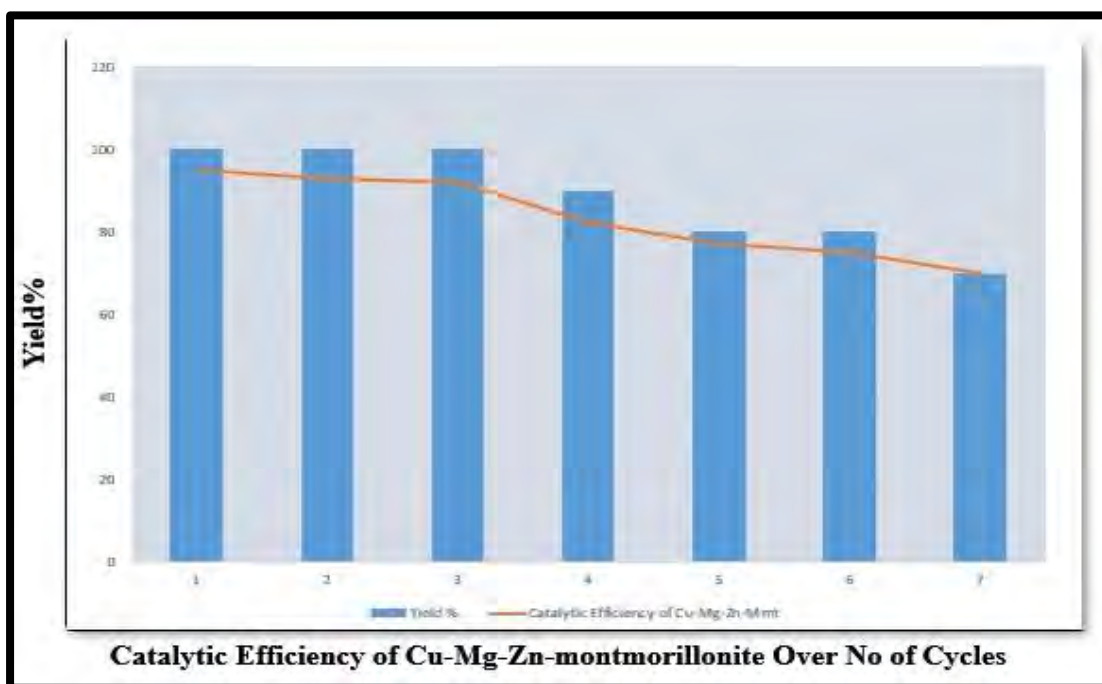


Figure 3.4.3.1: Reusability of Cu-Mg-Zn-Mmt Catalyst in Transesterification Reaction (blue bars are representing biodiesel yield) in Seven Consecutive Experiments

Table 3.4: Best Catalytic Yield against Selected FeedStocks

Plant	Mmt Catalyst	Yield %
<i>Brassica oleracea</i> L.	Al	91.40
<i>Carthamus oxycantha</i>	Cu-Mg-Zn	91.8
<i>Carthamus tinctorius</i>	Al	95
<i>Carthamus lanatus</i>	Cu-Mg-Zn	90
<i>Beaumontia grandiflora</i> Wall	Na-Ag	87
<i>Acacia concinna</i>	Na-Ag	90
<i>Sapindus trifoliatus</i>	Cu-Mg-Zn	95
<i>Sesamum indicum</i>	Cu-Mg-Zn	93
<i>Ricinus communis</i>	Cu-Mg-Zn	89
<i>Celastrus paniculatus</i>	Cu-Mg-Zn	92

4 Concluding Remarks and Recommendations

In this study, ten non-edible oil yielding seeds bearing plants are discussed with reference to their potential as a feed stock for the biodiesel industry. Scanning Electron Microscope was utilized for the micro morphological identification of the oil yielding seeds. A thorough discussion has been made to analyze their potential as a feed stock for biodiesel using different catalysts to cope with the energy demands of Pakistan Particularly and world in general. Among the ten discussed oil seeds bearing plants, three of them are novel to the field and explored for the very first time as a source for biodiesel, these include *Brassica oleracea* L, *Carthamus lanatus* and *Beaumontia grandiflora* Wall.

Information about the size variation and color was obtained via LM. Light microscopic studies revealed that size of the selected plants vary from 3mm to 112mm (length x width). And a great variation in color was observed from pitch black to greenish grey and various shades of brown to yellowish white. Seeds ultrastructure investigation through SEM shows great variations in shape, size, sculpturing and periclinal wall shape and arrangement. Seed shape varied from rounded, ellipsoidal, irregular, sub spherical, flatted, polygonal to reniform. The periclinal wall pattern show variation from flat to slightly concave-convex with straight, angular, undulate, or dentate seeds margin. Seeds wall structure display great verity from entire, angular, straight, irregular, polygonal, smooth, and elongated. Results of the current study would thus, propose that SEM could be used as a tool in refreshing the obscure micro morphological characters of various oil yielding seeds, helping researchers in their correct identification, exploration, authentication, and seeds classification in the future.

Physic-chemical properties of the extracted seeds oils were determined before their transesterification to the biodiesel. Free fatty acid analysis of the seeds oils was found to be less than 3 %, so only single step transesterification was performed for their conversion to the corresponding biodiesel. Inorganic clays such as Montmorillonite have been utilized for the synthesis of green based nano-catalysts. Such as Al-Mmt clat catalyst, Na-Ag-Mmt clay catalyst and Cu-Mg-Zn-Mmt clay catalyst. The synthesized catalysts were characterized using SEM, EDX, FT-IR and XRD. Table 4 shows the summary of comparative key findings using three catalysts on different seed oils.

The catalyst reusability study revealed that all the synthesized catalysts were active and proficiently used for maximum five-four times with no reduction in their catalytic power. On the contrary, a substantial fall in their catalysis was witnessed after fourth or third cycle of catalysis and might be linked to deactivation of catalyst's active site. Fuel properties of all the synthesized biodiesel from ten seed oils were determined and were well in line with international biodiesel standards. The use of renewable energy resources (biodiesel) to generate power is receiving attention around the world, and for Pakistan, it can address the current and upcoming energy stresses of the country. Pakistan is facing a severe economic crisis owed to an unceasingly rising gap between energy demand and energy supply. Thus, to conclude, the outcomes of the present project can be used at broad spectrum for mass production of biodiesel around the globe and especially in Pakistan. Findings of this study further suggest the utilization of Scanning Electron Microscopy as a tool to identify oil bearing seeds as a source of biodiesel to overcome the issue of inaccurate identification as well as adulteration of the feed stock. Three of the seeds oils utilized in this study i.e. *Brassica oleracea* L., *Carthamus lanatus* and *Beaumontia grandiflora* Wall are Novel feedstock for the biodiesel synthesis. All of these feedstocks need little or no care for cultivation and their seeds are available at cheap prices in the local market so, can be used at commercial level production of biodiesel as being both cost effective as well abundantly available. In this study clay based nano catalysts were used to assist the transesterification of the nonedible oils to the FAMES. And were found very effective as they gave the biodiesel yield of 95% (with Al-Mmt clay composite). The promising catalytic efficiency of the nano-sized clay hybrid composites further recommends their use in the transesterification as well other reaction. The study further indorses the bulk cultivation of such non-edible plants on waste, marginal and saline and waterlogged soil to improve the soil fertility usability a well. The study also proposes the emission analysis of produced biodiesel as well as synthesis of other green based catalysts i.e. nano-sized clay hybrid composites consuming low cost metals at commercial level to improve the quality and yield of biodiesel for industrial use globally.

Table 4: Comparative Key Findings of the Study

FEEDSTOCK	OIL PERCENTAGE	APPLIED CATALYSTS	OBTAINED BIODIESEL YIELD%	PROMINENT ESTER COMPOUND
<i>Brassica oleracea</i> L.	42.20%	Al-Mmt	91.40	Octadecanoic acid (C ₁₈ H ₃₄ O ₂)
		Na-Ag-Mmt	87	
		Cu-Mg-Zn-Mmt	91	
<i>Carthamus oxycantha</i>	29.20%	Al-Mmt	95	Ethyl 13-docosenoate (C ₂₄ H ₄₆ O ₂)
		Na-Ag-Mmt	91	
		Cu-Mg-Zn-Mmt	92	
<i>Carthamus tinctorius</i>	28.80%	Al-Mmt	87	9,12-Octadecadienoic acid (C ₁₈ H ₃₂ O ₂)
		Na-Ag-Mmt	89	
		Cu-Mg-Zn-Mmt	90	
<i>Carthamus lanatus</i>	22.40%	Al-Mmt	95	9-Octadecenoic acid (C ₁₇ H ₃₂ O ₂)
		Na-Ag-Mmt	100	
		Cu-Mg-Zn-Mmt	90	
<i>Beaumontia grandiflora</i> Wall	25.79%	Al-Mmt	95	9-Octadecadienoic acid (C ₁₈ H ₃₂ O ₂)
		Na-Ag-Mmt	100	
		Cu-Mg-Zn-Mmt	100	
<i>Acacia concinna</i>	22.00%	Al-Mmt	89	Octadecadienoic acid (C ₁₈ H ₃₂ O ₂)
		Na-Ag-Mmt	90	

		Cu-Mg-Zn-Mmt	87	
<i>Sapindus trifoliatus</i>	43%	Al-Mmt	90	Docosanoic acid (C ₂₃ H ₄₆ O ₂)
		Na-Ag-Mmt	93	
		Cu-Mg-Zn-Mmt	95	
<i>Sesamum indicum</i>	48%	Al-Mmt	91	Tetracosanoic acid (C ₂₅ H ₅₀ O ₂)
		Na-Ag-Mmt	90	
		Cu-Mg-Zn-Mmt	93	
<i>Ricinus communis</i>	54%	Al-Mmt	85.37	Erucic acid (C ₂₃ H ₄₄ O ₂)
		Na-Ag-Mmt	85	
		Cu-Mg-Zn-Mmt	89	
<i>Celastrus paniculatus</i>	55%	Al-Mmt	85	Methyl 9-octadecenoate (C ₁₉ H ₃₆ O ₂)
		Na-Ag-Mmt	87	
		Cu-Mg-Zn-Mmt	92	



REFERENCES

- Abdelshafeek, K. A., Abou-Setta, L. M., & Nazif, N. M. (2010). Study of some chemical constituents and antioxidant activity of *Beaumontia grandiflora* Wall. grown in Egypt. *Australian Journal of Basic and Applied Sciences*, 4(6), 10631069.
- Agarry, S. E., & Ogunleye, O. O. (2012). Box-Behnken design application to study enhanced bioremediation of soil artificially contaminated with spent engine oil using biostimulation strategy. *International Journal of Energy and Environmental Engineering*, 3(1), 31.
- Agarwal, H., Kumar, S. V., & Rajeshkumar, S. (2017). A review on green synthesis of zinc oxide nanoparticles—An eco-friendly approach. *Resource-Efficient Technologies*, 3(4), 406-413.
- Ajanovic, A. (2011). Biofuels versus food production: Does biofuels production increase food prices?. *Energy*, 36(4), 2070-2076.
- Akhtar, M. T., M. Ahmad, A. Shaheen, M. Zafar, R. Ullah, M. Asma, S. Sultana, M. Munir, N. Rashid, K. Malik, M. Saeed, & A. Waseem. (2019). Comparative study of liquid biodiesel from *sterculia foetida* (bottle tree) using CuO-CeO₂ and Fe₂O₃ nano catalysts. *Frontiers in Energy Research*, 7(4), 1-15.
- Akram, W., T. Saeed, A. Ahmad, N.A. Yasin, M. Akbar, W.U. Khan, S. Ahmed, J. Guo, W. Luo and T. Wu, 2019. Liquiritin elicitation can increase the content of medicinally important glucosinolates and phenolic compounds in Chinese kale plants. *Journal of the Science of Food and Agriculture*, 100(4), 1616-1624.
- Almadani, E. A., Harun, F. W., Radzi, S. M., & Muhamad, S. K. (2018). Cu²⁺ Montmorillonite K10 Clay Catalyst as a Green Catalyst for Production of Stearic Acid Methyl Ester: Optimization Using Response Surface Methodology (RSM). *Bulletin of Chemical Reaction Engineering & Catalysis*, 13(1), 187195.
- Alves, M. B., Medeiros, F., Sousa, M. H., Rubim, J. C., & Suarez, P. A. (2014). Cadmium and tin magnetic nanocatalysts useful for biodiesel production. *Journal of the Brazilian Chemical Society*, 25(12), 2304-2313.
- Alves, M. D. C., & Pozza, E. A. (2009). Scanning electron microscopy applied to seedborne fungi examination. *Microscopy Research and Technique*, 72(7), 482-488.

- Anisah, P. M., & Agustian, E. (2019). Effect of transesterification on the result of waste cooking oil conversion to biodiesel. In *Journal of Physics: Conference Series*, 1170(1), 012067. IOP Publishing.
- ANR, R., Saleh, A. A., Islam, M. S., Hamdan, S., & Maleque, M. A. (2016). Biodiesel production from crude *Jatropha* oil using a highly active heterogeneous nanocatalyst by optimizing transesterification reaction parameters. *Energy & Fuels*, 30(1), 334-343.
- Aranda, D. A., Santos, R. T., Tapanes, N. C., Ramos, A. L. D., & Antunes, O. A. C. (2008). Acid-catalyzed homogeneous esterification reaction for biodiesel production from palm fatty acids. *Catalysis letters*, 122(1-2), 20-25.
- Aransiola, E. F., Ojumu, T. V., Oyekola, O. O., Madzimbamuto, T. F., & IkhuOmogbe, D. I. O. (2014). A review of current technology for biodiesel production: State of the art. *Biomass and bioenergy*, 61, 276-297.
- Asif, S., Ahmad, M., Zafar, M., & Ali, N. (2017). Prospects and potential of fatty acid methyl esters of some non-edible seed oils for use as biodiesel in Pakistan. *Renewable and Sustainable Energy Reviews*, 74, 687-702.
- Atabani, A. E., Badruddin, I. A., Badarudin, A., Khayoon, M. S., & Triwahyono, S. (2014). Recent scenario and technologies to utilize non-edible oils for biodiesel production. *Renewable and Sustainable Energy Reviews*, 37, 840-851.
- Atabani, A. E., Silitonga, A. S., Badruddin, I. A., Mahlia, T. M. I., Masjuki, H. H., & Mekhilef, S. (2012). A comprehensive review on biodiesel as an alternative energy resource and its characteristics. *Renewable and Sustainable Energy Reviews*, 16(4), 2070-2093.
- Atabani, A. E., Silitonga, A. S., Ong, H. C., Mahlia, T. M. I., Masjuki, H. H., Badruddin, I. A., & Fayaz, H. (2013). Non-edible vegetable oils: a critical evaluation of oil extraction, fatty acid compositions, biodiesel production, characteristics, engine performance and emissions production. *Renewable and Sustainable Energy Reviews*, 18, 211-245.
- Atadashi, I. M., Aroua, M. K., Aziz, A. A., & Sulaiman, N. M. N. (2011). Refining technologies for the purification of crude biodiesel. *Applied energy*, 88(12), 4239-4251.
- Avramović, J. M., Veličković, A. V., Stamenković, O. S., Rajković, K. M., Milić, P. S., & Veljković, V. B. (2015). Optimization of sunflower oil ethanolysis

- catalyzed by calcium oxide: RSM versus ANN-GA. *Energy Conversion and Management*, 105, 1149-1156.
- Azam, M. M., Waris, A., & Nahar, N. M. (2005). Prospects and potential of fatty acid methyl esters of some non-traditional seed oils for use as biodiesel in India. *Biomass and bioenergy*, 29(4), 293-302.
- Balat, M. (2011). Potential alternatives to edible oils for biodiesel production—A review of current work. *Energy conversion and management*, 52(2), 1479-1492.
- Balat, M., & Balat, H. (2010). Progress in biodiesel processing. *Applied energy*, 87(6), 1815-1835.
- Bamgboye, A. I., & Hansen, A. C. (2008). Prediction of cetane number of biodiesel fuel from the fatty acid methyl ester (FAME) composition. *International Agrophysics*, 22(1), 21.
- Banik, S. K., Rouf, M. A., Rabeya, T., Khanam, M., Sajal, S. I., Sabur, S. B., & Islam, M. R. (2018). Production of biodiesel from neem seed oil. *Bangladesh Journal of Science and Industrial Research*, 53(3), 211-218.
- Baskar, G., & Soumiya, S. (2016). Production of biodiesel from castor oil using iron (II) doped zinc oxide nanocatalyst. *Renewable Energy*, 98, 101-107.
- Baskar, G., Gurugulladevi, A., Nishanthini, T., Aiswarya, R., & Tamilarasan, K. (2017). Optimization and kinetics of biodiesel production from Mahua oil using manganese doped zinc oxide nanocatalyst. *Renewable energy*, 103, 641-646.
- Baskar, G., Selvakumari, I. A. E., & Aiswarya, R. (2018). Biodiesel production from castor oil using heterogeneous Ni doped ZnO nanocatalyst. *Bioresource technology*, 250, 793-798.
- Betiku, E., & Adepoju, T. F. (2013). Methanolysis optimization of sesame (*Sesamum indicum*) oil to biodiesel and fuel quality characterization. *International Journal of Energy and Environmental Engineering*, 4(1), 9.
- Bhanumathy, M., Chandrasekar, S. B., Chandur, U., & Somasundaram, T. (2010). Phyto-pharmacology of *Celastrus paniculatus*: an Overview. *International Journal of Pharmaceutical Sciences and Drug Research*, 2(3), 176-181.
- Bhuiya, M. M. K., Rasul, M. G., Khan, M. M. K., Ashwath, N., & Azad, A. K. (2016). Prospects of 2nd generation biodiesel as a sustainable fuel—Part: 1 selection of feedstocks, oil extraction techniques and conversion technologies. *Renewable and Sustainable Energy Reviews*, 55, 1109-1128.

- Boatwright, J. S., Maurin, O., & van der Bank, M. (2015). Phylogenetic position of Madagascan species of *Acacia* s.l. and new combinations in Senegalia and *Vachellia* (Fabaceae, Mimosoideae, Acacieae). *Botanical Journal of the Linnean Society*, 179(2), 288-294.
- Borges, M. E., & Díaz, L. (2012). Recent developments on heterogeneous catalysts for biodiesel production by oil esterification and transesterification reactions: a review. *Renewable and Sustainable Energy Reviews*, 16(5), 2839-2849.
- Bu, Q., Lei, H., Wang, L., Wei, Y., Zhu, L., Zhang, X., Liu, Y., Yadavalli, G., & Tang, J. (2014). Bio-based phenols and fuel production from catalytic microwave pyrolysis of lignin by activated carbons. *Bioresource technology*, 162, 142-147.
- Candeia, R., Freitas, J., Souza, M., Conceição, M., Santos, I., Soledade, L., & Souza, A. (2007). Thermal and rheological behavior of diesel and methanol biodiesel blends. *Journal of thermal analysis and calorimetry*, 87(3), 653-656.
- Carapetian, J., & Zarei, G. (2005). Variation in Protein, oil and fatty acid contents in three wild species of safflower (*Carthamus*) from West Azerbaijan, Iran. *International Journal of Botany*, 1(2), 133-137.
- Carta, D., Corrias, A., Falqui, A., Brescia, R., Fantechi, E., Pineider, F., & Sangregorio, C. (2013). EDS, HRTEM/STEM, and X-ray absorption spectroscopy studies of co-substituted maghemite nanoparticles. *The Journal of Physical Chemistry C*, 117(18), 9496-9506.
- Chakraborty, R., & Sahu, H. (2014). Intensification of biodiesel production from waste goat tallow using infrared radiation: process evaluation through response surface methodology and artificial neural network. *Applied energy*, 114, 827-836.
- Chen, X., Du, W., & Liu, D. (2008). Response surface optimization of biocatalytic biodiesel production with acid oil. *Biochemical Engineering Journal*, 40(3), 423-429.
- Chhetri, A. B., Tango, M. S., Budge, S. M., Watts, K. C., & Islam, M. R. (2008). Nonedible plant oils as new sources for biodiesel production. *International Journal of Molecular Sciences*, 9(2), 169-180.
- Chisti, Y. (2007). Biodiesel from microalgae. *Biotechnology advances*, 25(3), 294-306.
- Choudhary, R., Sheoran, A., & Trivedi, S. (2012). A small kaolin beneficiation unit: state of art. *International Journal of Earth Sciences and Engineering*, 5(4), 775781.

- Chouhan, A. S., & Sarma, A. K. (2011). Modern heterogeneous catalysts for biodiesel production: A comprehensive review. *Renewable and Sustainable Energy Reviews*, 15(9), 4378-4399.
- Chuah, L. F., Yusup, S., Abd Aziz, A. R., Bokhari, A., Klemeš, J. J., & Abdullah, M. Z. (2015). Intensification of biodiesel synthesis from waste cooking oil (palm olein) in a hydrodynamic cavitation reactor: effect of operating parameters on methyl ester conversion. *Chemical Engineering and Processing: Process Intensification*, 95, 235-240.
- Clarke, L., Jiang, K., Akimoto, K., Babiker, M., Blanford, G., Fisher-Vanden, K., Hourcade J-C., Krey V & McCollum, D. (2014). Assessing transformation pathways. *Climate Change: Mitigation of Climate Change. IPCC Working Group III Contribution to AR5, Cambridge University Press.*
- Conti, J., Holtberg, P., Diefenderfer, J., LaRose, A., Turnure, J. T., & Westfall, L. (2016). International energy outlook 2016 with projections to 2040 (No. DOE/EIA-0484 (2016)). *USDOE Energy Information Administration (EIA), Washington, DC (United States). Office of Energy Analysis.*
- Dajue, L., & Mündel, H. H. (1996). Safflower, promoting the conservation and use of underutilized and neglected crops. 7. *Institute of Plant Genetics and Crop Plant Research, Gatersleben/International Plant Genetic Resources Institute, Rome, Italy*, 85.
- Daniyan, I. A., Bello, E. I., Ogedengbe, T. I., & Mogaji, P. B. (2019). Gas Chromatography and Fourier Transform Infrared Analysis of Biodiesel from Used and Unused Palm Olein Oil. In *International Journal of Engineering Research in Africa*, 42, 47-64. Trans Tech Publications.
- Dawood, S., Ahmad, M., Ullah, K., Zafar, M., & Khan, K. (2018). Synthesis and characterization of methyl esters from non-edible plant species yellow oleander oil, using magnesium oxide (MgO) nano-catalyst. *Materials Research Bulletin*, 101, 371-379.
- Demirbas, A. (2005). Biodiesel production from vegetable oils via catalytic and noncatalytic supercritical methanol transesterification methods. *Progress in energy and combustion science*, 31(5-6), 466-487.
- Demirbas, A. (2009). Potential resources of non-edible oils for biodiesel. *Energy Sources, Part B*, 4(3), 310-314.

- Demirbas, A. (2009). Progress and recent trends in biodiesel fuels. *Energy conversion and management*, 50(1), 14-34.
- Deng, Y., Hu, X., Cheng, L., Wang, H., Duan, L., & Qiu, R. (2018). Zirconocencatalysed biodiesel synthesis from vegetable oil with high free fatty acid contents. *Journal of Organometallic Chemistry*, 870, 116-120.
- Deodhar, K. A., & Shinde, N. W. (2015). *Celastrus paniculatus* Traditional uses and Ethnobotanical study. *Indian Journal of Advances in Plant Research*, 2(1), 18-21.
- Dharma, S., Masjuki, H., Ong, H. C., Sebayang, A., Silitonga, A., Kusumo, F., & Mahlia, T. (2016). Optimization of biodiesel production process for mixed *Jatropha curcas*–*Ceiba pentandra* biodiesel using response surface methodology. *Energy Conversion and Management*, 115, 178-190.
- Dhawale, V. P., Khobragade, V., & Kulkarni, S. D. (2018). Synthesis and Characterization of Aluminium Oxide (Al₂O₃) Nanoparticles and its Application in Azodye Decolourisation. *International Journal of Environmental Chemistry*, 2(1), 10-17.
- Dhingra, S., Dubey, K. K., & Bhushan, G. (2014). Enhancement in *Jatropha*-based biodiesel yield by process optimisation using design of experiment approach. *International Journal of Sustainable Energy*, 33(4), 842-853.
- Di Serio, M., Tesser, R., Pengmei, L., & Santacesaria, E. (2008). Heterogeneous catalysts for biodiesel production. *Energy & Fuels*, 22(1), 207-217.
- Dias, J. M., Alvim-Ferraz, M. C., Almeida, M. F., Díaz, J. D. M., Polo, M. S., & Utrilla, J. R. (2012). Selection of heterogeneous catalysts for biodiesel production from animal fat. *Fuel*, 94, 418-425.
- Du, W., Xu, Y., Liu, D., & Zeng, J. (2004). Comparative study on lipase-catalyzed transformation of soybean oil for biodiesel production with different acyl acceptors. *Journal of Molecular Catalysis B: Enzymatic*, 30(3-4), 125-129.
- Dwivedi, G., & Sharma, M. P. (2015). Application of Box–Behnken design in optimization of biodiesel yield from *Pongamia* oil and its stability analysis. *Fuel*, 145, 256-262.

- El Khier, M. K. S., Ishag, K. E. A., & Yagoub, A. A. (2008). Chemical composition and oil characteristics of sesame seed cultivars grown in Sudan. *Research Journal of Agriculture and Biological Sciences*, 4(6), 761-766.
- El-Taher, A. M., EL-Gendy, A. G., & Lila, M. I. (2019). Morphological and anatomical studies on some taxa of family Apocynaceae. *Al-Azhar Journal of Agricultural Research*, 44(1), 136-147.
- Enamala, M. K., Enamala, S., Chavali, M., Donepudi, J., Yadavalli, R., Kolapalli, B., Aradhyula, T. V., Velpuri, J., & Kuppam, C. (2018). Production of biofuels from microalgae-A review on cultivation, harvesting, lipid extraction, and numerous applications of microalgae. *Renewable and Sustainable Energy Reviews*, 94, 49-68.
- Endalew, A. K., Kiros, Y., & Zanzi, R. (2011). Heterogeneous catalysis for biodiesel production from *Jatropha curcas* oil (JCO). *Energy*, 36(5), 2693-2700.
- Endut, A., Abdullah, S. H. Y. S., Hanapi, N. H. M., Hamid, S. H. A., Lananan, F., Kamarudin, M. K. A., Umar, R., Juahir, H., & Khatoon, H. (2017). Optimization of biodiesel production by solid acid catalyst derived from coconut shell via response surface methodology. *International Biodeterioration & Biodegradation*, 124, 250-257.
- Etim, A. O., Betiku, E., Ajala, S. O., Olaniyi, P. J., & Ojumu, T. V. (2018). Potential of ripe plantain fruit peels as an ecofriendly catalyst for biodiesel synthesis: optimization by artificial neural network integrated with genetic algorithm. *Sustainability*, 10(3), 707-721.
- Ezebor, F., Khairuddean, M., Abdullah, A. Z., & Boey, P. L. (2014). Oil palm trunk and sugarcane bagasse derived heterogeneous acid catalysts for production of fatty acid methyl esters. *Energy*, 70, 493-503.
- Ezekannagha, C. B., Ude, C. N., & Onukwuli, O. D. (2017). Optimization of the methanolysis of lard oil in the production of biodiesel with response surface methodology. *Egyptian Journal of Petroleum*, 26(4), 1001-1011.
- Fan, X., Chen, F., & Wang, X. (2010). Ultrasound-assisted synthesis of biodiesel from crude cottonseed oil using response surface methodology. *Journal of oleo science*, 59(5), 235-241.
- Fan, X., Wang, X., & Chen, F. (2011). Biodiesel production from crude cottonseed oil: an optimization process using response surface methodology. *The Open Fuels & Energy Science Journal*, 4(1).

- Farahmandjou, M., & Golabiyan, N. (2015). New pore structure of nano-alumina (Al₂O₃) prepared by sol gel method. *Journal of Ceramic Processing Research*, 16(2), 1-4.
- Farooq, M., Ramli, A., Naeem, A., Mahmood, T., Ahmad, S., Humayun, M., & Islam, M. G. U. (2018). Biodiesel production from date seed oil (Phoenix dactylifera L.) via egg shell derived heterogeneous catalyst. *Chemical Engineering Research and Design*, 132, 644-651.
- Fatima, A., Zafar, M., Ahmad, M., Yaseen, G., Sultana, S., Gulfraz, M., & Khan, A. M. (2018). Scanning electron microscopy as a tool for authentication of oil yielding seed. *Microscopy Research and Technique*, 81(6), 624-629.
- Fauzi, A. H. M., & Amin, N. A. S. (2013). Optimization of oleic acid esterification catalyzed by ionic liquid for green biodiesel synthesis. *Energy Conversion and Management*, 76, 818-827.
- Ferella, F., Di Celso, G. M., De Michelis, I., Stanisci, V., & Vegliò, F. (2010). Optimization of the transesterification reaction in biodiesel production. *Fuel*, 89(1), 36-42.
- Feyzi, M., & Norouzi, L. (2016). Preparation and kinetic study of magnetic Ca/Fe₃O₄@ SiO₂ nanocatalysts for biodiesel production. *Renewable Energy*, 94, 579-586.
- Furat, S., & Uzun, B. (2010). The use of agro-morphological characters for the assessment of genetic diversity in sesame (Sesamum indicum L.). *Plant Omics*, 3(3), 85-91.
- Furuta, S., Matsushashi, H., & Arata, K. (2004). Biodiesel fuel production with solid superacid catalysis in fixed bed reactor under atmospheric pressure. *Catalysis communications*, 5(12), 721-723.
- Gama, P. E., Gil, R. A. D. S. S., & Lachter, E. R. (2010). Biodiesel production by in situ transesterification of sunflower seeds by homogeneous and heterogeneous catalysis. *Química Nova*, 33(9), 1859-1862.
- Gama, P. E., Lachter, E. R., San Gil, R. A., Coelho, A. V., Sidi, I. A., Poubel, R. L., Faro, A. C., & de Souza, A. L. (2015). Characterization and catalytic activity of K₂CO₃/Al₂O₃ in the transesterification of sunflower oil in conventional and microwave heating. *Química Nova*, 38(2), 185-190.
- García-Moreno, P. J., Khanum, M., Guadix, A., & Guadix, E. M. (2014). Optimization of biodiesel production from waste fish oil. *Renewable Energy*, 68, 618-624.

- Gecgel, U., Demirci, M., Esendal, E., & Tasan, M. (2007). Fatty acid composition of the oil from developing seeds of different varieties of safflower (*Carthamus tinctorius* L.). *Journal of the American Oil Chemists' Society*, 84(1), 47-54.
- Ghoreishi, S. M., & Moein, P. (2013). Biodiesel synthesis from waste vegetable oil via transesterification reaction in supercritical methanol. *The Journal of Supercritical Fluids*, 76, 24-31.
- Giera, M., Lingeman, H., & Niessen, W. M. (2012). Recent advancements in the LC- and GC-based analysis of malondialdehyde (MDA): a brief overview. *Chromatographia*, 75(9-10), 433-440.
- Gladis, T., & Hammer, K. (1990). The Gaterslebener Brassica collection — an introduction. *The crop*, 38 (3), 121-156.
- Gohain, M., Devi, A., & Deka, D. (2017). Musa balbisiana Colla peel as highly effective renewable heterogeneous base catalyst for biodiesel production. *Industrial Crops and Products*, 109, 8-18.
- G. mez-Bombarelli, R., Calle, E., & Casado, J. (2013). Mechanisms of lactone hydrolysis in acidic conditions. *The Journal of Organic Chemistry*, 78(14), 6880-6889.
- Gu, L., Huang, W., Tang, S., Tian, S., & Zhang, X. (2015). A novel deep eutectic solvent for biodiesel preparation using a homogeneous base catalyst. *Chemical Engineering Journal*, 259, 647-652.
- Gui, M. M., Lee, K. T., & Bhatia, S. (2008). Feasibility of edible oil vs. non-edible oil vs. waste edible oil as biodiesel feedstock. *Energy*, 33(11), 1646-1653.
- Gunstone, F. D., and Hamilton, R. J. (2001). *Oleochemical Manufacture and Applications* (4). Sheffield, UK: CRC Press.
- Gurunathan, B., & Ravi, A. (2015). Biodiesel production from waste cooking oil using copper doped zinc oxide nanocomposite as heterogeneous catalyst. *Bioresource technology*, 188, 124-127.
- Hameed, B. H., Lai, L. F., & Chin, L. H. (2009). Production of biodiesel from palm oil (*Elaeis guineensis*) using heterogeneous catalyst: an optimized process. *Fuel Processing Technology*, 90(4), 606-610.
- Hamze, H., Akia, M., & Yazdani, F. (2015). Optimization of biodiesel production from the waste cooking oil using response surface methodology. *Process Safety and Environmental Protection*, 94, 1-10.

- Han, H., & Guan, Y. (2009). Synthesis of biodiesel from rapeseed oil using K₂O/γ-Al₂O₃ as nano-solid-base catalyst. *Wuhan University Journal of Natural Sciences*, 14(1), 75-79.
- Harborne, J. B. (1977). Flavonoids and the evolution of the angiosperms. *Biochemical Systematics and Ecology*, 5(1), 7-22.
- Hasni, K., Ilham, Z., Dharma, S., & Varman, M. (2017). Optimization of biodiesel production from Brucea javanica seeds oil as novel non-edible feedstock using response surface methodology. *Energy Conversion and Management*, 149, 392-400.
- Hebbar, H. H., Math, M. C., & Yatish, K. V. (2018). Optimization and kinetic study of CaO nano-particles catalyzed biodiesel production from Bombax ceiba oil. *Energy*, 143, 25-34.
- Helwani, Z., Othman, M. R., Aziz, N., Fernando, W. J. N., & Kim, J. (2009). Technologies for production of biodiesel focusing on green catalytic techniques: a review. *Fuel Processing Technology*, 90(12), 1502-1514.
- Huaping, Z. H. U., Zongbin, W. U., Yuanxiong, C., Zhang, P., Shijie, D. U. A. N., Xiaohua, L. I. U., & Zongqiang, M. A. O. (2006). Preparation of biodiesel catalyzed by solid super base of calcium oxide and its refining process. *Chinese Journal of Catalysis*, 27(5), 391-396.
- Hulkoti, N. I., & Taranath, T. C. (2014). Biosynthesis of nanoparticles using microbes—a review. *Colloids and Surfaces B: Biointerfaces*, 121, 474-483.
- Issarakraisila, M., Ma, Q., & Turner, D. W. (2007). Photosynthetic and growth responses of juvenile Chinese kale (*Brassica oleracea* var. *alboglabra*) and Caisin (*Brassica rapa* subsp. *parachinensis*) to waterlogging and water deficit. *Scientia horticulturae*, 111(2), 107-113.
- Jahirul, M. I., Koh, W., Brown, R. J., Senadeera, W., O'Hara, I., & Moghaddam, L. (2014). Biodiesel production from non-edible beauty leaf (*Calophyllum inophyllum*) oil: Process optimization using response surface methodology (RSM). *Energies*, 7(8), 5317-5331.
- Jain, S., & Sharma, M. P. (2010). Prospects of biodiesel from Jatropha in India: a review. *Renewable and Sustainable Energy Reviews*, 14(2), 763-771.
- Janaun, J., & Ellis, N. (2010). Perspectives on biodiesel as a sustainable fuel. *Renewable and Sustainable Energy Reviews*, 14(4), 1312-1320.

- Jayed, M. H., Masjuki, H. H., Saidur, R., Kalam, M. A., & Jahirul, M. I. (2009). Environmental aspects and challenges of oilseed produced biodiesel in Southeast Asia. *Renewable and Sustainable Energy Reviews*, 13(9), 2452-2462.
- Jeong, G. T., & Park, D. H. (2009). Optimization of biodiesel production from castor oil using response surface methodology. *Applied biochemistry and biotechnology*, 156(1-3), 1-11.
- Kansedo, J., Lee, K. T., & Bhatia, S. (2009). Biodiesel production from palm oil via heterogeneous transesterification. *Biomass and bioenergy*, 33(2), 271-276.
- Karaj, S., & Müller, J. (2011). Optimizing mechanical oil extraction of *Jatropha curcas* L. seeds with respect to press capacity, oil recovery and energy efficiency. *Industrial Crops and Products*, 34(1), 1010-1016.
- Karmakar, A., Karmakar, S., & Mukherjee, S. (2010). Properties of various plants and animals feedstocks for biodiesel production. *Bioresource technology*, 101(19), 7201-7210.
- Kaur, M., & Ali, A. (2011). Lithium ion impregnated calcium oxide as nano catalyst for the biodiesel production from karanja and jatropha oils. *Renewable Energy*, 36(11), 2866-2871.
- Khan, H. A., & Pervaiz, S. (2013). Technological review on solar PV in Pakistan: Scope, practices and recommendations for optimized system design. *Renewable and Sustainable Energy Reviews*, 23, 147-154.
- Kim, H. J., Kang, B. S., Kim, M. J., Park, Y. M., Kim, D. K., Lee, J. S., & Lee, K. Y. (2004). Transesterification of vegetable oil to biodiesel using heterogeneous base catalyst. *Catalysis today*, 93-95, 315-320.
- Kim, K. S., Park, J. O., & Nam, S. C. (2013). Synthesis of iron-loaded zeolites for removal of ammonium and phosphate from aqueous solutions. *Environmental Engineering Research*, 18(4), 267-276.
- Knothe, G. (2005). Dependence of biodiesel fuel properties on the structure of fatty acid alkyl esters. *Fuel processing technology*, 86(10), 1059-1070.
- Kongjao, S., Damronglerd, S., & Hunsom, M. (2010). Purification of crude glycerol derived from waste used-oil methyl ester plant. *Korean Journal of Chemical Engineering*, 27(3), 944-949.
- Kouzu, M., Yamanaka, S. Y., Hidaka, J. S., & Tsunomori, M. (2009). Heterogeneous catalysis of calcium oxide used for transesterification of soybean oil with refluxing methanol. *Applied Catalysis A: General*, 355(1-2), 94-99.

- Kumar, D., Singh, B., Banerjee, A., & Chatterjee, S. (2018). Cement wastes as transesterification catalysts for the production of biodiesel from Karanja oil. *Journal of Cleaner Production*, 183, 26-34.
- Labhane, P. K., Huse, V. R., Patle, L. B., Chaudhari, A. L., & Sonawane, G. H. (2015). Synthesis of Cu doped ZnO nanoparticles: crystallographic, optical, FTIR, morphological and photocatalytic study. *Journal of Materials Science and Chemical Engineering*, 3(07), 39-50.
- Lakshmana Naik, R., Radhika, N., Sravani, K., Hareesha, A., Mohanakumari, B., & Bhavanasindhu, K. (2015). Optimized parameters for production of biodiesel from fried oil. *International Advanced Research Journal in Science, Engineering and Technology*, 2(6), 23.
- Lam, H. S., & Proctor, A. (2001). Rapid methods for milled rice surface total lipid and free fatty acid determination. *Cereal Chemistry*, 78(4), 498-499.
- Leamsamrong, K., W. Tongjaroenbuangam, S. Maneetong, A. Chantiratikul, O. Chinrasri., & P. Chantiratikul, 2019. Physicochemical contents, antioxidant activities, and acute toxicity assessment of selenium-enriched Chinese kale (*brassica oleracea* var. *Alboglabra* L.) seedlings. *Journal of Chemistry*, 2019. 112, doi.org/10.1155/2019/7983038.
- Lee, H. V., Yunus, R., Juan, J. C., & Taufiq-Yap, Y. H. (2011). Process optimization design for jatropha-based biodiesel production using response surface methodology. *Fuel Processing Technology*, 92(12), 2420-2428.
- Lee, J. S., & Saka, S. (2010). Biodiesel production by heterogeneous catalysts and supercritical technologies. *Bioresource technology*, 101(19), 7191-7200.
- Li, J., Wang, X., Zhu, W., & Cao, F. (2009). ZnO nanotubes with double acid sites as heterogeneous catalysts for the production of biodiesel from waste cooking oil. *ChemSusChem*, 2(2), 177-183.
- Li, W., Jiang, Z., Ma, F., Su, F., Chen, L., Zhang, S., & Guo, Y. (2010). Design of mesoporous $\text{SO}_4^{2-}/\text{ZrO}_2\text{-SiO}_2$ (Et) hybrid material as an efficient and reusable heterogeneous acid catalyst for biodiesel production. *Green Chemistry*, 12(12), 2135-2138.
- Li, Y., Ye, B., Shen, J., Tian, Z., Wang, L., Zhu, L., Ma, T., Yang, D., & Qiu, F. (2013). Optimization of biodiesel production process from soybean oil using the sodium

- potassium tartrate doped zirconia catalyst under Microwave Chemical Reactor. *Bioresource technology*, 137, 220-225.
- Lin, L., Cunshan, Z., Vittayapadung, S., Xiangqian, S., & Mingdong, D. (2011). Opportunities and challenges for biodiesel fuel. *Applied energy*, 88(4), 10201031.
- Liu, Y., Liu, S., He, D., Li, N., Ji, Y., Zheng, Z., Luo, F., Liu, S., Shi, Z., & Hu, C. (2015). Crystal facets make a profound difference in polyoxometalate-containing metal–organic frameworks as catalysts for biodiesel production. *Journal of the American Chemical Society*, 137(39), 12697-12703.
- Lovato, L., Pelegrini, B. L., Rodrigues, J., de Oliveira, A. J. B., & Ferreira, I. C. P. (2014). Seed oil of *Sapindus saponaria* L.(Sapindaceae) as potential C16 to C22 fatty acids resource. *Biomass and Bioenergy*, 60, 247-251.
- Luqman, M., Zafar, M., Ahmad, M., Ozturk, M., Sultana, S., Alam, F., & Ullah, F. (2019). Micromorphological observation of seed coat of *Eucalyptus* species (Myrtaceae) using scanning electron microscopy technique. *Microscopy Research and Technique*, 82(2), 75-84.
- Maciejewska-Rutkowska, I., & Bednorz, L. (2004). SEM and stereoscope microscope observations on the seeds of the Polish species of the genus *Sorbus* L.[Rosaceae]. *Acta societatis botanicorum poloniae*, 73(4), 293-300,
- Mageshwari, K., Mali, S. S., Sathyamoorthy, R., & Patil, P. S. (2013). Template-free synthesis of MgO nanoparticles for effective photocatalytic applications. *Powder technology*, 249, 456-462.
- Mahamuni, N. N., & Adewuyi, Y. G. (2009). Fourier transform infrared spectroscopy (FTIR) method to monitor soy biodiesel and soybean oil in transesterification reactions, petrodiesel– biodiesel blends, and blend adulteration with soy oil. *Energy & Fuels*, 23(7), 3773-3782.
- Mahesh, S. E., Ramanathan, A., Begum, K. M. S., & Narayanan, A. (2015). Biodiesel production from waste cooking oil using KBr impregnated CaO as catalyst. *Energy conversion and management*, 91, 442-450.
- Mahmudul, H. M., Hagos, F. Y., Mamat, R., Adam, A. A., Ishak, W. F. W., & Alenezi, R. (2017). Production, characterization and performance of biodiesel as an

- alternative fuel in diesel engines—A review. *Renewable and Sustainable Energy Reviews*, 72, 497-509.
- Manikandan, D., Mangalaraja, R. V., Ananthakumar, S., & Sivakumar, T. (2012). Synthesis of metal intercalated clay catalysts for selective hydrogenation reactions. *Catalysis in Industry*, 4(4), 215-230.
- Manyasree, D., Kiranmayi, P., & Kumar, R. (2018). Synthesis, characterization and antibacterial activity of aluminium oxide nanoparticles. *International Journal of Pharmacy and Pharmaceutical Sciences*, 10(1), 32-35.
- Maran, J. P., & Priya, B. (2015a). Comparison of response surface methodology and artificial neural network approach towards efficient ultrasound-assisted biodiesel production from muskmelon oil. *Ultrasonics Sonochemistry*, 23, 192-200.
- Maran, J. P., & Priya, B. (2015b). Modeling of ultrasound assisted intensification of biodiesel production from neem (*Azadirachta indica*) oil using response surface methodology and artificial neural network. *Fuel*, 143, 262-267.
- Mardhiah, H. H., Ong, H. C., Masjuki, H. H., Lim, S., & Lee, H. V. (2017). A review on latest developments and future prospects of heterogeneous catalyst in biodiesel production from non-edible oils. *Renewable and sustainable energy reviews*, 67, 1225-1236.
- McGlade, C., & Ekins, P. (2015). The geographical distribution of fossil fuels unused when limiting global warming to 2 C. *Nature*, 517(7533), 187-190.
- McKelvey, V. E. (1972). Mineral Resource Estimates and Public Policy: Better methods for estimating the magnitude of potential mineral resources are needed to provide the knowledge that should guide the design of many key public policies. *American Scientist*, 60(1), 32-40.
- Meher, L. C., Sagar, D. V., & Naik, S. N. (2006). Technical aspects of biodiesel production by transesterification—a review. *Renewable and sustainable energy reviews*, 10(3), 248-268.
- Mehta, B. K., Chhajlani, M., & Shrivastava, B. D. (2017, May). Green synthesis of silver nanoparticles and their characterization by XRD. In *Journal of physics: conference series*, 836 (1), 012050. Bristol, UK: IOP Publishing.
- Meinshausen, M., Meinshausen, N., Hare, W., Raper, S. C., Frieler, K., Knutti, R., Frame, D. J & Allen, M. R. (2009). Greenhouse-gas emission targets for limiting global warming to 2 C. *Nature*, 458(7242), 1158-1162.

- Mubarak, M., Shaija, A., & Suchithra, T. V. (2016). Optimization of lipid extraction from *Salvinia molesta* for biodiesel production using RSM and its FAME analysis. *Environmental Science and Pollution Research*, 23(14), 14047-14055.
- Mumtaz, M. W., Mukhtar, H., Anwar, F., & Saari, N. (2014). RSM based optimization of chemical and enzymatic transesterification of palm oil: biodiesel production and assessment of exhaust emission levels. *The Scientific World Journal*, 2014.
- Muppaneni, T., Reddy, H. K., Patil, P. D., Dailey, P., Aday, C., & Deng, S. (2012). Ethanolysis of camelina oil under supercritical condition with hexane as a co-solvent. *Applied Energy*, 94, 84-88.
- Muppaneni, T., Reddy, H. K., Ponnusamy, S., Patil, P. D., Sun, Y., Dailey, P., & Deng, S. (2013). Optimization of biodiesel production from palm oil under supercritical ethanol conditions using hexane as co-solvent: A response surface methodology approach. *Fuel*, 107, 633-640.
- Nafees, M., & Waseem, A. (2014). Organoclays as sorbent material for phenolic compounds: a review. *CLEAN–Soil, Air, Water*, 42(11), 1500-1508.
- Nafees, M., Waseem, A., & Khan, A. R. (2013). Comparative study of laterite and bentonite based organoclays: implications of hydrophobic compounds remediation from aqueous solutions. *Scientific World Journal*, 2013, 681769681774. doi: 10.1155/2013/681769.
- Nahar, K. (2013). Castor bean (*Ricinus communis* L.)-a biofuel plant: morphological and physiological parameters propagated from seeds in Bangladesh. *Asian Business Review*, 2(2), 122-124.
- Naidu, C. V., Rajendrudu, G., & Swamy, P. M. (2000). Effect of plant growth regulators on seed germination of *Sapindus trifoliatus* Vahl. *Seed Science and Technology* (Switzerland), 28(2), 249-252.
- Najafi, B., Faizollahzadeh Ardabili, S., Shamshirband, S., Chau, K. W., & Rabczuk, T. (2018). Application of ANNs, ANFIS and RSM to estimating and optimizing the parameters that affect the yield and cost of biodiesel production. *Engineering Applications of Computational Fluid Mechanics*, 12(1), 611-624.

- Narasimharao, K., Brown, D. R., Lee, A. F., Newman, A. D., Siril, P. F., Tavener, S. J., & Wilson, K. (2007). Structure–activity relations in Cs-doped heteropolyacid catalysts for biodiesel production. *Journal of catalysis*, 248(2), 226-234.
- Navajas, A., Campo, I., Moral, A., Echave, J., Sanz, O., Montes, M., Odriozola, J. A., Arzamendi, G., & Gandía, L. M. (2018). Outstanding performance of rehydrated Mg-Al hydrotalcites as heterogeneous methanolysis catalysts for the synthesis of biodiesel. *Fuel*, 211, 173-181.
- Nawaz, H., Shad, M. A., & Muzaffar, S. (2018). Phytochemical Composition and Antioxidant Potential of Brassica. Brassica Germplasm: Characterization, Breeding and Utilization, 7. doi: 10.5772/2018/76120.
- Nayebzadeh, H., Saghatoleslami, N., & Tabasizadeh, M. (2016). Optimization of the activity of KOH/calcium aluminate nanocatalyst for biodiesel production using response surface methodology. *Journal of the Taiwan Institute of Chemical Engineers*, 68, 379-386.
- Nematollahi, O., Hoghooghi, H., Rasti, M., & Sedaghat, A. (2016). Energy demands and renewable energy resources in the Middle East. *Renewable and Sustainable Energy Reviews*, 54, 1172-1181.
- Ngamcharussrivichai, C., Wiwatnimit, W., & Wangnoi, S. (2007). Modified dolomites as catalysts for palm kernel oil transesterification. *Journal of Molecular Catalysis A: Chemical*, 276(1-2), 24-33.
- Noichinda, S., Bodhipadma, K., Mahamontri, C., Narongruk, T., & Ketsa, S. (2007). Light during storage prevents loss of ascorbic acid, and increases glucose and fructose levels in Chinese kale (*Brassica oleracea* var. *alboglabra*). *Postharvest biology and technology*, 44(3), 312-315.
- Noor, M. Z. M., Sollahunddin, N. A., & Irawan, S. (2018). Surface Modification of Aluminium Oxide (Al₂O₃) Nanoparticles (NPs) on Detection of Crude Oil Production. *Multidisciplinary Digital Publishing Institute Proceedings*, 2(20), 1273-1278.
- Noshadi, I., Amin, N. A. S., & Parnas, R. S. (2012). Continuous production of biodiesel from waste cooking oil in a reactive distillation column catalyzed by solid heteropolyacid: optimization using response surface methodology (RSM). *Fuel*, 94, 156-164.

- Nuridin, M., Fatma, F., Natsir, M., & Wibowo, D. (2017). Characterization of methyl ester compound of biodiesel from industrial liquid waste of crude palm oil processing. *Analytical chemistry research*, 12, 1-9.
- Obadiah, A., Kannan, R., Ramasubbu, A., & Kumar, S. V. (2012). Studies on the effect of antioxidants on the long-term storage and oxidation stability of *Pongamia pinnata* (L.) Pierre biodiesel. *Fuel processing technology*, 99, 56-63.
- Ogunniyi, D. S. (2006). Castor oil: a vital industrial raw material. *Bioresource technology*, 97(9), 1086-1091.
- Okuda, N., & Fujime, Y. (1994, November). Plant growth characters of Chinese kale (*Brassica oleracea* L. var. *alboglabra*). In *ISHS Brassica Symposium-IX Crucifer Genetics Workshop* 407, 55-60. doi: 10.17660/ActaHortic.1996.407.4
- Olutoye, M. A., Lee, S. C., & Hameed, B. H. (2011). Synthesis of fatty acid methyl ester from palm oil (*Elaeis guineensis*) with $Ky (MgCa) 2xO_3$ as heterogeneous catalyst. *Bioresource technology*, 102(23), 10777-10783.
- Olutoye, M. A., Wong, S. W., Chin, L. H., Amani, H., Asif, M., & Hameed, B. H. (2016). Synthesis of fatty acid methyl esters via the transesterification of waste cooking oil by methanol with a barium-modified montmorillonite K10 catalyst. *Renewable Energy*, 86, 392-398.
- Omar, W. N. N. W., & Amin, N. A. S. (2011). Optimization of heterogeneous biodiesel production from waste cooking palm oil via response surface methodology. *Biomass and bioenergy*, 35(3), 1329-1338.
- Omer, A. M. (2008). Energy, environment and sustainable development. *Renewable and sustainable energy reviews*, 12(9), 2265-2300.
- Onukwuli, D. O., Emembolu, L. N., Ude, C. N., Aliozo, S. O., & Menkiti, M. C. (2017). Optimization of biodiesel production from refined cotton seed oil and its characterization. *Egyptian Journal of Petroleum*, 26(1), 103-110.
- Parawira, W. (2010). Biodiesel production from *Jatropha curcas*: A review. *Scientific Research and Essays*, 5(14), 1796-1808.
- Park, Y. M., Lee, D. W., Kim, D. K., Lee, J. S., & Lee, K. Y. (2008). The heterogeneous catalyst system for the continuous conversion of free fatty acids in used vegetable oils for the production of biodiesel. *Catalysis Today*, 131(1-4), 238243.
- Patil, P. D., Gude, V. G., Mannarswamy, A., Deng, S., Cooke, P., Munson-McGee, S., Rhodes, I., Lammers, p., & Nirmalakhandan, N. (2011). Optimization of direct

- conversion of wet algae to biodiesel under supercritical methanol conditions. *Bioresource technology*, 102(1), 118-122.
- Peng, X., Pan, Q., & Rempel, G. L. (2008). Bimetallic dendrimer-encapsulated nanoparticles as catalysts: a review of the research advances. *Chemical Society Reviews*, 37(8), 1619-1628.
- Phelan, J.R. and J. Vaughan, 1976. A chemotaxonomic study of brassica oleracea with particular reference to its relationship to brassica alboglabra. *Biochemical Systematics and Ecology*, 4(3): 173-178.
- Pinto, A. C., Guarieiro, L. L., Rezende, M. J., Ribeiro, N. M., Torres, E. A., Lopes, W. A., Pereira, P. A. D., & Andrade, J. B. D. (2005). Biodiesel: an overview. *Journal of the Brazilian Chemical Society*, 16(6B), 1313-1330.
- Pradhan, S., Madankar, C. S., Mohanty, P., & Naik, S. N. (2012). Optimization of reactive extraction of castor seed to produce biodiesel using response surface methodology. *Fuel*, 97, 848-855.
- Priscilla, S. J., Daniel, R., Gayathri, S., Rodney, J. D., Thomas, M., Ponraj, C., & Sivaji, K. (2017). Structural and Morphological properties of Lithium Doped Copper Oxide Nanoparticles. *International Journal of Materials Science*, 12(2), 345349.
- Qin, S., Sun, Y., Meng, X., & Zhang, S. (2010). Production and analysis of biodiesel from non-edible seed oil of Pistacia Chinensis. *Energy Exploration & Exploitation*, 28(1), 37-46.
- Rabelo, S. N., Ferraz, V. P., Oliveira, L. S., & Franca, A. S. (2015). FTIR analysis for quantification of fatty acid methyl esters in biodiesel produced by microwaveassisted transesterification. *International Journal of Environmental Science and Development*, 6(12), 964-969.
- Raheem, A., Prinsen, P., Vuppaladiyam, A. K., Zhao, M., & Luque, R. (2018). A review on sustainable microalgae based biofuel and bioenergy production: Recent developments. *Journal of cleaner production*, 181, 42-59.
- Rajan, R. N., Rajesh, R., & Elayidom, M. R. (2016, April). Optimization of production of transesterified Jatropha curcas oil using Response Surface Methodology. In 2016 *International Conference on Energy Efficient Technologies for Sustainability (ICEETS)*, 187-193. IEEE.

- Ramadan, M. F., Kinni, S. G., Rajanna, L. N., Seetharam, Y. N., Seshagiri, M., & Mörsel, J. T. (2009). Fatty acids, bioactive lipids and radical scavenging activity of *Celastrus paniculatus* Willd. seed oil. *Scientia Horticulturae*, 123(1), 104-109.
- Ramadhas, A. S., Jayaraj, S., & Muraleedharan, C. (2005). Biodiesel production from high FFA rubber seed oil. *Fuel*, 84(4), 335-340.
- Rashid, U., Anwar, F., Ashraf, M., Saleem, M., & Yusup, S. (2011). Application of response surface methodology for optimizing transesterification of *Moringa oleifera* oil: Biodiesel production. *Energy conversion and Management*, 52(8-9), 3034-3042.
- Rashtizadeh, E., Farzaneh, F., & Talebpour, Z. (2014). Synthesis and characterization of Sr₃Al₂O₆ nanocomposite as catalyst for biodiesel production. *Bioresource technology*, 154, 32-37.
- Sabzalian, M. R., Saeidi, G., & Mirlohi, A. (2008). Oil content and fatty acid composition in seeds of three safflower species. *Journal of the American Oil Chemists' Society*, 85(8), 717-721.
- Salaheldeen, M., M. K. Aroua, A. A. Mariod, S. F. Cheng, M. A. Abdelrahman, and A. E. Atabani. (2015). Physicochemical characterization and thermal behavior of biodiesel and biodiesel–Diesel blends derived from crude *Moringa peregrina* seed oil. *Energy Conversion and Management*, 92, 535–42.
- Santos, E. C., dos Santos, T. C., Guimarães, R. B., Ishida, L., Freitas, R. S., & Ronconi, C. M. (2015). Guanidine-functionalized Fe₃O₄ magnetic nanoparticles as basic recyclable catalysts for biodiesel production. *RSC Advances*, 5(59), 48031-48038.
- Saqib, M., Mumtaz, M. W., Mahmood, A., & Abdullah, M. I. (2012). Optimized biodiesel production and environmental assessment of produced biodiesel. *Biotechnology and Bioprocess Engineering*, 17(3), 617-623.
- Sarve, A., Sonawane, S. S., & Varma, M. N. (2015). Ultrasound assisted biodiesel production from sesame (*Sesamum indicum* L.) oil using barium hydroxide as a heterogeneous catalyst: comparative assessment of prediction abilities between response surface methodology (RSM) and artificial neural network (ANN). *Ultrasonics sonochemistry*, 26, 218-228.

- Saxena, V., Kumar, N., & Saxena, V. K. (2019). Multi-objective Process Optimization of Biodiesel Synthesis from Acacia concinna Seed Oil Using TOPSIS and GRA Approach. In *Advances in Interdisciplinary Engineering*, 353-361. *Springer, Singapore*. doi: 10.1007/978-981-13-6577-5_33.
- Schoonheydt, R. A., Johnston, C. T., Brigatti, M., & Mottana, A. (2011). The surface properties of clay minerals. *Layered Structures and their Application in Advanced Technologies*, 11, 337-373.
- Schuchardt, U., Sercheli, R., & Vargas, R. M. (1998). Transesterification of vegetable oils: a review. *Journal of the Brazilian Chemical Society*, 9(3), 199-210.
- Sekhar, M. C., Mamilla, V. R., Mallikarjun, M. V., & Reddy, K. V. K. (2009). Production of biodiesel from neem oil. *International journal of engineering studies*, 1(4), 295-302.
- Sekoai, P. T., Ouma, C. N. M., Du Preez, S. P., Modisha, P., Engelbrecht, N., Bessarabov, D. G., & Ghimire, A. (2019). Application of nanoparticles in biofuels: An overview. *Fuel*, 237, 380-397.
- Serin, H., Ozcanli, M., Kemal Gokce, M., & Tuccar, G. (2013). Biodiesel production from tea seed (*Camellia Sinensis*) oil and its blends with diesel fuel. *International journal of green energy*, 10(4), 370-377.
- Shah, Z., Cataluña Veses, R., & Silva, R. D. (2016). GC-MS and FTIR analysis of biooil obtained from freshwater algae (*spirogyra*) collected from freshwater. *International Journal of Environmental & Agriculture Research (IJOEAR)*. Bikaner, 2(2), 134-141.
- Shaheen, A., Sultana, S., Lu, H., Ahmad, M., Asma, M., & Mahmood, T. Assessing the Potential of Different Nano- composite (MgO, Al₂O₃-CaO and TiO₂) for Efficient Conversion of *Silybum eburneum* Seed Oil to Liquid Biodiesel. (2017). *Journal of Molecular Liquids*, 249, 511-521.
- Shahid, E. M., & Jamal, Y. (2011). Production of biodiesel: a technical review. *Renewable and Sustainable Energy Reviews*, 15(9), 4732-4745.
- Shameli, K., Ahmad, M. B., Zamanian, A., Sangpour, P., Shabanzadeh, P., Abdollahi, Y., & Zargar, M. (2012). Green biosynthesis of silver nanoparticles using *Curcuma longa* tuber powder. *International journal of nanomedicine*, 7, 56035610.
- Sharma, Y. C., & Singh, B. (2009). Development of biodiesel: current scenario. *Renewable and sustainable energy reviews*, 13(6-7), 1646-1651.

- Sharma, Y. C., Singh, B., & Upadhyay, S. N. (2008). Advancements in development and characterization of biodiesel: a review. *Fuel*, 87(12), 2355-2373.
- Sheykhluou, N., Valadabadi, S. A., Daneshian, J., & Khiavi, M. (2012). Study of new dry land safflower cultivars yield under different planting seasons in Zanjan area. *International Journal of Agriculture and Crop Sciences (IJACS)*, 4(20), 1546-1550.
- Shimelis, H., & Hugo, A. (2011). Determination of selection criteria for seed yield and seed oil content in Vernonia (Vernonia galamensis variety ethiopica). *Industrial Crops and Products*, 33(2), 436-439.
- Shin, H. Y., Lim, S. M., Kang, S. C., & Bae, S. Y. (2012). Statistical optimization for biodiesel production from rapeseed oil via transesterification in supercritical methanol. *Fuel processing technology*, 98, 1-5.
- Silitonga, A. S., Atabani, A. E., Mahlia, T. M. I., Masjuki, H. H., Badruddin, I. A., & Mekhilef, S. (2011). A review on prospect of Jatropha curcas for biodiesel in Indonesia. *Renewable and Sustainable Energy Reviews*, 15(8), 3733-3756.
- Silitonga, A. S., Mahlia, T. M. I., Ong, H. C., Riayatsyah, T. M. I., Kusumo, F., Ibrahim, H., Dharma, S., & Gumilang, D. (2017). A comparative study of biodiesel production methods for Reutealis trisperma biodiesel. *Energy Sources, Part A: Recovery, Utilization, and Environmental Effects*, 39(20), 2006-2014.
- Silva, G. F., Camargo, F. L., & Ferreira, A. L. (2011). Application of response surface methodology for optimization of biodiesel production by transesterification of soybean oil with ethanol. *Fuel Processing Technology*, 92(3), 407-413.
- Silva, P. L., Silva, C. M., Guimarães, L., & Pliego, J. R. (2015). Acid-catalyzed transesterification and esterification in methanol: a theoretical cluster-continuum investigation of the mechanisms and free energy barriers. *Theoretical Chemistry Accounts*, 134(1), 1591.
- Singh, S. P., & Singh, D. (2010). Biodiesel production through the use of different sources and characterization of oils and their esters as the substitute of diesel: a review. *Renewable and sustainable energy reviews*, 14(1), 200-216.
- Singh, V., Belova, L., Singh, B., & Sharma, Y. C. (2018). Biodiesel production using a novel heterogeneous catalyst, magnesium zirconate (Mg₂Zr₅O₁₂): Process optimization through response surface methodology (RSM). *Energy Conversion and Management*, 174, 198-207.

- Sokolova, V., Ludwig, A. K., Hornung, S., Rotan, O., Horn, P. A., Epple, M., & Giebel, B. (2011). Characterisation of exosomes derived from human cells by nanoparticle tracking analysis and scanning electron microscopy. *Colloids and Surfaces B: Biointerfaces*, 87(1), 146-150.
- Sokoto, M. A., Hassan, L. G., Dangoggo, S. M., Ahmad, H. G., & Uba, A. (2011). Influence of fatty acid methyl esters on fuel properties of biodiesel produced from the seeds oil of *Curcubita pepo*. *Nigerian Journal of Basic and Applied Sciences*, 19(1), 81-86.
- Sreedhar, N. (2014). Optimization of algal methyl esters using RSM and evaluation of biodiesel storage characteristics. *Bioresources and Bioprocessing*, 1(1), 19.
- Srivastava, A., & Prasad, R. (2000). Triglycerides-based diesel fuels. *Renewable and sustainable energy reviews*, 4(2), 111-133.
- Sultana, S., Ahmad, M., Zafar, M., Ullah, K., Ashraf, M. A., Ayoub, M., & Tareen, N. M. (2016). Biodiesel synthesis and characterization using welted thistle plant (*Carduus acanthoides*) as source of new non-edible seed oil. *International Journal of Green Energy*, 13(5), 462-469.
- Tahvildari, K., Anaraki, Y. N., Fazaeli, R., Mirpanji, S., & Delrish, E. (2015). The study of CaO and MgO heterogenic nano-catalyst coupling on transesterification reaction efficacy in the production of biodiesel from recycled cooking oil. *Journal of Environmental Health Science and Engineering*, 13(1), 73-81.
- Talebian-Kiakalaieh, A., Amin, N. A. S., Zarei, A., & Noshadi, I. (2013). Transesterification of waste cooking oil by heteropoly acid (HPA) catalyst: optimization and kinetic model. *Applied Energy*, 102, 283-292.
- Tan, K. T., Gui, M. M., Lee, K. T., & Mohamed, A. R. (2010). An optimized study of methanol and ethanol in supercritical alcohol technology for biodiesel production. *The Journal of Supercritical Fluids*, 53(1-3), 82-87.
- Tan, Y. H., Abdullah, M. O., Nolasco-Hipolito, C., & Zauzi, N. S. A. (2017). Application of RSM and Taguchi methods for optimizing the transesterification of waste cooking oil catalyzed by solid ostrich and chicken-eggshell derived CaO. *Renewable Energy*, 114, 437-447.
- Tariq, M., Ali, S., Ahmad, F., Ahmad, M., Zafar, M., Khalid, N., & Khan, M. A. (2011). Identification, FT-IR, NMR (1H and 13C) and GC/MS studies of fatty acid methyl esters in biodiesel from rocket seed oil. *Fuel Processing Technology*, 92(3), 336-341.

- Tariq, N., Majeed, M. I., Hanif, M. A., & Rehman, R. (2020). Pholi (Wild Safflower). In *Medicinal Plants of South Asia*, 557-569. Elsevier.
- Thangaraj, B., & Piraman, S. (2016). Heteropoly acid coated ZnO nanocatalyst for *Madhuca indica* biodiesel synthesis. *Biofuels*, 7(1), 13-20.
- Thangaraj, B., Jia, Z., Dai, L., Liu, D., & Du, W. (2016). Lipase NS81006 immobilized on Fe₃O₄ magnetic nanoparticles for biodiesel production. *Ovidius University Annals of Chemistry*, 27(1), 13-21.
- Thangaraj, B., Muniyandi, B., Ranganathan, S., & Xin, H. (2015). Functionalized magnetic nanoparticles for catalytic application—a review. *Reviews in Advanced Sciences and Engineering*, 4(2), 106-119.
- Tiwari, A. K., Kumar, A., & Raheman, H. (2007). Biodiesel production from jatropha oil (*Jatropha curcas*) with high free fatty acids: an optimized process. *Biomass and bioenergy*, 31(8), 569-575.
- Ullah, H., Nafees, M., Iqbal, F., Awan, M. S., Shah, A., & Waseem, A. (2017). Adsorption Kinetics of Malachite Green and Methylene Blue from Aqueous Solutions Using Surfactant-modified Organoclays. *Acta Chimica Slovenica*, 64(2), 449-460. doi: 10.17344/acsi.2017.3285.
- Ullah, K., Sharma, V. K., Ahmad, M., Lv, P., Krahl, J., & Wang, Z. (2018). The insight views of advanced technologies and its application in bio-origin fuel synthesis from lignocellulose biomasses waste, a review. *Renewable and sustainable energy reviews*, 82, 3992-4008.
- Ullah, K., Sharma, V. K., Dhingra, S., Braccio, G., Ahmad, M., & Sofia, S. (2015). Assessing the lignocellulosic biomass resources potential in developing countries: A critical review. *Renewable and Sustainable Energy Reviews*, 51, 682-698.
- Uprety, B. K., Chaiwong, W., Ewelike, C., & Rakshit, S. K. (2016). Biodiesel production using heterogeneous catalysts including wood ash and the importance of enhancing byproduct glycerol purity. *Energy Conversion and Management*, 115, 191-199.
- Uzun, B. B., Kılıç, M., Özbay, N., Pütün, A. E., & Pütün, E. (2012). Biodiesel production from waste frying oils: Optimization of reaction parameters and determination of fuel properties. *Energy*, 44(1), 347-351.

- Van de Voort, F. R., Sedman, J., & Pinchuk, D. (2011). An overview of progress and new developments in FTIR lubricant condition monitoring methodology. *Journal of ASTM International*, 8(5), 1-14.
- Velasco, L., Goffman, F. D., & Becker, H. C. (1998). Variability for the fatty acid composition of the seed oil in a germplasm collection of the genus Brassica. *Genetic Resources and Crop Evolution*, 45(4), 371-382.
- Verma, P., & Sharma, M. P. (2016a). Comparative analysis of effect of methanol and ethanol on Karanja biodiesel production and its optimisation. *Fuel*, 180, 164-174.
- Verma, P., & Sharma, M. P. (2016b). Review of process parameters for biodiesel production from different feedstocks. *Renewable and Sustainable Energy Reviews*, 62, 1063-1071.
- Verma, P., Dwivedi, G., & Sharma, M. P. (2017). Comprehensive analysis on potential factors of ethanol in Karanja biodiesel production and its kinetic studies. *Fuel*, 188, 586-594.
- Verma, P., Sharma, M. P., & Dwivedi, G. (2016). Evaluation and enhancement of cold flow properties of palm oil and its biodiesel. *Energy Reports*, 2, 8-13.
- Vicente, G., Martinez, M., & Aracil, J. (2007). Optimisation of integrated biodiesel production. Part I. A study of the biodiesel purity and yield. *Bioresource technology*, 98(9), 1724-1733.
- Viter, R., & Iatsunskyi, I. (2018). Optical Spectroscopy for Characterization of Metal Oxide Nanofibers. *Handbook of Nanofibers*, 1-35.
- Vorontsov, A. V., & Tsybulya, S. V. (2018). Influence of nanoparticles size on XRD patterns for small monodisperse nanoparticles of Cu₀ and TiO₂ anatase. *Industrial & Engineering Chemistry Research*, 57(7), 2526-2536.
- Vyas, A. P., Verma, J. L., & Subrahmanyam, N. (2010). A review on FAME production processes. *Fuel*, 89(1), 1-9.
- Wagner, G. W., Koper, O. B., Lucas, E., Decker, S., & Klabunde, K. J. (2000). Reactions of VX, GD, and HD with nanosize CaO: autocatalytic dehydrohalogenation of HD. *The Journal of Physical Chemistry B*, 104(21), 5118-5123.
- Wan, T., Yu, P., Wang, S., & Luo, Y. (2009). Application of sodium aluminate as a heterogeneous base catalyst for biodiesel production from soybean oil. *Energy & Fuels*, 23(2), 1089-1092.

- Wan, Z., Lim, J. K., & Hameed, B. H. (2015). Chromium–tungsten heterogeneous catalyst for esterification of palm fatty acid distillate to fatty acid methyl ester. *Journal of the Taiwan Institute of Chemical Engineers*, 54, 64-70.
- Wang, J., Chen, Y., Wang, X., & Cao, F. (2009). Aluminumdodecatungstophosphate (Al₁₀.9H₀.3PW₁₂O₄₀) nanotube as a solid acid catalyst one-pot production of biodiesel from waste cooking oil. *BioResources*, 4(4), 1477-1486.
- Wen, L., Wang, Y., Lu, D., Hu, S., & Han, H. (2010). Preparation of KF/CaO nanocatalyst and its application in biodiesel production from Chinese tallow seed oil. *Fuel*, 89(9), 2267-2271.
- Wong, Y. C., Tan, Y. P., Taufiq-Yap, Y. H., Ramli, I., & Tee, H. S. (2015). Biodiesel production via transesterification of palm oil by using CaO–CeO₂ mixed oxide catalysts. *Fuel*, 162, 288-293.
- Woodford, J. J., Parlett, C. M., Dacquin, J. P., Cibin, G., Dent, A., Montero, J., Wilson, K., & Lee, A. F. (2013). Identifying the active phase in Cs-promoted MgO nanocatalysts for triglyceride transesterification. *Journal of Chemical Technology & Biotechnology*, 89(1), 73-80.
- Worapun, I., Piantong, K., & Thaiyasuit, P. (2012). Optimization of biodiesel production from crude palm oil using ultrasonic irradiation assistance and response surface methodology. *Journal of Chemical Technology & Biotechnology*, 87(2), 189-197.
- Xiong, G., Pal, U., Serrano, J. G., Ucer, K. B., & Williams, R. T. (2006). Photoluminescence and FTIR study of ZnO nanoparticles: the impurity and defect perspective. *physica status solidi c*, 3(10), 3577-3581.
- Xue, J. (2013). Combustion characteristics, engine performances and emissions of waste edible oil biodiesel in diesel engine. *Renewable and Sustainable Energy Reviews*, 23, 350-365.
- Yan, S., DiMaggio, C., Mohan, S., Kim, M., Salley, S. O., & Ng, K. S. (2010). Advancements in heterogeneous catalysis for biodiesel synthesis. *Topics in catalysis*, 53(11-12), 721-736.
- Yuan, X., Liu, J., Zeng, G., Shi, J., Tong, J., & Huang, G. (2008). Optimization of conversion of waste rapeseed oil with high FFA to biodiesel using response surface methodology. *Renewable Energy*, 33(7), 1678-1684.

- Yusuf, N. N. A. N., Kamarudin, S. K., & Yaakub, Z. (2011). Overview on the current trends in biodiesel production. *Energy conversion and management*, 52(7), 2741-2751.
- Zhang, D., Zhou, C.-H., Lin, C.-X., Tong, D.-S., & Yu, W.-H. (2010). Synthesis of clay minerals. *Applied Clay Science*, 50(1), 1-11.
- Zhang, J., Chen, S., Yang, R., & Yan, Y. (2010). Biodiesel production from vegetable oil using heterogenous acid and alkali catalyst. *Fuel*, 89(10), 2939-2944.
- Zhang, S., Zu, Y. G., Fu, Y. J., Luo, M., Zhang, D. Y., & Efferth, T. (2010). Rapid microwave-assisted transesterification of yellow horn oil to biodiesel using a heteropolyacid solid catalyst. *Bioresource technology*, 101(3), 931-936.
- Zhang, X., Rong, J., Chen, H., He, C., & Wang, Q. (2014). Current status and outlook in the application of microalgae in biodiesel production and environmental protection. *Frontiers in Energy Research*, 2, 32-46.
- Zhao, C., Lv, P., Yang, L., Xing, S., Luo, W., & Wang, Z. (2018). Biodiesel synthesis over biochar-based catalyst from biomass waste pomelo peel. *Energy Conversion and Management*, 160, 477-485.
- Zhao, Q., Wang, H., Zheng, H., Sun, Z., Shi, W., Wang, S., Wang, X., & Jiang, Z. (2013). Acid–base bifunctional HPA nanocatalysts promoting heterogeneous transesterification and esterification reactions. *Catalysis Science & Technology*, 3(9), 2204-2209.
- Zhou, C. H. (2011). An overview on strategies towards clay-based designer catalysts for green and sustainable catalysis. *Applied Clay Science*, 53(2), 87-96.





RESEARCH ARTICLE

MICROSCOPY
RESEARCH TECHNIQUE

WILEY

Implication, visualization, and characterization through scanning electron microscopy as a tool to identify nonedible oil seeds

Saman Ilyas Cheema¹ | Mushtaq Ahmad¹ | Riaz Ullah² | Ramzi A. Mothana² | Omar M. Noman² | Muhammad Zafar¹ | Shazia Sultana¹ | Ayesha Hameed¹ | Saeeda Naz¹ | Maryam Tanveer Akhtar³

¹Department of Plant Sciences, Quaid-i-Azam University, Islamabad, Pakistan

²Department of Pharmacognosy, College of Pharmacy, King Saud University, Riyadh, Saudi Arabia

³Department of Environmental Science, International Islamic University, Islamabad, Pakistan

Correspondence

Muhammad Zafar, Department of Plant Sciences, Quaid-i-Azam University, Islamabad, Pakistan.

Email: zafar@qau.edu.pk

Funding information

King Saud University, Grant/Award Number: RSP/2020/119

Review Editor: Paul Verkade

Abstract

Second-generation biofuels prove to be a distinctive and renewable source of sustainable energy and cleaner environment. The current study focuses on the exploration and identification of four nonedible sources, that is, *Brassica oleracea* L., *Carthamus oxyacantha* M.Bieb., *Carthamus tinctorius* L., and *Beaumontia grandiflora* Wall., utilizing light microscopy (LM) and scanning electron microscopy (SEM) for studying the detailed micromorphological features of these seeds. LM revealed that size ranges from 3 to 20 mm. furthermore, a great variety of color is observed from pitch black to greenish gray and yellowish white to off white. Seeds ultrastructure study with the help of SEM revealed a great variety in shape, size, color, sculpturing and periclinal wall shape, and so on. Followed by the production of fatty acid methyl esters from a novel source, that is, seeds oil of *Brassica oleracea* L. (seed oil content 42.20%, FFA content 0.329 mg KOH/g) using triple metal impregnated montmorillonite clay catalyst (Cu-Mg-Zn-Mmt). Catalyst was characterized using SEM-EDX, FT-IR. Maximum yield of *Brassica oleracea* L. biodiesel (87%) was obtained at the conditions; 1:9 of oil to methanol ratio, 0.5 g of catalyst, 5 hr reaction time, and 90°C of temperature. Synthesized biodiesel was characterized by FT-IR, GC-MS, and NMR. Fuel properties of the *Brassica oleracea* L. FAMES were determined and found in accordance with ASTM standards.

KEYWORDS

biodiesel, nanocatalyst, nonedible sources, renewable energy, scanning electron microscopy, seed identification, seed ultrastructure

1 | INTRODUCTION

The world is running out of fossil fuel resources due to rapid increase in the population. And global population is estimated to reach nine million by the mid of this millennium. With most part of population residing in the developing and poor countries of the world (Asif, Ahmad, Zafar, & Ali, 2017). Energy and population growth have a

direct relation, that is, more population results in more food demand as well as that of energy resources for life sustenance. And one thing that is becoming crystal clear with time is that fossil fuels are squeezing fast (Rasmuson & Zetterstrom, 1992). World energy resources can be categorized into two main classes, that is, conventional or non-renewable and nonconventional or renewable. In current global scenario where the world is facing the problems of fossil fuel shortage